

**PRIMARY AND RECALL CYTOTOXIC T LYMPHOCYTE RESPONSES TO  
AUTOLOGOUS ANTIGEN IN HIV-1-INFECTED SUBJECTS**

by

**Kellie N. Smith**

B.S., Villa Julie College, 2008

Submitted to the Graduate Faculty of

Department of Molecular Virology and Microbiology

School of Medicine

in partial fulfillment of the requirements for the degree of

Doctor of Philosophy

University of Pittsburgh

2013

UNIVERSITY OF PITTSBURGH

School of Medicine

This dissertation was presented

by

**Kellie N. Smith**

It was defended on

November 21, 2013

and approved by

*Dissertation Advisor:* Charles R. Rinaldo, PhD  
Chairman and Professor, Department of Infectious Diseases and Microbiology  
Graduate School of Public Health, University of Pittsburgh  
Professor, Department of Pathology  
School of Medicine, University of Pittsburgh

*Committee Member:* Lisa Butterfield, PhD  
Professor, Division of Hematology/Oncology  
School of Medicine, University of Pittsburgh

*Committee Member:* Phalguni Gupta, PhD  
Assistant Chairman and Professor, Department of Infectious Diseases and Microbiology  
Graduate School of Public Health, University of Pittsburgh

*Committee Member:* Todd Reinhart, ScD  
Professor, Department of Infectious Diseases and Microbiology  
Graduate School of Public Health, University of Pittsburgh

*Committee Member:* Walter Storkus, PhD  
Professor, Department of Dermatology and Immunology  
School of Medicine, University of Pittsburgh

**PRIMARY AND RECALL CYTOTOXIC T LYMPHOCYTE RESPONSES TO  
AUTOLOGOUS ANTIGEN IN HIV-1-INFECTED SUBJECTS**

Kellie N. Smith, PhD

University of Pittsburgh, 2013

Copyright © by Kellie N. Smith

2013

**PRIMARY AND RECALL CYTOTOXIC T LYMPHOCYTE RESPONSES TO  
AUTOLOGOUS ANTIGEN IN HIV-1-INFECTED SUBJECTS**

Kellie N. Smith, PhD

University of Pittsburgh, 2013

Human immunodeficiency virus type-1 (HIV-1) affects more than 30 million people worldwide and has accounted for over 30 million deaths. The advent of combination antiretroviral therapy (cART) resulted in a drastic decrease in AIDS-associated morbidity and mortality. Despite this, cART fails to completely eradicate the virus from infected patients, as cessation of treatment results in a rebound in viremia and a resumption of disease progression. Partial immune reconstitution is achieved under suppressive therapy, thus causing research efforts to begin development of curative strategies for HIV-1-infected patients. We believe the best method of HIV-1 eradication will be through cytotoxic T lymphocyte (CTL) elimination of the latently-infected reservoir, which may be difficult given the propensity of the virus to undergo mutations that evade CTL recognition. Dendritic cells, the most potent antigen-presenting cells, can reveal broad and robust HIV-1-specific T cell responses in subjects on cART and can prime CD8<sup>+</sup> T cells specific for various HIV-1 antigens. We therefore believe the best method of inducing a potent anti-HIV-1 CTL response will be through the use of a DC-based immunotherapy targeting the patient's own, unique (autologous) virus. It is unclear, however, if the naïve T cell repertoire and function has been sufficiently restored to respond to autologous virus containing multiple mutational variants. In the present study, we longitudinally evaluated autologous HIV-1 evolution and changes in T cell responses throughout untreated and treated HIV-1 infection in subjects from the Multicenter AIDS Cohort Study (MACS). We show that dendritic cells reveal autologous

antigen-specific T cell responses at all stages of disease progression and are potent inducers of polyfunctional T cell responses after long-term suppressive cART. We developed and utilized an *in vitro* model of DC immunotherapy targeting naïve and memory CD8<sup>+</sup> T cell subsets to show for the first time that naïve CD8<sup>+</sup> T cells from subjects on cART can be primed to target the latent HIV-1 reservoir. Taken together, these findings shed new light on T cell responses to autologous HIV-1 viral variants and support the use of a DC immunotherapy in subjects on cART.

# TABLE OF CONTENTS

<b>LIST OF TABLES.....</b>	<b>XIIII</b>
<b>LIST OF FIGURES .....</b>	<b>XIV</b>
<b>PREFACE .....</b>	<b>XIX</b>
<b>1.0 HUMAN IMMUNODEFICIENCY VIRUS TYPE-1 .....</b>	<b>1</b>
1.1.1 <i>Life cycle .....</i>	<i>1</i>
1.1.2 <i>Pathogenesis.....</i>	<i>3</i>
1.1.3 <i>Genetic evolution .....</i>	<i>4</i>
1.1.4 <i>Combination antiretroviral therapy .....</i>	<i>5</i>
1.2 CTL AND HIV-1 INFECTION .....	6
1.2.1 <i>CTL in chronic infection.....</i>	<i>7</i>
1.2.2 <i>Barriers to CTL-mediated viral clearance .....</i>	<i>8</i>
1.3 DENDRITIC CELLS AND HIV-1 INFECTION .....	11
1.3.1 <i>Impact of chronic HIV-1 infection on DC function .....</i>	<i>12</i>
1.3.2 <i>DC as an immunotherapy in subjects on cART .....</i>	<i>12</i>
1.4 STATEMENT OF THE PROBLEM.....	19
1.4.1 <i>Specific aim I: describe the clinical correlates and signatures of HIV-1 evolution in chronic, untreated infection .....</i>	<i>21</i>
1.4.2 <i>Specific aim II: evaluate the effects of viral evolution on the generation and detection of HIV-1-specific T cell responses .....</i>	<i>21</i>
1.4.3 <i>Specific aim III: determine the residual capacity of naïve and memory T cells to respond to DC stimulation and eradicate the HIV-1 reservoir in subjects on cART.....</i>	<i>22</i>

<b>2.0</b>	<b>.....CLINICAL CORRELATES AND SIGNATURES OF SELECTIVE PRESSURE IN HUMAN IMMUNODEFICIENCY VIRUS TYPE-1 GAG AND ENV .....</b>	<b>23</b>
2.1	BACKGROUND.....	24
2.2	METHODS .....	26
2.2.1	<i>Study participants.....</i>	26
2.2.2	<i>Clinical and virologic characteristics.....</i>	27
2.2.3	<i>HIV-1 gag and env-gp120 sequencing.....</i>	27
2.2.4	<i>Genetic sequence analysis.....</i>	28
2.2.5	<i>Identification of sites under selection.....</i>	29
2.2.6	<i>Protein sequence and epitope analysis .....</i>	30
2.2.7	<i>Statistics .....</i>	31
2.3	RESULTS.....	31
2.3.1	<i>Clinical characteristics in chronic, untreated HIV-1 infection.....</i>	31
2.3.2	<i>Correlates of HIV-1 gag and env evolution.....</i>	34
2.3.3	<i>Mechanisms of viral evolution.....</i>	42
2.3.4	<i>Positive selection as a driving force for viral evolution.....</i>	47
2.3.5	<i>Positive selection in MHC class I-restricted epitopes.....</i>	49
2.3.6	<i>The impact of protein evolution on predicted epitope processing and presentation .....</i>	51
2.4	DISCUSSION .....	56
2.5	ACKNOWLEDGEMENTS.....	61
<b>3.0</b>	<b>THE EFFECTS OF REGULATORY T CELLS AND DENDRITIC CELLS ON T CELL RESPONSES TO AUTOLOGOUS HIV-1 EPITOPE VARIANTS.....</b>	<b>62</b>
3.1	ABSTRACT .....	62
3.2	BACKGROUND.....	63

3.3	METHODS.....	66
3.3.1	<i>Study subjects.....</i>	66
3.3.2	<i>Isolation of HIV-1 pre- and post-cART.....</i>	67
3.3.3	<i>HIV-1 genetic sequencing .....</i>	68
3.3.4	<i>Identification of epitopes and peptide synthesis.....</i>	68
3.3.5	<i>T<sub>reg</sub> depletion .....</i>	69
3.3.6	<i>PBMC and T<sub>reg</sub> staining.....</i>	70
3.3.7	<i>Generation of monocyte-derived dendritic cells (DC) .....</i>	71
3.3.8	<i>IFN-<math>\gamma</math> ELISpot assay .....</i>	71
3.3.9	<i>Intracellular cytokine staining .....</i>	72
3.3.10	<i>Statistical analyses.....</i>	73
3.4	RESULTS.....	73
3.4.1	<i>Changes in HIV-1 Gag and Env epitopes in chronic infection.....</i>	73
3.4.2	<i>Longitudinal T cell responses to autologous HIV-1 epitope variants.....</i>	79
3.4.3	<i>The effects of regulatory T cells on HIV-1-specific responses .....</i>	86
3.4.4	<i>Broad DC enhancement of T cell responses to autologous epitope variants.....</i>	90
3.4.5	<i>The combined effect of T<sub>reg</sub> depletion and DC addition on recall T cell responses</i>	93
3.4.6	<i>Comparison of T<sub>reg</sub> depletion and DC addition for the detection of recall HIV-1-specific T cell responses .....</i>	96
3.4.7	<i>DC enhance cytokine secretion in HIV-1-specific CD8<sup>+</sup> T cells.....</i>	98
3.4.8	<i>DC induce a disease state-dependent enhancement in the cytokine profile of epitope variant-specific CD8<sup>+</sup> T cells .....</i>	103
3.5	DISCUSSION .....	106
3.6	ACKNOWLEDGEMENTS .....	110



<b>4.0 PRIMARY AND RECALL T CELL RESPONSES TO AUTOLOGOUS EPITOPE VARIANTS</b>	
<b>IN CHRONIC HIV-1 INFECTION .....</b>	<b>111</b>
4.1 ABSTRACT .....	111
4.2 BACKGROUND.....	112
4.3 METHODS.....	114
4.3.1 <i>Study participants</i> .....	114
4.3.2 <i>Clinical and virologic characteristics</i> .....	115
4.3.3 <i>Sequencing and phylogenetic analysis</i> .....	116
4.3.4 <i>Synthetic peptides</i> .....	116
4.3.5 <i>In silico and in vitro analysis of peptide binding affinity</i> .....	117
4.3.6 <i>Generation of dendritic cells (DC)</i> .....	118
4.3.7 <i>In vitro priming</i> .....	118
4.3.8 <i>IFN<math>\gamma</math> ELISPOT assay</i> .....	119
4.3.9 <i>Statistical analysis</i> .....	120
4.4 RESULTS.....	121
4.4.1 <i>Clinical and virologic characteristics of the study participant</i> .....	121
4.4.2 <i>Dynamics of viral evolution and epitope variants</i> .....	122
4.4.3 <i>Autologous HIV-1 peptide binding affinity for MHC class I</i> .....	124
4.4.4 <i>Impact of peptide:MHC binding affinity on the breadth of memory T cell</i> <i>responses to autologous contemporaneous HIV-1 peptide sequences</i> .....	129
4.4.5 <i>The changing magnitude of T cell memory responses targeting autologous HIV-1</i> <i>variant sequences</i> .....	132
4.4.6 <i>Broad and high magnitude primary T cell responses to naturally-evolving</i> <i>variants in HIV-1-positive and healthy donors</i> .....	138
4.5 DISCUSSION .....	143

4.6	ACKNOWLEDGEMENTS .....	148
<b>5.0</b>	<b>THE ROLE OF DEFECTIVE AND CROSS-REACTIVE RECALL T CELL RESPONSES IN HIV-1 INFECTION .....</b>	<b>149</b>
5.1	ABSTRACT .....	149
5.2	BACKGROUND.....	150
5.3	METHODS.....	152
5.3.1	<i>Media, reagents, and cell lines.....</i>	<i>152</i>
5.3.2	<i>Human subjects.....</i>	<i>153</i>
5.3.3	<i>Selection of HIV-1 epitopes.....</i>	<i>153</i>
5.3.4	<i>HIV-1 genetic sequencing.....</i>	<i>154</i>
5.3.5	<i>Dengue virus epitope sequences.....</i>	<i>154</i>
5.3.6	<i>Synthetic peptides.....</i>	<i>154</i>
5.3.7	<i>Analysis of peptide:MHC class I affinity.....</i>	<i>155</i>
5.3.8	<i>HLA typing.....</i>	<i>155</i>
5.3.9	<i>Generation of DC.....</i>	<i>155</i>
5.3.10	<i>Induction and expansion of primary CTL.....</i>	<i>156</i>
5.3.11	<i>Short term expansion of CTL.....</i>	<i>156</i>
5.3.12	<i>CTL and DC co-cultures.....</i>	<i>157</i>
5.3.13	<i>HIV-1 infection and transmission assay.....</i>	<i>157</i>
5.3.14	<i>Flow cytometry.....</i>	<i>158</i>
5.3.15	<i>ELISpot assays.....</i>	<i>158</i>
5.3.16	<i>Cytotoxicity assays.....</i>	<i>159</i>
5.3.17	<i>DC production of immune mediators.....</i>	<i>159</i>
5.3.18	<i>Scanning electron microscopy (SEM).....</i>	<i>160</i>
5.3.19	<i>Live cell imaging.....</i>	<i>160</i>

5.3.20	<i>Statistical analysis</i> .....	161
5.4	RESULTS.....	161
5.4.1	<i>Use of DC to induce broadly cross-reactive HIV-1-specific CTL from HIV-1 naïve donors</i> .....	161
5.4.2	<i>Phenotypic characterization of cross-reactive CTL lines</i> .....	165
5.4.3	<i>Cytolytic function of cross-reactive HIV-1-specific CTL</i> .....	169
5.4.4	<i>Activation and programming of variant antigen-expressing DC by cross-reactive CTL</i> .....	172
5.4.5	<i>Expression levels of cognate antigen can determine killer versus helper role of CTL</i> .....	176
5.4.6	<i>CTL programmed DC show enhanced ability to mediate HIV-1 transmission to T cells</i> .....	177
5.5	DISCUSSION .....	179
5.6	ACKNOWLEDGEMENTS .....	184

## **6.0 PRIMARY *IN VITRO* DC STIMULATION OF NAÏVE CD8<sup>+</sup> T CELLS FACILITATES**

<b>ELIMINATION OF THE HIV-1 RESERVOIR</b> .....	<b>185</b>	
6.1	BACKGROUND.....	186
6.2	METHODS.....	189
6.2.1	<i>Study subjects</i> .....	189
6.2.2	<i>Induction and isolation of HIV-1 from latently-infected CD4<sup>+</sup> T cells</i> .....	190
6.2.3	<i>HIV-1 sequencing and peptide synthesis</i> .....	191
6.2.4	<i>Isolation of monocytes and peripheral blood lymphocytes</i> .....	192
6.2.5	<i>Purification of naïve and non-naïve CD4<sup>+</sup> and CD8<sup>+</sup> T cells</i> .....	192
6.2.6	<i>Generation of monocyte-derived DC and CTL effector populations</i> .....	193
6.2.7	<i>IFN<math>\gamma</math> ELISpot</i> .....	194

6.2.8	<i>Generation of autologous HIV-1-infected CD4<sup>+</sup> T cells</i> .....	195
6.2.9	<i>HIV-1-specific cytotoxicity assay</i> .....	195
6.2.10	<i>Statistical analyses</i> .....	196
6.3	RESULTS.....	197
6.3.1	<i>Primary CD8<sup>+</sup> T cell responses induced from pre-seroconversion and post-cART naïve precursors</i> .....	197
6.3.2	<i>Ex vivo T cells recognize autologous Gag p17 and p24 with variable breadth and magnitude</i> .....	201
6.3.3	<i>T cells primed to autologous HIV-1 in vitro are of higher breadth and magnitude than responses detected ex vivo</i> .....	204
6.3.4	<i>DC sensitization of non-naïve T cells results in responses of variable breadth and magnitude against autologous Gag antigens</i> .....	209
6.3.5	<i>Analysis of CTL effector function against autologous HIV-1-infected CD4<sup>+</sup> T cells</i> .....	214
6.4	DISCUSSION .....	216
6.5	ACKNOWLEDGEMENTS .....	220
<b>7.0</b>	<b>DISCUSSION AND SUMMARY</b> .....	<b>221</b>
	<b>APPENDIX A: LIST OF ABBREVIATIONS</b> .....	<b>230</b>
	<b>APPENDIX B: SUPPLEMENTAL FIGURES</b> .....	<b>232</b>
	<b>BIBLIOGRAPHY</b> .....	<b>233</b>

## LIST OF TABLES

Table 1. Factors involved in the generation of a dendritic cell immunotherapy for HIV-1 .....	15
Table 2. HIV-1 plasma viral load, T cell count, and number of unique <i>gag</i> and <i>env</i> sequences obtained from each post-seroconversion time point .....	35
Table 3. Molecular HLA genotypes used in epitope prediction models.....	49
Table 4. Known MHC class I-restricted HIV-1 Gag and Env epitopes for each subject .....	50
Table 5. HIV-1 Gag and Env epitope variants that evolved throughout infection .....	76
Table 6. Longitudinal HIV-1 peptide sequences and their predicted and experimental HLA A and B affinity .....	125
Table 7. Early memory anti-HIV CTL responses to early and late epitope variants.....	162

## LIST OF FIGURES

Figure 1. The HIV-1 life cycle.....	2
Figure 2. Typical course of untreated HIV-1 infection.....	4
Figure 3. Clinical and virologic data.....	32
Figure 4. Correlates of HIV-1 <i>gag</i> and <i>env</i> divergence .....	37
Figure 5. Comparison of divergence in HIV-1 <i>gag</i> and <i>env</i> .....	38
Figure 6. Correlates of HIV-1 <i>gag</i> and <i>env</i> pairwise diversity .....	39
Figure 7. Comparison of pairwise diversity in HIV-1 <i>gag</i> and <i>env</i> .....	40
Figure 8. Phylogenetic trees derived from autologous <i>gag</i> and <i>env</i> sequences.....	41
Figure 9. Correlations between divergence and pairwise diversity .....	42
Figure 10. Correlates of positive and negative selection .....	45
Figure 11. Positive selection as a function of viral divergence and diversity.....	48
Figure 12. Longitudinal changes in the frequency of predicted MHC class I and II-restricted epitopes .....	53
Figure 13. Longitudinal changes in predicted proteasomal cleavage sites .....	55
Figure 14. The effects of amino acid substitutions on predicted MHC class I affinity in autologous HIV-1 HLA A*2402-restricted epitope variants .....	78
Figure 15. PBMC responses to autologous HIV-1 epitope variants in subject S2 .....	81
Figure 16. PBMC responses to autologous HIV-1 epitope variants in subject S3 .....	83
Figure 17. PBMC responses to autologous HIV-1 epitope variants in subject S8 .....	85
Figure 18. Longitudinal responses to autologous HIV-1 epitope variants in PBMC and T <sub>reg</sub> <sup>neg</sup> PBMC .....	87

Figure 19. DC stimulation reveals T cell responses specific for autologous epitope variants at all stages of disease progression .....	91
Figure 20. The combined effect of DC addition and T <sub>reg</sub> depletion on recall HIV-1-specific responses <i>in vitro</i> .....	94
Figure 21. DC addition reveals higher magnitude HIV-1-specific responses than T <sub>reg</sub> depletion	97
Figure 22. DC enhance CD8 <sup>+</sup> T cell secretion of some type 1 cytokines in response to autologous, contemporaneous HIV-1 epitope variants during late disease progression .....	99
Figure 23. DC enhance CD8 <sup>+</sup> T cell secretion of type 1 cytokines in response to autologous, contemporaneous HIV-1 epitope variants early post-cART.....	100
Figure 24. DC enhance CD8 <sup>+</sup> T cell secretion of type 1 cytokines in response to autologous, contemporaneous HIV-1 epitope variants late post-cART.....	102
Figure 25. DC effects on multifunctional CD8 <sup>+</sup> T cell responses specific for autologous contemporaneous HIV-1 epitope variants pre- and post-cART .....	104
Figure 26. Clinical course of HIV-1 infection in the study participant .....	121
Figure 27. Dynamics of genetic diversity and divergence of HIV-1 .....	123
Figure 28. Proportion of HIV-1 epitope variants exhibiting differential MHC class I affinities .....	128
Figure 29. The percent of autologous HIV-1 epitope variants that induced T cell responses...	130
Figure 30. Longitudinal changes in T cell responses against contemporaneous Gag epitope variants.....	133
Figure 31. Longitudinal changes in T cell responses against contemporaneous Env epitope variants.....	134

Figure 32. Longitudinal changes in T cell responses against contemporaneous Nef epitope variants.....	135
Figure 33. T cell responses specific for HIV-1 epitope variants with differential MHC class I affinity.....	137
Figure 34. <i>In vitro</i> -induced primary T cell responses specific for autologous HIV-1 epitope variants.....	139
Figure 35. Primary T cell responses induced in vitro against autologous epitope variants with differential MHC class I affinities. ....	141
Figure 36. Primary T cell responses specific for patient-derived HIV-1- epitope variants induced in HIV-1-negative donors. ....	142
Figure 37. Chronological evolution of autologous HIV-1 Gag, Env, and Nef epitope variants	163
Figure 38. <i>In vitro</i> induction of broadly reactive primary HIV-1 specific CTL.....	164
Figure 39. Differential expression of the T cell co-receptor CD8 on cross-reactive CTL.....	166
Figure 40. CTL induced early post-seroconversion respond to late autologous HIV-1 epitope variants.....	169
Figure 41. Dysfunctional cytolytic capacity of cross-reactive HIV-1-specific CTL.....	170
Figure 42. Cross-reactive CTL induce micro/nanotube extensions on DC expressing variant peptide.....	172
Figure 43. Cross-reactive HIV-1-specific CTL induce mature proinflammatory programmed DC .....	174
Figure 44. Concentration of cognate Ag determines differential shift in CTL killer versus helper activity.....	177



Figure 45. DC matured by cross-reactive CTL are superior mediators of HIV-1 transmission to CD4 <sup>+</sup> T cells.....	178
Figure 46. Primary CD8 <sup>+</sup> T cell responses specific for autologous epitope variants induced pre-seroconversion and post-cART in subject S1 .....	198
Figure 47. Comparison of primary and recall CD8 <sup>+</sup> T cell responses to autologous HIV-1 epitope variants in subject S1 .....	200
Figure 48. <i>Ex vivo</i> T cell responses to autologous, contemporaneous Gag peptide antigen .....	203
Figure 49. Primary T cell responses specific for contemporaneous Gag p17 and p24 peptide antigens .....	205
Figure 50. Priming of naïve T cells to autologous HIV-1 induces antigen-specific responses that are of greater magnitude than the endogenous recall response.....	207
Figure 51. Primary stimulation of naïve T cells increases the breadth of responses to autologous HIV-1 antigen .....	208
Figure 52. T cell responses detected to autologous Gag peptides following DC <i>in vitro</i> sensitization.....	210
Figure 53. Comparison of IFN $\gamma$ responses to all autologous Gag antigens evaluated in <i>ex vivo</i> , primary, and secondary T cells .....	211
Figure 54. Comparison of IFN $\gamma$ responses specific for autologous Gag antigens that induced responses in <i>ex vivo</i> T cells.....	213
Figure 55. <i>Ex vivo</i> , primary, and secondary CTL-mediated reductions in autologous CD4 <sup>+</sup> T cells infected with the autologous HIV-1 reservoir virus .....	215
Figure 56. Proposed effects of DC immunotherapy on naïve and memory CD8 <sup>+</sup> T cells in HIV-1-infected subjects on cART.....	228

Figure 57. Effects of T<sub>reg</sub> depletion on remaining T cell populations ..... 232

## PREFACE

### SPECIAL THANKS AND ACKNOWLEDGEMENTS

*“Biologists often talk about the ecology of an organism: the tallest oak in the forest is the tallest not just because it grew from the hardest acorn; it is the tallest also because no other trees blocked its sunlight, the soil around it was deep and rich, no rabbit chewed through its bark as a sapling, and no lumberjack cut it down before it matured.”*

-Malcolm Gladwell, *Outliers*

This is not the story of a tall tree. It is the story of the sunlight that warmed me, the soil in which I put my roots, and the rabbits and lumberjacks I was lucky enough to avoid. I would like to especially thank:

My mentor, Dr. Charles R. Rinaldo for his support and guidance during my time as a graduate student in his laboratory. I was very “green” when I started graduate school and I am forever grateful for Dr. Rinaldo’s faith that I would succeed. I would also like to thank him for the many opportunities he gave me to travel around the world to present our work and for putting his faith in me as the “travel guide” wherever we went.

All members of the Rinaldo lab, past and present. Particularly, Dr. Robbie B. Mailliard for his continued and unwavering support and mentorship over the years and for his ability to always see the good in people. Weimin Jiang for being a constant motivator, for staying with me until the wee hours of the night for my sorts, and for being a wonderful friend. LuAnn Borowski and Aarika

Yates for their guidance and help with my many flow cytometry woes and for always listening when I needed to talk. Dr. Ron Fecek for help with my experimental designs and for always taking time to help me and others. Blair Gleeson for running experiments for me when I was away or when I really just needed a helping hand. Taylor Poston for just being awesome and making the lab a happier place. Dr. Lauren Lepone for forcing me to get out of the house and go see that movie with you when I was feeling particularly low. I will never forget that.

Dr. Phalguni Gupta and Dr. Todd Reinhart for their mentorship and guidance with my work over the years. Dr. Gupta, for making me face my fear of the “tuk tuk”. The members of the Gupta lab, particularly Dr. Chengli Shen for assistance with genetic sequence analysis, and Deena and Lori, for going out of their way and taking time from their busy days to help with my project, and for becoming great friends.

The members of my committee, Dr. Lisa Butterfield, Dr. Phalguni Gupta, Dr. Todd Reinhart, and Dr. Walter Storkus, for their invaluable scientific expertise and suggestions, and for always being available when I needed guidance.

The faculty, students, and staff of IDM, particularly Judy Malenka, Debbie Laurie, Nancy Heath, Robin Tierno, Meredith Maverro, and Nancy McCarthy, for treating me as one of your own and making me feel like part of the IDM family. Also the faculty, students, and staff of the MVM department for their help and support and all the participants in the Pitt Men’s Study and the Multicenter AIDS Cohort study, without whom none of this work would have been possible.

All the wonderful friends I have made since moving to Pittsburgh, particularly Marc, Brian, Jonathan, and Lauren for making my time outside the lab much more enjoyable. Ann, for becoming a great friend and showing me that wonderful people can do extraordinary things.

My dear friends Matt, Heidi, and Janine, for sticking with me these 5 and a half years and making me realize that “out of sight, out of mind” just doesn’t apply to us.

Mike, my wonderful husband and partner in crime, for sticking with me through the ups and downs. I don’t think any other man could have been this patient and understanding, and I am forever grateful to you. My wonderful parents, brother, and grandparents for always believing in me and pushing me to be the best. I would not have been able to do this without your unwavering support and the drive you instilled in me. I owe this to you.

## **1.0 HUMAN IMMUNODEFICIENCY VIRUS TYPE-1**

Human immunodeficiency virus type-1 (HIV-1) affects more than 30 million people worldwide and accounts for 1.8 million deaths per year (329). Adult HIV-1 prevalence has exceeded 20% in some countries in Sub-Saharan Africa, including Swaziland (26%), Botswana (23.4%), and Lesotho (23.3%) (329). While combination antiretroviral therapy (cART) has drastically reduced AIDS-associated morbidity and mortality, the treatment is lifelong and results in many undesirable side effects (338). Additionally, inaccessibility to or failure to adhere to cART has resulted in a continuation of viral spread, even in the United States where treatment is readily obtainable (52). Current research is focused on the development of a prophylactic HIV-1 vaccine and/or curative approaches to completely eradicate infection in those already infected with the virus. There is no doubt that developing a cure will provide the best chance of HIV-1 eradication and will allow those already infected to live healthy, normal lives in the absence of cART.

### **1.1.1 Life cycle**

HIV-1 is a single-stranded, positive sense RNA virus and is the etiologic agent of acquired immunodeficiency syndrome (AIDS). The virus is present in blood and other bodily fluids and is contracted upon transfer of these fluids between people. HIV-1 is approximately 120nm in

diameter and contains two copies of the genome that encodes nine genes (66). The viral capsid is surrounded by an envelope composed of host cell phospholipids and the viral proteins gp120 and gp41. These two proteins interact with CD4 and CCR5 or CXCR4 on the surface of host cells to gain entry, therefore making CD4<sup>+</sup> T cells and macrophages the primary targets for HIV-1 infection (65, 214, 224) (Figure 1).

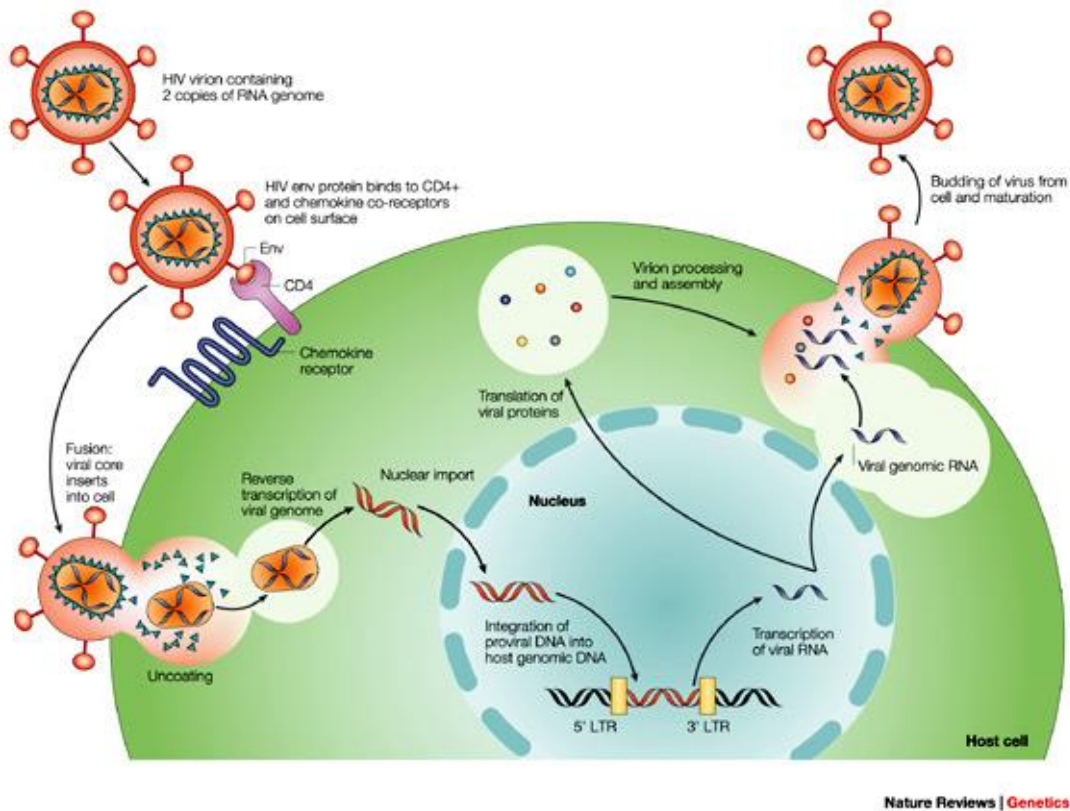


**Figure 1. The HIV-1 life cycle**

Viral entry into host cells requires the CD4 molecule and either the CCR5 or CXCR4 chemokine receptor. Entry is followed by a cascade of viral uncoating, reverse transcription, nuclear import, synthesis of viral proteins, and budding from the host membrane. Reproduced with permission from Rambaut et al. (274) ©2004 Nature Publishing Group.

The viral envelope fuses with the host cell membrane and releases the virion contents into the cytosol (54). It is here where RNA reverse transcription generates complementary DNA (cDNA) that is imported into the nucleus. This process of reverse transcription is extremely error-

prone and often results in mutations conferring drug resistance, immunological escape, or costs in viral fitness. The cDNA is then integrated into the host genome and establishes latency. Following cell activation, the viral genome is transcribed into mRNA, exported from the nucleus, and translated into viral proteins (150, 153). Virion assembly then occurs in the cytosol, incorporating two copies of the single-stranded (+) sense RNA genome within the Gag capsid proteins. The assembled virion then buds from the cell membrane, incorporating portions of the host cell membrane in its envelope, and is released to infect new target cells (367).

### 1.1.2 Pathogenesis

HIV-1 is a lentivirus, and as such is slowly-replicating and can latently reside within infected cells for many years. HIV-1 preferentially infects CD4<sup>+</sup> T cells and thus results in their gradual depletion over many years of infection. In approximately half of those infected with the virus, an acute mononucleosis-like syndrome develops within 6 weeks of infection (322). During this period there are high levels of viremia and a subsequent detectable immune response to HIV-1 (64, 76). Within 6 months after seroconversion, there is a peak in plasma viral load and a decline in the number of CD4<sup>+</sup> T cells in circulation. This is followed by a period of gradual deterioration of the immune system lasting 6-10 years in patients with typical disease progression. When the CD4<sup>+</sup> T cell count falls below 200 cells/mm<sup>3</sup>, patients are classified as having acquired immunodeficiency syndrome (AIDS). Due to the lack of a fully competent immune system, patients almost surely succumb to opportunistic infections, such as *Pneumocystis carinii* pneumonia, *Toxoplasma gondii*, and Kaposi's sarcoma, within two years of an AIDS diagnosis without antiretroviral treatment (**Figure 2**) (255).



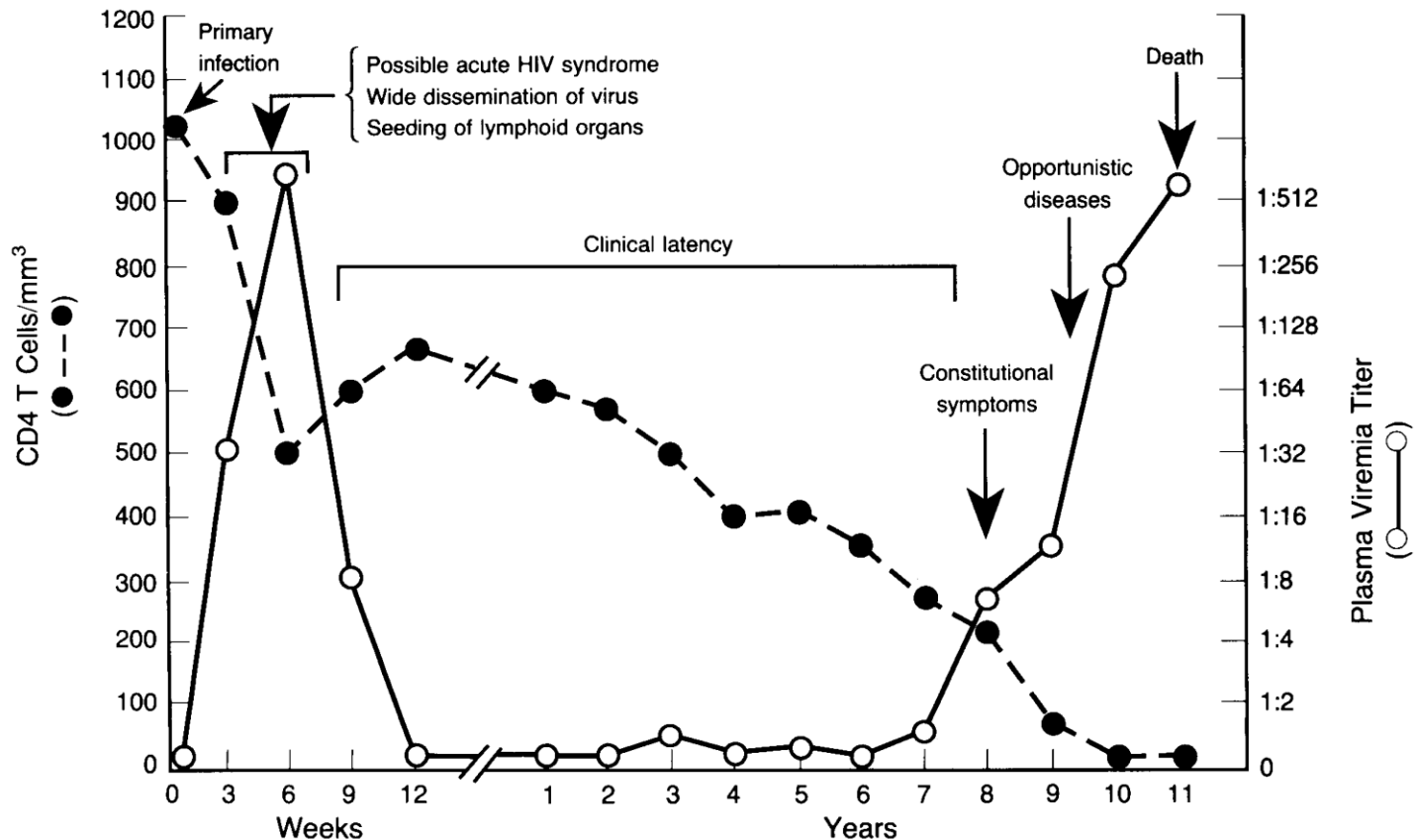


**Figure 2. Typical course of untreated HIV-1 infection**

Acute HIV-1 results in viral dissemination and an almost immediate drop in CD4+ T cells in the blood. Clinical latency is established after ~1 year of infection and is followed by a period of gradual CD4+ T cell decline. Patients are classified as having acquired immunodeficiency syndrome (AIDS) after CD4+ T cells fall below 200 cells/mm<sup>3</sup>. Patients typically succumb to opportunistic infections within 2 years after an AIDS diagnosis. Reproduced with permission from Pantaleo et al. (268) ©1993 Massachusetts Medical Society

### 1.1.3 Genetic evolution

Much of the pathogenesis associated with HIV-1 infection can be attributed to its high rate of genetic evolution. Diversification of the viral repertoire within infected hosts is a hallmark of HIV-1 infection and is thought to be the result of multiple host and viral factors (274). High viral replication rate, error-prone reverse transcription, strong neutralizing antibody responses, and CD8+ cytotoxic T lymphocyte (CTL) selective forces are all thought to contribute to the evolution

and eventual immune escape of HIV-1 within chronically-infected subjects (80, 188, 274, 278, 344).

HIV-1 has extensive intrahost genetic variability that can be observed early after infection (333). The error-prone reverse transcriptase enzyme makes ~0.2 errors per genome replication cycle (34), which results in a substantial number of mutations in the  $\sim 10^{10}$  new virions that are produced each day during untreated infection (4). Positive selection is also a major driving force of viral evolution and has been well characterized in HIV-1 and in SIV models (75, 80, 131, 227, 318). Mutations resulting from positive selection allow the virus to evade host immune responses. Indeed, disease progression is positively correlated with high genetic diversity and divergence and escape from adaptive immune responses, particularly in the *env* gene (149, 201, 307). This persistent variation occurs within hosts and between hosts, thereby complicating prophylactic and therapeutic vaccine efforts. Moreover, the highly mutable nature of this virus leaves it susceptible to drug resistance in individuals on combined antiretroviral therapy (cART) (57). Luckily, in those who do not develop drug resistance, cART reduces viremia to undetectable levels and slows or ceases viral evolution (55, 126).

#### **1.1.4 Combination antiretroviral therapy**

Following the advent of combination antiretroviral therapy (cART) in 1996, HIV-1 infection was reduced from a death sentence to a manageable chronic disease. After 52 weeks of cART, there are significant increases in CD4<sup>+</sup> T cell counts and undetectable levels of plasma HIV-1 RNA (<20 copies/ml) in >50% of patients (234). Prolonged use of cART has enabled

patients to live near-normal life spans without HIV-1 disease progression, but often results in many adverse side effects and/or drug-resistant viral strains.

Increases in several liver enzymes and liver toxicity are observed after long-term use of cART. These HIV-1 medications can lead to anemia, neutropenia, thrombocytopenia, and idiopathic thrombocytopenic purpura (192). Other treatment effects include increases in hyperglycemia and dyslipidemia secondary to insulin resistance and glucose intolerance. Because of this, subjects on cART have an increased risk for type 2 diabetes, cardiovascular disease, and heart attacks (338). When patients fail to adhere to their prescribed dosing regimen or cease treatment altogether, viral replication resumes and drug-resistant mutations arise (98). It was initially proposed that cART would only need to be used for a few years, thus mitigating any potential side effects in favor of HIV-1 eradication. Mathematical models inaccurately predicted HIV-1 eradication from the body within 2-3 years of the start of cART (258). Because latency is established early in infection, resurgence in HIV-1 replication occurs shortly after cessation of cART and presents a mechanism of lifelong viral persistence, even in patients who have been on treatment for many years (61, 109, 110, 221, 340, 352). It is therefore necessary to explore curative approaches that would allow HIV-1-infected patients to live drug- and disease-free.

## **1.2 CTL AND HIV-1 INFECTION**

Cytotoxic T lymphocytes (CTL) are a specialized subset of CD8<sup>+</sup> T cells that enact killer effector functions on cancer cells, damaged cells, or cells infected with pathogens. These cells express a T cell receptor (TCR) that can recognize a specific MHC class I-bound antigen on the target cell (237). CTL are generated from naïve CD8<sup>+</sup> precursors and are the result of priming by

a professional APC, such as a DC. Upon encountering an infected cell, CTL secrete the type-1-associated cytokines IL-2, IFN $\gamma$ , and TNF $\alpha$ , and the cytotoxins granzyme and perforin (237). Part of the dysfunction in chronic HIV-1 infection is that CTL are not effective at eliminating infected cells, thus allowing unchecked viral replication and disease progression (22). An anti-HIV-1 CTL response should recognize the autologous virus with high breadth and magnitude if it is to be successful at eradicating infection (19, 83).

### **1.2.1 CTL in chronic infection**

HIV-1-specific CD8<sup>+</sup> T cell responses are effective at imposing immunological pressure in acute infection, as evidenced by the induction of a large turnover and mutation rate in the virus population (89, 313, 336). Depletion of CD8<sup>+</sup> T cells in the non-human primate model results in enhanced disease progression, thus supporting the protective role of these cells (299). Long term control of both HIV-1 and simian immunodeficiency virus (SIV) infections is associated with a broad and high magnitude CTL response (253, 289), particularly to Gag epitopes (33, 179, 285). However, the failure of CD8<sup>+</sup> cytotoxic T lymphocytes (CTL) to control virus in chronic infection results in progression to AIDS and can be attributed to several factors. Viral evolution, specifically in CTL epitopes, can impede its recognition by naïve and memory CD8<sup>+</sup> T cells, resulting in a limited repertoire of T cell-mediated immune responses against the mutated region (6, 7, 19, 22, 30, 134-137, 145).

The breadth and magnitude of CD8<sup>+</sup> T cell responses are thought to be critical indicators in the control of HIV-1 infection as well as prevention of AIDS (19, 83). Therefore, the induction of strong and broadly reactive memory CTL responses is believed to be necessary to respond to the diverse viral sequences generated during the course of infection. Indeed, the failure of the STEP

prophylactic vaccine trial has been linked in part to induction of limited CTL responses and failure to cross-react with circulating viral strains (25, 73). There is also a correlation between the larger number of T cell responses targeting different SIV proteins and control of viral load in non-human primates (204, 277). Strong cellular HIV-1-specific responses are thought to contribute to long term viral control in long term nonprogressors, a subset of HIV-1-infected individuals who maintain plasma viral loads below 50 copies/ml and live >10 years without developing AIDS (24). Understanding CD8<sup>+</sup> T cell failure and the mechanisms underlying successful control in HIV-1 infection are therefore paramount for the design of successful therapeutic strategies.

### **1.2.2 Barriers to CTL-mediated viral clearance**

Several hypotheses have emerged to explain the failure of CTL generated during natural infection to eradicate virally-infected cells, despite displaying a polyfunctional phenotype associated with cytolytic activity (155). The propensity of HIV-1 to undergo mutations that eventually lead to CTL escape is undoubtedly a primary mechanism by which the virus persists (58, 165). More recently, however, other mechanisms have been described. Alterations in T cell homeostasis and prolonged antigenemia promote an environment of chronic immune activation that disrupts the generation and effector function of HIV-1-specific CTL in progressive infection (17, 91, 146, 366). Additionally, perturbations in regulatory T cells (T<sub>reg</sub>) lead to alterations in homeostasis and can result in the suppression of HIV-1-specific responses (14, 21, 112, 164, 243, 302, 314). In concert, these three factors heavily contribute to the demise of CTL control in chronic infection and eventual progression to AIDS.

### **1.2.2.1 Escape**

An undisputed mechanism by which HIV-1 evades host recognition in chronic infection is the rapid rate at which the virus evolves. Mutations in CTL epitopes can alter peptide:MHC affinity and could consequently ablate T cell recognition of the mutated epitope (58, 165). Mechanisms promoting the establishment of escape mutations and thus evasion of clearance of HIV-1-infected cells by CTL include interaction defects between a viral epitope and its cognate MHC class I molecule or between an MHC class I molecule/epitope complex and its T cell receptor (TCR) (202) and impairment at the level of epitope processing (7, 93, 360). Disease progression has been shown to be positively associated with synonymous HIV-1 substitution rates and high HIV-1 genetic diversity (149, 201). There is a temporal association between *env* divergence and diversity and progression to AIDS, as well as the emergence of CXCR4-tropic viral strains in chronically infected individuals (307). These observations underscore the role of viral evolution on HIV-1 disease progression. It is therefore imperative to overcome these complications of natural infection in order to design HIV-1 vaccines capable of eliciting antiviral immunity targeting the diverse viral strains in infected individuals.

### **1.2.2.2 Regulatory mechanisms**

Alterations in T cell homeostasis during chronic infection largely impact the naïve subset and partially result from decreases in thymic output (17, 91, 366). Progressive infection is also accompanied by decreases in the naïve CD8<sup>+</sup> T cell subset despite increases in total CD8<sup>+</sup> T cells (284). These perturbations in the naïve CD8<sup>+</sup> T cell repertoire could reduce the number and likelihood of mutated epitopes being recognized. Additionally, HIV-1 infection is accompanied by a progressive decrease in CD4<sup>+</sup> T cells, of which a subpopulation is capable of suppressing immune responses and promoting tolerance in healthy states and in a variety of disease models

(191, 291). As HIV-1 is a disease of chronic immune activation, an increase or decrease in these regulatory T cells ( $T_{reg}$ ) could be beneficial to the virus. An increase leading to more suppression of anti-HIV-1 CTL responses and a decrease leading to enhanced immune activation.

Reports on the perturbations in these regulatory T cells ( $T_{reg}$ ) during chronic HIV-1 infection have been variable, with most showing an increase in the frequency of  $T_{reg}$  with disease progression and/or overall  $CD4^+$  T cell depletion (14, 21, 112, 164, 243, 302, 314). These cells have also been implicated in HIV-1 pathogenesis and disease progression (59, 212). In subjects receiving successful combination antiretroviral therapy (cART),  $T_{reg}$  levels return to those seen in uninfected subjects (39, 235, 302), suggesting any effects imposed by  $T_{reg}$  during untreated infection should be mitigated during cART. Interestingly,  $T_{reg}$  also suppress HIV-1-specific T cell responses following DC immunotherapy in subjects on cART (213), highlighting their role in suppressing existing  $CD8^+$  T cell responses and those generated *de novo* under suppressive cART.

### **1.2.2.3 Immune activation and exhaustion**

HIV-1 primarily infects  $CD4^+$  T cells, thus resulting in the gradual decline of these cells in the blood of infected individuals (106). However, cellular apoptosis in infected individuals is not specific to infected  $CD4^+$  T cells and is observed in other cells types (108, 229). A large body of evidence has pointed to chronic immune activation as a driving force in the failure of HIV-1-specific immunity to control virus in chronic infection (146). This activation, subsequent to prolonged antigenemia, affects multiple cells in the innate and adaptive arms of the immune system (230) and results in continuous activation of naïve  $CD4^+$  and  $CD8^+$  T cells and the eventual depletion of these subsets. The generation of new, primary CTL against late-evolving virus is therefore difficult to achieve and results in a CTL population that is unable to eradicate HIV-1 in progressive infection (92, 136, 284).

More recently, the upregulation of inhibitory receptors such as programmed death-1 (PD-1), CTLA-4, and Tim-3 has been shown to result from continued immune activation. The downstream effects of these markers may interfere with the generation of new CTL or the function of existing recall CTL (79, 173, 323). Indeed, the persistent activation that induces expression of these markers has detrimental effects on CD4<sup>+</sup> (142, 143, 226, 361) and CD8<sup>+</sup> (53, 231, 331) HIV-1-specific immunity. Potential therapies aimed at inducing CTL *de novo* or enhancing the exiting, dysfunctional CD8<sup>+</sup> T cell response should take this exhaustion into consideration.

### 1.3 DENDRITIC CELLS AND HIV-1 INFECTION

Dendritic cells (DC) are the most potent antigen-presenting cells (APC) and are lauded as being the sentinels of infection. These cells respond to invading pathogens and coordinate the innate and adaptive arms of the immune system (326). Upon encountering a pathogen, immature, undifferentiated DC (iDC) undergo a maturation to become professional mature APC. This maturation is accompanied by the secretion of cytokines in accordance with the type of immune cells that need to be attracted to combat the residing pathogen (266, 317). Optimal priming of CD8<sup>+</sup> T cells requires maturation of DC with a type-1-polarizing cocktail containing IFN $\gamma$ . This maturation protocol generates IL-12p70-producing DC with increased expression of activation and costimulatory molecules (104). These factors are involved in activation of memory antigen-specific CD8<sup>+</sup> T cell memory responses and are likely involved in priming of CD8<sup>+</sup> T cells (273). These *in vitro*, T cell memory and priming models represent a promising approach to generate potent CD8<sup>+</sup> T cell-driven immunotherapeutic approaches (69, 219).



### 1.3.1 Impact of chronic HIV-1 infection on DC function

There is the potential for HIV-1 infection of DC by both CXCR4- and CCR5-tropic strains, with the virus replicating more efficiently in immature than mature DC (264). Additionally, DC in untreated infection are circulating in a semi-mature state (88) and are more likely to induce T<sub>reg</sub> that can suppress anti-HIV-1 responses (190). Luckily, DC are not major reservoirs for HIV-1 infection during cART (250). While many aspects of the immune system become dysfunctional in chronic HIV-1 infection and remain dysfunctional after treatment, myeloid DC retain the ability to process and present antigen (68) and stimulate HIV-1-specific IFN- $\gamma$  production in CD8<sup>+</sup> (105, 156, 158) and CD4<sup>+</sup> T cells (240). Although monocytes can be infected with HIV-1 *in vivo*, functional monocyte-derived DC can be generated from HIV-1-infected patients on cART (70). These DC also secrete high levels of the Th-1-stimulating cytokine IL-12p70 if treated with CD40L and IFN- $\gamma$  or the  $\alpha$ DC1 maturation cocktail (104, 156). These findings therefore support the functional integrity of DC in HIV-1-infected persons on cART and underscore their potential usefulness in immunotherapy.

### 1.3.2 DC as an immunotherapy in subjects on cART

We and others propose that the afferent arm of the CTL response can be induced by autologous dendritic cells (DC) (119, 248, 280, 334, 337), the most potent antigen presenting cells (APC), which are capable of enhancing the breadth, magnitude, and polyfunctionality of the efferent arm, i.e., HIV-1-specific memory and naïve T cell responses (67, 155-157, 211). A key issue in this approach is how these DC are educated *in vitro* to result in the greatest breadth and magnitude of anti-HIV-1 T cell reactivity after they are given *in vivo*. During cART, myeloid DC

obtained from blood monocytes and matured with mixtures of different cytokines and T cell co-stimulatory molecules retain their capacity to process and present antigen (68, 295) and stimulate HIV-1-specific IFN- $\gamma$  production in CD8<sup>+</sup> (105, 156, 158) and CD4<sup>+</sup> T cells (240). In particular, we have shown that subjects on cART secrete high levels of IL-12p70 if treated with CD40L and IFN- $\gamma$  or the  $\alpha$ DC1 maturation cocktail that is being used in cancer immunotherapy trials (104, 156). We have also shown the generation of broadly reactive and polyfunctional primary CD8<sup>+</sup> T cell responses from HIV-1 naïve adults against HIV-1 and other viral epitopes (67).

Several different methods have been proposed to enhance immune responses in persons on cART, of which the methods and principles have been extensively reviewed elsewhere (119, 180, 212, 280, 292, 337). These methods include cytokine-based therapies, specifically administration of IL-2, IFN- $\alpha$ , and IL-7; blockade of inhibitory molecules such as PD-1/PD-1L or inhibition of regulatory T cells; and induction of HIV-1-specific responses via therapeutic vaccination. The most promising of these strategies is therapeutic vaccination using autologous, myeloid-derived DC that promote effective cell-mediated antiviral immunity against the autologous HIV-1 reservoir. The goal of this approach is to induce CD4<sup>+</sup> and CD8<sup>+</sup> cytotoxic T cell (CTL) responses against the autologous HIV-1 reservoir. Because DC induce T cell immunity in response to microbial pathogens (326), they are an attractive tool for creating effective, long-lasting immunity in viral infections and cancer. Indeed, this method was first explored in patients with B cell lymphoma (152), and recent clinical trials have shown promising results in cancer patients using autologous, myeloid-derived DC loaded with tumor antigens (100, 249, 315).

Several clinical trials have explored the use of DC in HIV-1 immunotherapy and have reported varying levels of success. There are several approaches and methodologies that can be implemented in a DC therapeutic vaccine, of which some are outlined in **Table 1**. Connolly et al.

showed a transient increase in HIV-1-specific IFN- $\gamma$  production by T cells following DC vaccination (70), while Lu et al. reported decreases in plasma HIV-1 viremia that correlated with IL-2 and IFN $\gamma$  production by HIV-1-specific CD4<sup>+</sup> T cells (210). More recently, García et al. reported inverse correlations between the change in post-vaccination viral load and the increase in HIV-1-specific T cell responses (116), and in a separate study saw significant decreases in plasma viral load that were associated with increases in HIV-1-specific T cell responses (117). DC electroporated with mRNA encoding Tat, Rev, and Nef were used to vaccinate 17 HIV-1 infected patients on cART and, following treatment interruption, 6/17 patients remained off drug therapy (5). Additionally, Van Gulck et al. showed an increase in the breadth and magnitude of HIV-1-specific IFN $\gamma$  production following DC vaccination of 6 subjects on cART (335). Despite these promising results, long-lasting control of HIV-1 replication remains elusive.

**Table 1. Factors involved in the generation of a dendritic cell immunotherapy for HIV-1**

<b>DC immunotherapy (immunovaccine) for HIV infection: Major issues</b> (Modified from Rinaldo, J Intern Med 2009)	
<b>Type of DC</b>	<ul style="list-style-type: none"> <li>• Myeloid MDDC, plasmacytoid DC</li> <li>• Langerhans cells, interstitial myeloid DC</li> </ul>
<b>Type of T cell</b>	<ul style="list-style-type: none"> <li>• Naïve CD4<sup>+</sup>, CD8<sup>+</sup></li> <li>• Memory CD4<sup>+</sup>, CD8<sup>+</sup></li> </ul>
<b>DC maturation, processing and migration</b>	<ul style="list-style-type: none"> <li>• Toll-like receptor agonists</li> <li>• CD40L, Cytokines IFN<math>\gamma</math>, TNF<math>\beta</math>, IFN<math>\alpha</math>, IL-1<math>\beta</math></li> <li>• PGE2</li> <li>• C-type lectins (DEC 205, DC-SIGN)</li> </ul>
<b>Immunovaccine delivery</b>	<ul style="list-style-type: none"> <li>• IV, SC, ID, intranodal, intralymphatic</li> <li>• Dose and treatment intervals</li> </ul>
<b>DC lifespan</b>	<ul style="list-style-type: none"> <li>• Anti-apoptotic mediators (Bcl-2, Bcl-xL, Akt1, CpG, TRANCE)</li> </ul>
<b>T cell regulation</b>	<ul style="list-style-type: none"> <li>• Regulatory cells: Treg; MDSC</li> <li>• Regulatory molecules: PD-1, LAG-3, Tim-3, CTLA-4, IL-10</li> </ul>
<b>Patient and HIV infection</b>	<ul style="list-style-type: none"> <li>• Initiation and duration of antiviral therapy</li> <li>• HLA, other genetic markers</li> <li>• cART regimen, antiviral effects</li> <li>• Viral immune escape variants</li> </ul>
<b>HIV antigen</b>	<ul style="list-style-type: none"> <li>• Consensus versus autologous strains</li> <li>• Whole inactivated virus; infected apoptotic cells; exosomes</li> <li>• Recombinant proteins; peptides</li> <li>• RNA; DNA</li> <li>• Microbial vectors; VLPs</li> </ul>
<b>Immunologic end-points</b>	<ul style="list-style-type: none"> <li>• Increase killing of HIV-1 infected cells</li> <li>• Increase breadth and magnitude of CTL to Gag, other HIV proteins</li> <li>• Increase in polyfunctional T cells</li> <li>• Normalize T cell numbers and activation levels</li> </ul>
<b>Virologic end-points</b>	<ul style="list-style-type: none"> <li>• Lower viral set-point and viral load</li> <li>• Elimination of virus reservoir</li> </ul>

### 1.3.2.1 Immunotherapy targeting naïve T cells

A major issue in our immunotherapy approach is which subset or subsets of T cells should be targeted for enhancement of antiviral activity by HIV-1 antigen-loaded DC. We propose that DC immunotherapy should target naïve T cell precursors in order to prime CTL *de novo*, and avoid or even inhibit activation of the existing, dysfunctional memory T cell population in an effort to revitalize their CTL function. We have previously proposed that CTL should be primed from naïve precursors, as the endogenous memory T cell population has already failed to control virus prior to cART (280). This is problematic, however, as studies have revealed decreases in the prevalence and function of naïve T cells following HIV-1 infection compared to uninfected controls (17, 91, 145, 364).

Abnormalities in T cell receptor (TCR) diversity and function, including responsiveness to neo-antigens, have also been reported and are reviewed elsewhere (178). It is plausible that naïve T cells present in long term, HIV-1 chronically infected subjects on cART do not have the appropriate TCR repertoire or functional capacity to respond to primary stimulation against autologous HIV-1, or that viral escape has specifically evaded potential recognition by this new repertoire of naïve T cells. Moreover, alterations in T cell homeostasis during chronic, untreated HIV-1 infection largely impact the naïve subset and partially result from decreases in thymic output (17, 91, 366). Under cART, however, there is a progressive restoration of naïve CD4<sup>+</sup> T cells that results in normalization of their frequency in subjects who began treatment with higher baseline CD4<sup>+</sup> T cell counts (>200 cells/μl) (341, 359). Subjects who began treatment with <200 CD4<sup>+</sup> T cells/μl experienced partial restoration in CD4<sup>+</sup> T cell numbers but not normalization of the naïve CD4<sup>+</sup> T cell compartment, suggesting delayed initiation of cART may adversely affect immune reconstitution even in the absence of viral burden (341).

To develop an effective CTL-mediated immunotherapy that would allow reduction or cessation of cART, it is essential to evaluate the effects of untreated HIV-1 infection on the naïve CD8<sup>+</sup> T cell compartment. Progressive HIV-1 infection is accompanied by decreases in the naïve CD8<sup>+</sup> T cell subset despite increases in total CD8<sup>+</sup> T cells (284). Cossarizza et al. assessed CD4<sup>+</sup> and CD8<sup>+</sup> v-beta TCR repertoires in acutely- and chronically-infected subjects pre- and post-cART. Although the naïve CD4<sup>+</sup> compartment was only restored in subjects receiving cART in acute infection, the naïve CD8<sup>+</sup> compartment was restored with cART irrespective of when treatment began (74). These findings suggest naïve CD8<sup>+</sup> T cells in subjects on cART possess the breadth and specificity required to respond to an array of diverse HIV-1 antigens.

Perturbations in the normal distribution of TCRs within the naïve T cell repertoire of untreated HIV-1 infected persons have been noted (71). These alterations lead to TCR clones being both more or less prevalent in HIV-1-infected subjects compared to healthy, uninfected age-matched donors (120, 127). Baum et al. showed that, while HIV-1-infected persons exhibited a 10 fold decrease in TCR repertoire diversity in the blood, the diversity of purified T cell populations was comparable between HIV-1-infected and HIV-uninfected subjects (29). They therefore postulate that changes in TCR repertoire diversity are the result of changes in T cell subpopulations and not the direct result of specific clonal deletion or expansion within the naïve compartment. These findings further underscore the potential efficacy of an immunotherapy aimed to stimulate primary anti-HIV-1 CTL responses from naïve CD8<sup>+</sup> T cell precursors.

While changes in the frequency of naïve T cells may play a role in the generation of an effective immune response, their function in response to neoantigen is of equal importance. Lange et al. evaluated antibody concentrations, lymphocyte proliferation, and delayed-type hypersensitivity responses following tetanus toxoid, diphtheria-toxoid, and key hole limpet

hemocyanin immunization and showed that delayed initiation of cART predicted an impaired response to vaccination, despite partial restoration of CD4<sup>+</sup> T cell numbers (197). Gelinck et al. reported significantly lower concentrations of anti-rabies IgG and IgM following rabies vaccination in HIV-1 infected subjects compared to uninfected donors (122). While both of these studies demonstrated an impaired capacity to generate primary immune responses against neoantigens, they also focused solely on Th2-driven responses mediated primarily by CD4<sup>+</sup> T cells. Although their frequency within the CD4 compartment may be restored if cART is implemented early, the overall number of CD4<sup>+</sup> T cells in many HIV-1-infected subjects does not rebound to normal levels, even after long-term suppressive cART (17, 18, 232, 251, 265).

Dysfunctional naïve CD4<sup>+</sup> T cells may exist in subjects on cART, but immunotherapies for these subjects that induce a CD8<sup>+</sup> T cell-mediated response would mostly need CD4<sup>+</sup> T cell functionality for bystander “help” (31, 44, 279, 301, 327, 328). Additionally, these studies compare HIV-1-infected subjects on cART to uninfected donors, which is difficult when assessing naïve T cell function in response to primary stimulation without accounting for a variety of factors, including HLA type, individual differences in autologous APC, age, comorbidities, and duration of infection. It is more beneficial to look within HIV-1-infected individuals to determine if the proposed immunotherapy generates a response greater than that generated from natural infection. Although the *de novo* response generated in an HIV-1-infected person on cART may not be equivalent to that which is generated in an uninfected person, it may be sufficient for viral clearance.

### **1.3.2.2 Effects of immunotherapy on memory T cells**

A more recent and less-explored consideration is the effect of existing HIV-1-specific memory T cells on the efficacy of a DC immunotherapy that aims to prime CTL from naïve

precursors. Despite their failure to control virus during treatment interruption, HIV-1-specific CD8<sup>+</sup> T cells persist in the blood of subjects on cART. While only a small fraction of PBMC and purified CD8<sup>+</sup> T cells from these subjects secrete IFN- $\gamma$  in response to HIV-1 peptide antigens, DC loaded with these same antigens reveal broad and robust T cell responses (154, 155). Additionally, peptide-loaded DC enhance the percent of T cells that secrete multiple type 1 cytokines and chemokines, including IL-2, IFN $\gamma$ , TNF $\alpha$ , and MIP-1 $\beta$ , and induce translocation of the CD107a LAMP protein to the plasma membrane. Additionally, DC stimulate proliferation of T cells in response to MHC class I-restricted HIV-1 peptide epitopes (155, 157). As the assays used in these studies range from 6-18h, it is highly unlikely that DC are inducing primary responses, but are rather revealing T cell responses that were undetectable with standard assay procedures. These findings show that HIV-1-specific T cells persist during cART and are capable of secreting high levels of type 1 cytokines in response to HIV-1 antigens, yet do not eradicate HIV-1-infected cells. These studies also suggest that these quiescent memory T cells can be awoken with the proper stimulus.

#### **1.4 STATEMENT OF THE PROBLEM**

While cART has reduced HIV-1 infection from a death sentence to a chronic illness, patients must be treated for life and often times suffer adverse side effects from prolonged use of these medications. Additionally, the prohibitive cost of lifelong treatment, especially in resource-limited countries, reduces the adherence to medications and perpetuates HIV-1 spread. It is therefore imperative that we identify the mechanisms by which HIV-1 evades host recognition and that we develop methods of eradicating the latent reservoir in subjects on cART.



We propose that a DC immunotherapy could induce an effective anti-HIV T cell response capable of eliminating the viral reservoir. To test this hypothesis, we first need to determine the effects of DC on T cell responses at all stages of disease progression and then determine if regulatory mechanisms have any impact on the DC-T cell interaction. We then need to determine if naïve and memory T cells from subjects on prolonged cART are capable of responding to a DC immunotherapy. The naïve repertoire may be irreparably damaged or dysfunctional, and the HIV-1-specific memory populations may be too exhausted to respond to this type of therapy.

A barrier to addressing these problems is the lack of longitudinal cohorts in which to evaluate the changes in T cell responses over time. Many subjects in the Multicenter AIDS Cohort Study (MACS) enrolled in the late 1980's and early 1990's, eventually seroconverted to HIV<sup>+</sup> status, received cART, and are still enrolled in the study. We therefore have the unique opportunity to analyze clinical correlates of longitudinal infection and viral evolution and to determine the residual capacity of T cells to respond to a DC immunotherapy after enduring years of chronic infection and cART treatment. In the present study, we chose three subjects from the MACS and examined signatures of HIV-1 *gag* and *env* viral evolution throughout untreated infection. We then used these sequences to identify variants of known and predicted HLA A\*2402-restricted epitopes and evaluated T cell responses to these autologous variants with and without the addition of DC and regulatory T cell depletion. The study culminated by determining the residual capacity of naïve and memory T cells from cART to respond to DC stimulation against the autologous HIV-1 reservoir.

**1.4.1 Specific aim I: describe the clinical correlates and signatures of HIV-1 evolution in chronic, untreated infection**

*Hypothesis:*

*HIV-1 evolution is observed in gag and env and can be correlated with signatures of immunological pressure.*

HIV-1 infection is characterized by increases in viral divergence and diversity. This diversity is thought to contribute to immunologic failure in chronic infection. Viral evolution may be predictive of immune pressure on viral proteins and changes in clinical parameters. These hypotheses are addressed in chapter 2.

**1.4.2 Specific aim II: evaluate the effects of viral evolution on the generation and detection of HIV-1-specific T cell responses**

*Hypothesis:*

*T cell responses to autologous HIV-1 epitope variants are generated in vivo and can be enhanced by DC addition and/or regulatory T cell depletion*

The failure of CTL to control HIV-1 infection may be the result of mutations that ablate T cell epitope recognition. Responses to autologous epitope variants decrease throughout chronic infection, thus suggesting T cells were unable to mount immunity against the dominant variants that evolved. Responses against these variants may have been generated *in vivo*, but are suppressed

by regulatory T cells or need additional stimulation by DC to be detected or mediate a clinically beneficial anti-HIV-1 response. These hypotheses are addressed in chapters 3, 4, and 5.

**1.4.3 Specific aim III: determine the residual capacity of naïve and memory T cells to respond to DC stimulation and eradicate the HIV-1 reservoir in subjects on cART**

*Hypothesis:*

*DC-induced primary HIV-1-specific T cells can eliminate autologous HIV-1-infected CD4<sup>+</sup> T cells and do so more efficiently than re-stimulated memory T cells*

Chronic HIV-1 infection induces perturbations in the naïve T cell repertoire and results in a viral quasispecies that evades host recognition. cART reduces viral load to undetectable levels, but removal from treatment results in rebounds in viral load and resumption of disease progression. The breadth and magnitude of the endogenous CTL response is not sufficient to eradicate infection after cART interruption. DC priming of naïve T cells or reconditioning of memory T cells may provide the stimulus needed to generate potent CTL specific for the autologous reservoir. These hypotheses are addressed in chapter 6.

## 2.0 CLINICAL CORRELATES AND SIGNATURES OF SELECTIVE PRESSURE IN HUMAN IMMUNODEFICIENCY VIRUS TYPE-1 GAG AND ENV

HIV-1 evades host recognition by rapidly mutating away from adaptive immune responses. A comprehensive understanding of the evolutionary mechanisms behind mutational escape in two of the key proteins involved in the viral life cycle, Gag and Env, is needed to develop effective immunotherapies for HIV-1-infected persons. We longitudinally evaluated genetic and amino acid evolution of autologous HIV-1 sequences in three untreated subjects in the Multicenter AIDS Cohort Study throughout chronic infection. Single-genome sequencing of *gag* p17-p6 and *env* gp120 was performed at 5 to 6 sequential time points in each subject. The frequency of sites under positive selection increased throughout infection and these sites were found within and adjacent to several known MHC class I-restricted epitopes. Positive selection in *gag* was associated with a decrease in CD4<sup>+</sup> T cells and an increase in CD8<sup>+</sup> T cells, whereas negative selection was associated with these parameters in *env*. While increases in divergence and diversity were not associated with a rise in HIV-1 viral load or CD8<sup>+</sup> T cells, these two evolutionary parameters were strongly correlated with the percent of *gag* and *env* sites under positive selection. The data presented here display differential correlates of genetic evolution in *gag* and *env* with chronic HIV-1 infection and provide novel insight into the effects of evolutionary mechanisms on protein and epitope evolution. These findings are important for understanding the natural evolution of HIV-1 infection and for development of prophylactic and therapeutic vaccines.

HIV-1 *gag* and *env* sequencing and the generation of phylogenetic trees were performed by our collaborators in the laboratory of Dr. Jim Mullins at the University of Washington. I performed all the remaining data analyses and statistical computations discussed in this chapter.

## 2.1 BACKGROUND

Human immunodeficiency virus type-1 (HIV-1) is known to rapidly mutate and evolve in the absence of combination antiretroviral therapy (cART). Diversification of the viral repertoire within infected hosts is a hallmark of HIV-1 infection and is thought to be the result of multiple host and viral factors. High viral replication rate, error-prone reverse transcription, strong neutralizing antibody responses, and CD8<sup>+</sup> cytotoxic T lymphocyte (CTL) selective forces are all thought to contribute to the evolution and eventual immune escape of HIV-1 within chronically-infected subjects (188, 261, 274, 278, 344). HIV-1 infection is also associated with a progressive increase in the percent of CD8<sup>+</sup> T cells circulating in peripheral blood, presumably due to chronic immune activation, antigenic stimulation, and generation of CTL responses against the Gag proteins (135, 139). Antibody and CD4<sup>+</sup> T cell-mediated helper responses, however, are predominantly formed against Env (90). To date, the correlates of viral evolution and escape from these adaptive host responses are not fully understood.

Phylogenetic studies of acute infection have provided an understanding of early evolutionary events. The observation that a single viral variant establishes infection, despite the subject being exposed to a pool of variants, has implications in the design of prophylactic vaccines (2, 23, 84, 114, 128, 138, 147, 174, 176, 199, 270, 282, 293, 307, 348). The results of studies evaluating evolution within chronically infected subjects, however, could be useful in the design of therapeutic vaccines, as clinical and virologic parameters during untreated HIV-1 infection can be predictors of disease outcome (228), cART treatment success (99, 103, 118, 134, 222, 353), and could potentially be predictors of a successful immunotherapy response. Several studies have described the evolution of the *env* gene in natural HIV-1 infection, but many have failed to compare this evolution to the more conserved *gag*. Understanding *gag* evolution is important

because protective CTL responses have been shown to target regions of the Gag protein (32, 179, 285), whereas T cell responses to Env are associated with higher viral load (179). Delineating the role of HIV-1 evolution in escape from adaptive immune responses, particularly CTL escape, is crucial in efforts to develop an effective immunotherapy against the autologous virus within infected subjects on cART (280).

Divergence from a common ancestor and intrahost diversity are the classical indicators of viral evolution, whereas the ratio of non-synonymous to synonymous mutations (dN/dS) is often a marker of directional selective pressures (125, 283). Several studies have attempted to associate these evolutionary parameters with clinical outcomes. Disease progression has been shown to be positively associated with synonymous HIV-1 substitution rates and high HIV-1 genetic diversity (149, 201). We previously published a study of 9 HIV-1 infected men who have sex with men (MSM) describing changes in T cell subsets and divergence and diversity of the C2-V5 region of the envelope (*env*) gene throughout 6 to 12 years of untreated infection (307). This study identified a temporal association between divergence and diversity and the progression to AIDS, as well as the emergence of CXCR4-tropic viral strains.

In the present study, we longitudinally evaluated the diverse *gag* and *env* quasispecies in 3 HIV-1 infected subjects from the Multicenter AIDS Cohort Study (MACS). We assessed divergence and diversity throughout infection and identified potential clinical correlates of viral evolution. To ascertain the mechanisms behind this evolution, we analyzed the cognate protein sequences for evidence of immune selective pressures within and outside of CTL epitopes. The data presented here provide a novel, in-depth analysis of natural HIV-1 evolution in the absence of cART. These data support an increased role for selective forces in the evolution of conserved and variable HIV-1 genes and have novel implications for therapeutic vaccine development.

## 2.2 METHODS

### 2.2.1 Study participants

Three HIV-1 infected subjects were chosen from the MACS, a natural history study of men who have sex with men (MSM) for which the methodologies have been described previously (159, 171). Human subject approval was obtained from the University of Pittsburgh Institutional Review Board. These subjects were chosen based on their prolonged enrollment in the study (>10 years), typical course of disease progression, favorable response to combination antiretroviral therapy (cART), and the presence of at least one common HLA allele. HLA A, B, and DR genotypes of each subject were determined by high resolution PCR genotyping (Tissue Typing Laboratory, University of Pittsburgh Medical Center). The HLA type of each subject is shown in **Table 3**. All three subjects were enrolled in the MACS prior to seroconversion to HIV-1. Seropositivity was confirmed by positive enzyme-linked immunosorbent assay (ELISA) for the presence of HIV-1 p24 and a Western blot with bands corresponding to at least two of the Gag, Pol, and Env proteins (171). Blood specimens and epidemiological and clinical data were collected at each visit, as described previously (307). All three subjects progressed to AIDS as defined by the CDC ( $<200$  CD4<sup>+</sup> T cells/mm<sup>3</sup>) within 8.3 years after seroconversion. All three subjects received combination ART and maintained plasma HIV-1 RNA below 20 copies/ml at most post-ART visits.

### 2.2.2 Clinical and virologic characteristics

At each biannual visit, plasma samples and peripheral blood mononuclear cells (PBMC) were collected from the study subjects and were stored at -80°C and -140°C, respectively, as described previously (159, 171). T cell phenotypes were determined by flow cytometry as previously described (123, 298). HIV-1 plasma viremia was determined by extracting RNA using a COBAS® Ampliprep Instrument (Roche Diagnostics, Indianapolis, IN) and performing RT-PCR on a COBAS® Taqman® 48 Analyzer (Roche Diagnostics) using the COBAS® Ampliprep/COBAS® Taqman® HIV-1 test. This assay is capable of detecting 20 to 10<sup>6</sup> HIV-1 RNA copies/ml of plasma. Negative, low positive, and high positive controls were used in each extraction and amplification per the manufacturer's instructions.

### 2.2.3 HIV-1 *gag* and *env-gp120* sequencing

Five post-seroconversion time points for S2 and S8 and six post-seroconversion time points for S3 were chosen for HIV-1 *gag* p17-p6 and *env* gp120 sequencing. Viral RNA was manually extracted from plasma using a viral RNA mini kit (Qiagen, Valencia, CA). cDNA synthesis was performed using Nef3 (TAAGTCATTGGTCTTAAAGGTACC) and RT2 (GTATGTCATTGACAGTCCAGC) primers with SuperScript III Reverse Transcriptase (200 U/ml; Invitrogen, Carlsbad, CA). Endpoint dilution methodology was used prior to viral gene amplification to avoid template resampling. Multiplex first-round PCR was performed with the Gag1 (GAGGCTAGAAGGAGAGAGATGG) and RT2 primers to amplify *gag* and the Ed3 (TTAGGCATCTCCTATGGCAGGAAGAAGCGG) and Nef3 (TAAGTCATTGGTCTTAAAGGTACC) primers to amplify *env-gp120*. Singleplex second



round PCR was performed with Gag2 (GTGCGAGAGCGTCGGTATTAAGCG) and RSP15R (CAATTCCCCCTATCATTTTTGGTTTCC) primers for *gag* and Gp120 forward (GGCCGCGTCGACAAGAGCAGAAGACAGTGGCAATGA) and reverse (GGCCGCGGATCCGTGCTTCCTGCTGCTCCCAAGAAC) primers for *env*. PCR products were run on a QIAxcel automated electrophoresis system (Qiagen, Valencia, CA) and Sanger sequencing was performed on samples with positive bands (High Throughput Genomics Center, Seattle, WA). We obtained 5 to 36 unique *gag* sequences and 9 to 32 unique *env* sequences from each subject at each time point.

#### **2.2.4 Genetic sequence analysis**

Nucleotide sequences were aligned with MUSCLE (203, 309) in SeaView, version 4.4. (133), and manually codon-edited with CLC sequence viewer, version 6.7.1 (CLC Bio, Aarhus, Denmark). All Env sequences were evaluated for CCR5 and CXCR4 coreceptor specificity using the position-specific site matrix (PSSM) web tool (163) (<http://indra.mullins.microbiol.washington.edu/webpssm>). Viral divergence from the most recent common ancestor (MRCA) and pairwise diversity were determined using the general time reversible model of substitution (GTR) and an HXB2 sequence as the outgroup within the DIVEIN web tool (86, 196). Phylogenetic trees were constructed with BEAST 1.7.4 (96) using the time of sequence sampling to estimate evolutionary rates throughout the tree. Each sample used the GTR with gamma substitution model and assumed a random-clock model. MCMC chains were run for 30 million generations and manually examined in tracer to ensure thorough mixing. Trees were edited using FigTree, version 1.3.1 (<http://tree.bio.ed.ac.uk/software/figtree/>). Four subtype reference sequences from HIV-1 subtype B were used as outgroup sequences and were obtained

from the Los Alamos Database. Reference numbers for these outgroup sequences are: Ref.B.FR.83.HXB2\_LAI\_IIIB\_BRU.K03455, Ref.B.NL.00.671\_00T36.AY423387, Ref.B.TH.90.BK132.AY173951, and Ref.B.US.98.1058\_11.AY331295 (<http://www.hiv.lanl.gov/content/sequence/NEWALIGN/align.html>). Potential N-linked glycosylation sites (PNGS) in Env were predicted using N-GLYCOSITE (365).

### 2.2.5 Identification of sites under selection

*Gag* and *env* codon alignments were evaluated at each time point for evidence of positive and negative diversifying selection. In positive selection, nonsynonymous mutations that infer an adaptive benefit are selected for at a greater rate than neutral or synonymous mutations. In negative selection,  $dN/dS$  is abnormally low and usually at or close to zero (125, 283). To estimate the rate of positive and negative selection, we used the fixed-effects likelihood (FEL) method with the GTR substitution model (196) in HyPhy as described previously (147). Sites with  $dN/dS$  ( $\omega$ ) of  $>1$  and  $P < 0.1$  were considered to be under positive selection, whereas sites with  $\omega$  of  $<0.2$  and  $P < 0.1$  were considered to be under negative selection. Codons corresponding to the variable loops of *env* were removed for selection analyses to avoid false identification of sites under positive selection.

To determine neutrality of viral evolution, Tajima's  $D$  (316) and the  $D^*$  of Fu and Li (113) were calculated for *gag* and *env* at each time point using the DnaSP software package (203) and using the heuristic assumption of free recombination among genes (309) and no recombination within them.

To identify sites under directional selective pressure, HIV-1 *gag* and *env* nucleotide sequences were first translated to amino acids using the ExPasy Bioinformatics Resource Portal

Translate Tool (16). Sequences coding for early stop mutations were excluded from protein sequence analysis and the variable loops in Env were removed for selection analyses due to the inability to assign homology. We determined the rate and number of sites under directional selection for each subject at each time point using the directional evolution of protein sequences (DEPS) method (<http://www.datamonkey.org>) (187).

### 2.2.6 Protein sequence and epitope analysis

Predicted N-linked glycosylation sites in Env were identified using the N-Glycosite web tool:

(<http://www.hiv.lanl.gov/content/sequence/GLYCOSITE/glycosite.html>) (365).

Phylogenetically informative sites were identified using the InSites approach (<http://indra.mullins.microbiol.washington.edu/DIVEIN/insites.html>) on the DIVEIN web tool (86). This tool functions by omitting mutations that only occur once and are therefore possibly introduced by polymerase errors during PCR.

Changes in the number of predicted MHC class I epitopes were evaluated using netMHCpan version 2.8 (151, 241) and SYFPEITHI (275), whereas changes in MHC class II epitopes were evaluated using netMHCIIpan version 3.0 (170). Peptide sequences with a predicted  $IC_{50}$  of less than 500 nM or 9mer sequences containing at least one preferred anchor residue were considered “predicted epitopes”. A combined predictor was also used to identify potential MHC class I-restricted epitopes. This algorithm combines proteasomal cleavage, TAP transport, and MHC class I affinity to produce a score for each peptide designating its potential of being a class I epitope (<http://tools.immuneepitope.org/processing/>). Peptide sequences with an overall score

greater than -2.0 were considered “predicted epitopes”. NetChop version 3.1 (242) was used to identify potential sites of proteasomal cleavage.

### **2.2.7 Statistics**

Spearman correlations were calculated to determine the association between CD4<sup>+</sup> T cell number and viral load, CD8<sup>+</sup> T cell number and viral load, as well as divergence and diversity correlations with viral load, CD4<sup>+</sup>T cell number, and CD8<sup>+</sup> T cell number. Linear regression was performed to identify the association between disease progression/years post-seroconversion and divergence, diversity, and sites under positive selection. Two-way ANOVA with Bonferroni multiple comparisons post-test was used to determine significant differences within subjects at each time point. All statistics were computed using GraphPad Prism 5 (GraphPad Software, Inc., La Jolla, CA) and were calculated with an  $\alpha$  of 0.05.

## **2.3 RESULTS**

### **2.3.1 Clinical characteristics in chronic, untreated HIV-1 infection**

In the present study, three HIV-1 infected subjects from the Multicenter AIDS Cohort Study (MACS) were chosen for longitudinal analysis. These subjects were chosen based on their prolonged enrollment in the study (>10 years), typical course of disease progression, and the presence of at least one common HLA allele. For each subject (designated as S2, S3 and S8), HIV-1 plasma viral loads and CD4<sup>+</sup> and CD8<sup>+</sup> T cell counts were determined biannually for >10 years

post-seroconversion (**Figure 3A**). All three subjects progressed to AIDS ( $<200$  CD4<sup>+</sup> T cells/ $\mu$ l) between 7.0 and 8.25 years after infection and subsequently received and responded favorably to combination antiretroviral therapy (cART). S8 was not infected with HIV-1 until 1992, hence he was administered cART earlier in his disease progression compared to S2 and S3, who were infected in 1987 and 1988, respectively, and received cART in 1996.

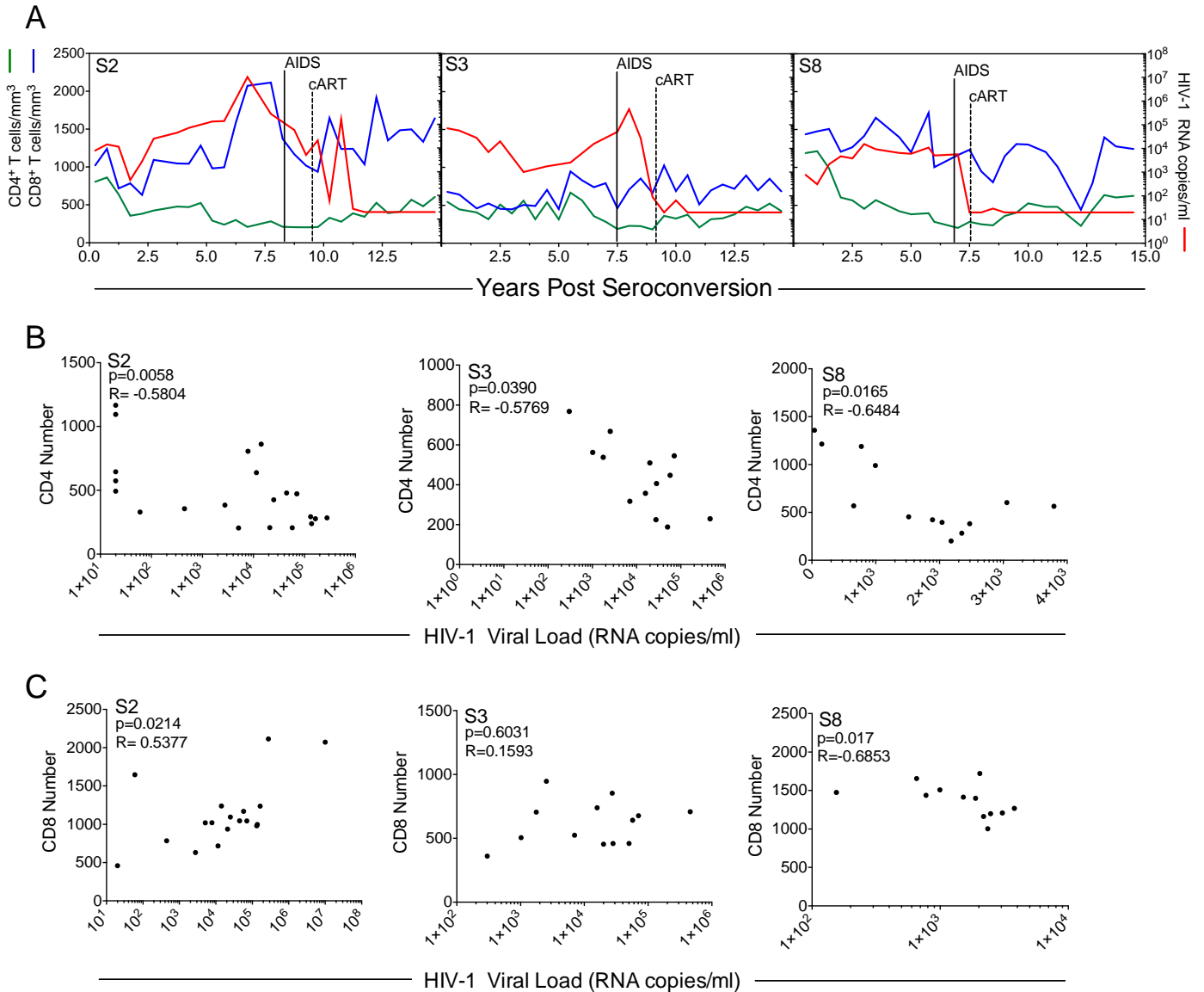


**Figure 3. Clinical and virologic data**

HIV-1 plasma RNA and CD4<sup>+</sup> and CD8<sup>+</sup> T cell counts were determined biannually for the three study subjects. (A) CD4<sup>+</sup> (green line) and CD8<sup>+</sup> (blue line) T cell counts and viral load (red line) are shown longitudinally for S2, S3, and S8. All three subjects progressed to AIDS (CD4<sup>+</sup> T cell count below 200 cells/ $\mu$ l) and received

antiretroviral therapy (ART, dotted line). Autologous Gag and Env sequences were obtained from multiple time points that spanned >6.5 years post-seroconversion (shaded region). Pre-ART (B) CD4<sup>+</sup> T cell number and (C) CD8<sup>+</sup> T cell number are shown as functions of viral load.

We observed an inversion of the CD4:CD8 T cell ratio following infection, albeit at varying degrees in each subject. The lowest ratio observed in S2 was 0.10, compared to 0.27 and 0.17 in S3 and S8, respectively. We also observed the steepest increase to peak viremia in S2, averaging an increase of 787,665 copies/ml per year. This was significantly greater than the rates to peak viremia observed in S3 (21,304 copies/ml per year) and S8 (908 copies/ml per year) ( $p=0.019$ ). Despite a gradual decline in CD4<sup>+</sup> T cell number to <200 cells/ $\mu$ l and an inversion in the CD4:CD8 ratio, S8 maintained relatively low viremia, reaching a peak of 15,456 copies/ml. This therefore demonstrated typical disease progression accompanied by atypical HIV-1 viral load. Interestingly, while S8 maintained the highest CD4<sup>+</sup> T cell count of the three subjects evaluated, he also experienced the most drastic reduction in T cell number, dropping 76% from 1,189 CD4<sup>+</sup> T cells/ $\text{mm}^3$  at his first post-seroconversion visit to 283 CD4<sup>+</sup> T cells/ $\text{mm}^3$  at his last pre-ART visit.

We next examined CD4<sup>+</sup> T cell counts as a function of viral load to determine if HIV-1 viremia was a predictor of CD4<sup>+</sup> T cell number within infected individuals before administration of cART. As expected, we saw significant negative correlations between these two parameters in all 3 subjects (**Figure 3B**). We additionally expected to see positive correlations between viral load and CD8<sup>+</sup> T cell number, which would suggest increased level of viral antigen led to CD8<sup>+</sup> T cell expansion, but observed this correlation only in subject S2 ( $p=0.0214$ ,  $R=-0.5377$ ). Interestingly, subject S8 displayed a negative correlation between CD8<sup>+</sup> T cell numbers and viral load ( $p=0.017$ ,  $R=-0.6853$ ) (**Figure 3C**). Only S3 showed a negative correlation between CD4<sup>+</sup> and CD8<sup>+</sup> T cell number (data not shown). When T cell and viral load data from all subjects were combined, viral load was negatively correlated with CD4<sup>+</sup> T cell number ( $p<0.0001$ ). No

association was seen between CD8<sup>+</sup> T cell number and viral load or between CD4<sup>+</sup> and CD8<sup>+</sup> T cell number when the subjects were combined (data not shown).

Taken together, these data demonstrate varying correlates of disease progression in each subject. Despite progression to AIDS, each subject had unique patterns of CD4<sup>+</sup> T cell depletion, CD8<sup>+</sup> T cell expansion, and increases in HIV-1 viral load. Moreover, these data show that high levels of viral antigen may directly contribute to CD4<sup>+</sup> T cell depletion, but are not sufficient to induce CD8<sup>+</sup> T cell expansion in all subjects. Of note, these findings indicate that raw CD4<sup>+</sup> T cell number may not be the best indicator or correlate of disease progression when comparing individuals, as baseline lymphocyte numbers differ greatly between individuals.

### **2.3.2 Correlates of HIV-1 *gag* and *env* evolution**

Prior studies have documented continuous HIV-1 evolution that produces a pool of unique viral strains, termed quasispecies, in untreated subjects (307, 349). It has yet to be fully determined if stochastic evolutionary processes, selection processes, or a combination of both contribute to viral evolution and disease progression in chronic untreated infection. To identify correlates of quasispecies evolution in our study subjects, we performed single-genome HIV-1 *gag* p17-p6 and *envelope* (*env*) gp120 sequencing on plasma samples from 5 to 6 pre-cART time points for each subject. A total of 325 *gag* and 328 *env* sequences were obtained, with an average of 20 and 21 sequences per time point, respectively. The numbers of *gag* and *env* sequences obtained from each subject at each time point are shown in **Table 2**. Sequencing spanned >6.5 years of untreated HIV-1 infection, with at least one early infection time point per subject that contained viruses predicted by PSSM (163) to primarily use the CCR5 co-receptor, as is expected in acute HIV-1 infection (297).

**Table 2. HIV-1 plasma viral load, T cell count, and number of unique *gag* and *env* sequences obtained from each post-seroconversion time point**

Subject	YPS <sup>a</sup>	HIV-1 Viral Load <sup>b</sup>	No. of Sequences <sup>c</sup>		T Cell Counts (cells/mm <sup>3</sup> )		
			Gag	Env	CD3	CD4	CD8
S2	0.2	7,844	11	13	2,015	806	1,021
	1.2	11,430	12	14	1,340	638	718
	3.4	44,749	20	31	1,525	479	1,046
	5.6	138,153	22	25	1,264	239	997
	9.6	20,926	25	27	1,215	207	937
S3	0.2	70,873	21	20	1,304	545	677
	1.5	28,240	15	11	969	406	459
	2.5	19,992	24	21	936	510	454
	5.3	2,539	27	19	1,670	668	947
	6.4	15,869	36	21	1,162	357	739
	8.3	71,057	27	32	1,117	225	853
S8	0.5	776	14	9	2,616	1,189	1,438
	1.4	2,146	5	13	2,517	990	1,508
	2.4	3,794	28	25	1,961	564	1,268
	5.0	10,897	22	23	1,595	382	1,199
	6.6	5,645	16	24	1,299	283	1,003

<sup>a</sup>Years post-seroconversion

<sup>b</sup>Plasma RNA copies/ml

<sup>c</sup>Number of unique sequences obtained at each time point from HIV-1 *gag* and *env* single genome sequencing

Divergence from the most recent common ancestor (MRCA) was determined for *gag* and *env* at each time point (**Figure 4A**). For ease of interpretation and comparability between subjects, we grouped the time points into the following ranges: 0-1, 1-2, 2-4, 4-6, 6-8, and >8 years post-seroconversion. Overall, the rate at which *gag* diverged from the founding virus differed between the subjects ( $p=0.0011$ ). There was a linear correlation between *gag* divergence and the time post-



seroconversion in S3 ( $p=0.0021$ ,  $r^2=0.9256$ ) and S8 ( $p=0.0253$ ,  $r^2=0.8520$ ). We did not see this correlation in S2. *Gag* divergence in S3 was significantly greater than that of S2 and S8 at each time point tested ( $p<0.0001$  for all). In *env*, divergence was linearly correlated with years post-seroconversion in S2 ( $p=0.0201$ ,  $r^2=0.8725$ ) and S3 ( $p=0.0020$ ,  $r^2=0.9271$ ). *Env* divergence in S8 increased at all time points except 2-4 years post-seroconversion, at which point divergence dropped below that seen 0-1 years post-seroconversion. *Env* divergence in S3 was significantly greater than that of S2 and S8 at all time points except 1-2 years post-seroconversion ( $p<0.0001$  for all), during which time there were no differences in divergence between the subjects. *Env* divergence in S2 was also significantly greater than divergence in S8 2-4 years post-seroconversion ( $p<0.0001$  for all). Although there was an overall positive slope in divergence in S8 throughout disease progression, this association did not reach significance ( $p=0.0518$ ,  $r^2=0.7663$ ).

Although there was an increasing trend in *gag* and *env* divergence as HIV-1 plasma viremia increased, this association did not reach significance when the subjects were combined ( $p=0.0697$  in *gag*,  $p=0.0718$  in *env*), suggesting a limited role of uncontrolled viral replication in inducing divergence (**Figure 4B**). To avoid the issue of having a highly variable dataset when combining raw numbers of CD4<sup>+</sup> and CD8<sup>+</sup> T cells between subjects, we evaluated divergence as a function of the CD4<sup>+</sup> and CD8<sup>+</sup> percent of the total lymphocyte population. Divergence was not due to an expansion or depletion of T cell subsets, as neither the percent of CD4<sup>+</sup> T cells (**Figure 4C**) nor the percent of CD8<sup>+</sup> T cells (**Figure 4D**) in peripheral blood correlated with divergence in *gag* or *env*. Based on these data, we conclude that *gag* and *env* divergence from MRCA is not a linear process in all HIV-1 infected subjects. Furthermore, uncontrolled viral replication alone is not responsible for this divergence, nor is it the cause of changes in CD4<sup>+</sup> and CD8<sup>+</sup> T cell percentages

within infected individuals. These data implicate selective pressures that may be driving HIV-1 evolution and suggest that increases in antigenic variability are not sufficient to induce CD4<sup>+</sup> T cell depletion or CD8<sup>+</sup> T cell expansion.

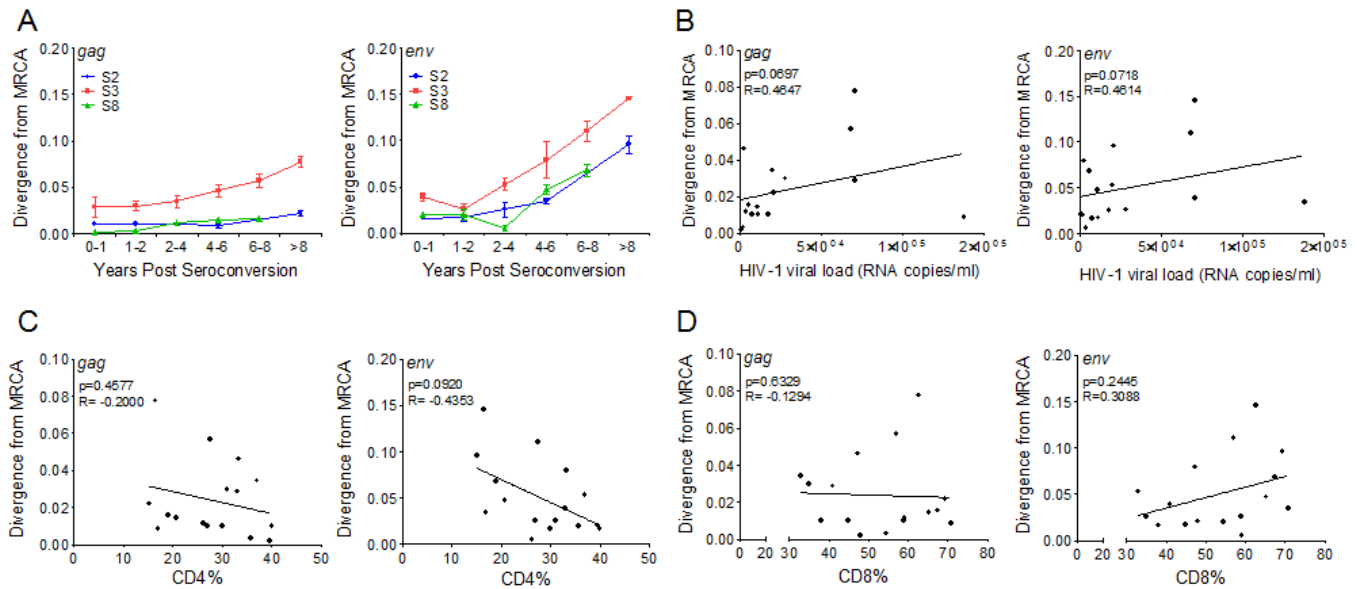


**Figure 4. Correlates of HIV-1 *gag* and *env* divergence**

Divergence from the most recent common ancestor (MRCA) was determined using the general time reversible (GTR) model of substitution with autologous *gag* and *env* sequences from 5 to 6 time points in each subject. (A) Divergence during untreated HIV-1 infection in S2 (blue line), S3 (red line), and S8 (green line). Spearman correlations were performed to evaluate (B) *gag* and *env* divergence as a function of HIV-1 viral load, (C) *gag* and *env* divergence as a function of CD4<sup>+</sup> T cell percent, and (D) *gag* and *env* divergence as a function of CD8<sup>+</sup> T cell percent. Error bars represent the standard deviation of 5 to 36 sequences.

Linear regression analyses showed the rate at which *env* divergence increased throughout infection was greater than that of *gag* in S2 ( $p=0.0091$ ), S3 ( $p=0.0052$ ), and S8 ( $p=0.0317$ ) (Figure 5). Interestingly, there was a decrease in *env* divergence 1-2 and 2-4 years post-seroconversion in subjects S3 and S8, respectively, followed by steady increases in divergence at all remaining time points.

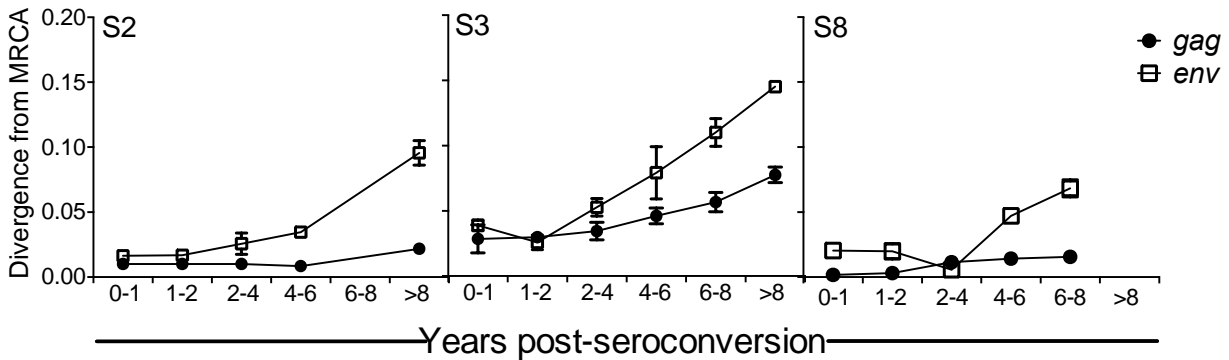


**Figure 5. Comparison of divergence in HIV-1 *gag* and *env***

Divergence from the most recent common ancestor (MRCA) was calculated for the autologous *gag* and *env* sequences obtained from subjects S2 (left panel), S3 (middle panel), and S8 (right panel) at each post-seroconversion time point. Error bars represent the standard deviation of 5 to 36 sequences.

We then evaluated the *gag* and *env* pairwise diversity of the viral quasispecies present within each subject at each time point (**Figure 6A**). There was a significant linear correlation between *gag* diversity and years post-seroconversion in S2 ( $p=0.0074$ ,  $r^2=0.9336$ ) and S8 ( $p=0.0391$ ,  $r^2=0.8046$ ). In S3, however, we observed increases in *gag* diversity through 4-6 years post-seroconversion and then a gradual decrease back to levels observed 0-1 years post-seroconversion, showing no overall correlation with disease progression. Nonetheless, *gag* diversity in S3 was significantly higher than the diversity seen in S8 at all time points and higher than the diversity in S2 at four out of five time points ( $p<0.0001$  for all).

Diversity in *gag* correlated with HIV-1 viral load ( $p=0.0338$ ,  $R=0.5324$ ), whereas this correlation was not observed with *env* diversity (**Figure 6B**). In accordance with our findings with divergence, diversity in neither *gag* nor *env* correlated with the percent of CD4<sup>+</sup> T cells (**Figure 6C**) or the percent of CD8<sup>+</sup> T cells (**Figure 6D**) in peripheral blood.

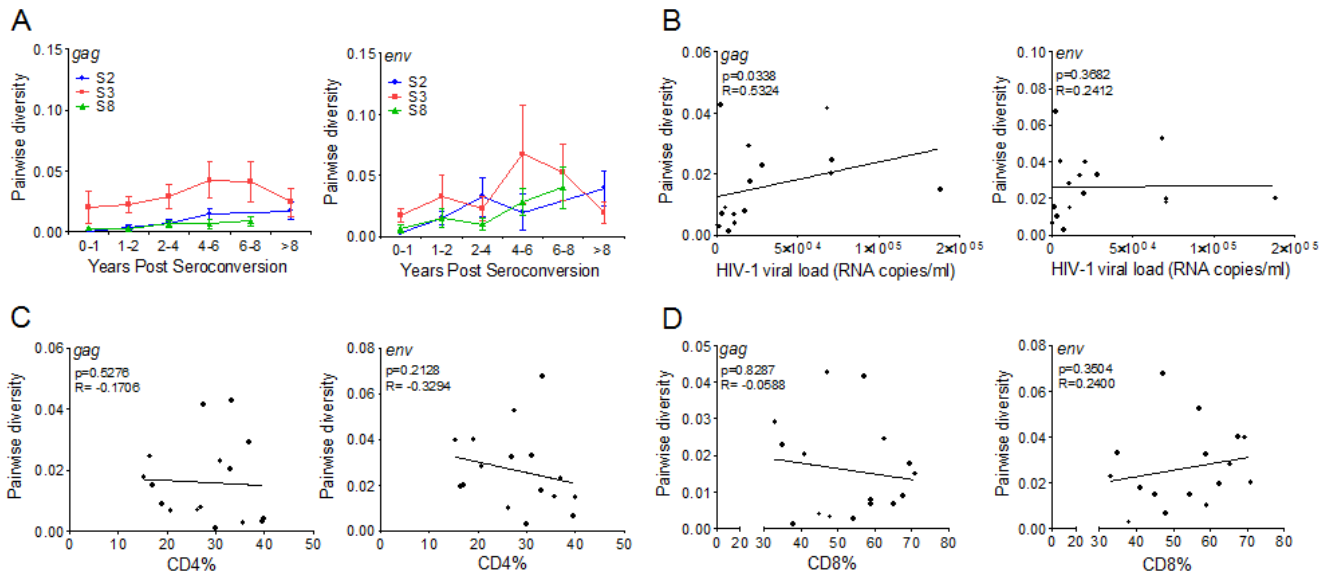


**Figure 6. Correlates of HIV-1 gag and env pairwise diversity**

Pairwise diversity at each time point was calculated using the general time reversible (GTR) model of substitution. This method identifies genetic distances between each sequence in a quasispecies at a particular time point. (A) gag and env pairwise diversity throughout untreated HIV-1 infection in S2 (blue line), S3 (red line), and S8 (green line). Spearman correlations were performed to evaluate (B) gag and env diversity as a function of HIV-1 viral load, (C) gag and env diversity as a function of CD4<sup>+</sup> T cell number, and (D) gag and env diversity as a function of CD8<sup>+</sup> T cell number. Error bars represent the standard deviation of 5 to 36 sequences.

There was a positive linear correlation between env diversity and the time post-seroconversion only in S8 ( $p=0.0095$ ,  $r^2=0.9219$ ). Env diversity in S2 had an overall increasing trend during infection, although this did not reach significance ( $p=0.0769$ ,  $r^2=0.7010$ ). In S3, we saw a similar trend in env diversity as we saw in gag, with diversity increasing and then gradually returning to baseline at >8 years post-seroconversion and no correlation with disease progression. This is not unexpected, as a previous report on env C2-V5 sequence evolution in MACS subjects showed plateaus and declines in diversity in some subjects, which correlated with the T cell inflection point in chronic, untreated HIV-1 infection (307). Env diversity was different between S2 and S3 at 1-2 ( $p<0.05$ ) and 4-6 ( $p<0.0001$ ) years post-seroconversion. There were also differences between S2 and S8 at 2-4 years post-seroconversion ( $p<0.0001$ ) in env diversity.

Interestingly, the rate at which *env* diversity increased was significantly greater than that of *gag* only in S8 ( $p=0.0033$ ) (**Figure 7**), suggesting *env* divergence from the most recent common ancestor may increase at a rate faster than that observed in *gag*, the intrahost variability of *env* at a specific time point is not consistently higher than the variability of *gag*.

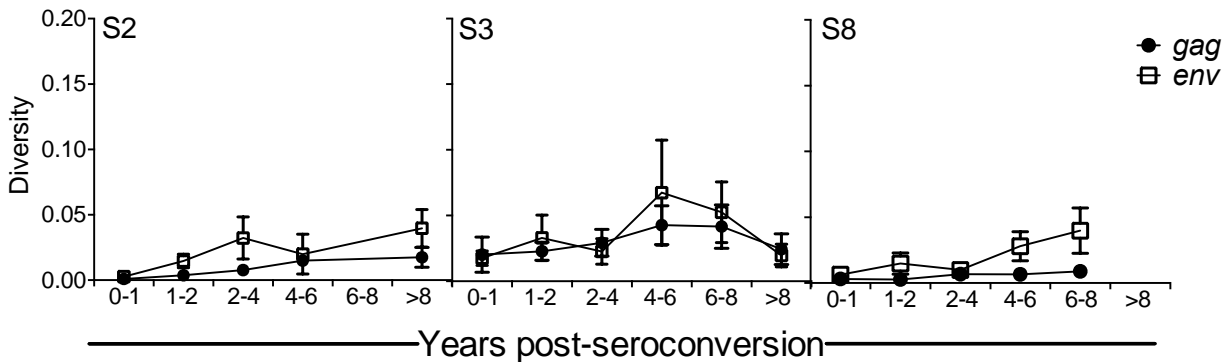


**Figure 7. Comparison of diversity in HIV-1 *gag* and *env***

Pairwise diversity was calculated for the autologous *gag* and *env* sequences obtained from subjects S2 (left panel), S3 (middle panel), and S8 (right panel) at each post-seroconversion time point. Error bars represent the standard deviation of 5 to 36 sequences.

Phylogenetic trees constructed for *gag* and *env* confirmed our calculations showing an increase in evolution over time (**Figure 8**). The rate of evolution differed between subjects and within subjects at different time points. Divergence in *gag* and *env* began to increase 5.61 years post-seroconversion in subject S2 (**Figure 8A**). Among the three, sequences obtained from subject S3 seemed to have the greatest evolution and divergence from the HXB2 outgroup sequence (**Figure 8B**). While *gag* and *env* sequences obtained from subject S8 were highly divergent from the outgroup (**Figure 8C**), they did not evolve at the rates seen in subjects S2 and S3. Interestingly, some sequences obtained from subjects S2 and S3 exhibited signatures of reversion to the ancestral sequence beginning at the second time point evaluated

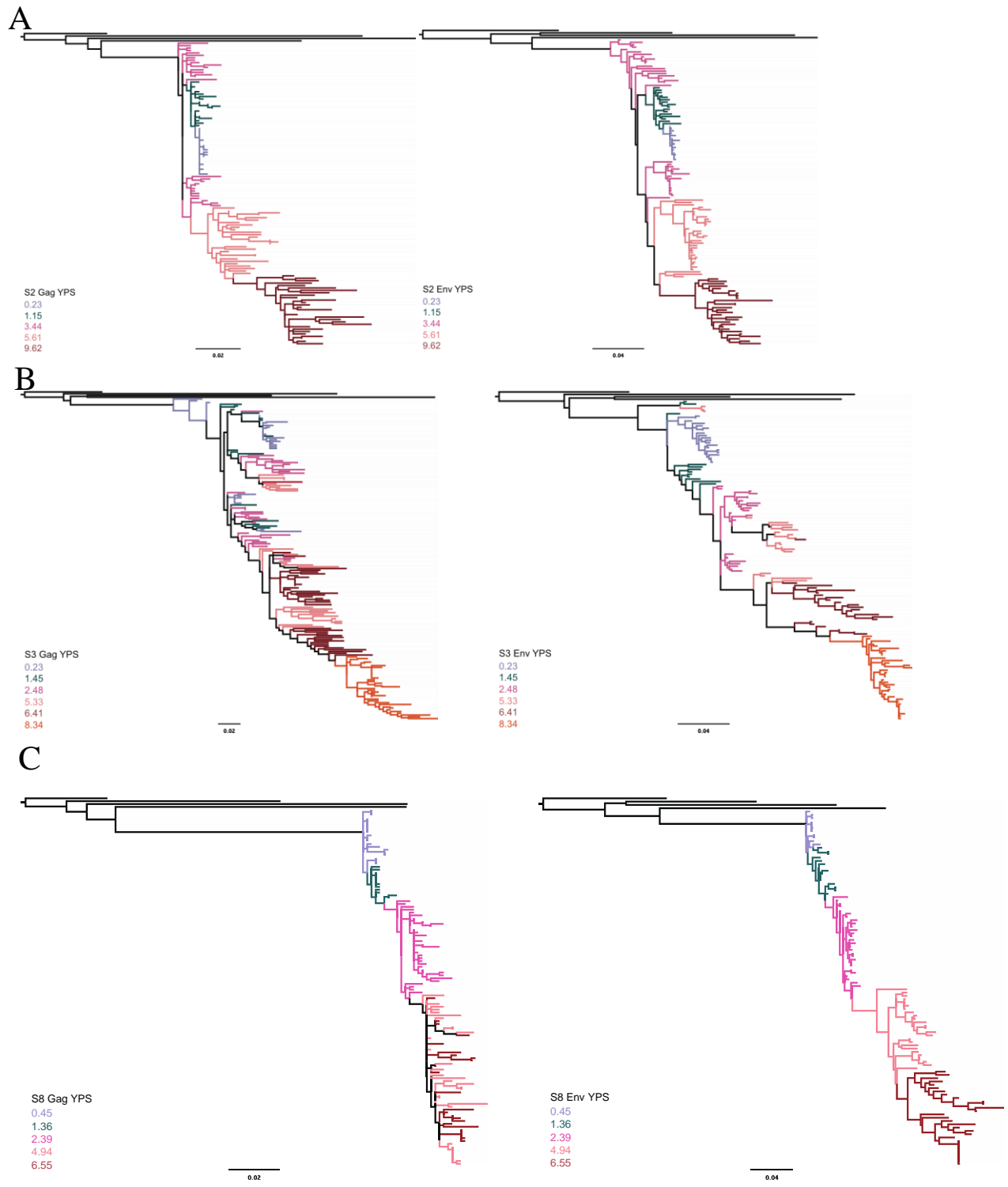


**Figure 8. Phylogenetic trees derived from autologous *gag* and *env* sequences**  
 Phylogenetic trees were constructed from the autologous HIV-1 *gag* and *env* sequences derived from subjects (A) S2, (B) S3, and (C) S8 using 4 HIV-1 subtype B reference outgroup sequences.

Divergence from MRCA highly correlated with diversity in *gag* ( $p < 0.0001$ ,  $R = 0.8794$ ) and *env* ( $p = 0.0009$ ,  $R = 0.7441$ ), showing a linear association between these two evolutionary parameters (**Figure 9**). Overall, these data suggest that HIV-1 viral load alone may contribute to increases in *gag* diversity but is not a direct contributor of increases in *env* diversity. Additionally, these results fail to directly correlate  $CD4^+$  T cell depletion and  $CD8^+$  T cell expansion to viral evolution, suggesting a role for adaptive immunological pressures that does not solely rely on T cell expansion.

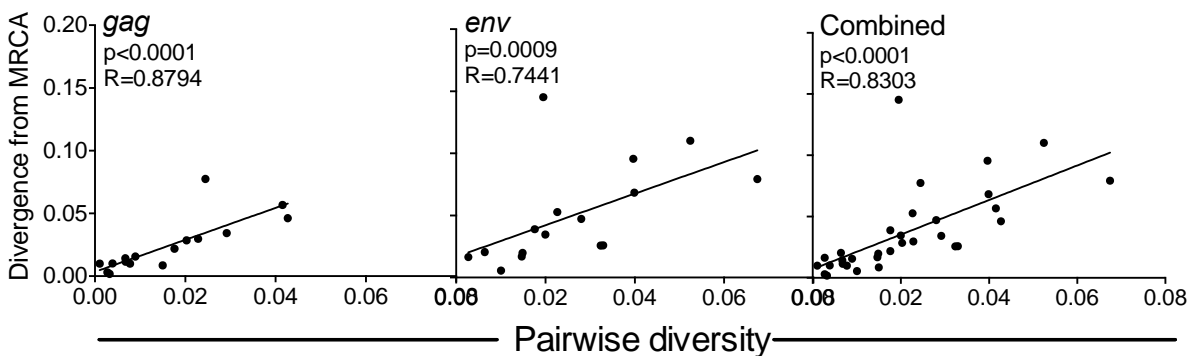


**Figure 9. Correlations between divergence and pairwise diversity**

Divergence from the most recent common ancestor (MRCA) and pairwise diversity were combined from the three subjects and plotted for *gag* (left), *env* (center), and both genes combined (right). R and p values from Spearman correlations are shown.

### 2.3.3 Mechanisms of viral evolution

The HIV-1 *gag* and *env* evolution observed in these subjects could have resulted from stochastic events or could have been the result of adaptive selective pressure. To evaluate these two potential mechanisms, we first assessed how the data conformed to the neutral theory, given that plasma HIV-1 viral load was increasing throughout infection and could have influenced

genetic diversity. Both Tajima's  $D$  (316) and Fu and Li's  $D^*$  (113) tests revealed deviations from neutrality in *gag* at 1 to 2 time points in each subject, whereas deviations from neutrality in *env* were observed only in S2 at 2 timepoints (data not shown). These findings implicate stochastic evolution in the divergence and diversity seen at most time points. More specifically, these findings suggest that evolution of *env* may have been more the result of replication errors during demographic expansion of the viral population, whereas evolution of *gag* may have resulted from other processes, such as selective pressures.

Although the entire *gag* and *env* genes exhibited patterns of random evolution at most time points, it is possible that selective pressures acted on a small number of sites within these genes to induce significant rates of non-synonymous mutations. To determine if selective pressures at individual amino acid sites could have induced the evolution observed in these subjects, we used a fixed effects likelihood (FEL) method to identify codons that were under diversifying and/or directional positive selection. This model operates by calculating the non-synonymous to synonymous substitution ratio in a maximum likelihood framework ( $dN/dS$ ). In positive selection, certain codons are advantageous and are indicated by a relatively high  $dN/dS$  ratio due to the rapid fixation of the favorable mutation in the population (125, 283). To avoid false identification of sites under positive selection, codons corresponding to the variable loops in *env* were removed for these analyses. The percent of *gag* codons that were under positive selection increased throughout infection and was associated with disease progression in S2 ( $p=0.0142$ ,  $r^2=0.8983$ ), S3 ( $p=0.0006$ ,  $r^2=0.9619$ ) and S8 ( $p=0.0045$ ,  $r^2=0.9522$ ) (**Figure 10A**). This was also seen in *env*, with the percent of sites under positive selection correlating with disease progression in S2 ( $p=0.0013$ ,  $r^2=0.9789$ ), S3 ( $p=0.0012$ ,  $r^2=0.9451$ ), and S8 ( $p=0.0073$ ,  $r^2=0.9344$ ). The rate at which positively-selected sites accumulated throughout infection was not different between the subjects, averaging



0.92% per year in *gag* and 1.54% per year in *env*. Of note, there was no difference in the mean frequency of codons under positive selection between *gag* and *env* at any of the time points, implying positive selective pressures were acting uniformly on the two genes.

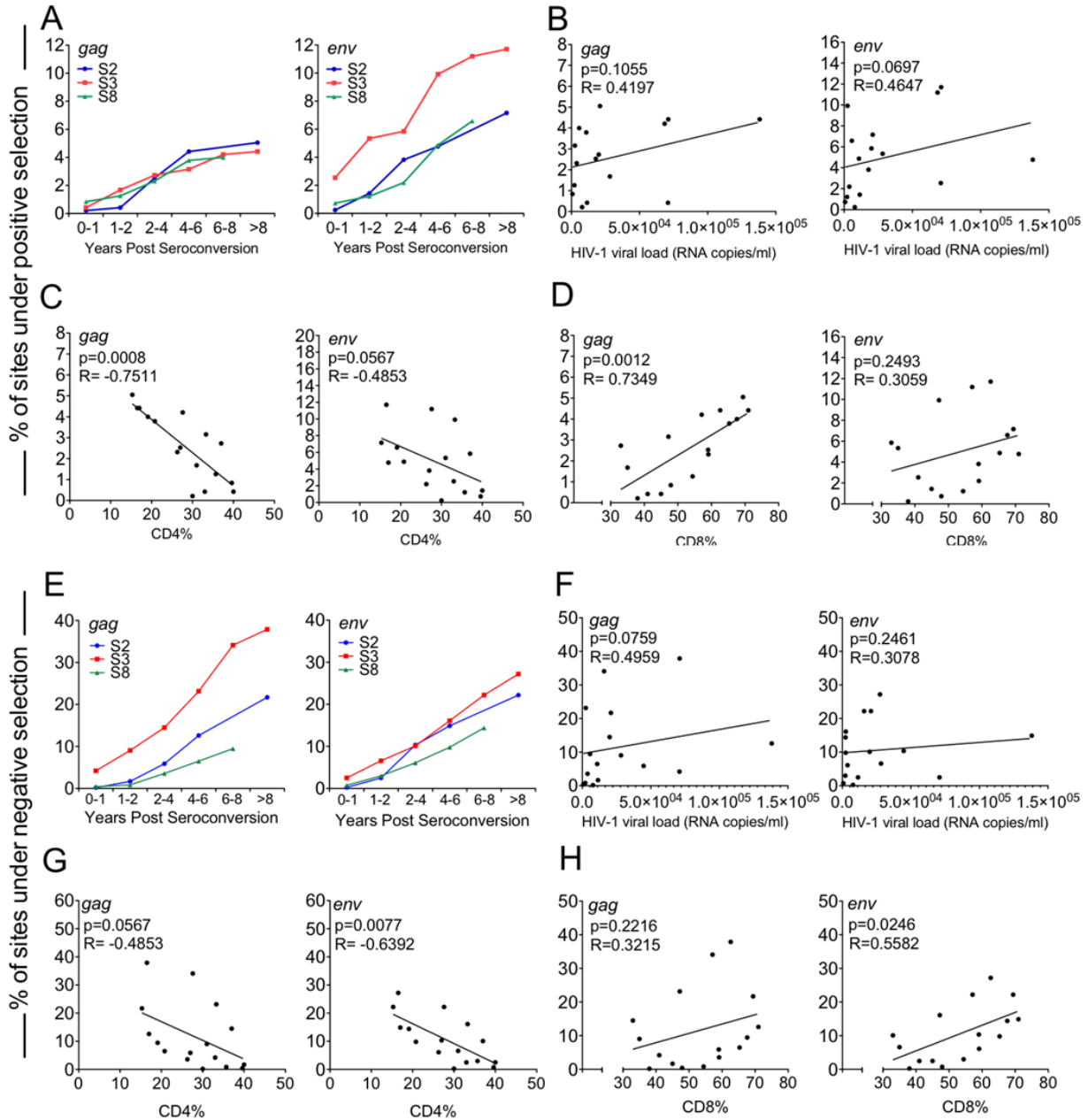


**Figure 10. Correlates of positive and negative selection**

The percent of *gag* and *env* codons under positive and negative selection were determined for each subject at each time point. (A) The percent of *gag* (left panel) and *env* (right panel) codons undergoing positive selection as determined by identifying sites under directional and diversifying selection. Spearman correlations were performed between the percent of sites under positive selection and HIV-1 plasma viral load (B), CD4<sup>+</sup> T cells (C), and (D) CD8<sup>+</sup> T cells. (E) The percent of *gag* (left panel) and *env* (right panel) codons under negative selection was determined longitudinally for each subject. Spearman correlations show the association between the percent of codons under negative selection and (F) HIV-1 viral load, (G) CD4<sup>+</sup> T cells, and (H) CD8<sup>+</sup> T cells.

We combined positive selection data from the three subjects and performed Spearman correlations between the percent of sites under positive selection and viral load, CD4<sup>+</sup>, and CD8<sup>+</sup> T cell percentages at each time point. No correlation was observed between positive selection in *gag* and HIV-1 plasma viremia (**Figure 10B**). There was a positive association between these two parameters in *env*, although this did not reach significance ( $p=0.0697$ ,  $R=0.4647$ ). Lower CD4<sup>+</sup> T cell percentages correlated with a greater percentage of sites under positive selection in *gag* ( $p=0.0008$ ,  $R=-0.7511$ ), but did not reach significance in *env* ( $p=0.0567$ ,  $R=-0.4853$ , **Figure 10C**). Likewise, we observed a positive correlation between CD8<sup>+</sup> T cell percentages and the number of sites under positive selection in *gag* ( $p=0.0012$ ,  $R=0.7349$ ), but did not see any association with CD8<sup>+</sup> T cells in *env* (**Figure 10D**).

We then identified *gag* and *env* sites that were undergoing negative selection, at which the  $dN/dS$  ratio is unusually low. In negative selection, conserved amino acids accrue a higher proportion of synonymous mutations than nonsynonymous due to nonsynonymous mutations being selected against. Using the FEL method we found that negative selection in *gag* and *env* correlated positively with disease progression in all three subjects ( $p<0.004$ ,  $r^2>0.95$  for all, **Figure 10E**). There was no difference in the rate at which sites under negative selection accumulated between *gag* and *env* in S2 ( $p=0.8929$ ). Negatively selected sites accumulated faster in *gag* than in *env* in S3 ( $p=0.0048$ ), and faster in *env* than in *gag* in S8 ( $p=0.0318$ ). There were no correlations between the percent of sites under negative selection and HIV-1 plasma viremia in *gag* or *env*, although the association approached significance in *env* ( $p=0.0759$ ,  $R=0.4959$ ). The percent of *env* sites under negative selection was negatively correlated with CD4<sup>+</sup> T cell percent ( $p=0.0077$ ,  $R = -0.6392$ ). We did not see this correlation in *gag* (**Figure 10G**). Accordingly, there was a positive correlation between CD8<sup>+</sup> T cell percentage and the number of sites under negative

selection in *env* ( $p=0.0246$ ,  $R=0.5582$ ) but not in *gag* (**Figure 10H**). Interestingly, negatively-selected sites accumulated at a faster rate than positively selected sites in *gag* and *env* in all subjects ( $P<0.0003$  for all).

We conclude that adaptive selective pressures, in addition to random mutations, are acting on both *gag* and *env* in chronic, untreated HIV-1 infection. The analyses of positive and negative selection show that increases in positively-selected sites are accompanied by a higher proportion of negatively-selected sites. Additionally, there are differential correlates of positive and negative selection between the two genes. Specifically, the expansion and depletion of T cell subsets correlates with positive selection in *gag* and negative selection in *env*.

### **2.3.4 Positive selection as a driving force for viral evolution**

The evidence presented above suggests uncontrolled viral replication alone is not responsible for the increases in divergence and diversity observed in chronic HIV-1 infection, and that positive selection at specific amino acid residues could have induced the evolution observed in these subjects. To determine the effects of adaptive selection on viral evolution, we performed Spearman correlations between divergence and diversity and positive selection in *gag* and *env*. We observed strong correlations between the percent of sites under positive selection and divergence (**Figure 11A**,  $p<0.0001$ ,  $R=0.7104$ ) and diversity (**Figure 11B**,  $p<0.0001$ ,  $R=0.7179$ ) when data from the three subjects were combined. We observed similar results when correlations were performed on *gag* and *env* separately (data not shown).

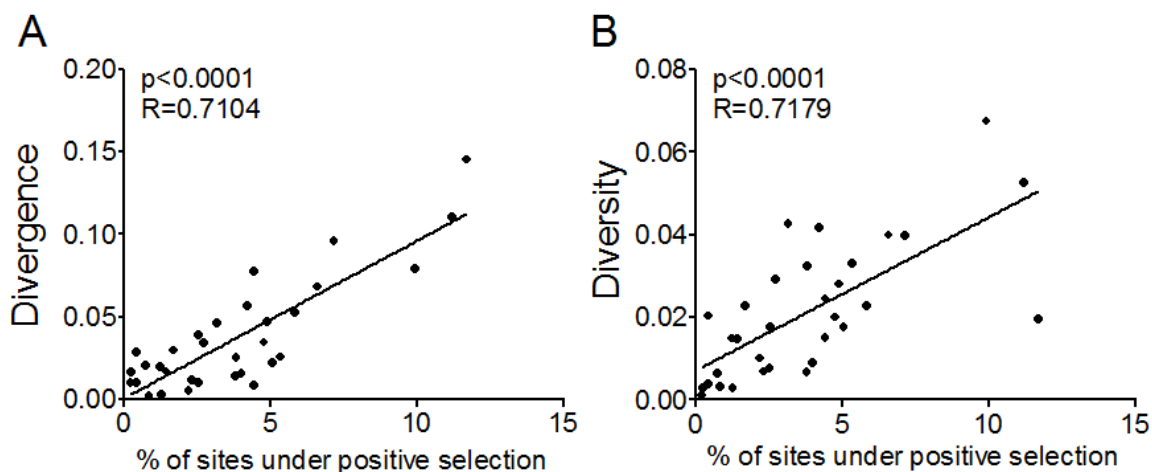


**Figure 11. Positive selection as a function of viral divergence and diversity**

Longitudinal data from all three subjects were combined to perform Spearman correlation analyses between the percent of *gag* and *env* codons under positive selection within each subject and (A) divergence and (B) diversity of the corresponding gene at the corresponding timepoint.

Analysis of phylogenetically-informative sites (86) revealed an increase in the number of mutated amino acid sites throughout infection as well as the presence of compensatory and mutually exclusive mutation patterns at these sites in all three subjects (data not shown). On average, less than 10% of amino acids in Gag and Env were considered phylogenetically informative, providing further evidence that evolution of entire HIV-1 genes may be due to evolution at a few highly-mutable sites. Of note, in all three subjects  $\geq 70\%$  of mutated Gag and Env amino acid sites were under positive selection, suggesting non-synonymous mutations were often the result of selective pressure. Env amino acid sequences showed no increase in potential N-linked glycosylation sites (PNGS) in any of the subjects throughout infection (data not shown), suggesting a limited role of this mechanism in escape from adaptive immune responses.

Together, these data provide strong evidence for the role of positive selection at a limited number of sites in the evolution of entire HIV-1 genes.

### 2.3.5 Positive selection in MHC class I-restricted epitopes

To identify the effects of protein evolution on cytotoxic T-lymphocyte (CTL) epitopes, we identified amino acid changes that occurred within epitopes known to be targeted, processed, and presented as defined by the Los Alamos Database (<http://www.hiv.lanl.gov>) for each individual's HLA A and B alleles (**Table 3**).

**Table 3. Molecular HLA genotypes used in epitope prediction models.**

Subject	HLA Alleles				
	A <sup>a</sup>	B <sup>a</sup>	DRB1 <sup>b</sup>	DRB3 <sup>b</sup>	DRB4 <sup>b</sup>
S2	2402, 2902	0801, 3501	1104, 1302	0202, 0301	
S3	2402, 0301	1518, 3502	1104, 0401	0202	0101
S8	2402, 1101	4001, 5101	0701, 1301	0202	0101

<sup>a</sup>HLA A and B alleles were used for MHC class I peptide affinity predictions, proteasomal cleavage, and TAP binding predictions

<sup>b</sup>HLA-DR alleles were used for MHC class II peptide affinity predictions

We excluded epitopes that occurred in the variable regions of Env from our analysis. The known Gag and Env epitopes evaluated for each subject are shown in **Table 4**.

**Table 4. Known MHC class I-restricted HIV-1 Gag and Env epitopes for each subject**

Subject	Epitope	Position	HLA Restriction	AA Change? <sup>a</sup>	Pos. Selection? <sup>b</sup>
S2	KYKCLKHIVW	p17 <sub>28-36</sub>	A*2402	yes	yes
	ELRSLYNTV	p17 <sub>74-82</sub>	B*0801	yes	yes
	LYNTVATLY	p17 <sub>78-86</sub>	A*2902	yes	yes
	EVKDTKEAL	p17 <sub>93-101</sub>	B*0801	yes	yes
	NYPIVQNL	p17/p24 <sub>131-138</sub>	A*2402	yes	yes
	HPVHAGPIA	p24 <sub>216-224</sub>	B*3501	yes	yes
	IYKRWIILGL	p24 <sub>263-272</sub>	A*2402	yes	yes
	DYVDRFYKT	p24 <sub>295-303</sub>	A*2402	yes	no
	LFCASDAKAY	gp120 <sub>52-61</sub>	A*2402	no	no
SFPEIPIHY	gp120 <sub>209-217</sub>	A*2902	yes	yes	
S3	KYKCLKHIVW	p17 <sub>28-36</sub>	A*2402	yes	no
	NYPIVQNL	p17/p24 <sub>131-138</sub>	A*2402	no	no
	VKVVEEKAF	p24 <sub>156-164</sub>	B*15	yes	yes
	GHQAAMQML	p24 <sub>193-201</sub>	B*15	no	no
	PIIPVGEIY	p24 <sub>254-262</sub>	B*3502	no	no
	IYKRWIILGL	p24 <sub>263-272</sub>	A*2402	no	no
	DYVDRFYKT	p24 <sub>295-303</sub>	A*2402	no	no
	VTVYYGVPVWK	gp120 <sub>36-46</sub>	A*0301	no	no
	LFCASDAKAY	gp120 <sub>52-61</sub>	A*2402	yes	no
S8	KYKCLKHIVW	p17 <sub>28-36</sub>	A*2402	yes	yes
	VLYCVHQG	p17 <sub>84-91</sub>	A*1101	no	no
	VEIKDTKEAL	p17 <sub>92-101</sub>	B*4001	yes	yes
	NYPIVQNL	p17/p24 <sub>131-138</sub>	A*2402	no	no
	VKVVEEKAF	p24 <sub>156-164</sub>	B*15	yes	yes
	SEGATPQDL	p24 <sub>176-184</sub>	B*4001	no	no
	GHQAAMQML	p24 <sub>193-201</sub>	B*15	no	no
	IYKRWIILGL	p24 <sub>263-272</sub>	A*2402	no	no
	GLNKIVRMY	p24 <sub>269-277</sub>	B*15	no	no
	DYVDRFYKT	p24 <sub>295-303</sub>	A*2402	no	no
	NANPDCKTI	p24 <sub>325-333</sub>	B*5001	no	no
	ACQGVGGPGHK	p24 <sub>349-359</sub>	A*1101	yes	no
	VTVYYGVPVWK	gp120 <sub>36-46</sub>	A*0301	no	no
	LFCASDAKAY	gp120 <sub>52-61</sub>	A*2402	yes	no
	SFNCGGEFF	gp120 <sub>375-383</sub>	B*15	yes	no
LPCRICKII	gp120 <sub>414-424</sub>	B*5001	no	no	

<sup>a</sup>Identifies if there were amino acid changes within the epitope at any time during untreated HIV-1 infection

<sup>b</sup>Identifies if any amino acid changes within the epitope were the result of positive selection

In S2, 6/7 (85.7%) Gag epitopes and 1/2 (50.0%) Env epitopes mutated throughout infection. Only 2/7 (28.6%) Gag epitopes and 0/2 (0.0%) Env epitopes contained sites undergoing

positive selection. In S3, 2/7 (28.6%) Gag epitopes and 1/2 (50.0%) Env epitopes mutated, with 0/7 (0.0%) Gag and 0/2 (0.0%) Env epitopes containing sites under positive selection. Lastly, in S8 4/12 (33.3%) Gag epitopes and 2/4 (50.0%) Env epitopes mutated, with 2/12 (16.7%) Gag and 2/4 (50.0%) Env epitopes under positive selection (**Table 4**). Interestingly, the percent of epitopes with mutations was significantly higher than the percent of epitopes with positively-selected sites ( $p=0.0014$ , data not shown), suggesting that mutations within epitopes are not always the direct result of positive selection. Epitope evolution was not specific to either protein, as there was no difference in the mean percent of epitopes that mutated between Gag and Env. Interestingly, none of the subjects exhibited evidence of positive selection in the optimal HLA A24-restricted Gag epitope KW9 (p17<sub>28-36</sub>, KYKCLKHIVW), despite variation of this epitope in all subjects. Additionally, the observed lack of selection in CTL epitopes was likely not due to viral fitness costs, as no compensatory mutations were found in or near known epitopes.

### **2.3.6 The impact of protein evolution on predicted epitope processing and presentation**

We have previously shown that the number of predicted epitopes in autologous full-length HIV-1 sequences decreases during the first 50 days of infection (147). To date, we have yet to fully understand how selective processes affect the HIV-1 proteome in chronic infection, particularly in CTL epitopes and regions involved in epitope processing. We therefore generated consensus Gag and Env sequences for each subject at each time point and used netMHCpan, a prediction model for peptide:MHC class I affinity, to identify potential epitopes for each subject's cognate HLA-A and -B molecules. For comparability between the two proteins, which are different lengths, we calculated the number of predicted epitopes per amino acid. Surprisingly, predicted MHC class I-restricted epitopes were more prevalent in Env than in Gag in all subjects



at all time points (**Figure 12A**). In fact, Env epitopes were more than 1.5 times more prevalent than Gag epitopes in S8 at every time point. There was no observable change in the number of predicted MHC class I epitopes throughout infection in Gag or Env.

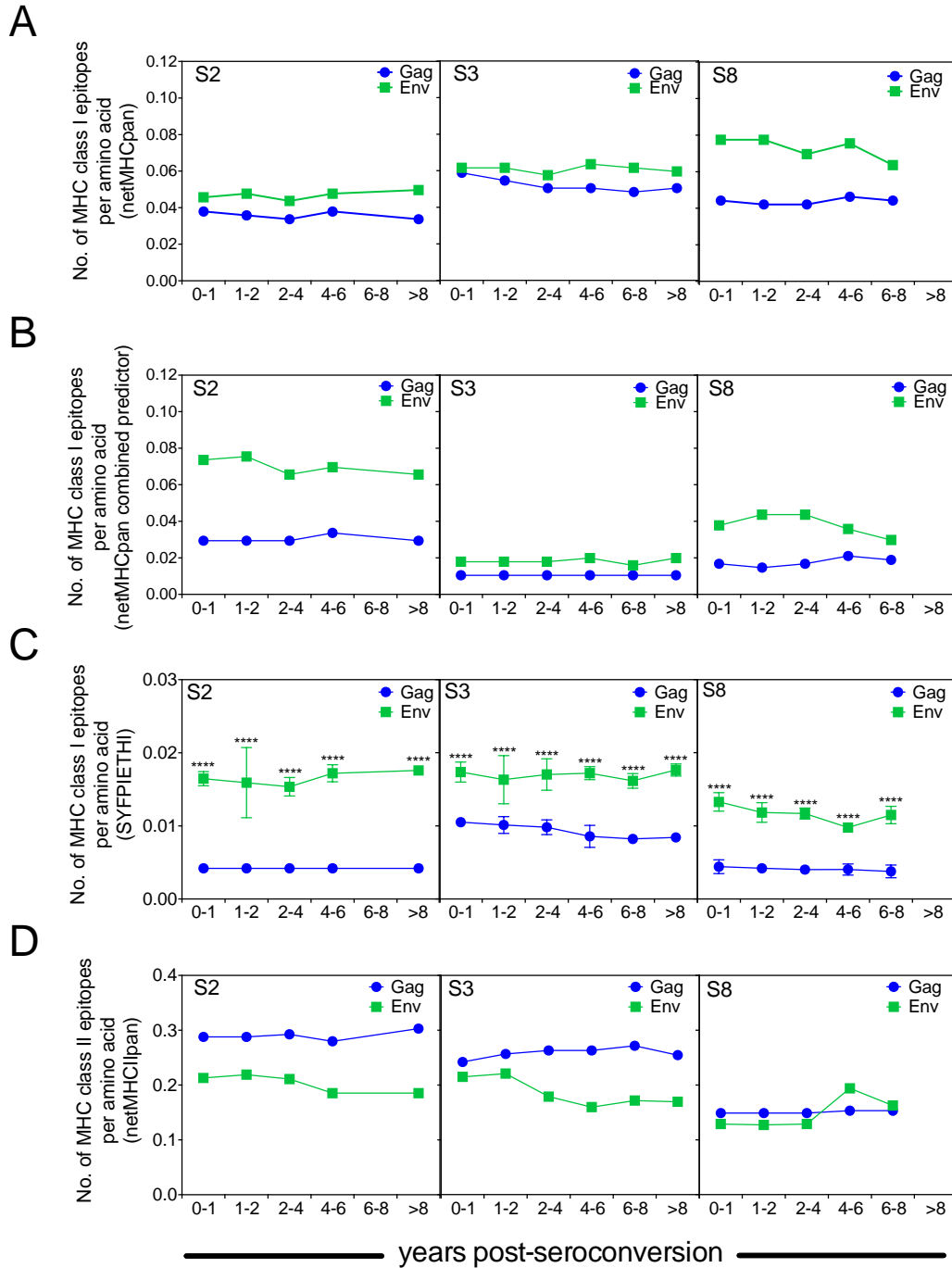


**Figure 12. Longitudinal changes in the frequency of predicted MHC class I and II-restricted epitopes**

Autologous Gag and Env sequences were evaluated for the presence of predicted MHC class I and II epitopes, as well as proteasomal cleavage sites. The number of predicted Gag and Env epitopes for each subject at each time point as determined by (A) netMHCpan, (B) a combined MHC class I affinity, proteasomal processing, and TAP binding predictor, and (C) SYFPEITHI calculations. (D) The number of predicted MHC class II epitopes at each time point for each subject as determined by netMHCIIpan. For comparability between Gag and Env, data are shown as the number of predicted epitopes per amino acid, as there were 475 Gag and 507 Env amino acids in each sequence. Error bars represent the standard deviation of 5 to 36 sequences. \* $p < 0.05$ , \*\* $p < 0.01$ , \*\*\* $p < 0.001$ , \*\*\*\* $p < 0.0001$

A similar pattern was observed when using a combined prediction model within the Immune Epitope Database (IEDB), which combines predictions of MHC class I affinity, proteasomal cleavage, and TAP binding to give an overall epitope “score” (260, 319). When these three components were evaluated in autologous Gag and Env sequences, Env had consistently more frequent predicted MHC class I epitopes than Gag (**Figure 12B**). Of note, there was a two-fold higher frequency of class I-restricted Env epitopes than Gag epitopes in S2 at all time points. This method is unable to predict an epitope score for HLA B\*1518 and B\*3502, so only predictions for HLA A alleles were performed in S3. SYFPEITHI calculations also showed a similar trend when looking at predicted HLA A\*2402-restricted epitopes within autologous sequences. As this method is able to evaluate multiple sequences at a time, we were able to identify predicted high-affinity peptide sequences in each of the 325 Gag and 328 Env sequences and calculated a mean and standard deviation for each time point within each subject. At all time points in all subjects, class I-restricted epitopes were significantly more prevalent in Env than in Gag ( $p < 0.0001$  for all, **Figure 12C**). Shockingly, when evaluating the prevalence of MHC class II-restricted epitopes throughout infection, Gag had more epitopes than Env at all time points in all subjects with the exception of 4-6 and 6-8 years post-seroconversion in S8 (**Figure 12D**). NetChop predictions performed on all autologous Gag and Env sequences from each time point showed no deviations in the number of predicted proteasomal cleavage sites throughout infection, but significantly more frequent sites in Gag than in Env at all time points except 2-4 years post-seroconversion in S8 (**Figure 13**).

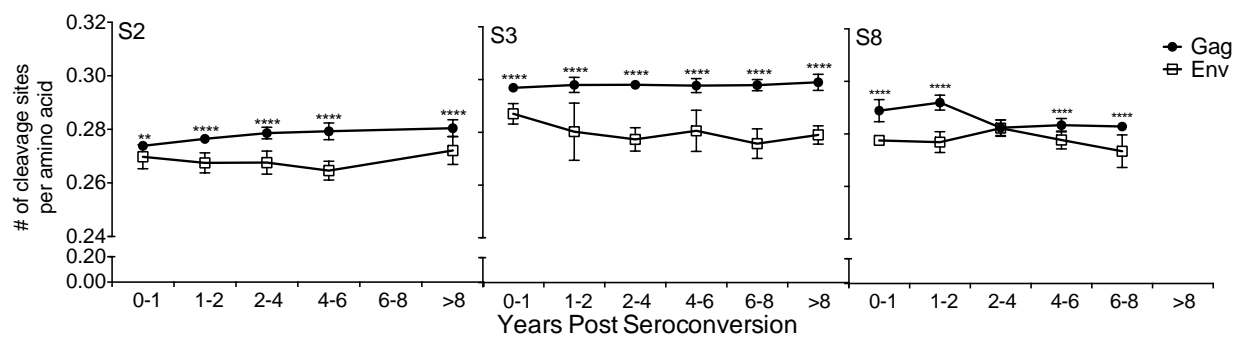


**Figure 13. Longitudinal changes in predicted proteasomal cleavage sites**

NetChop was used to identify the number of predicted cleavage sites in Gag and Env in each subject throughout untreated HIV-1 infection. Error bars represent the standard deviation of 5 to 36 sequences obtained at each time point. \* $p < 0.05$ , \*\* $p < 0.01$ , \*\*\* $p < 0.001$ , \*\*\*\* $p < 0.0001$

The number of predicted epitopes in Gag and Env was not correlated with viral load,  $CD4^+$  T cell, or  $CD8^+$  T cell percentages (data not shown). There were additionally no correlations between the number of predicted Gag cleavage sites and viral load,  $CD4^+$  T cell, or  $CD8^+$  T cell percentages (data not shown). When all subjects were combined, there was a significant correlation between the number of Env cleavage sites and  $CD8^+$  T cells ( $p=0.0128$ ), but not with viral load or  $CD4^+$  T cells.

From these data, we conclude that neither the number of predicted epitopes nor the number of cleavage sites change throughout infection. Because netMHCpan and SYFPEITHI base their epitope predictions on the presence of amino acid sequences with high affinity for the subject's HLA alleles, we can conclude that epitope affinity for MHC class I was not likely to be altered during infection. Taken together, these data demonstrate varying patterns of epitope frequency and cleavage site evolution. Overall, predicted MHC class I epitopes were more prevalent in Env, whereas predicted MHC class II epitopes and proteasomal cleavage sites were more prevalent in

Gag, suggesting differential mechanisms of escape and epitope processing and presentation between the two proteins.

## 2.4 DISCUSSION

In the present study, we evaluated *gag* and *env* viral evolution and the correlates of adaptive selective pressures in three untreated HIV-1 infected subjects. We performed in-depth analyses of *gag* and *env* viral evolution at multiple time points within each subject and evaluated between 5 and 36 sequences from each time point. Here we described trends of nucleotide and amino acid evolution within each individual and identified patterns and correlates of disease progression and signatures of selective pressure.

We found that the gradual increase in plasma viremia was not sufficient to induce CD8<sup>+</sup> T cell expansion, although it may be directly related to CD4<sup>+</sup> T cell depletion. The increase in CD8<sup>+</sup> T cells observed in chronic HIV-1 infection could be due to a chronic state of immune activation that is independent of the level of HIV-1 in the blood. This is evidenced by longitudinal clinical data as well as the clinical characteristics of our study subjects (**Figure 3A**) in which CD8<sup>+</sup> T cells remain high and the CD4:CD8 ratio remains skewed during cART and even when plasma viral load has decreased to undetectable levels.

Interestingly, we did not observe any correlations when looking at the raw number of CD4<sup>+</sup> and CD8<sup>+</sup> T cells, as these values varied greatly between subjects. S8, for example, had 1,189 CD4<sup>+</sup> T cells/mm<sup>3</sup> at the first post-seroconversion timepoint, compared to 545 and 806 cells/mm<sup>3</sup> in S2 and S3, respectively. While common practice is to evaluate the raw CD4<sup>+</sup> T cells count as a measure of disease progression, it may be more telling to look at how the T cell repertoire has

changed over time. Although S8 had the highest pre-cART CD4<sup>+</sup> T cell count of the subjects evaluated in this study, he also experienced the most drastic change, with a 76.2% reduction in CD4<sup>+</sup> T cell numbers by the last pre-cART time point. Therefore, even though the clinical parameters observed in this subject may hint to a slightly slower disease progression, the rate at which he lost CD4<sup>+</sup> T cells was much more rapid than the other two subjects.

A recent study of 37 high-risk Kenyan women examined *gag* and *env* sequences at one acute and one chronic infection time point. In chronic infection, *gag* divergence was positively correlated with viral load and was negatively correlated with CD4<sup>+</sup> T cell number, whereas no correlations were observed with *env* divergence and diversity (262). This study went further to evaluate the impact of genetic evolution on MHC class I epitopes and found that the percentage of *gag* epitopes that were variable was positively associated with viral load, suggesting a crucial role of *gag* evolution in disease progression.

We previously reported longitudinal increases in *env* divergence and diversity in treatment-naïve HIV-1 infected subjects (307). Prior to this study, analyses of *gag* evolution and the effects of genetic evolution on cognate protein sequences had yet to be fully explored. More importantly, which virologic and/or immunologic factors induce these increases in genetic diversity? Here we determined that *gag* and *env* divergence and diversity was not the direct result of uncontrolled viral replication. Because of this, it can be hypothesized that random genetic drift was not the sole culprit for the high evolutionary rates observed in these subjects. Indeed, bursts of nonsynonymous substitutions in multiple HIV-1 proteins have been shown to be the result of positive selection as opposed to random genetic drift (30).

In both *gag* and *env*, we were able to detect the signature of positive selection, providing further evidence that adaptive processes greatly contribute to viral evolution. Although neutrality

tests suggested *gag* and *env* evolution was the result of viral expansion, identification of sites under positive selection revealed the majority of non-synonymous mutations were due to positive selective pressure. Perhaps stochastic evolutionary events that resulted in non-synonymous mutations, but conferred no immunological benefit to the virus, were eliminated from the viral repertoire. We also observed rates of negative selection that were much higher than the rate of positive selection. We are not the first to show that negative selection is more common than positive selection, as this is the basis of the neutral theory of molecular evolution (124, 181-183), whereby most sites are evolving neutrally and very few are under positive selection, while a substantially higher proportion are under negative selection. We do show, however, that selection is differentially correlated with T cell subsets in *gag* and *env*, but is nonetheless detected in both of these genes.

Sites under positive selection accumulated at an equal rate in *gag* and *env*, hence we can conclude that the driving force for adaptive selection was acting uniformly on both genes. As the associations did approach significance, it would be of interest to examine more subjects in this fashion to determine if a significant correlation is observed between genetic evolution and HIV-1 viral load. Additionally, neither decreases in CD4<sup>+</sup> T cells nor increases in CD8<sup>+</sup> T cells were predictive of viral evolution, again showing that disease progression alone was not sufficient to induce evolution in these genes. As CD4<sup>+</sup> T cell depletion is a hallmark of progressive HIV-1 infection, it is plausible to suspect the quantity of CD4<sup>+</sup> and CD8<sup>+</sup> T cells may not be as important as the quality of these cells in containing viral evolution. These findings are contradictory to a previous study, which observed positive correlations between divergence and viral load, and inverse correlations between divergence and CD4<sup>+</sup> T cell number in *gag* sequences obtained from chronically-infected subjects (262). This study looked at one acute and one chronic infection time

point in each subject, whereas our study looked at 5 to 6 time points throughout infection, giving a broader range of T cell and viral load fluctuations. Additionally, these discrepancies may be due to using CD4<sup>+</sup> T cell number instead of percentage as the correlating factor. As the total number of lymphocytes varies greatly within the human population, it is more appropriate to look at CD4<sup>+</sup> T cells as a percent of lymphocytes when combining data from multiple subjects. The number of CD4<sup>+</sup> T cells may not be comparable between subjects, but the percent of CD4<sup>+</sup> T cells within the lymphocyte pool may be more telling of trends within multiple subjects.

Notably, the number of codons under positive and negative selection did not differ between *gag* and *env*, suggesting the high divergence and diversity observed in *env* was not due to increased selective pressures but was potentially due to higher rates of random polymerase errors. This furthermore shows that adaptive selection was equally targeted against the two proteins in spite of significant differences in genetic evolution. Additionally, diversifying selection (positive and negative selection) was inversely correlated with CD4<sup>+</sup> T cells and positively correlated with CD8<sup>+</sup> T cells in *env* but not in *gag*, suggesting selection in *env* is more predictive of clinical outcome. It may therefore be pertinent to expand studies of selection, particularly CTL-mediated selection, to include analysis of *env* in addition to *gag*, as many CTL studies primarily focus on amino acid changes within the Gag protein. Observing these correlations in positive and negative selection, despite the lack of correlations observed between divergence and diversity and clinical parameters, implicates a specific adaptive selective force that is acting in response to the Env protein, i.e. genetic evolution is not a stochastic event but is not the best correlate of clinical outcome in chronic HIV-1 infection.

Despite the evidence presented here for adaptive selective pressures against *gag* and *env*, these mechanisms were unsuccessful in controlling HIV-1 replication and in preventing disease



progression. That is, there is strong evidence for adaptive selective mechanisms within our study subjects, yet all three still progressed to AIDS, suggesting an unsuccessful immune response may have been generated. We suspect the adaptive responses generated to Gag and Env were unable to eliminate viral targets but succeeded in inducing an environment of chronic inflammation upon recognition, but not elimination, of their antigens. A primary mechanism by which HIV-1 evades immune recognition is by evolution within epitopes that is secondary to CTL selective pressures (9, 10, 35, 43, 58, 244-247, 271). Our observation that positive selection was not specific to CTL epitopes suggests an efficient epitope-specific response was not generated during natural HIV-1 infection. Of note, we did not observe amino acid changes within all of the known CTL epitopes. It is plausible that mutations within these epitopes were detrimental to viral fitness, but there was no evidence for compensatory mutations within or near any of the known CTL epitopes.

Reports on the efficacy of CTL pressure are somewhat conflicting. Allen et al. longitudinally examined viral evolution and T cell responses to CTL epitopes in four HIV-1 infected subjects and noted that nearly two-thirds of mutations could be attributed to CD8<sup>+</sup> T cell selective pressures (6). This same group, however, observed occasions of limited evolution in persistently-targeted CD8<sup>+</sup> T cell epitopes, suggesting that T cell responses in chronic infection may not always exert functional immunological pressure (186). These studies demonstrate contrasting models of CTL selective pressure that may not be mutually exclusive. For the purposes of therapeutic vaccine development, perhaps responses should focus on inducing selection within dominant Gag and Env CTL epitopes, particularly the well-defined KW9 epitope. A focus of future work is to perform intensive longitudinal analyses on all known and predicted CTL epitopes within these subjects and correlate these responses with the in-depth evolutionary data presented here.

In summary, our study provides the first in depth analysis of longitudinal and sequential *gag* and *env* genetic and protein evolution in untreated, chronically-infected subjects. The results reported here provide novel insight into the natural evolution of HIV-1 and could potentially impact the design of therapeutic vaccinations aimed at targeting autologous Gag and Env epitopes. Identifying the immunological implications and evolutionary correlates of adaptive immune pressures, particularly those in CTL epitopes, is important for development of immunotherapies that target autologous epitope variants and aim to cure HIV-1 infection.

## 2.5 ACKNOWLEDGEMENTS

We would like to thank Dr. Jim Mullins and his laboratory, specifically Kim Wong and Brendan Larsen, for generating and help with analyzing our sequencing data, Weimin Jiang and Kelley Gordon for excellent technical assistance, William Buchanan for clinical assistance, Dr. John Mellors for use of his Roche COBAS® TaqMan® HIV-1 Test instrumentation, and the volunteers of the Pittsburgh site of the Multicenter AIDS Cohort Study. This work was supported by the National Institutes of Allergy and Infectious Diseases grants U01 AI-35041, R37 AI-41870, and T32 AI-065380.

### 3.0 THE EFFECTS OF REGULATORY T CELLS AND DENDRITIC CELLS ON T CELL RESPONSES TO AUTOLOGOUS HIV-1 EPITOPE VARIANTS

#### 3.1 ABSTRACT

Recall T cell responses to HIV-1 antigens are often used as a surrogate for the endogenous immune response that is generated during infection. HIV-1 immunotherapies aim to induce T cell immunity against viral antigens for which there are no effective T cell responses generated during natural infection. The current methods of identifying antigen specific T cell responses in HIV-1 infection use bulk PBMC and ignore regulatory mechanisms that could be masking these responses and/or antigen presenting cells that could reveal otherwise hidden responses. It has yet to be shown how regulatory mechanisms, such as regulatory T cells ( $T_{reg}$ ), and enhancing mechanisms, such as dendritic cells (DC), suppress or enhance detection of responses to autologous epitope variants in chronic HIV-1 infection. In the present study, HIV-1 *gag* and *env* were sequenced from three A\*2402 subjects at multiple post-seroconversion time points. Peptides representing autologous variants of thirteen known or predicted MHC class I-restricted epitopes were synthesized and used as antigen in IFN $\gamma$  ELISpot and intracellular polyfunctional cytokine assays. Longitudinal PBMC responses were compared to responses observed with removal of  $T_{reg}$  from PBMC and/or addition of autologous monocyte-derived DC. Addition of DC to ELISpot assays significantly enhanced the detection of antigen-specific responses regardless of disease state. Removal of  $T_{reg}$ , however, had minimal effect on the detection of T cell responses. Using DC and  $T_{reg}$  removal only modestly enhanced responses at some time points when compared to the condition with only DC addition. Secretion of multiple type 1 cytokines was enhanced by DC and the effect DC had on the

polyfunctionality of CD8<sup>+</sup> T cells was most apparent late post-cART. For the first time, we have shown that T cell responses specific for autologous HIV-1 antigens are generated at all states of disease progression, but are slightly masked by regulatory mechanisms and are significantly enhanced when stimulated by a professional antigen-presenting cell. We additionally show that DC can reveal polyfunctional T cell responses after many years of treatment. These data underscore the potential efficacy of a DC immunotherapy that aims to awaken a dormant autologous HIV-1-specific CD8<sup>+</sup> T cell response.

HIV-1 *gag* and *env* sequencing was performed by our collaborators in the laboratory of Dr. Jim Mullins at the University of Washington. I performed all experiments and data and statistical analyses and generated all graphs. Interpretation of the data was assisted by Dr. Charles R. Rinaldo and Dr. Robbie B. Mailliard.

### **3.2 BACKGROUND**

HIV-1-specific CD8<sup>+</sup> T cell responses are effective at imposing immunological pressure in acute infection, as evidenced by the induction of a large turnover and mutation rate in the virus population (89, 313, 336). However, the failure of CD8<sup>+</sup> cytotoxic T lymphocytes (CTL) to control virus in chronic infection results in progression to AIDS and can be attributed to several factors. Viral evolution, specifically in CTL epitopes, can interfere with recognition by naïve CD8<sup>+</sup> T cells, resulting in a limited repertoire of T cell-mediated immune responses against the mutated region. In the absence of an effective CTL response that is specific for these mutated epitopes, the virus persists and disease progression continues (6, 7, 19, 22, 30, 134-137, 145). Additionally, prolonged antigenemia and changes in regulatory mechanisms lead to a disruption in T cell

homeostasis, correlate with disease progression, and may negatively regulate the HIV-1-specific CD8<sup>+</sup> T cell response (107, 236). To fully understand the mechanisms of viral pathogenesis and develop effective treatments for HIV-1-infected subjects, the effects of viral evolution and regulatory mechanisms on HIV-1-specific T cell responses must be evaluated.

Alterations in T cell homeostasis during chronic infection largely impact the naïve subset and partially result from decreases in thymic output (17, 91, 366). Progressive infection is also accompanied by decreases in the naïve CD8<sup>+</sup> T cell subset despite increases in total CD8<sup>+</sup> T cells (284). These perturbations in the naïve CD8<sup>+</sup> T cell repertoire could reduce the number and likelihood of mutated epitopes being recognized. Additionally, HIV-1 infection is accompanied by a progressive decrease in CD4<sup>+</sup> T cells, of which a subpopulation is capable of suppressing immune responses and promoting tolerance in healthy states and in a variety of disease models (191, 291). As HIV-1 is a disease of chronic immune activation, an increase or decrease in these regulatory T cells (T<sub>reg</sub>) could be beneficial to the virus. An increase leading to more suppression of anti-HIV-1 CTL responses and a decrease leading to enhanced immune activation.

Reports on the perturbations in these regulatory T cells (T<sub>reg</sub>) during chronic HIV-1 infection have been variable, with most showing an increase in the frequency of T<sub>reg</sub> with disease progression and/or overall CD4<sup>+</sup> T cell depletion (14, 21, 112, 164, 243, 302, 314). These cells have also been implicated in HIV-1 pathogenesis and disease progression (59, 212). In subjects receiving successful combination antiretroviral therapy (cART), T<sub>reg</sub> levels return to those seen in uninfected subjects (39, 235, 302), suggesting any effects imposed by T<sub>reg</sub> during untreated infection should be mitigated during cART. Interestingly, T<sub>reg</sub> also suppress HIV-1-specific T cell responses following DC immunotherapy in subjects on cART (213)

While many aspects of the immune system become dysfunctional in chronic HIV-1 infection and remain dysfunctional even when subjects receive cART, myeloid dendritic cells (DC), the most potent antigen presenting cells (APC), retain the ability to process and present antigen (68, 295) and to stimulate HIV-1-specific IFN $\gamma$  production in CD8<sup>+</sup> (105, 156, 158) and CD4<sup>+</sup> T cells (240). These cells may be a valuable tool in analysis of the antigen recognition repertoire of CD8<sup>+</sup> T cells or in immunotherapies that strive to enhance a dysfunctional HIV-1 recall CD8<sup>+</sup> T cell response. Indeed, we have previously shown that DC stimulation reveals CD8<sup>+</sup> T cell responses to consensus MHC class I-restricted HIV-1 epitopes that were otherwise masked in subjects on cART (155). It is currently unclear if DC can also reveal responses to the subject's own, unique (autologous) virus, and if this DC enhancement changes with untreated and treated HIV-1 infection. As a successful immunotherapy will likely enhance the breadth and magnitude of the autologous HIV-1-specific T cell response (3, 37, 259), it is pertinent to ascertain the best method of detecting and enhancing these responses.

In the present study, we longitudinally evaluate recall T cell responses to autologous HIV-1 epitope variants at multiple pre- and post-cART time points. We use T<sub>reg</sub> depletion and DC addition to determine the best method of revealing and enhancing the HIV-1-specific response. While both methods enhanced the response at multiple time points, DC were more able to consistently reveal a response of high breadth and magnitude. Additionally, the ability of DC stimulation to reveal bifunctional and polyfunctional cytokine responses increased as subjects regained immunological function during cART. Taken together, the findings presented here demonstrate a unique ability of DC to reveal HIV-1-specific responses to a multitude of autologous epitope variants regardless of disease state and to enhance CD8<sup>+</sup> T cell cytokine profiles after long-

term treatment, thus supporting the use of these cells in an immunotherapy for HIV-1-infected subjects on cART.

### **3.3 METHODS**

#### **3.3.1 Study subjects**

Three HIV-1 infected subjects were chosen from the MACS, a natural history study of men who have sex with men for which the methodologies have been described previously (87, 171). Human subject approval was obtained from the University of Pittsburgh Institutional Review Board. These subjects were chosen based on their prolonged enrollment in the study (>10 years), typical course of disease progression, favorable response to combination antiretroviral therapy (cART), and the presence of at least one common HLA allele. Positivity for HLA A\*2402 was confirmed by high resolution PCR genotyping (Tissue Typing Laboratory, University of Pittsburgh Medical Center). All three subjects were enrolled in the MACS prior to seroconversion to HIV-1. Seropositivity was confirmed by positive enzyme-linked immunosorbent assay (ELISA) for the presence of HIV-1 p24 and a Western blot with bands corresponding to at least two of the Gag, Pol, and Env proteins (171). Blood specimens and epidemiological and clinical data were collected at each visit, as described previously (307). All three subjects progressed to AIDS as defined by the CDC ( $<200$  CD4<sup>+</sup> T cells/mm<sup>3</sup>) within 8.3 years after seroconversion. All three subjects received cART and maintained plasma HIV-1 RNA below 20 copies/ml at most post-ART visits.

### 3.3.2 Isolation of HIV-1 pre- and post-cART

Five post-seroconversion time points for S2 and S8, six post-seroconversion time points for S3, and one post-cART time point for S2 and S3 were chosen for HIV-1 *gag* p17-p6 and *env* gp120 sequencing. HIV-1 was obtained from freeze-thawed plasma for all pre-cART time points. Under cART, plasma viremia was reduced to <50 copies/ml in all subjects. We therefore used a previously described virus culture assay to induce HIV-1 production by latently-infected CD4<sup>+</sup> T cells obtained during cART (195, 311). Briefly, 1x10<sup>6</sup> CD4<sup>+</sup> T cells were isolated from cryopreserved PBMC obtained <2 years post-cART using a negative CD4<sup>+</sup> T cell enrichment kit per the manufacturer's instructions (STEMCELL Technologies Inc, Vancouver, BC). 1x10<sup>7</sup> fresh, irradiated PBMC from an HIV-1-negative donor were co-cultured with patient-derived CD4<sup>+</sup> T cells in IMDM supplemented with 10% heat-inactivated fetal bovine serum (FBS), 50 µg/ml gentamicin (Life Technologies, Carlsbad, CA), 100 U/ml IL-2 (Prometheus Labs, San Diego, CA), and 1 µg/ml PHA (Sigma-Aldrich, St. Louis, MO) at 37°C in a 5% CO<sub>2</sub> atmosphere. On day 2, 4x10<sup>6</sup> CD4<sup>+</sup> lymphoblasts that had been activated for 2 days with 100 U/ml IL-2 and 0.5 µg/ml PHA were added to the virus cultures. On day 7 and every 7 days thereafter, CD4<sup>+</sup> lymphoblasts were again added to the virus cultures, splitting cells and replenishing media as needed. The presence of HIV-1 in culture supernatants was evaluated every 3 days by p24 ELISA (Zeptometrix, Buffalo, NY). Cultures were terminated and supernatants were collected when the concentration of p24 reached or exceeded 20,000 pg/ml.



### 3.3.3 HIV-1 genetic sequencing

Viral RNA was manually extracted from plasma or cell culture supernatants using a viral RNA mini kit (Qiagen, Valencia, CA). cDNA synthesis was performed using Nef3 (TAAGTCATTGGTCTTAAAGGTACC) and RT2 (GTATGTCATTGACAGTCCAGC) primers with SuperScript III Reverse Transcriptase (200 U/ml; Invitrogen, Carlsbad, CA). Endpoint dilution methodology was used prior to viral gene amplification to avoid template resampling. Multiplex first-round PCR was performed with the Gag1 (GAGGCTAGAAGGAGAGAGATGG) and RT2 primers to amplify *gag* and the Ed3 (TTAGGCATCTCCTATGGCAGGAAGAAGCGG) and Nef3 (TAAGTCATTGGTCTTAAAGGTACC) primers to amplify *env*-gp120. Singleplex second round PCR was performed with Gag2 (GTGCGAGAGCGTCGGTATTAAGCG) and RSP15R (CAATTCCCCCTATCATTTTTGGTTTCC) primers for *gag* and Gp120 forward (GGCCGCGTCGACAAGAGCAGAAGACAGTGGCAATGA) and reverse (GGCCGCGGATCCGTGCTTCCTGCTGCTCCCAAGAAC) primers for *env*. PCR products were run on a QIAxcel automated electrophoresis system (Qiagen, Valencia, CA) and Sanger sequencing was performed on samples with positive bands (High Throughput Genomics Center, Seattle, WA). We obtained 5 to 36 unique *gag* sequences and 9 to 32 unique *env* sequences.

### 3.3.4 Identification of epitopes and peptide synthesis

Six HLA A\*24-restricted HIV-1 Gag and Env epitopes were identified for each subject using the Los Alamos Database (<http://www.hiv.lanl.gov>). The combined epitope prediction model within The Immune Epitope Database (260, 319) was used to identify seven additional

predicted A\*2402-restricted epitopes within autologous sequences from the three study subjects. This prediction model ranks potential epitopes within an input sequence based on predicted proteasomal cleavage, TAP transport, and MHC class I affinity using the netMHCpan prediction method (151, 260, 319). A PEPscreen custom library representing the epitope variants that evolved in each study subjects was synthesized (Sigma-Aldrich). Each peptide was resuspended in 100 $\mu$ l DMSO and further resuspended in AIM V at a final concentration of 1 mg/ml or 100  $\mu$ g/ml. Peptides were stored at -80°C.

### **3.3.5 T<sub>reg</sub> depletion**

To investigate the effects of regulatory T cells (T<sub>reg</sub>) on HIV-1-specific CD8<sup>+</sup> T cell responses, cryopreserved PBMC were thawed and depleted of T<sub>reg</sub> using a T<sub>reg</sub> CD4<sup>+</sup>CD25<sup>+</sup> two-step isolation kit per the manufacturer's instructions (Miltenyi Biotec, Gladbach, Germany). This column-based kit uses magnetic beads to first isolate CD4<sup>+</sup> T cells via negative selection and then isolate CD25<sup>+</sup> T cells from within the CD4<sup>+</sup> subset via positive selection. The labeled CD4 negative cells from the first separation were resuspended in the recommended assay buffer and rested at 4°C. Following positive isolation and removal of CD4<sup>+</sup>CD25<sup>+</sup> T cells from the CD4<sup>+</sup> subset, the CD4 negative population and the CD4<sup>+</sup> non-T<sub>reg</sub> population were reconstituted to generate the T<sub>reg</sub><sup>neg</sup> PBMC condition. To account for any potential effects this isolation procedure may have on T cell function, the CD4<sup>+</sup> negative bead selection was performed on the PBMC condition, after which all subsets were reconstituted.

### 3.3.6 PBMC and T<sub>reg</sub> staining

To determine T<sub>reg</sub> frequency in peripheral blood and the efficiency of T<sub>reg</sub> depletion, aliquots from T<sub>reg</sub><sup>neg</sup> PBMC, PBMC before magnetic bead selection, and PBMC after reconstitution were stained for cell surface markers and intracellular FoxP3. Cells ( $5 \times 10^4$ ) were resuspended in 100  $\mu$ l PBS with 1  $\mu$ l LIVE/DEAD Aqua Viability Dye (Invitrogen, Carlsbad, CA) and incubated for 30 minutes at room temperature in the dark. Cells were washed and resuspended in 100  $\mu$ l PBS and stained with CD3-APC, CD4-APC-Cy7, CD8-PerCP-Cy5.5, CD39-PE-Cy7, and CD25-PE (all BD Pharmingen). Cells were washed twice and resuspended in 100  $\mu$ l Cytofix/Cytoperm (BD Biosciences, San Jose, CA) and incubated for 20 minutes at 4C. Cells were again washed and then stained for intracellular FoxP3 expression using a FoxP3 staining kit per the manufacturer's instructions (Biolegend, San Diego, CA). Briefly, cells were resuspended in 100  $\mu$ l FOXP3 Fix/Perm solution and incubated at room temperature in the dark for 20 minutes. Cells were washed once with PBS and once with 1X FOXP3 Perm Buffer. Cells were resuspended in 1ml of 1X FOXP3 Perm Buffer and incubated at room temperature in the dark for 15 minutes. Cells were again washed and incubated with 100  $\mu$ l 1X FOXP3 Perm Buffer with 3  $\mu$ l FOXP3-AlexaFluor488 for 30 minutes at room temperature in the dark. Following two washes with PBS, cells were resuspended in 0.5ml PBS and analyzed on a BD LSR Fortessa flow cytometer using BD FACSDiva software. Graphs displaying flow cytometry data were generated using FLOWJo version 9.6.4 (Ashland, OR).

### 3.3.7 Generation of monocyte-derived dendritic cells (DC)

Leukapheresis was performed on each study subject while under cART to obtain PBMC. Monocytes were isolated from PBMC by Percoll (GE Healthcare Life Sciences, Uppsala, Sweden) density separation. Immature DC were generated by culturing monocytes in IMDM containing 10% FBS with GM-CSF and IL-4 (both 1000 U/ml; R&D Systems, Minneapolis, MN). On day 5, immature DC were treated with 0.5 µg/ml soluble CD40L (Enzo, Farmingdale, NY) for 48h. Maturation status of the DC was confirmed by expression of CD83, CD86, and CCR7 as determined by flow cytometry.

### 3.3.8 IFN-γ ELISpot assay

IFN-γ production was measured by a standard overnight ELISpot assay. Briefly, 96-well nitrocellulose plates (EMD Millipore, Billerica, MA) were coated with anti-IFN-γ monoclonal antibody (10 µg/ml; Mabtech, Stockholm, Sweden) and incubated overnight at 4°C. Plates were washed and blocked with IMDM supplemented with 10% heat-inactivated FBS for 2h at 37°C. PBMC or T<sub>reg</sub><sup>neg</sup> PBMC (1x10<sup>5</sup>/well) were tested in singlet or duplicate for reactivity to peptides representing the autologous HIV-1 epitope variants that had evolved before and at the time point of PBMC sampling. Responders were stimulated overnight at 37°C with peptide alone (5µg/ml) or 1x10<sup>4</sup> autologous DC pre-pulsed with peptide (5 µg/ml) in IMDM supplemented with 10% heat-inactivated FBS. Responders in media alone or with DC alone served as negative controls and a peptide pool consisting of CMV, EBV, and flu (CEF) peptides was used as a positive control for all responder conditions. ELISpot plates were washed and processed as described previously (67, 156). Spots were counted using an automated ELISpot plate reader (AID, Straßberg, Germany)

and are shown as the number of background-subtracted antigen-specific spot-forming cells (SFC) per  $10^6$ . Background was calculated as the mean number of SFC/ $10^6$  in duplicate control wells without peptide plus 2 standard deviations.

### **3.3.9 Intracellular cytokine staining**

PBMC were also evaluated for polyfunctional cytokine secretion in response to peptide alone or peptide-loaded DC. PBMC obtained from each subject during late infection (<1 year pre-cART), early cART (first post-cART visit with HIV-1 viral load <50 copies/ml), and late cART (>15 years post-cART) were thawed and resuspended in AIM V with CD28/CD49d FastImmune™ co-stimulatory reagent (BD Biosciences), Golgistop (BD Biosciences), and Golgiplug (BD Biosciences). Peptides representing variants of known HLA A\*24 HIV-1 Gag and Env epitopes that were in circulation at the time of PBMC sampling (“contemporaneous variants”) were added to PBMC or pre-loaded into DC before adding to PBMC at a final concentration of 5  $\mu\text{g/ml}$ . Cells were incubated for 6h at 37°C, washed with PBS, and stained with LIVE/DEAD Aqua Viability Dye (Invitrogen) for 30 minutes at room temperature in the dark. Cells were washed and stained for surface expression of CD3-PE-TexasRed (Invitrogen), CD4-APC (BD Biosciences), and CD8-APC-Cy7 (BD Biosciences). Cells were again washed and fixed with 100  $\mu\text{l}$  Cytofix/Cytoperm (BD Biosciences) and then incubated with 1X Perm/Wash buffer (BD Biosciences) for 30 minutes at room temperature in the dark. Cells were washed and resuspended in 50  $\mu\text{l}$  1X Perm/Wash buffer containing IFN- $\gamma$ -Alexa Fluor 700 (BD Pharmingen), TNF- $\alpha$ -eFluor 450 (eBioscience), and MIP-1 $\beta$ -APC (BD Pharmingen) and incubated for 20 minutes at room temperature in the dark. Cells were washed, resuspended in PBS, and analyzed on a BD LSR

Fortessa flow cytometer using BD FACSDiva software. Data were analyzed using Flow Jo version 9.6.4.

### **3.3.10 Statistical analyses**

Comparisons between the percent of epitopes with variants of higher, lower, or higher and lower affinity were performed using a repeated measures one-way ANOVA, while the comparison between the percent of variants with higher or lower affinity than the founder were performed using student's T test. Evaluation of the differences in IFN $\gamma$  production between T cell conditions at longitudinal time points was performed using a two-way ANOVA with Sidak's multiple comparisons post-test. Paired T tests were used to compare cytokine secretion with and without the addition of DC. All graphs and statistical analyses were generated using GraphPad Prism 6 (GraphPad Software, Inc., La Jolla, CA).

## **3.4 RESULTS**

### **3.4.1 Changes in HIV-1 Gag and Env epitopes in chronic infection**

A proposed mechanism by which infected subjects fail to control HIV-1 replication is the lack of cytotoxic T lymphocytes (CTL) that recognize the patient's own, unique virus ("autologous virus"), presumably due to mutations within CTL epitopes that ablate MHC class I affinity and/or T cell recognition (58, 165). We therefore aimed to longitudinally assess the changes in predicted MHC class I affinity of Gag and Env epitope variants derived from autologous HIV-1 sequences.

We chose 3 subjects from the Multicenter AIDS Cohort Study (MACS) who share the HLA A\*2402 allele, received and responded to combination antiretroviral therapy (cART), and are still enrolled in the study. In subjects S2, S3, and S8 there was a gradual rise in HIV-1 plasma viremia and CD8<sup>+</sup> T cells and a decline in CD4<sup>+</sup> T cells concordant with progression to AIDS (<200 CD4<sup>+</sup> T cells/mm<sup>3</sup>), indicating typical patterns of disease progression.

Autologous HIV-1 was sequenced from plasma obtained from 5 to 6 post-seroconversion, pre-cART time points in all three subjects. Additionally, HIV-1 was isolated from CD4<sup>+</sup> T cells at one post-cART time point in subjects S2 and S3. We were unable to isolate autologous HIV-1 from CD4<sup>+</sup> T cells in subjects S8, potentially due to the low HIV-1 viral load exhibited in this subject at all stages of disease progression. The source of autologous HIV-1 likely did not affect the resulting sequences, as virus recovered from plasma was shown to be identical to virus obtained from CD4<sup>+</sup> T cells (13). We performed single genome HIV-1 *gag* and *env* gp120 sequencing on the autologous virus obtained from each subject at each time point. Nucleotide sequences were translated to their corresponding amino acid sequences. We identified 6 known Gag and Env HLA A\*2402-restricted epitopes using The Los Alamos Database (<http://www.hiv.lanl.gov/content/immunology>) and 7 predicted epitopes using the Immune Epitope Database combined predictor with the netMHCpan MHC class I prediction method (151, 260, 319). We then identified the variants of these epitopes that evolved in each subject throughout infection. The epitopes studied and the variants that evolved *in vivo* are shown in **Table 5**. Interestingly, not all epitopes evolved throughout infection, despite each subject being infected for >7 years without receiving cART. Of note, the Gag p24 AFSPEVIPMF and DYVDRFYKT epitopes did not evolve in any of the subjects throughout infection. In Gag p17 NYPIVQNI, Gag

p24 IYKRWIILGL, and Env gp120 LYKYKVVKI, amino acid changes were observed in only 1 out of the 3 subjects.



**Table 5. HIV-1 Gag and Env epitope variants that evolved throughout infection**

Epitope location <sup>a</sup>	Amino acid sequence <sup>b</sup>	Subject <sup>c</sup>	Autologous variant sequence <sup>d</sup>	Time of evolution (YPS) <sup>e</sup>	Predicted MHC class I affinity (nM) <sup>f</sup>	Epitope location <sup>a</sup>	Amino acid sequence <sup>b</sup>	Subject <sup>c</sup>	Autologous variant sequence <sup>d</sup>	Time of evolution (YPS) <sup>e</sup>	Predicted MHC class I affinity (nM) <sup>f</sup>			
Gag p17 <sub>28-36</sub>	<b>KYKCLKHIVW</b>	S2	KYKCLKHIVW	0.2	954.7	Env gp120 <sub>52-61</sub>	<b>LFCASDAKAY</b>	S2	<u>LFCASDAKAY</u>	0.2	29256.5			
			KYELKHKHIVW	0.2	738.1				<u>LFCASDAKAY</u>	0.2	29256.5			
			KYQLKHKHIVW	0.2	155.3				S3	<u>LFCASDAKAY</u>	0.2	29256.5		
			<u>KYRLKHKHIVW</u>	1.2	1164.5				S8	LFCASDARAY	0.5	27869.6		
	S3	KYKCLKHIVW	0.2	954.7	<u>LFCASDAKAY</u>		5.0	29256.5	Env gp120 <sub>158-165</sub>	SFNISTS	S2	TFNITTSI	0.2	1515.1
		<u>OYKCLKHIVW</u>	0.2	1616.7	<u>TFNITTSI</u>		9.6	1382.9						
		RKYLKHKHIVW	2.5	561.2	S3		<u>TFNITTSI</u>	0.2			1321.7			
		<u>RYRLKHLVW</u>	0.5	233.0	S8		<u>TFNITTSI</u>	5.3			3088.4			
	S8	<u>KYRLKHLVW</u>	5.0	432.5	Env gp120 <sub>168-176</sub>		KVQKEYAFF	S2	KMQKEYALF	0.2	17.9			
		RFAVNPGLL	0.2	626.9	<u>KVQKEYALF</u>				3.4	139.7				
		<u>RFAVNPGLL</u>	3.4	245.9	S3				KVQKEYALF	0.2	139.7			
		RFAVNPGLI	0.5	293.8	<u>KVQKEHALF</u>				2.5	394.3				
Gag p17 <sub>43-51</sub>	RFAVNPGLL	S2	RFAVNPGLL	0.2	626.9	KVQKEYALF	5.3	159.8						
			<u>RFAVNPGLL</u>	3.4	245.9	<u>KVQKERALF</u>	5.3	1054.2						
			RFAVNPGLI	2.4	626.9	<u>KVRQKEYALF</u>	5.3	768.5						
			<u>RFAVNPGLM</u>	2.4	1246.9	S8	KMKGEYAFF	0.5	157.9					
RFAVNPGLI	0.5	293.8	<u>KMKREYAFF</u>	0.5	132.5									
<u>RFAVNPGLL</u>	2.4	626.9	KIKREYAFF	2.4	1141.8									
RFAVNPGLM	2.4	1246.9	KIKREYAAF	5.0	3502.7									
Gag p17 <sub>131-132</sub> /p24 <sub>1-6</sub>	NYPIVQNI	S2	NYPIVQNI	0.2	74.0	KIKREYATF	5.0	1256.3						
			<u>NYPIVQNL</u>	9.6	214.7	KRKREYATF	5.0	7219.6						
		S3	<u>NYPIVQNL</u>	0.2	214.7	KRRREYATF	6.6	9284.2						
			<u>NYPIVQNL</u>	0.5	214.7	Env gp120 <sub>311-320</sub>	RGPGRAFVTI	S2	MGPGGAFYAT	0.2	26383.6			
		S8	<u>NYPIVQNL</u>	0.5	214.7				<u>IGPGRAFYAT</u>	3.4	27231.5			
			Gag p24 <sub>31-40</sub>	AFSPEVIPMF	S2			<u>AFSPEVIPMF</u>	0.2	274.3	S3	IGPGRAFYAT	0.2	27231.5
<u>AFSPEVIPMF</u>	0.2	274.3						<u>IGPGRAFYAA</u>	6.4	19176.8				
Gag p24 <sub>129-138</sub>	IYKRWILGL	S2	IYKGWILGL	0.2	107.3	S8	<u>IGPGRAFYTT</u>	0.5	21484.4					
			<u>IYKRWILGL</u>	0.2	78.9		IGPGGAFYTT	2.4	21701.3					
		<u>IYKRWILGL</u>	0.2	78.9	IGPGRAFYAT		5.0	27231.5						
		<u>IYKRWILGL</u>	0.5	78.9	Env gp120 <sub>383-391</sub>		FYCNSTQLF	S2	<u>FYCNTTQLF</u>	0.2	8.9			
Gag p24 <sub>163-171</sub>	DYVDRFYKT	S2	<u>DYVDRFYKT</u>	0.2		19856.1			FYCNTTPLF	3.4	13.8			
			S3	<u>DYVDRFYKT</u>		0.2		19856.1	FYCNTTKLF	9.6	34.9			
S8	<u>DYVDRFYKT</u>	0.5		19856.1		FYCSTKQLF		9.6	21.7					
	Gag p24 <sub>129-138</sub>	IYKRWILGL	S2	<u>IYKRWILGL</u>		0.2		78.9	S3	FYCNSTQLF	0.2	11.5		
<u>IYKRWILGL</u>				0.2		78.9		FYCNTTQLF		1.5	8.9			
<u>IYKRWILGL</u>				0.2	78.9	FYCNTAQLF	2.5	11.9						
<u>IYKRWILGL</u>				0.5	78.9	FYCNTTKLF	5.3	35.0						
S3			<u>IYKRWILGL</u>	0.2	78.9	FYCDTTKLF	5.3	80.0						
			<u>IYKRWILGL</u>	0.5	78.9	<u>FYCNTTRLF</u>	8.3	28.5						
			<u>IYKRWILGL</u>	0.5	78.9	FYCNTTHLF	8.3	6.0						
			<u>IYKRWILGL</u>	0.5	78.9	S8	FYCNTAQLF	0.5	11.9					
<u>IYKRWILGL</u>			0.5	78.9	FYCNTTQLF		2.4	8.9						
<u>IYKRWILGL</u>			0.5	78.9	<u>FYCNTSOLE</u>		2.4	9.4						
<u>IYKRWILGL</u>			0.5	78.9	Env gp120 <sub>434-443</sub>		MYAPPISGQI	S2	MYAPPISGQI	0.2	89.0			
S3			MYAPPISGLI	0.2		21.4								
	MYAPPISGQI	1.2	121.0	MYAPPISGLI		5.3		41.0						
MYAPPISGLI	8.3	52.9	MYAPPISGVI	5.0		46.8								
MYAPPISGLI	8.3	82.5	Env gp120 <sub>483-491</sub>	LYKYKVVKI	S2	<u>LYKYKVVKI</u>	0.2	301.8						
MYAPPISGLI	8.3	82.5				S3	LYKYKVVKI	0.2	301.8					
MYAPPISGLI	8.3	82.5			<u>LYKYKVVEI</u>	8.3	237.6							
MYAPPISGLI	8.3	82.5			S8	<u>LYKYKVVKI</u>	0.5	301.8						

<sup>a</sup>HXB2 location of each HIV-1 epitope within the Gag p17 and p24 (left table) and Env gp120 (right table) proteins

<sup>b</sup>HXB2 consensus amino acid sequences for known and predicted HLA A\*2402-restricted HIV-1 Gag and Env epitopes. Known epitopes as identified by the Los Alamos Database are in bold. Non-bolded sequences show the HXB2 sequence of regions predicted to be CTL epitopes in autologous sequences derived from all three subjects. Predicted epitopes were identified using the Immune Epitope Database combined predictor, which assigns an overall score taking into account MHC class I affinity, proteasomal processing, and TAP affinity.

<sup>c</sup>Subjects S2, S3, and S8 were chosen from the Multicenter AIDS Cohort Study for analysis.

<sup>d</sup>Autologous epitope variants were identified by single-genome gag p17-p6 and env gp120 sequencing of autologous HIV-1 derived from plasma at 5 to 6 pre-cART time points and 1 post-cART time point in subjects S2 and S3. Underlined variants were the dominate form of the epitope (>55% of the variant pool) that was observed at the last pre-cART time point.

<sup>e</sup>The time at which the epitope variant was detected by single genome sequencing. YPS, years post-seroconversion.

<sup>f</sup>Predicted affinity for HLA A\*2402 as determined using netMHCpan. A lower value indicates a higher predicted affinity. nM, nanomolar

Previous studies have suggested that the failure of CTL to be generated against HIV-1 variants in chronic infection is due to amino acid mutations within CTL epitopes that ablate epitope affinity for MHC class I (58, 165). Surprisingly, not all variants had a lower predicted affinity for the HLA A\*2402 molecule in comparison to the founder variant that was present at the first post-seroconversion time point. Of the 9 epitopes that contained amino acid changes in subject S2, 5 evolved to variants with lower predicted MHC class I affinity, 3 evolved to variants with higher predicted affinity, and 1 evolved to variants with higher and lower predicted affinity (**Table 5**). In subject S3, 8 epitopes contained mutations, of which 4 evolved to variants with lower predicted affinity, 3 evolved to variants with higher predicted affinity, and 1 evolved to variants with higher and lower predicted affinity. Of the 7 epitopes that contained amino acid changes in subject S8, 5 evolved to variants with lower predicted affinity and 2 evolved to variants with higher predicted affinity. When data from the three subjects were combined, an average of 59% of epitopes only contained variants with lower affinity than the founder, whereas 33.1% only contained variants with higher MHC class I affinity, and 7.9% of epitopes contained variants with higher and lower predicted affinity (**Figure 14A**).

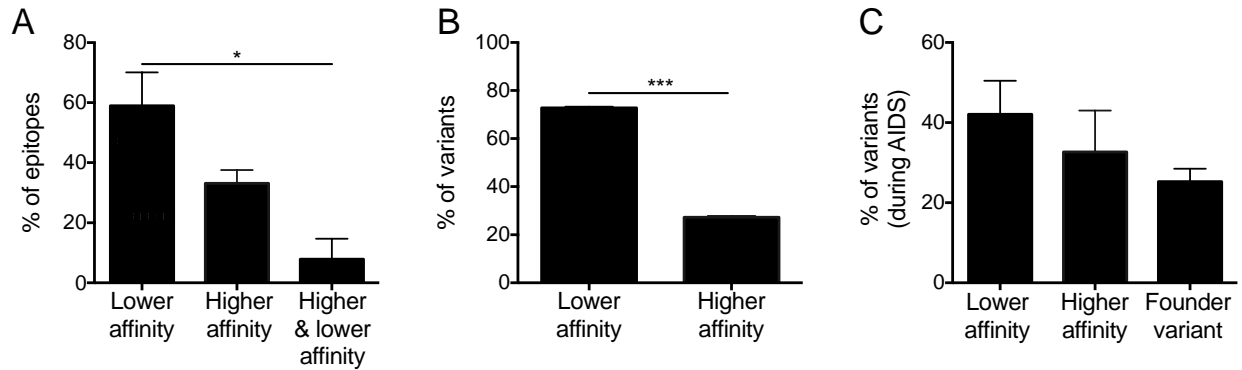


**Figure 14. The effects of amino acid substitutions on predicted MHC class I affinity in autologous HIV-1 HLA A\*2402-restricted epitope variants**

Autologous variants of known and predicted epitopes were identified by single genome sequencing of plasma HIV-1 in subjects S2, S3, and S8 (shown in Table 4). Predicted affinity for HLA A\*2402 was determined using netMHCpan (151, 241). (A) The percent of mutated epitopes that acquired variants with lower, higher, or lower and higher predicted MHC class I affinity than the founder variants present at the first post-seroconversion time point. (B) The percent of epitope variants within each subject that were of lower and higher predicted MHC class I affinity than the founder variants. (C) The percent of variants in circulation during AIDS that were of lower or higher predicted MHC class I affinity than the founder or the percent of variants that were the same as the founder. Data are shown as the mean of the three subjects +/-SD. \* $p < 0.05$ , \*\*\* $p < 0.001$

There was a significant difference between the three groups ( $p=0.03$ ), but post test comparisons only showed a significant difference between the percent of epitopes that contained variants with lower MHC class I affinity and the percent that contained variants with both patterns of affinity ( $p=0.04$ ). Despite the lower percent of epitopes that contained variants with higher MHC class I affinity, this was not significantly different from the percent containing lower-affinity variants ( $p=0.10$ ). When we combined all variants from each subject, we observed significantly more lower-affinity variants than those with higher predicted affinity ( $p=0.0002$ ) (**Figure 14B**).

Despite these variable patterns of predicted MHC class I affinity within autologous epitope variants, it is possible that the variants with higher predicted affinity did not make up a large percentage of the variants in circulation in the end stages of disease progression. It could be argued that, while variants with higher affinity evolved throughout infection, they were only transient blips and were not representative of the dominating, “escape” variant that persisted while subjects

progressed to AIDS. To address this concern, we determined the frequency of each variant within its cognate epitope at the last pre-cART time point in subjects S2, S3, and S8, at which point all three subjects had AIDS as defined by the CDC ( $CD4^+$  T cell count  $<200$  cells/mm<sup>3</sup>). We were able to identify the variant that made up  $>55\%$  of the epitopic pool and determined this to be the “dominant” variant at that time point (**Table 5**). When the subjects were averaged, 42.1% of the dominant variants during AIDS were of lower predicted MHC class I affinity than the founder variant, with 32.7% having a higher predicted affinity, and 25.3% were the founders that maintained dominance despite the evolution of other variants (**Figure 14C**). No significant difference was observed between these two groups, indicating variants with lower MHC class I affinity were not specifically selected for during progression to AIDS.

### **3.4.2 Longitudinal T cell responses to autologous HIV-1 epitope variants**

To identify the impact of amino acid substitutions within CTL epitopes on T cell responses, we synthesized the variants shown in **Table 5** and used them to stimulate autologous PBMC obtained from the time points at which sequences were derived. PBMC were tested against all autologous epitope variants that had evolved by the time of PBMC sampling. For subject S8, PBMC from the two post-cART time points were tested against the variants that had evolved by the last pre-cART time point. For subjects S2 and S3, PBMC from the last post-cART time point were tested for reactivity to variants that had evolved by the first post-cART time point. For each subject, there were 5 to 6 pre-cART time points, one early post-cART time point ( $<0.5$  years post-cART), and one late post-cART time point ( $>15$  years post-cART) evaluated for T cell responses.

In subject S2, we evaluated 5 pre-cART, one early post-cART (10.1 years post-seroconversion; <0.5 years post-cART), and one late post-cART (25.9 years post-seroconversion; >15 years post-cART) time point. IFN $\gamma$  responses of varying magnitude were detected to 100% of the variants at at least one time point (**Figure 15**). Variants of known Gag epitopes induced moderate to robust responses 0.2 years post-seroconversion, but these responses waned with disease progression and slightly rebounded 25.9 years post-seroconversion (**Figure 15A**). A similar trend was observed in the responses to variants of predicted Gag epitopes, with early responses waning and a partial rebound at the last time point (**Figure 15B**). IFN $\gamma$  production in response to variants of known Env epitopes was low throughout infection but was revealed 25.9 years post-seroconversion during late post-cART (**Figure 15C**), while variants of predicted Env epitopes induced T cell responses that waned by 9.6 years post-seroconversion and rebounded at the last time point (**Figure 15D**). Of note, no differences were observed in the IFN $\gamma$  production against known and predicted epitope variants nor between Gag and Env variants at any time point, suggesting responses were generated equally against the two proteins and our prediction methods may have accurately identified new A\*2402-restricted HIV-1 epitopes.

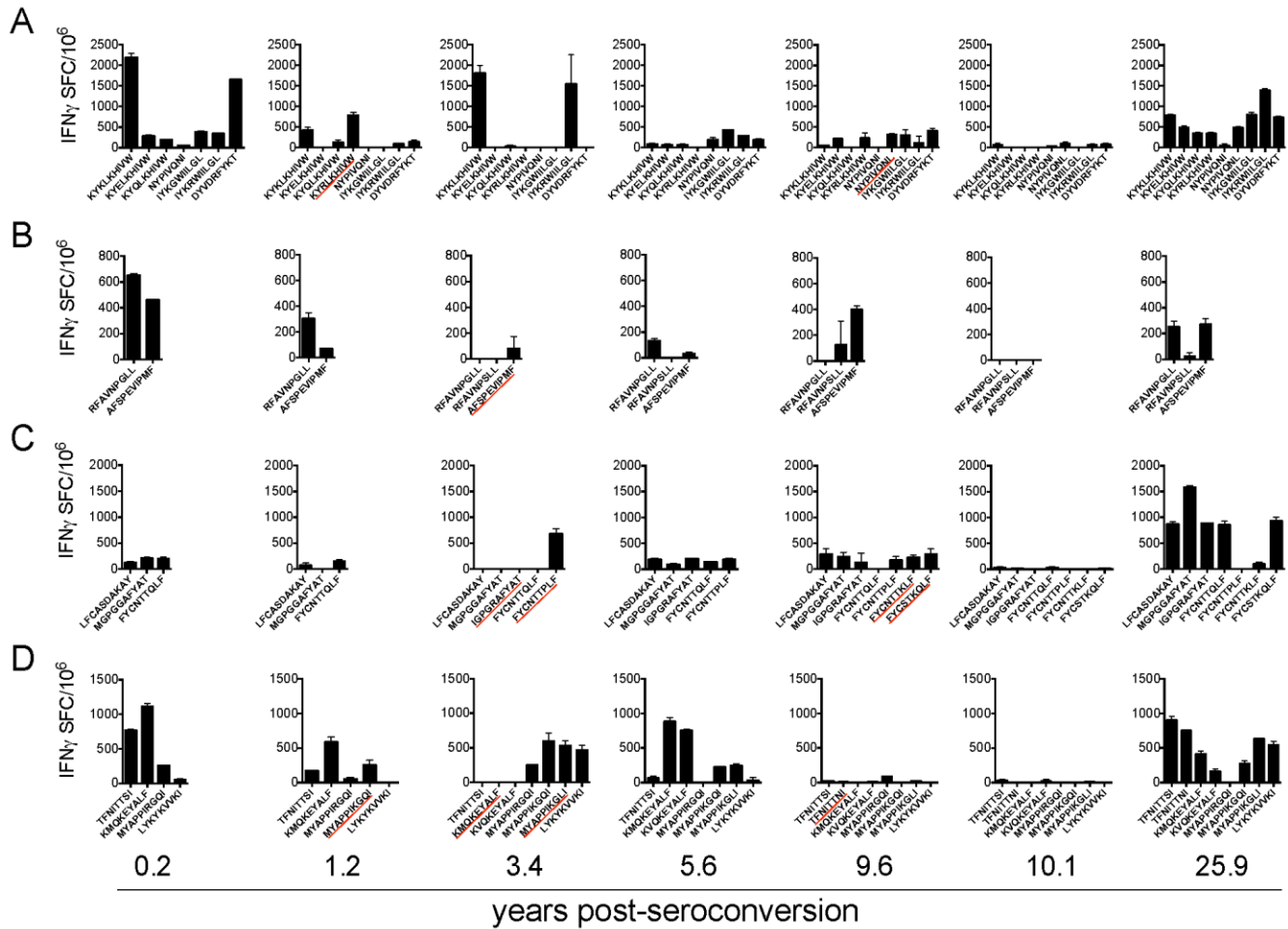


**Figure 15. PBMC responses to autologous HIV-1 epitope variants in subject S2**

PBMC were tested by IFN $\gamma$  ELISpot for reactivity to autologous variants of known (A) and predicted (B) Gag epitopes and known (C) and predicted (D) Env epitopes. Each graph represents the responses observed at each post-seroconversion time point. Variants are shown in the order of their evolution. 10.1 and 25.9 years post-seroconversion are post-cART time points. Data are shown as the mean number of spot forming cells (SFC) above background per  $10^6$  PBMC. Background was calculated as the mean number of SFC with PBMC alone plus 2 standard deviations. Error bars represent the standard deviation of duplicate wells. Variants underlined in red were detected for the first time at the corresponding time point.

In subject S3, we analyzed 6 pre-cART time points, an early post-cART time point (8.8 years post-seroconversion, <0.5 years post-cART), and a late post-cART time point (23.5 years post-seroconversion, >15 years post-cART) for T cell responses to autologous HIV-1 peptide epitopes (**Figure 16**). Responses to variants of known and predicted Gag epitopes were detected prior to cART but were lost early post-cART. As seen in subject S2, these responses rebounded

after long-term cART (**Figure 16A-B**). A similar trend was seen in T cell responses to variants of known and predicted Env epitopes, whereby responses of moderate magnitude were detected to all variants pre-cART, with a loss of responses early post-cART and restoration late post-cART (**Figure 16C-D**). Of note, responses were detected to all founder variants and the supposed “escape” variants that evolved throughout infection, albeit at only a moderate magnitude. No significant differences were observed between responses detected against Gag and Env variants or between variants of known and predicted epitopes (data not shown).

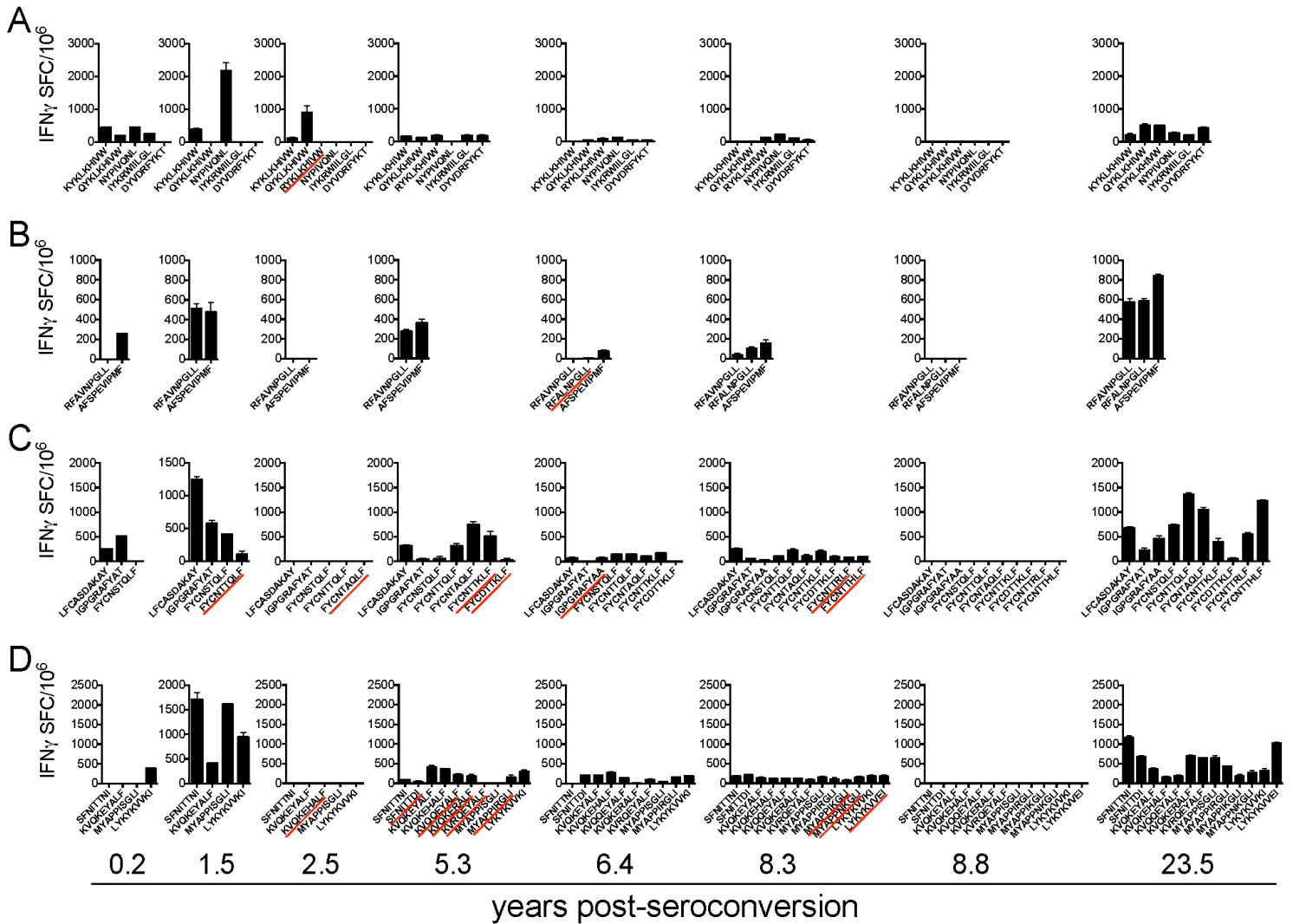


**Figure 16. PBMC responses to autologous HIV-1 epitope variants in subject S3**

PBMC were tested by IFN $\gamma$  ELISpot for reactivity to autologous variants of known (A) and predicted (B) Gag epitopes and known (C) and predicted (D) Env epitopes. Each graph represents the responses observed at each post-seroconversion time point. Variants are shown in the order of their evolution. 8.8 and 23.5 years post-seroconversion are early post-cART and late post-cART time points, respectively. Data are shown as the mean number of spot forming cells (SFC) above nonspecific background per 10<sup>6</sup> PBMC, +/- standard deviation from duplicate wells. Variants underlined in red were detected for the first time at the corresponding time point.

In subject S8, we evaluated PBMC responses at 5 pre-cART time points, one early post-cART time point (8.0 years post-seroconversion, <0.5 years post-cART), and one late post-cART time point (20.5 years post-seroconversion, ~13.0 years post-cART). T cell responses were detected to all autologous epitope variants except the KIKREYATF variant, with the breadth of



responses being most prominent 20.5 years post-seroconversion (**Figure 17**). Responses to variants of known and predicted Gag epitopes were minimal 0.5 years post-seroconversion, but increased by 1.4 years post-seroconversion (**Figures 17A and B**). The detection of responses was sporadic at the remaining time points, with responses to all Gag epitope variants detected during late post-cART. A similar trend was observed in T cell responses to variants of known and predicted Env epitopes (**Figures 17C and D**), with minimal responses detected 0.5 years post-seroconversion, variable responses at the remaining time points, and the number of variants recognized peaking late post-cART. No significant differences were observed in IFN $\gamma$  ELISpot responses against variants of known or predicted epitopes, nor between variants from Gag and Env.

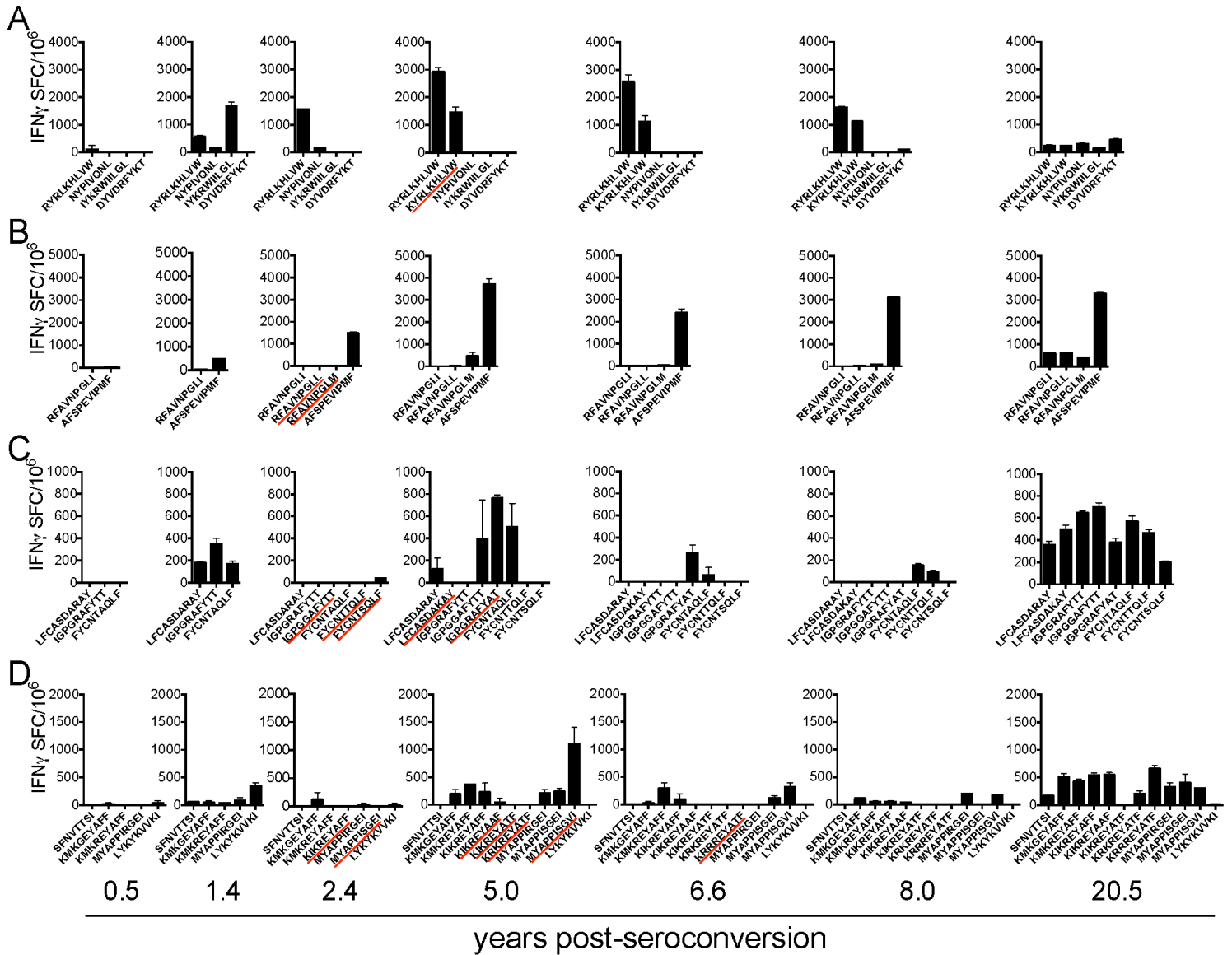


**Figure 17. PBMC responses to autologous HIV-1 epitope variants in subject S8**

PBMC were tested by IFN $\gamma$  ELISpot for reactivity to autologous variants of known (A) and predicted (B) Gag epitopes and known (C) and predicted (D) Env epitopes. Each graph represents the responses observed at each post-seroconversion time point. Variants are shown in the order of their evolution. 8.0 and 20.5 years post-seroconversion are early post-cART and late post-cART time points, respectively. Data are shown as the mean number of spot forming cells (SFC) above nonspecific background per 10<sup>6</sup> PBMC, +/- standard deviation from duplicate wells. Variants underlined in red were detected for the first time at the corresponding time point.

IFN $\gamma$  ELISpot data from these three subjects show PBMC responses were generated to autologous HIV-1 Gag and Env epitope variants, albeit at varying levels throughout infection with minimal magnitude. There were mostly no differences between T cell responses detected against

Gag and Env epitope variants, nor against variants of known and predicted epitopes. Interestingly, there were also no differences between the responses detected to variants that were of higher or lower predicted MHC class I affinity than the founder variant, and there was no correlation between predicted affinity and IFN production at any time point in any of the subjects (data not shown). While most of the epitopes evolved to produce at least one variant, T cell responses were still detected, indicating the epitope did not fully escape T cell recognition.

### **3.4.3 The effects of regulatory T cells on HIV-1-specific responses**

Regulatory T cells ( $T_{reg}$ ) are a  $CD4^+$  subset that suppress antigen-specific responses and could possibly impede an effective anti-HIV T cell response. Additionally, the loss of  $CD4^+$  T cells in chronic HIV-1 infection could contribute to enhanced immune activation. To longitudinally identify the effects of  $T_{reg}$  on responses specific for autologous HIV-1 epitope variants in chronic and treated infection, we combined the PBMC responses shown in figures 13, 14, and 15 for subjects S2, S3, and S8, respectively, to generate an average response to all variants tested at each time point. We then compared these responses to those detected in PBMC depleted of  $T_{reg}$  ( $T_{reg}^{neg}$  PBMC) at the same time points. The  $T_{reg}$  depletion method was successful at removing  $> 80\%$  of  $CD4^+CD25^+$  T cells and increased the frequency of  $CD8^+$  T cells by  $<4\%$  (**Appendix B, figure 57**).

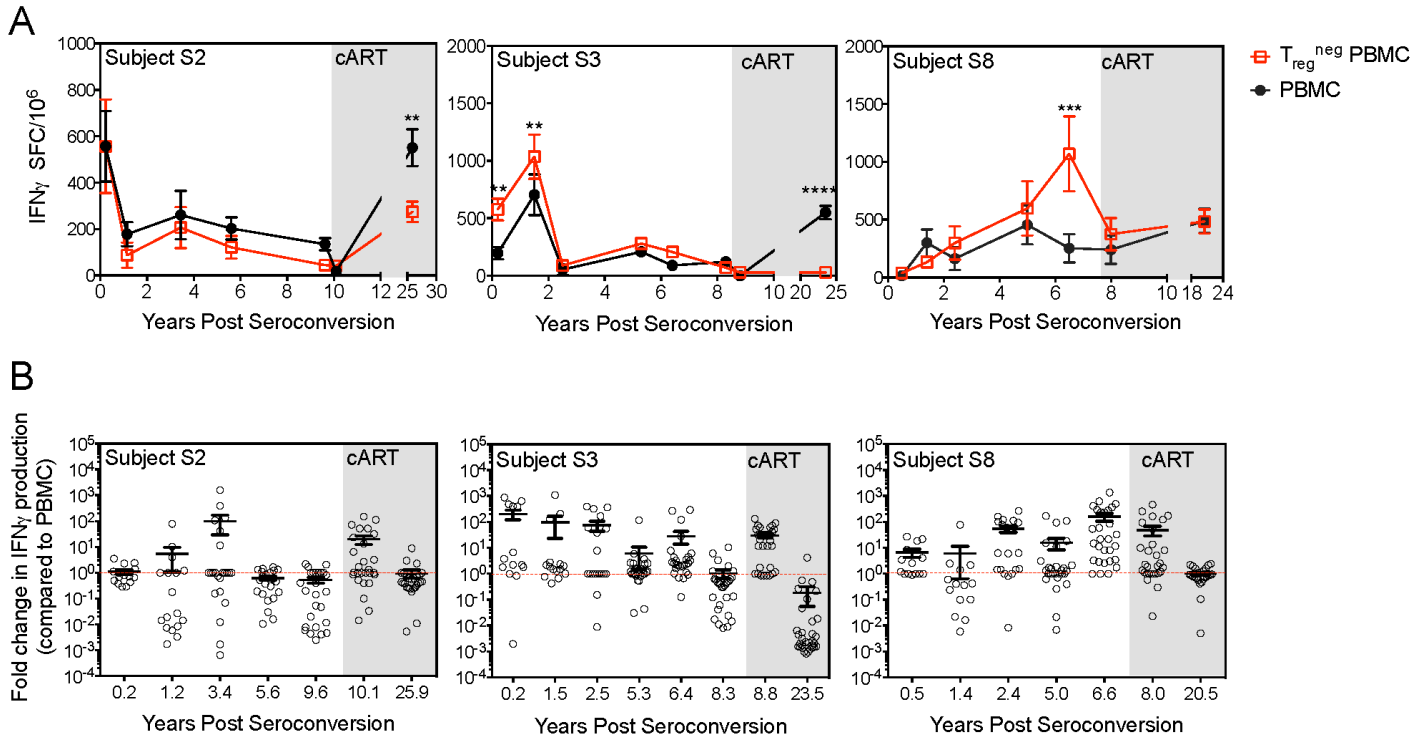


**Figure 18. Longitudinal responses to autologous HIV-1 epitope variants in PBMC and T<sub>reg</sub><sup>neg</sup> PBMC**

PBMC were depleted of T<sub>reg</sub> and evaluated by IFN $\gamma$  ELISpot for responses against the autologous HIV-1 Gag and Env epitope variants that had evolved by each time point. (A) Responses to autologous HIV-1 epitope variants detected in PBMC (filled black circle) were averaged at each time point and compared to those detected in T<sub>reg</sub><sup>neg</sup> PBMC (red square) to the same variants. The mean response of all variants  $\pm$  SEM is shown at each time point for subjects S2 (left panel), S3 (middle panel), and S8 (right panel). Responses are shown as spot-forming cells (SFC) per 10<sup>6</sup>. (B) The fold change in IFN $\gamma$  production of T<sub>reg</sub><sup>neg</sup> PBMC compared to PBMC is shown at each time point. Open circles represent the fold change detected in an individual epitope variant. Error bars represent the mean fold change  $\pm$  SEM. The dashed red line is shown to mark a fold change of 1, or no change in response. Post-cART time points are indicated by the gray box. \* $p < 0.05$ , \*\* $p < 0.01$ , \*\*\* $p < 0.001$ , \*\*\*\* $p < 0.0001$ .

In subject S2, the mean PBMC response decreased from 557 SFC/10<sup>6</sup> 0.2 years post-seroconversion to 178 SFC/10<sup>6</sup> 1.2 years post-seroconversion, but had little variation at the remaining pre-cART time points (**Figure 18A, left panel**). Early post-cART, the mean PBMC response dropped to 18 SFC/10<sup>6</sup> PBMC and rebounded late post-cART (25.9 years post-seroconversion) to 551 SFC/10<sup>6</sup> PBMC. T<sub>reg</sub><sup>neg</sup> PBMC responses mirrored this pattern throughout infection and were not significantly higher than the PBMC response at any of the time points

tested. Interestingly, the PBMC response was significantly higher than the  $T_{reg}^{neg}$  PBMC response late post-cART ( $p=0.006$ ). Surprisingly, there was no significant linear trend in PBMC ( $p=0.224$ ) or  $T_{reg}^{neg}$  PBMC ( $p=0.233$ ) responses pre-cART. We therefore concluded that disease progression, accompanied by an increase in viral load and a decrease in  $CD4^+$  T cells, was not sufficient to also cause a decrease in the HIV-1-specific response that was generated *in vivo*.

In subject S3, the mean PBMC response increased from 197 SFC/ $10^6$  0.2 years post-seroconversion to 704 SFC/ $10^6$  1.5 years post-seroconversion (**Figure 18A, middle panel**). By 2.5 years post-seroconversion, the PBMC response decreased to 54 SFC/ $10^6$  and only slightly varied from this during the remaining pre-cART time points. The trend of  $T_{reg}^{neg}$  PBMC responses mirrored the PBMC response and was significantly higher than PBMC at 0.2 ( $p=0.002$ ) and 1.5 ( $p=0.003$ ) years post-seroconversion. The PBMC response was significantly higher than the  $T_{reg}^{neg}$  PBMC response 23.5 ( $p<0.0001$ ) years post-seroconversion. While decreasing trends were observed in the average PBMC and  $T_{reg}^{neg}$  PBMC responses, there were no significant linear associations with disease progression.

In subject S8, we observed a slightly different trend in T cell responses compared to subjects S2 and S3. PBMC responses slightly increased throughout untreated infection but did not exhibit a significant upward trend (**Figure 18A, right panel**). The highest PBMC response was observed 23.5 years post-seroconversion, during late cART. The  $T_{reg}^{neg}$  PBMC response gradually increased throughout untreated infection with a significant increase of 161 SFC/ $10^6$ /year ( $p=0.003$ ), indicating  $T_{reg}$  depletion revealed an increase in antigen-specific T cell responses throughout infection. IFN $\gamma$  production by  $T_{reg}^{neg}$  PBMC was significantly higher than the PBMC response 6.6 years post-seroconversion ( $p=0.0009$ ). Contrary to subjects S2 and S3, we observed

no timepoints in subject S8 at which the PBMC response was higher than the  $T_{reg}^{neg}$  PBMC response.

While evaluating the average responses over multiple epitope variants is useful in identifying longitudinal trends, it does not show if there is a universal  $T_{reg}$  effect among all epitope variants. The significant differences observed between the PBMC and  $T_{reg}^{neg}$  PBMC conditions at a few time points could be the result of reactivity to a few isolated variants. We next aimed to assess the effect of  $T_{reg}$  on the PBMC response to each individual variant by determining the fold change in IFN $\gamma$  production induced by  $T_{reg}$  depletion (**Figure 18B**). We observed no common trend among the three subjects. In subject S2, the effect of  $T_{reg}$  depletion increased 1.2 and 3.4 years post-seroconversion and decreased to baseline levels 5.6 and 9.6 years post-seroconversion, exhibiting no significant trend with disease progression. The  $T_{reg}$  effect increased early post-cART and returned to baseline late post-cART (**Figure 18B, left panel**). In subject S3, the fold change decreased throughout untreated infection and was negatively associated with disease progression prior to cART ( $p=0.018$ ). The  $T_{reg}$  effect rebounded early post-cART to an average fold change of 29.8. Late post-cART, the average fold change was 0.18, indicating lower responses in  $T_{reg}^{neg}$  PBMC compared to PBMC (**Figure 18B, middle panel**). In subject S8, the fold change decreased 1.4 years post-seroconversion and then continually increased throughout untreated infection. While there was an increasing trend in the fold change prior to cART, this association did not reach significance ( $p=0.143$ ). There was a drop in the fold change early post-cART, and by late post-cART the average fold change was 0.83, indicating slightly lower  $T_{reg}^{neg}$  PBMC responses compared to PBMC (**Figure 18B, right panel**).

In summary, the data presented here indicate varying patterns of T cell response throughout infection and varying levels of the  $T_{reg}$  effect on IFN $\gamma$  secretion. Surprisingly, no changes in

PBMC or  $T_{reg}^{neg}$  PBMC responses were noted in subjects S2 and S3 during untreated infection, despite disease progression. Subject S8 displayed a unique pattern, with  $T_{reg}^{neg}$  PBMC responses significantly increasing throughout untreated infection. In S2 and S3, we observed one time point at which the PBMC response was significantly higher than the  $T_{reg}^{neg}$  PBMC response. Together, these data suggest a variable degree of suppressive activity imposed by  $T_{reg}$  in HIV-1 infection that may be patient- and disease state-dependent.

#### **3.4.4 Broad DC enhancement of T cell responses to autologous epitope variants**

We have previously shown that dendritic cell (DC) stimulation enhances T cell responses to consensus HIV-1 peptide antigens in subjects on cART (155). We next aimed to determine the longitudinal effects of DC stimulation on the detection of T cell responses (PBMC+DC) to autologous epitope variants and to compare these responses to those detected in PBMC alone. Immature DC were derived from monocytes obtained from our three study subjects during cART and were matured with CD40L and loaded with the autologous HIV-1 epitope variants that had evolved by the time of PBMC sampling. PBMC obtained from the same time points shown above were co-cultured with antigen-loaded DC or peptide alone and were evaluated for responses by IFN $\gamma$  ELISpot. The responses to all variants within each subject were averaged at each time point and are shown in **Figure 19A**.

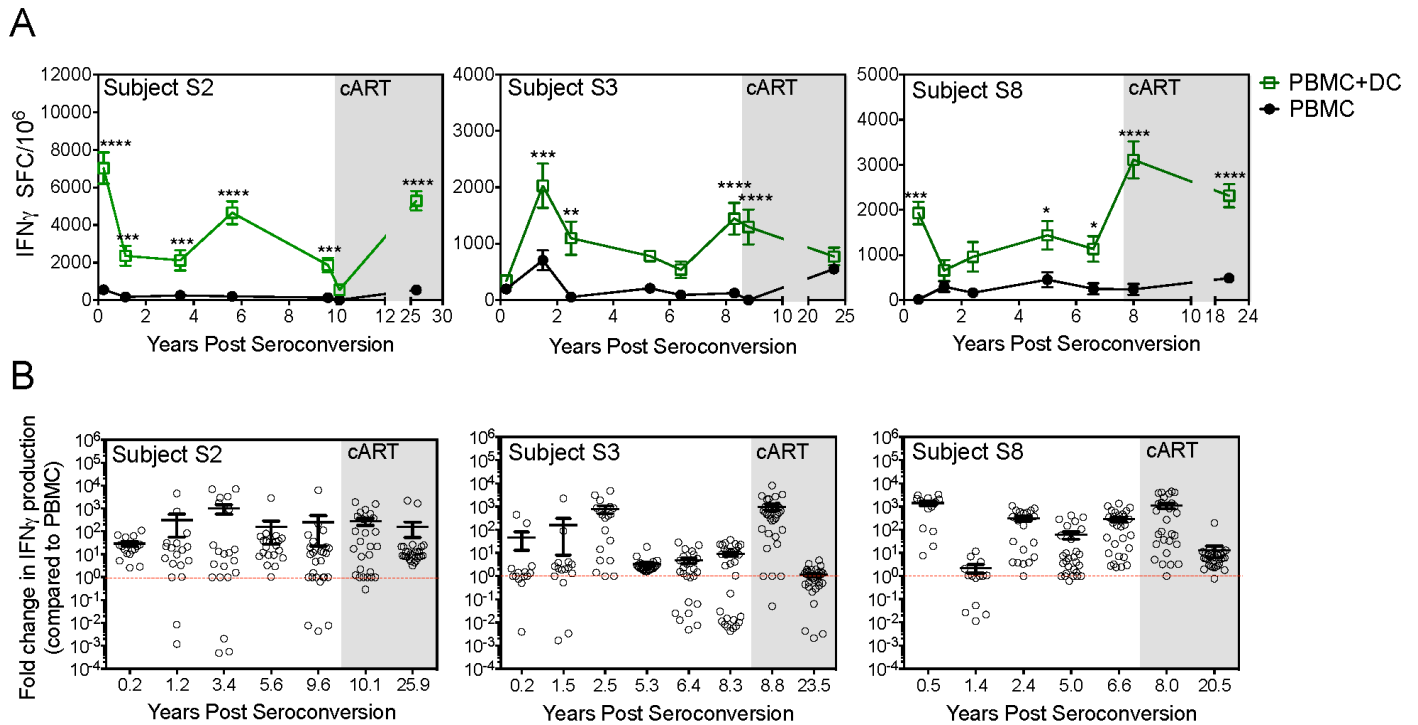


**Figure 19. DC stimulation reveals T cell responses specific for autologous epitope variants at all stages of disease progression**

Autologous DC were generated for each patient and were derived from monocytes obtained during late post-cART. DC were matured with CD40L for 48h and were loaded with individual autologous HIV-1 epitope variants. PBMC with or without antigen-loaded DC were evaluated by IFN $\gamma$  ELISpot for responses against the autologous HIV-1 Gag and Env epitope variants that had evolved by each time point. (A) Responses to autologous HIV-1 epitope variants detected in PBMC (filled black circle) were averaged at each time point and compared to those detected in PBMC+DC (green square) to the same variants. The mean response of all variants  $\pm$  SEM is shown at each time point for subjects S2 (left panel), S3 (middle panel), and S8 (right panel). Responses are shown as spot-forming cells (SFC) per 10<sup>6</sup>. (B) The fold change in IFN $\gamma$  production of PBMC+DC compared to PBMC is shown at each time point. Open circles represent the fold change detected in an individual epitope variant. Error bars represent the mean fold change  $\pm$  SEM. The dashed red line is shown to mark a fold change of 1, or no change in response. Post-cART time points are indicated by the gray box. \* $p$ <0.05, \*\* $p$ <0.01, \*\*\* $p$ <0.001, \*\*\*\* $p$ <0.0001.

In subject S2, DC stimulation significantly enhanced T cell responses to autologous epitope variants at 0.2 ( $p$ <0.0001), 1.2 ( $p$ =0.001), 3.4 ( $p$ =0.001), 5.6 ( $p$ <0.0001), 9.6 ( $p$ =0.001), and 25.9 ( $p$ <0.0001) years post-seroconversion (**Figure 19A, left panel**). At 1.2 years post-seroconversion, the mean response dropped from 7,029 SFC/10<sup>6</sup> to 2360 SFC/10<sup>6</sup>. There was a slight increase in the response 5.6 years post-seroconversion, followed by two timepoints of subsequent decreases in response. IFN $\gamma$  production rebounded to 5,295 SFC/10<sup>6</sup> at 25.9 years post-seroconversion.



Prior to cART, there was no significant trend in IFN $\gamma$  production by PBMC+DC ( $p=0.394$ ), indicating no correlation of this response with disease progression. In subject S3, the PBMC+DC response peaked at 2,029 SFC/10<sup>6</sup> 1.5 years post-seroconversion and decreased at the next 3 study time points (**Figure 19A, middle panel**). There was an increase in response to 1,444 SFC/10<sup>6</sup> at the last pre-cART time point, followed by decreases at each of the post-cART time points. The PBMC+DC response was significantly higher than the PBMC response at 1.5 ( $p=0.001$ ), 2.5 ( $p=0.002$ ), 8.3 ( $p<0.0001$ ), and 8.8 ( $p<0.0001$ ) years post-seroconversion. There was no correlation of this response with years post-seroconversion ( $p=0.953$ ) prior to cART. In subject S8, there was a decrease in response 1.4 years post-seroconversion to 659 SFC/10<sup>6</sup>, followed by increases in mean IFN $\gamma$  production at the next two time points (**Figure 19A, right panel**). There was a slight decrease in response at the last pre-cART time point, followed by a drastic increase to 3,109 SFC/10<sup>6</sup> at 8.0 years post-seroconversion and a drop to 2,315 SFC/10<sup>6</sup> 20.5 years post-seroconversion. Addition of DC significantly enhanced the PBMC response at 0.5 ( $p=0.001$ ), 5.0 ( $p=0.005$ ), 6.6 ( $p=0.01$ ), 8.0 ( $p<0.0001$ ), and 20.5 ( $p<0.0001$ ) years post-seroconversion. There was no association of the PBMC+DC response with years post-seroconversion throughout untreated infection ( $p=0.845$ ).

When we looked at the fold change in IFN $\gamma$  production induced by DC stimulation, we saw average fold changes that were  $>1$  in all subjects at all timepoints, indicating DC stimulation enhanced HIV-1-specific T cell responses regardless of disease state (**Figure 19B**). Additionally, there were no significant linear trends in the fold change induced by DC throughout infection. Interestingly, there was a decrease in the fold change late post-cART compared to the early post-cART time point in all three subjects. In subjects S3 and S8, this decrease was significant ( $p<0.0001$  for both).

Together, these data show that DC stimulation can enhance IFN $\gamma$  production by T cells specific for autologous HIV-1 epitope variants at most post-seroconversion time points and at all stages of disease progression. This trend was observed in all three subjects. Additionally, the PBMC+DC response did not change throughout untreated infection, indicating disease progression had little effect on the ability of DC to reveal HIV-1-specific responses.

### **3.4.5 The combined effect of T<sub>reg</sub> depletion and DC addition on recall T cell responses**

While we only observed a moderate enhancement in T cell responses with T<sub>reg</sub> removal, we hypothesized that T<sub>reg</sub> depletion combined with the addition of antigen-loaded DC could further enhance the T cell response above that which was observed with DC addition alone. We therefore co-cultured autologous DC loaded with the contemporaneous, autologous epitope variants shown in **Table 5** with T<sub>reg</sub><sup>neg</sup> PBMC and evaluated T cell responses by IFN $\gamma$  ELISpot, while concurrently evaluating PBMC responses to the same epitope variants. We then calculated an average response for each condition at each time point (**Figure 20A**).

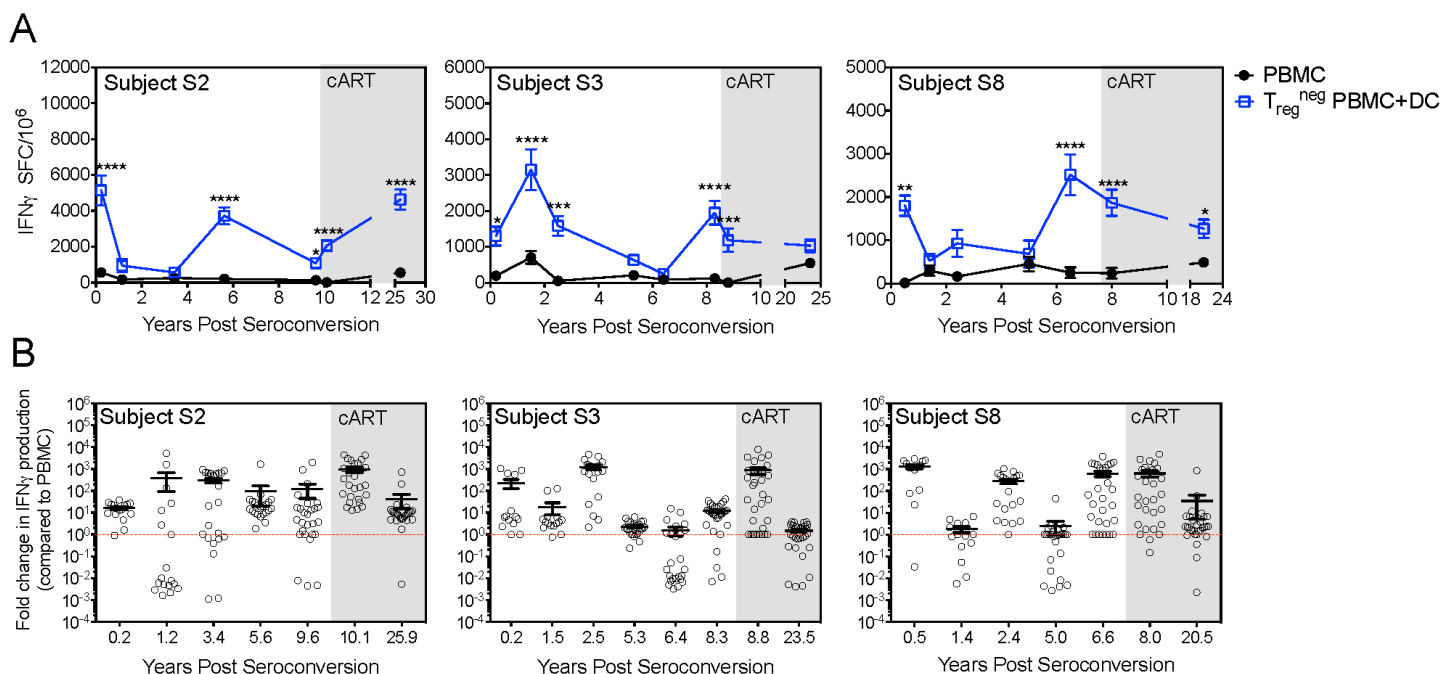


**Figure 20. The combined effect of DC addition and T<sub>reg</sub> depletion on recall HIV-1-specific responses *in vitro***

Autologous DC were generated for each patient and were derived from monocytes obtained during late post-cART. DC were matured with CD40L for 48h and were loaded with individual autologous HIV-1 epitope variants. PBMC with or without antigen-loaded DC were evaluated by IFN $\gamma$  ELISpot for responses against the autologous HIV-1 Gag and Env epitope variants that had evolved by each time point. (A) Responses to autologous HIV-1 epitope variants detected in PBMC (filled black circle) were averaged at each time point and compared to those detected in T<sub>reg</sub><sup>neg</sup> PBMC+DC (blue square) to the same variants. The mean response of all variants +/- SEM is shown at each time point for subjects S2 (left panel), S3 (middle panel), and S8 (right panel). Responses are shown as spot-forming cells (SFC) per 10<sup>6</sup>. (B) The fold change in IFN $\gamma$  production of PBMC+DC compared to PBMC is shown at each time point. Open circles represent the fold change detected in an individual epitope variant. Error bars represent the mean fold change +/- SEM. The dashed red line is shown to mark a fold change of 1, or no change in response. Post-cART time points are indicated by the gray box. \*p<0.05, \*\*p<0.01, \*\*\*p<0.001, \*\*\*\*p<0.0001.

In Subject S2, the mean IFN $\gamma$  production by the T<sub>reg</sub><sup>neg</sup> PBMC+DC condition at 0.2 years post-seroconversion was 5,153 SFC/10<sup>6</sup> (**Figure 20A, left panel**). By 1.2 years post-seroconversion this response had dropped to 946 SFC/10<sup>6</sup>. The response decreased slightly 3.4 years post-seroconversion and rebounded to 3,723 SFC/10<sup>6</sup> at 5.6 years post-seroconversion. Following a decrease at 9.6 years post-seroconversion, the average response of the T<sub>reg</sub><sup>neg</sup> PBMC+DC condition increased at both post-cART time points. The combination of T<sub>reg</sub> depletion and DC addition significantly enhanced IFN $\gamma$  production at 0.2 (p<0.0001), 5.6 (p<0.0001), 9.6

( $p=0.03$ ), 10.1 ( $p<0.0001$ ), and 25.9 ( $p<0.0001$ ) years post-seroconversion. There was no significant association of the  $T_{reg}^{neg}$  PBMC+DC response with pre-cART disease progression, despite showing an average loss of 185 SFC/ $10^6$ /year.

In subject S3, the mean response of the  $T_{reg}^{neg}$  PBMC+DC condition increased from 1303 SFC/ $10^6$  at 0.2 years post-seroconversion to 3,150 SFC/ $10^6$  at 1.5 years post-seroconversion (**Figure 20A, middle panel**). The response gradually decreased until 6.4 years post-seroconversion when the response reached a low of 247 SFC/ $10^6$ . At the last pre-cART time point, IFN $\gamma$  production increased to 1952 SFC/ $10^6$  and then decreased at each post-cART time point.  $T_{reg}^{neg}$  PBMC+DC responses were significantly higher than those detected in the PBMC condition at 0.2 ( $p=0.013$ ), 1.5 ( $p<0.0001$ ), 2.5 ( $p=0.0002$ ), 8.3 ( $p<0.0001$ ), and 8.8 ( $p<0.0001$ ) years post-seroconversion. There was no linear trend in the  $T_{reg}^{neg}$  PBMC+DC responses throughout untreated infection.

When evaluating  $T_{reg}^{neg}$  PBMC+DC responses in subject S8, we observed a decrease from 1,803 SFC/ $10^6$  at 0.5 years post-seroconversion to 526 SFC/ $10^6$  at 1.4 years post-seroconversion (**Figure 20A, right panel**). The mean response only slightly varied until 6.5 years post-seroconversion, when the mean response peaked at 2,516 SFC/ $10^6$  at the last pre-cART time point and then decreased at each of the post-cART time points. The  $T_{reg}^{neg}$  PBMC+DC response was significantly higher than the PBMC response at 0.5 ( $p=0.002$ ), 6.5 ( $p<0.0001$ ), 8.0 ( $p<0.0001$ ), and 20.5 ( $p=0.024$ ) years post-seroconversion. Similar to subjects S2 and S3, there was no linear trend in  $T_{reg}^{neg}$  PBMC+DC responses prior to cART in subject S8.

We then evaluated the fold change induced by the  $T_{reg}^{neg}$  PBMC+DC condition compared to the PBMC condition within each autologous epitope variant (**Figure 20B**). The average fold change was  $>1$  at all time points in each subject, indicating  $T_{reg}$  depletion combined with the

addition of DC was able to enhance the PBMC response to autologous Gag and Env epitope variants regardless of disease progression.

In summary, these data show that  $T_{reg}$  depletion combined with the addition of DC is able to reveal T cell responses specific for HIV-1 epitope variants at all stages of disease progression. Furthermore, the responses detected with this condition did not decrease throughout chronic infection and further verify that high-magnitude responses were generated against late-evolving variants and can be detected late in infection.

#### **3.4.6 Comparison of $T_{reg}$ depletion and DC addition for the detection of recall HIV-1-specific T cell responses**

We were able to show significant increases in HIV-1-specific responses with the removal of  $T_{reg}$  in some cases and with the addition of DC at most timepoints. We next aimed to determine which method,  $T_{reg}$  depletion, DC addition, or the combination of both techniques, was most efficient at revealing epitope variant-specific IFN $\gamma$  production and if the best method of detection was dependent on disease progression. We therefore compared the mean responses detected in the  $T_{reg}^{neg}$  PBMC to those detected in the PBMC+DC condition at each time point in each subject (**Figure 21A**). In subject S2, the PBMC+DC response was significantly higher than the  $T_{reg}^{neg}$  PBMC response at each time point except early post-cART at 10.1 years post-seroconversion ( $p < 0.001$  for all, **Figure 21A, left panel**). In subject S3, DC addition revealed higher IFN $\gamma$  production than  $T_{reg}$  depletion at 1.5 ( $p = 0.009$ ), 2.5 ( $p = 0.003$ ), 8.3 ( $p < 0.0001$ ), 8.8 ( $p < 0.0001$ ), and 23.5 ( $p = 0.002$ ) years post-seroconversion (**Figure 21A, middle panel**). In subject S8, we observed the least number of time points at which the PBMC+DC response was significantly greater than the  $T_{reg}^{neg}$  PBMC response. These time points were 0.5 ( $p = 0.002$ ), 8.0 ( $p < 0.0001$ ),

and 20.5 ( $p < 0.0001$ ) years post-seroconversion (**Figure 21A, right panel**). Not surprisingly,  $T_{reg}$  depletion did not enhance the PBMC+DC response at any time point in subjects S2 and S3 (**Figure 21B, left and middle panels**). In subject S8, we only saw a significant enhancement at 6.5 ( $p = 0.003$ ) and 8.0 ( $p = 0.007$ ) years post-seroconversion (**Figure 21B, right panel**).

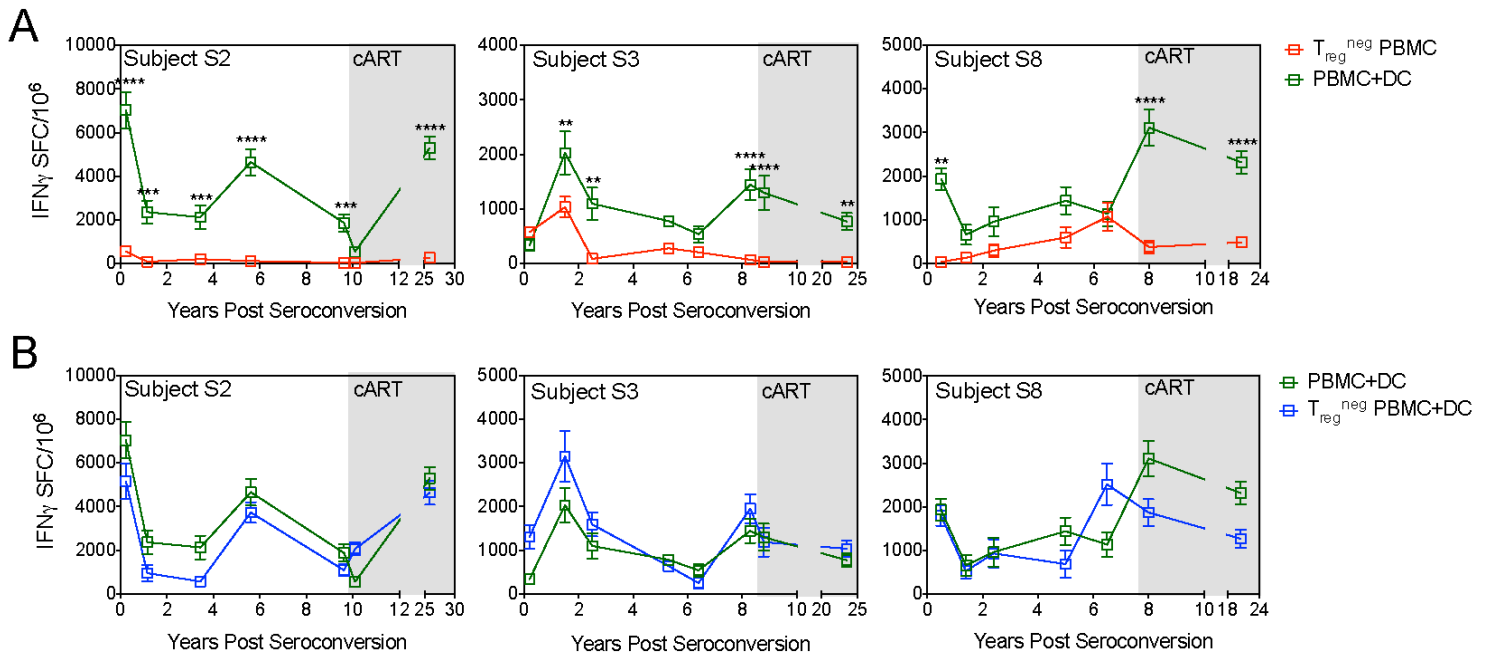


**Figure 21. DC addition reveals higher magnitude HIV-1-specific responses than  $T_{reg}$  depletion**

The longitudinal responses shown in figures 18, 19, and 20 were compared within each subject at each time point to determine the best method of revealing T cell responses specific for autologous HIV-1 epitope variants. (A) Responses to autologous HIV-1 epitope variants detected in PBMC+DC (green square) were averaged at each time point and compared to those detected in (A)  $T_{reg}^{neg}$  PBMC (red square) or (B)  $T_{reg}^{neg}$  PBMC +DC (blue square) to the same variants. The mean response of all variants  $\pm$  SEM is shown at each time point for subjects S2 (left panel), S3 (middle panel), and S8 (right panel). Responses are shown as spot-forming cells (SFC) per  $10^6$ . Post-cART time points are indicated by the gray box. \* $p < 0.05$ , \*\* $p < 0.01$ , \*\*\* $p < 0.001$ , \*\*\*\* $p < 0.0001$ .

In summary, the data presented here suggest DC addition is the best and most consistent method of detecting T cell responses specific for autologous HIV-1 epitope variants throughout chronic and treated HIV-1 infection. While  $T_{reg}$  depletion slightly increases recall IFN $\gamma$  production, it does not reveal the magnitude of responses seen with DC addition. Additionally,

we observed no additive effect of combining the DC addition with T<sub>reg</sub> depletion, therefore suggesting DC addition alone is sufficient to reveal robust recall T cell responses at all stages of disease progression.

### **3.4.7 DC enhance cytokine secretion in HIV-1-specific CD8<sup>+</sup> T cells**

We showed above that DC enhance IFN $\gamma$  secretion specific for autologous epitope variants at multiple stages of disease progression. We therefore aimed to determine if DC could enhance T cell production of other type 1 immune mediators in response to these autologous epitope variants. To address this, we co-cultured PBMC obtained from each subject during AIDS, early post-cART, and late post-cART with autologous HIV-1 epitope variants alone or loaded onto CD40L-matured, monocyte-derived DC. For practicality purposes, we only used variants of the known Gag and Env epitopes (**Table 5**) that were in viral circulation at the time of PBMC sampling (contemporaneous variants). Following a 6h co-culture, PBMC were stained for the type 1-associated molecules IFN $\gamma$ , CD107a, MIP-1 $\beta$ , TNF $\alpha$ , and IL-2.

We first evaluated cytokine/chemokine secretion by CD8<sup>+</sup> T cells obtained from the last pre-cART time point with peptide alone or peptide-loaded DC (**Figure 22**).

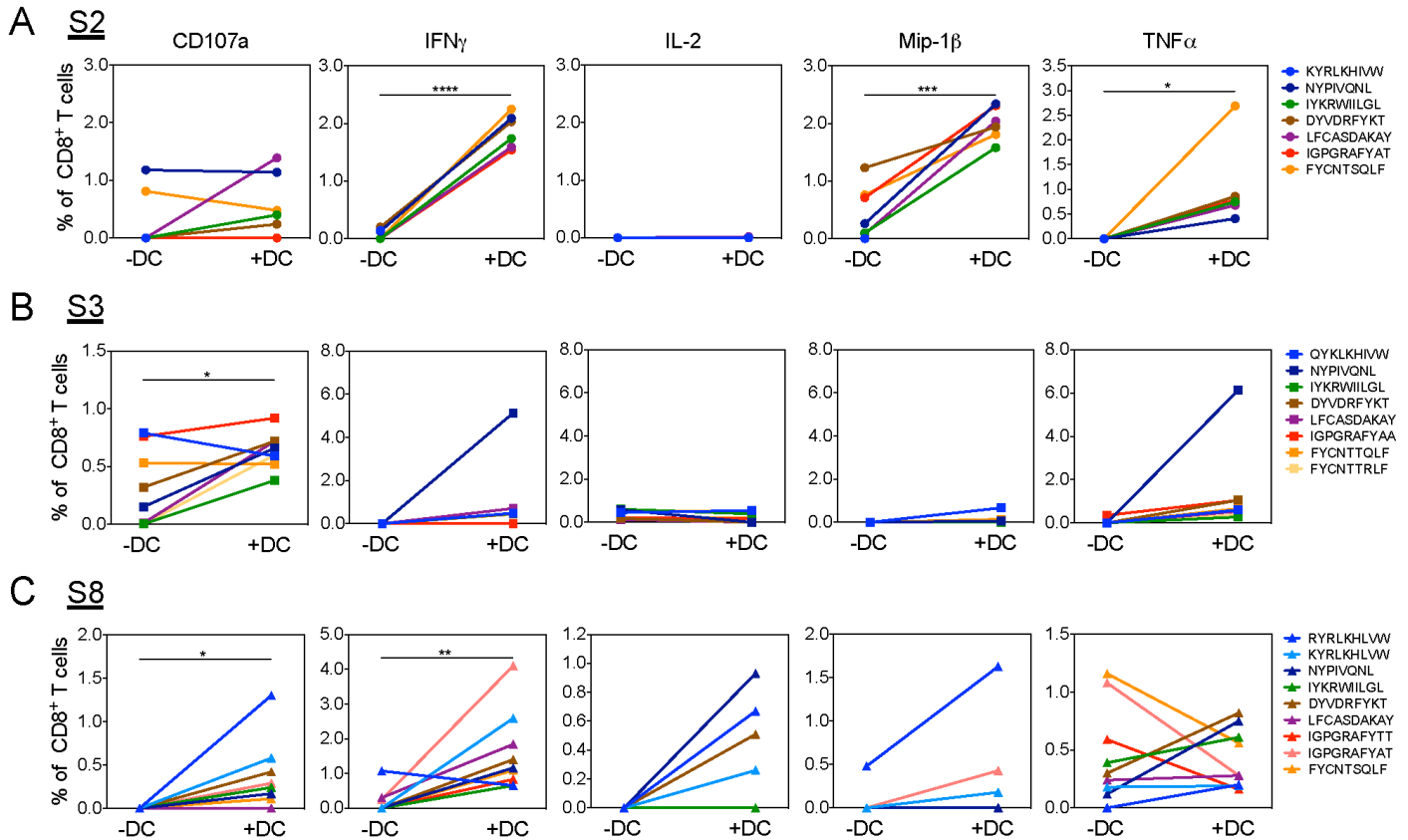


**Figure 22. DC enhance the percent of CD8<sup>+</sup> T cells staining positive for proinflammatory molecules in response to autologous, contemporaneous HIV-1 epitope variants during late disease progression**

Autologous monocyte derived DC were matured with CD40L and loaded with autologous HIV-1 epitope variants. PBMC derived from the last pre-cART time point were incubated with peptide alone or peptide-loaded DC. For practicality, only the variants of known Gag and Env epitopes that were in circulation at the last pre-cART time point were used. PBMC and PBMC+DC were also incubated with SEB or media alone for positive and negative controls, respectively. PBMC were then stained for CD107a, IFN $\gamma$ , IL-2, MIP-1 $\beta$ , and TNF $\alpha$ . Background was determined as the percent of CD8<sup>+</sup> T cells staining positive for the relevant cytokine in the negative control condition. Data are shown as the percent of CD8<sup>+</sup> T cells that are antigen-specific (background subtracted) in (A) subject S2, (B) subject S3, and (C) subject S8. \* $p < 0.05$ , \*\* $p < 0.01$ , \*\*\* $p < 0.001$ , \*\*\*\* $p < 0.0001$ .

In each subject, this study visit was after at least one time point with a CD4<sup>+</sup> T cell count that was below 200 cells/mm<sup>3</sup> and was therefore in the advanced stage of disease progression. In subject S2, DC significantly enhanced the percent of CD8<sup>+</sup> T cells specific for IFN $\gamma$  ( $p < 0.0001$ ), MIP-1 $\beta$  ( $p = 0.001$ ), and TNF $\alpha$  ( $p = 0.03$ ) (**Figure 22A**). Surprisingly, only CD107a secretion was enhanced by DC in subject S3 ( $p = 0.023$ ) (**Figure 22B**). In subject S8, CD107a ( $p = 0.03$ ) and IFN $\gamma$  ( $p = 0.008$ ) were enhanced by DC (**Figure 22C**). While we observed increases in IL-2 production



in response to 4 of the variants tested when using DC, the mean percent of CD8<sup>+</sup> T cells specific for this cytokine was not significantly different (p=0.06). Of interest, there was no common immune mediator that was enhanced by DC in all three subjects, implying this enhancement is not cytokine-specific and may result in differential CD8<sup>+</sup> T cell immune profiles.

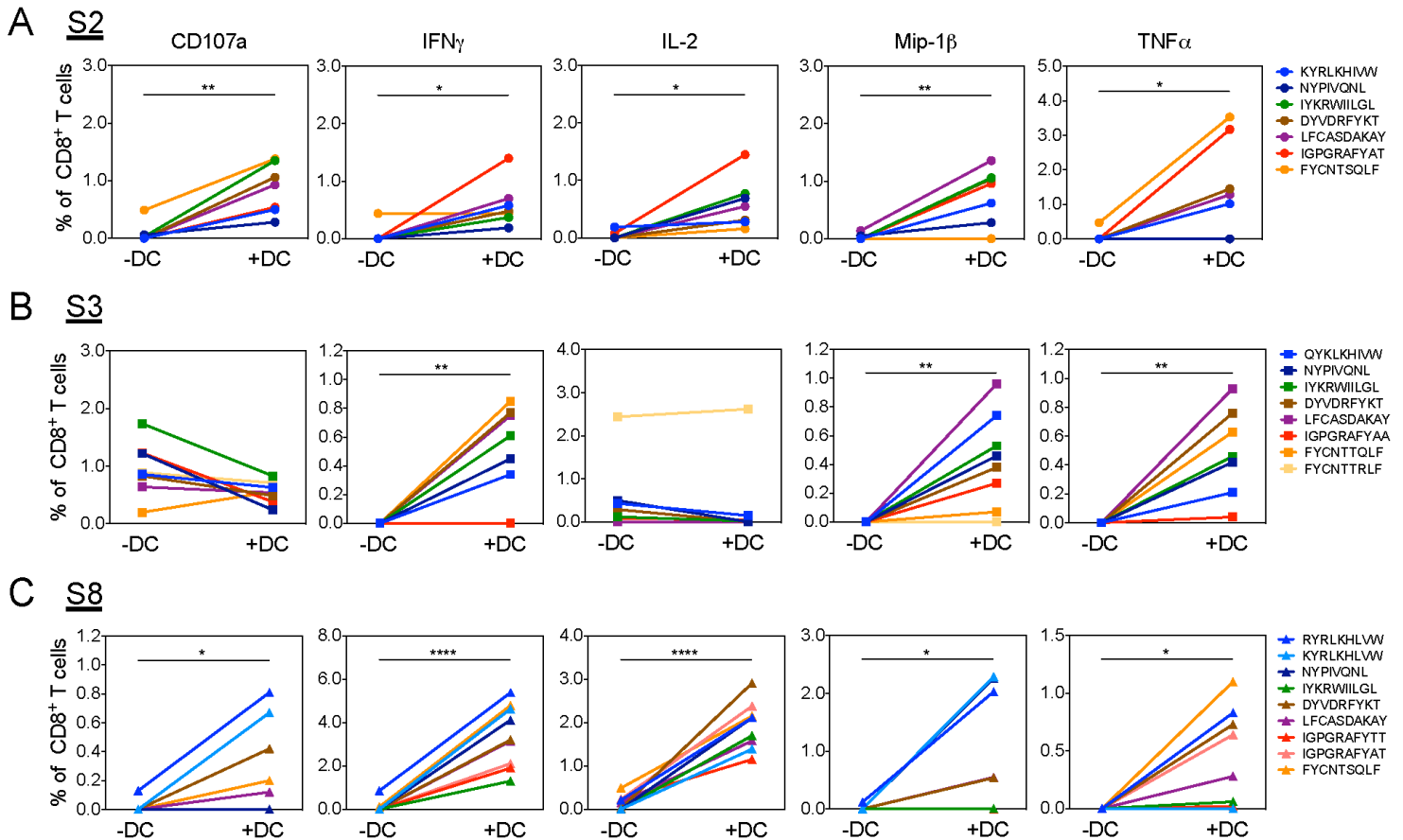


**Figure 23. DC enhance the percent of CD8<sup>+</sup> T cells staining positive for proinflammatory molecules in response to autologous, contemporaneous HIV-1 epitope variants early post-cART**

Autologous monocyte derived DC were matured with CD40L and loaded with autologous HIV-1 epitope variants. PBMC derived from the first post-cART time point (<6 months post-cART) were incubated with peptide alone or peptide-loaded DC. For practicality, only the variants of known Gag and Env epitopes that were in circulation at the last pre-cART time point were used. PBMC and PBMC+DC were also incubated with SEB or media alone for positive and negative controls, respectively. PBMC were then stained for CD107a, IFN $\gamma$ , IL-2, MIP-1 $\beta$ , and TNF $\alpha$ . Background was determined as the percent of CD8<sup>+</sup> T cells staining positive for the relevant cytokine in the negative control condition. Data are shown as the percent of CD8<sup>+</sup> T cells that are antigen-specific (background subtracted) in (A) subject S2, (B) subject S3, and (C) subject S8. \*p<0.05, \*\*p<0.01, \*\*\*p<0.001, \*\*\*\*p<0.0001.

To determine if cART impacted the ability of DC to stimulate cytokine production, we evaluated responses in CD8<sup>+</sup> T cells obtained from the first post-cART time point, which was less than 6 months after starting treatment (**Figure 23**). In subject S2, DC induced significant increases in the percent of CD8<sup>+</sup> T cells that stained positive for all immune mediators evaluated; CD107a (p=0.002), IFN $\gamma$  (p=0.02), IL-2 (p=0.01), MIP-1 $\beta$  (p=0.006), and TNF $\alpha$  (p=0.03) (**Figure 23A**). In subject S3, we observed higher IFN $\gamma$  (p=0.005), MIP-1 $\beta$  (p=0.007), and TNF $\alpha$  (p=0.002) production with antigen-loaded DC (**Figure 23B**). In subject S8, DC induced significant increases in the production of all immune mediators evaluated; CD107a (p=0.04), IFN $\gamma$  (p<0.0001), IL-2 (p<0.0001), MIP-1 $\beta$  (p=0.03), and TNF $\alpha$  (p=0.02) (**Figure 23C**). Of note, IFN $\gamma$ , MIP-1 $\beta$ , and TNF $\alpha$  were significantly increased in each subject following DC addition. This is in contrary to our findings at the last pre-cART time point, at which there were no common mediators enhanced by DC among the three subjects.

We finally aimed to evaluate the effect of DC on antigen-specific CD8<sup>+</sup> T cell responses late post-cART, after >13 years of treatment in each subject (**Figure 24**). In subject S2, we observed a higher percent of CD8<sup>+</sup> T cells staining positive for CD107a (p=0.0001), IFN $\gamma$  (p=0.0002), IL-2 (p=0.001), and TNF $\alpha$  (p=0.017) (**Figure 24A**) when T cells were exposed to antigen-loaded DC. We observed an increase in the production of 4 out of the 5 immune mediators in subject S3 when DC were added; CD107a (p=0.0003), IFN $\gamma$  (p=0.041), IL-2 (p=0.005), and MIP-1 $\beta$  (p=0.033) (**Figure 24B**). In subject S8, we only observed a DC enhancement in CD107a (p<0.0001), IFN $\gamma$  (p<0.0001), and IL-2 (p<0.0001) (**Figure 24C**). While DC addition revealed increases in MIP-1 $\beta$ - and TNF $\alpha$ -positive CD8<sup>+</sup> T cells, these changes were not significant (p=0.06 and 0.07, respectively). The percent of CD8<sup>+</sup> T cells producing CD107a, IFN $\gamma$ , and IL-2 was significantly enhanced by DC in all three subjects at this late post-cART time point, showing a

shift from early post-cART in the common DC-enhanced immune mediators among the three subjects.

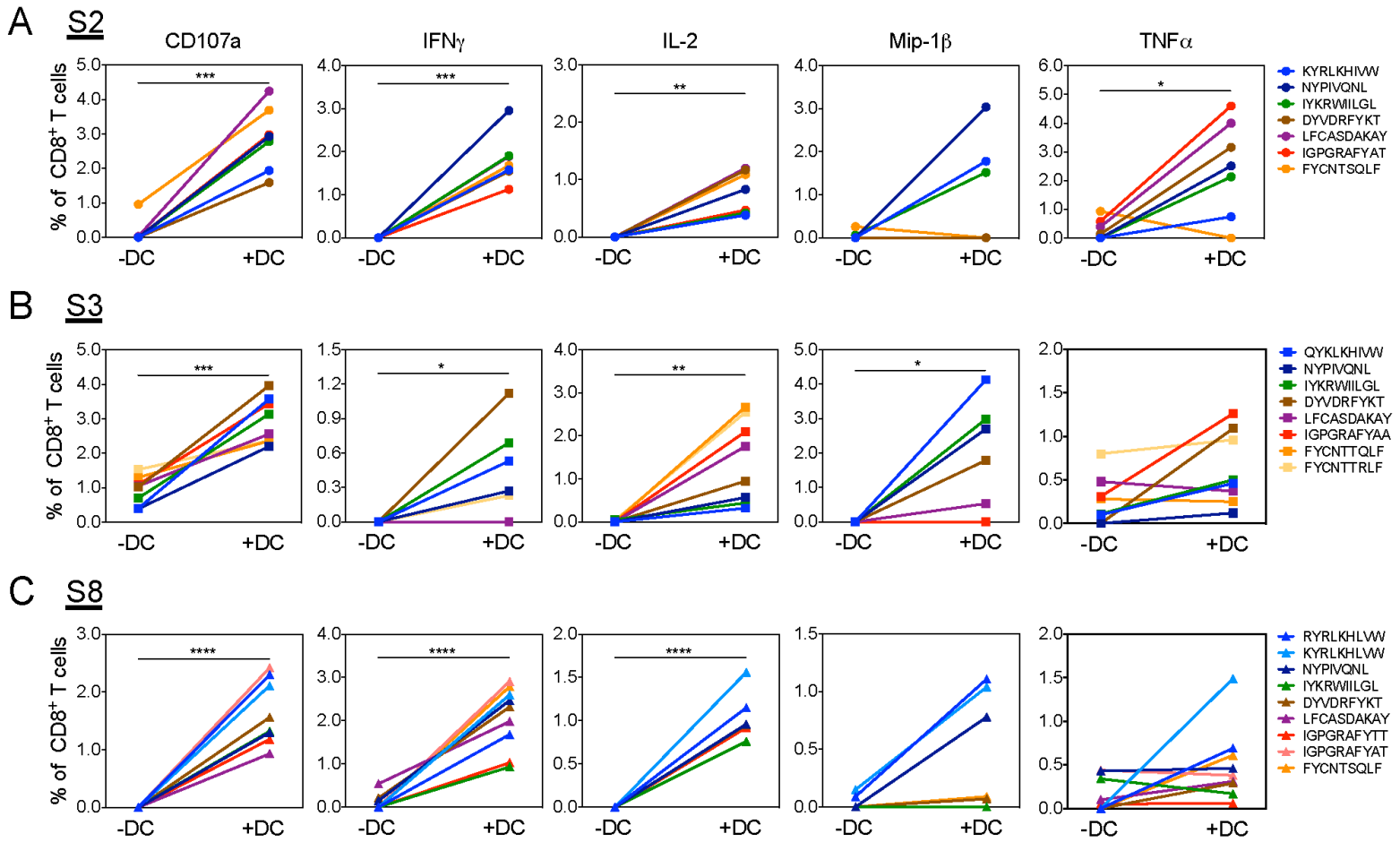


**Figure 24. DC enhance the percent of CD8<sup>+</sup> T cells staining positive for proinflammatory molecules in response to autologous, contemporaneous HIV-1 epitope variants late post-cART**

Autologous monocyte derived DC were matured with CD40L and loaded with autologous HIV-1 epitope variants. PBMC derived from the last post-cART time point (>13 years post-cART) were incubated with peptide alone or peptide-loaded DC. For practicality, only the variants of known Gag and Env epitopes that were in circulation at the last pre-cART time point were used. PBMC and PBMC+DC were also incubated with SEB or media alone for positive and negative controls, respectively. PBMC were then stained for CD107a, IFN $\gamma$ , IL-2, MIP-1 $\beta$ , and TNF $\alpha$ . Background was determined as the percent of CD8<sup>+</sup> T cells staining positive for the relevant cytokine in the negative control condition. Data are shown as the percent of CD8<sup>+</sup> T cells that are antigen-specific (background subtracted) in (A) subject S2, (B) subject S3, and (C) subject S8. \*p<0.05, \*\*p<0.01, \*\*\*p<0.001, \*\*\*\*p<0.0001.

The intracellular cytokine data presented here show a differential DC-induced increase in type 1-associated cytokines between the three subjects. Late post-seroconversion, we observed the lowest number of cytokines in which there was a DC enhancement effect. In subjects S2 and S8, the highest number of cytokines for which there was a DC enhancement was observed early post-seroconversion, whereas this was observed late post-seroconversion in subject S8. Nonetheless, antigen-loaded DC were able to reveal cytokine specific CD8<sup>+</sup> T cells at all three time points in each subject.

#### **3.4.8 DC induce a disease state-dependent enhancement in the cytokine profile of epitope variant-specific CD8<sup>+</sup> T cells**

We have previously shown that DC reveal polyfunctional cytokine production by CD8<sup>+</sup> T cells in response to consensus Gag peptides in subjects on cART (155). We therefore aimed to determine if DC enhance epitope variant-specific polyfunctionality of CD8<sup>+</sup> T cells derived from our study subjects during chronic infection, early post-cART, and late post-cART. These findings would allow us to evaluate the potential efficacy of a DC immunotherapy aimed at enhancing the polyfunctionality of HIV-1-specific CD8<sup>+</sup> T cells and would shine light on the effects of DC on polyfunctional responses at various stages of disease progression. To address this, we loaded autologous CD40L-matured DC with the autologous contemporaneous epitope variants found in subjects S2, S3, and S8 late post-seroconversion. These are the same variants used in Figures 22, 23, and 24. We then incubated PBMC from the last pre-cART time point (“late post-seroconversion”), the first post-cART time point (<2 years post-cART), and a late post-cART time point (>13 years post-cART) with peptide-loaded DC or peptide alone and stained for

polyfunctional expression of the immune mediators CD107a, IFN $\gamma$ , IL-2, TNF $\alpha$ , and MIP-1 $\beta$  (Figure 25).

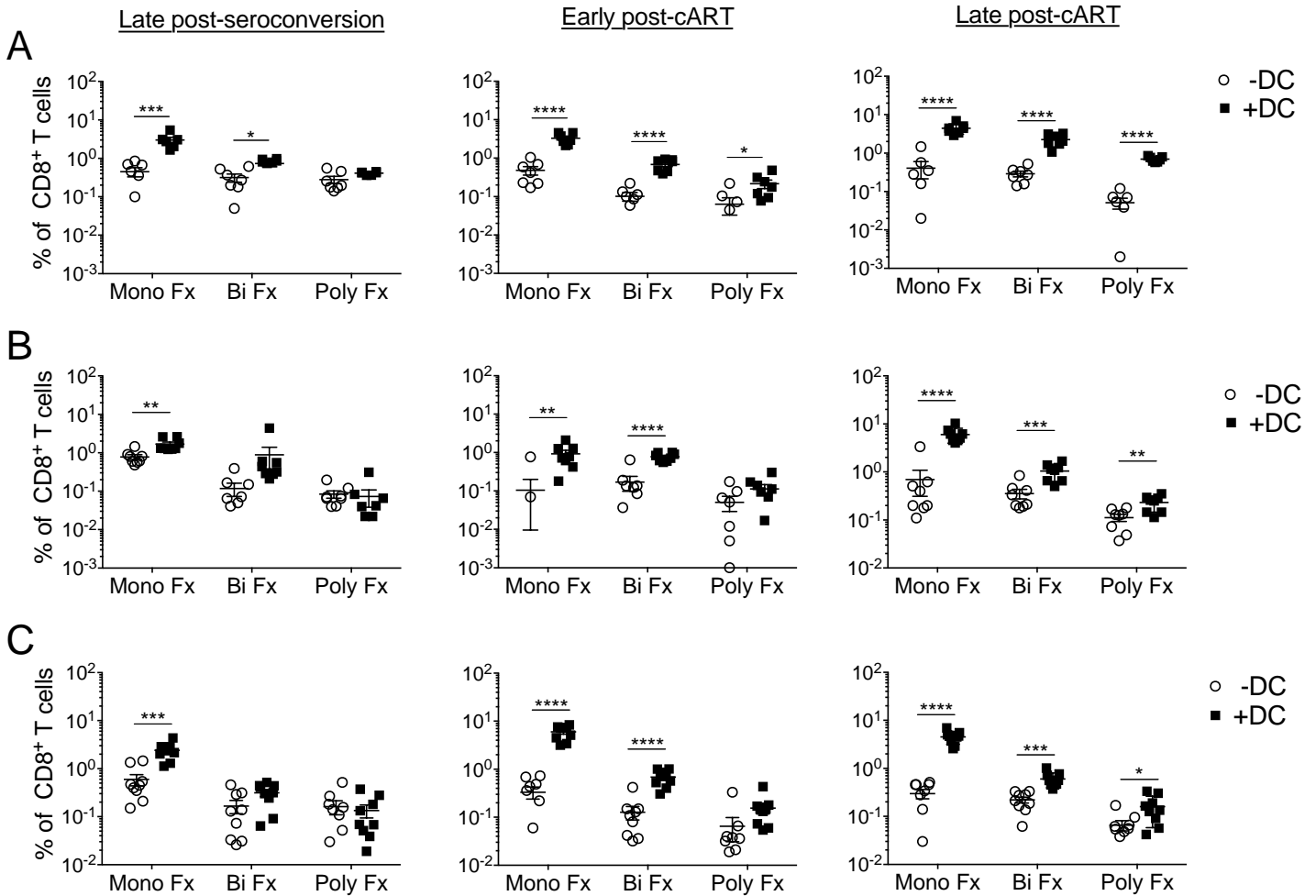


**Figure 25. DC effects on multifunctional CD8<sup>+</sup> T cell responses specific for autologous contemporaneous HIV-1 epitope variants pre- and post-cART**

Autologous monocyte derived DC were matured with CD40L and loaded with autologous HIV-1 epitope variants. PBMC derived from late post-seroconversion (the last pre-cART time point), early post-cART (<2 years post-cART), and late post-cART (>13 years post-cART) were incubated with peptide alone or peptide-loaded DC. For practicality, only the variants of known Gag and Env epitopes that were in circulation at the last pre-cART time point were used. PBMC and PBMC+DC were also incubated with SEB or media alone for positive and negative controls, respectively. PBMC were then stained for CD107a, IFN $\gamma$ , IL-2, MIP-1 $\beta$ , and TNF $\alpha$ . Background was determined as the percent of CD8<sup>+</sup> T cells staining positive for the relevant cytokine in the negative control condition. Data are shown as the percent of CD8<sup>+</sup> T cells above background that are producing one (mono fx), two (bi fx), and 3 or more (poly fx) immune mediators in (A) subject S2, (B) subject S3, and (C) subject S8. \* $p$ <0.05, \*\* $p$ <0.01, \*\*\* $p$ <0.001, \*\*\*\* $p$ <0.0001.

In Figure 25A, B, and C, we show the polyfunctional profile of CD8<sup>+</sup> T cells in subjects S2, S3, and S8, respectively. Late post-seroconversion, after many years of untreated HIV-1 infection, we observed a DC-mediated increase in the percent of monofunctional (p=0.0005) and bifunctional (p=0.015) CD8<sup>+</sup> T cells in subject S2 (**Figure 25A**). At this time point, we only observed increases in monofunctionality in subjects S3 (**Figure 25B**, p=0.002) and S8 (**Figure 25C**, p=0.0001). Early post-cART, DC increased the percent of CD8<sup>+</sup> T cells that were monofunctional (p<0.0001), bifunctional (p<0.0001), and polyfunctional (p=0.031) in subject S2. We saw a significant enhancement of the monofunctional response in subjects S3 (p=0.004) and S8 (p<0.0001), as well as an increase in the bifunctional response (p<0.0001 for both) when using DC early post-cART. Finally, DC increased the late post-cART monofunctional response (p<0.0001 for all), as well as the bifunctional (p= <0.0001, 0.0009, and 0.0001) and polyfunctional (p= <0.0001, 0.005, and 0.021) responses in subjects S2, S3, and S8, respectively.

The data presented here suggest a restoration in the ability of DC to reveal polyfunctional CD8<sup>+</sup> T cell responses as immune reconstitution occurs during cART. While monofunctional responses were significantly enhanced by DC late post-seroconversion, the bifunctional response was not increased in subjects S3 and S8 until early post-cART and the polyfunctional response was not increased by DC until late post-cART. While the bifunctional response was enhanced by DC late post-seroconversion in subject S2, the polyfunctional response was not revealed until early post-cART, again demonstrating a disease state-dependent ability of the DC to reveal multifunctional cytokine profiles in HIV-1-specific CD8<sup>+</sup> T cells.

### 3.5 DISCUSSION

Cytotoxic T lymphocytes (CTL) play a vital role in controlling HIV-1 infection (253, 289). The failure to control HIV-1 replication in chronic infection has been attributed to a decline in CTL responses that are specific for the autologous virus (6, 7, 19, 22, 30, 134-137, 145). Indeed, mutations within CTL epitopes have been shown to ablate MHC class I affinity and would therefore prevent the generation of a primary CD8<sup>+</sup> T cell response against that epitope. In this study, we employed several methods of detecting and enhancing T cell responses specific for autologous HIV-1 epitope variants at multiple stages of infection, before and after combination antiretroviral therapy (cART). Using these methods, we show that regulatory T cells (T<sub>reg</sub>) have limited, if any, suppressive effect on IFN $\gamma$  production, while dendritic cells (DC) reveal broad and robust responses regardless of disease progression. These results were expanded using a DC-enhanced polychromatic flow cytometry assay to detect multiple immune mediators in response to autologous HIV-1 epitope variants that were in circulation immediately prior to or after cART (contemporaneous variants). By using this approach, we observed DC enhancement of multiple cytokine production by HIV-1-specific CD8<sup>+</sup> T cells that was associated with suppression of viremia subsequent to cART.

The known and predicted HLA A\*2402-restricted epitopes used in our study exhibited various patterns of evolution. While many of the epitopes incurred amino acid changes throughout infection, there was no universal effect of these changes on the predicted MHC class I affinity, indicating HIV-1 evolution did not specifically evade MHC class I loading by antigen presenting cells (APC) or expression on the surface of infected cells. This observation would suggest that APC priming of naïve CD8<sup>+</sup> T cells could have occurred *in vivo* if the T cell receptor (TCR) repertoire was sufficient to recognize these antigens. Indeed, we detected PBMC responses to

>95% of variants irrespective of the predicted MHC class I affinity, showing amino acid mutations within epitopes did not ablate priming to these variants *in vivo*. Moreover, IFN $\gamma$  production to variants of novel predicted epitopes was of a similar magnitude to the response against variants of known epitopes, therefore highlighting the potential of these predicted epitope regions to be classified as HLA A\*2402 epitopes.

Our failure to identify a link between IFN $\gamma$  production and MHC class I affinity is not surprising. While decreased binding of mutated epitopes to MHC class I is a primary mechanism by which HIV-1 and SIV evade CD8<sup>+</sup> T lymphocyte responses (7, 26, 43, 58, 75, 102, 130, 131, 177, 227, 271), detection of IFN $\gamma$  production is not necessarily indicative of a cytolytic CD8<sup>+</sup> T cell response that can control infection (94, 144, 160, 217). The three subjects used in our study exhibited characteristics of normal disease progression, and therefore resident CTL were unable to control viral replication in chronic infection. A CTL response with high breadth and magnitude, specifically to the Gag proteins, has been associated with SIV and HIV-1 control (33, 179, 253, 285, 289). However, high-avidity CD8<sup>+</sup> T cells have been detected in progressive infection and therefore point to poor immune selection pressure exerted by these cells (94). Indeed, the PBMC responses to autologous epitope variants described in this study were broad and within a wide range of magnitudes despite the continuation of disease progression, thus indicating ineffective selective pressure on the virus. While we are not making the claim that our detection of cytokine secretion is indicative of CTL activity, we are concluding that a primary response to these epitope variants was generated *in vivo*, although this response was likely of variable efficacy, as disease progression continued and many of the epitope variants persisted throughout infection. Future studies should focus on the changes in cytolytic effector function against a select number of epitope



variants throughout HIV-1 infection. Nonetheless, these findings provide an in-depth understanding of the breadth of T cell responses that are generated to autologous HIV-1 antigens.

$T_{reg}$  have been implicated in the pathogenesis of HIV-1 infection and have become targets for exploitation in immunotherapies (212, 213). Additionally, we previously reported on the ability of mature, autologous DC to reveal and enhance HIV-1-specific T cell responses in subjects on cART (155). Not much is known about the role of  $T_{reg}$  in suppressing responses or the ability of DC to enhance responses during progressive infection. After detecting moderate responses to autologous epitope variants in PBMC, we next determined the individual and combined effects of  $T_{reg}$  depletion and DC addition on longitudinal  $CD8^+$  T cell  $IFN\gamma$  production throughout untreated and treated HIV-1 infection. Surprisingly,  $T_{reg}$  depletion only slightly enhanced responses at a relatively small number of time points in two of the subjects. The  $T_{reg}$  effect on PBMC responses did not universally increase throughout infection and therefore showed this mechanism of regulation is not necessarily correlated with disease progression. Addition of DC to PBMC did not enhance the number of epitope variants that were recognized, as the breadth was already >95% when evaluating PBMC, but the magnitude was significantly enhanced at most time points in each subject.

Regardless of disease progression, DC were functional at enhancing  $IFN\gamma$  production against autologous epitope variants as judged in our overnight ELISpot assays. More importantly, we observed similar responses to variants that evolved early and late post-seroconversion, thus supporting the ability of DC to present mutated epitopes to their cognate  $CD8^+$  T cell. We hypothesized that combining  $T_{reg}$  depletion and DC addition might result in an additive T cell response that was greater than the two methods used individually. We did not observe this, and in fact observed few differences between the PBMC+DC and PBMC- $T_{reg}$ +DC conditions, thereby

suggesting DC addition is superior at revealing HIV-1-specific T cell responses and T<sub>reg</sub> depletion provides minimal, if any, help in enhancing these responses. Of note, DC enhanced T cell responses late post-cART in 2 of the 3 subjects, suggesting a DC-mediated therapy for subjects on long-term suppressive cART may be successful in reinvigorating quiescent memory responses that are specific for the autologous reservoir.

Production of multiple cytokines by CD8<sup>+</sup> T cells has been associated with CTL effector function and control of HIV-1 infection (11, 12, 36, 141, 324). We therefore expanded our analysis of DC-mediated enhancement of HIV-1-specific CD8<sup>+</sup> T cell responses by evaluating intracellular cytokine secretion late post-seroconversion and during early and late cART time points with and without DC. As the subjects in our study regained their health under suppressive cART, DC were more able to reveal polyfunctional cytokine secretion by CD8<sup>+</sup> T cells. These findings suggest that a DC immunotherapy aimed at reinvigorating the dysfunctional CTL response may be effective. Our IFN $\gamma$  ELISpot analysis showed variable effects of DC addition as subjects received cART, but staining for multiple immune mediators gave a broader picture of how cART restores the ability of T cells to respond to HIV-1-specific stimuli. While our ELISpot data suggest DC would be efficient at inducing T cell responses at all disease time points, ICS shows DC enhancement is more pronounced after long-term cART.

We recognize our in-depth study was performed in a limited number of subjects and was done so to evaluate a broad array of autologous epitope variants. Continuing studies should incorporate a large cohort of subjects and should focus on a few epitopes and their variants. Additionally, using the data here to identify and focus on a select number of epitopes would allow for the analysis of cytolytic effector function by cells stimulated with antigen-loaded DC. Nonetheless, our extensive in-depth study allowed us to show DC enhancement to almost every

epitope variant evaluated and can therefore be lauded as a general phenomenon within our study subjects. Together, the data presented in this study highlight the ability of T cells to respond to autologous HIV-1 epitope variants at all stages of disease progression and support the use of DC immunotherapy in subjects on cART.

### **3.6 ACKNOWLEDGEMENTS**

We would like to thank Dr. John Mellors for access to his Taqman® assay, and Kelly Gordon and Weimin Jiang for technical assistance. Additionally, we would like to acknowledge James I. Mullins, PhD and the staff of his laboratory, particularly Kim Wong and Brendan Larsen, for performing the HIV-1 single genome sequencing and assistance with the analysis of these data, and the volunteers of the Pittsburgh site of the Multicenter AIDS Cohort Study. This work was supported in part by NIH grants R01-AI-40388, R37-AI-41870, U01-AI-35041 and T32-AI065380.

## 4.0 PRIMARY AND RECALL T CELL RESPONSES TO AUTOLOGOUS EPITOPE VARIANTS IN CHRONIC HIV-1 INFECTION

### 4.1 ABSTRACT

It is unclear if HIV-1 variants lose the ability to prime naïve CD8<sup>+</sup> cytotoxic T lymphocytes (CTL) during progressive, untreated infection. We conducted a comprehensive longitudinal analysis of viral evolution and its impact on primary and memory CD8<sup>+</sup> T cell responses pre-seroconversion (SC), post-SC, and during combination antiretroviral therapy (cART). Memory T cell responses targeting autologous virus variants reached a nadir by 8 years post-SC with development of AIDS, followed by transient enhancement of anti-HIV-1 CTL responses upon initiation of cART. We show broad and high magnitude primary T cell responses to late variants pre-SC, comparable to primary anti-HIV-1 responses induced in T cells from uninfected persons. Despite evolutionary changes, CD8<sup>+</sup> T cells could still be primed to HIV-1 variants. Hence, vaccination against late, mutated epitopes could be successful in enhancing primary reactivity of T cells for control of the residual reservoir of HIV-1 during cART.

I performed >50% of the experiments discussed in this chapter, generated all graphs, and performed most of the statistical analyses and data interpretation. A modified version of the work in this chapter has been published as: The impact of viral evolution and frequency of variant epitopes on primary and memory human immunodeficiency virus type-1-specific CD8<sup>+</sup> T cell responses. \*Melhem NM, \***Smith KN**, Huang XL, Colleton BA, Jiang W, Mailliard RB, Mullins JI, and Rinaldo CR. *Virology*. (IN PRESS).

**\*These authors contributed equally to this work and share primary authorship**

## 4.2 BACKGROUND

CD8<sup>+</sup> cytotoxic T lymphocytes (CTL) are a crucial component of the immunological defense against human immunodeficiency virus type 1 (HIV-1) infection (22). The appearance of CTL responses is associated with the early decline of plasma viremia during HIV-1 infection (189). Depletion of CD8<sup>+</sup> T cells in the non-human primate model results in enhanced disease progression, supporting the protective role of these cells (299). Long term control of both HIV-1 and simian immunodeficiency virus (SIV) infections is associated with a broad and high magnitude CTL response (253, 289), particularly to Gag epitopes (33, 179, 285). However, despite the establishment of HIV-1-specific CTL responses during early HIV-1 infection, they fail to control persistent, chronic HIV-1 infection. A hallmark of HIV-1 pathogenesis is the ability of the virus to escape host CTL responses through mutations within and adjacent to CTL epitopes during the early and chronic phases of the infection (8, 9, 93, 246). HIV-1 prophylactic and therapeutic vaccine strategies have yet to establish protective CD8<sup>+</sup> CTL responses to overcome the propensity of the virus to undergo escape mutations.

The breadth and magnitude of CD8<sup>+</sup> T cell responses are thought to be critical indicators in the control of HIV-1 infection as well as prevention of AIDS (19, 83). Therefore, the induction of strong and broadly reactive memory CTL responses is believed to be necessary to respond to the diverse viral sequences generated during the course of infection. Indeed, the failure of the STEP prophylactic vaccine trial has been linked in part to induction of limited CTL responses and failure to cross-react with circulating viral strains (25, 73). There is also a correlation between the larger number of T cell responses targeting different SIV proteins and control of viral load in non-human primates (204, 277). These emphasize the importance of understanding the mechanisms

underlying the ability of CD8<sup>+</sup> T cell responses to control HIV-1 replication for the design of successful vaccine strategies.

Mechanisms promoting the establishment of escape mutations and thus evasion of clearance of HIV-1-infected cells by CTL include interaction defects between a viral epitope and its cognate MHC class I molecule or between an MHC class I molecule/epitope complex and its T cell receptor (TCR) (202) and impairment at the level of epitope processing (7, 93, 360). It is imperative to overcome these complications of natural infection in order to design HIV-1 vaccines capable of eliciting antiviral immunity targeting the diverse viral strains circulating during the course of infection and spreading from person to person. We have previously shown the generation of broadly reactive and polyfunctional primary CD8<sup>+</sup> T cell responses from HIV-1 naïve adults against HIV-1 and other viral epitopes (67). Optimal priming of CD8<sup>+</sup> T cells requires maturation of DC with CD40L and IFN- $\gamma$ . This maturation protocol generates IL-12-producing DC (104) with increased expression of activation and costimulatory molecules. These factors are involved in activation of memory antigen-specific CD8<sup>+</sup> T cell memory responses and are likely involved in priming of CD8<sup>+</sup> T cells (273). These *in vitro*, T cell memory and priming models represent a promising approach to evaluate the immunogenicity of potential HIV-1 epitopes for vaccine design (219).

To better understand the relationship between viral evolution and its impact/effect on primary and memory responses, we examined autologous HIV-1 *gag*, *env*, and *nef* sequences derived at multiple points up to approximately 12 years post-seroconversion (SC) in a participant in the Multicenter AIDS Cohort Study (MACS) (87, 171). The breadth and magnitude of primary T cell responses were compared to memory, recall T cell responses observed early and late during infection as well as during cART. Our results reveal memory T cell responses specific for prior

and contemporaneous HIV-1 variants. We further demonstrate the development of strong primary responses in pre-SC naïve T cells to naturally evolving HIV-1 variant sequences in an entirely autologous system. These primary CD8<sup>+</sup> T cell responses were of similar breadth to memory responses and of higher magnitude, thus supporting the use of such models in immunotherapy of HIV-1 infection in persons on cART.

## 4.3 METHODS

### 4.3.1 Study participants

Human subject approval was obtained for this study from the institutional review board of the University of Pittsburgh. The participant in this study (subject 8) is enrolled in the Multicenter AIDS Cohort Study (MACS), a natural history study of HIV-1 infection in men who have sex with men (87, 171). The age of the study participant upon enrollment in the study was 24.8 years. The subject's MHC class I alleles as determined by high resolution PCR genotyping (Tissue Typing Laboratory, University of Pittsburgh Medical Center) are HLA-A\*0201 A\*2402 B\*0702 B\*4001 C\*0304 C\*00702. Subject 8 was HIV-1 seronegative upon enrollment in the MACS in November, 1984, and seroconverted to HIV-1 between October 1987 and May 1988. HIV-1 seropositivity was confirmed by a positive enzyme-linked immunosorbent assay (ELISA) for the presence of HIV-1 p24 and a Western blot with bands corresponding to at least 2 of either Gag, Pol, and Env (171). Blood specimens, and epidemiologic and clinical data were obtained at semiannual visits (307). Participant 8 progressed to AIDS as defined by the CDC ( $<200$  CD4<sup>+</sup> T cells/mm<sup>3</sup>) 6.2 years post-SC. cART was initiated July, 1996 at 8.4 years post-SC. This treatment regimen, consisting

of Retrovir (zidovudine azidothymidine, GlaxoSmithKline), Epivir (lamiduvudine 3TC, GlaxoSmithKline) and Invirase (saquinovir mesylate, Roche), was administered for 1 year. At 9.4 years post-SC, Viracept (nelfinavir mesylate, Agouron), Sustiva (efavirenz, Bristol-Meyers Squibb) and Ziagen (abacavir sulfate, GlaxoSmithKline) replaced the previous regimen. This treatment was finally replaced with Atrilpa (efavirenz/emtricitabine/tenofovir, Bristol-Meyers Squibb) at 20.5 years post SC and was maintained for the period of study. Blood was also obtained from 2 anonymous, healthy HIV-1 negative donors (Central Blood Bank, Pittsburgh, PA) who were typed as HLA-A2/B7 by flow cytometry for use in the T cell priming study.

#### **4.3.2 Clinical and virologic characteristics**

At each clinic visit pre- or post-SC and during cART, plasma samples and peripheral blood mononuclear cells (PBMC) were collected and stored at -80°C and -140 °C, respectively. Plasma samples and PBMC were used to determine HIV-1 load and CD4<sup>+</sup> and CD8<sup>+</sup> T cell counts, respectively. T cell phenotypes were determined by flow cytometry as previously described (123, 298). For HIV-1 plasma viremia, RNA was extracted from plasma using a COBAS<sup>®</sup> Ampliprep Instrument (Roche Diagnostics, Indianapolis, IN) and amplified by RT-PCR on a COBAS<sup>®</sup> Taqman<sup>®</sup> 48 Analyzer (Roche Diagnostics) using the COBAS<sup>®</sup> Ampliprep/COBAS<sup>®</sup> Taqman HIV-1 Test. This assay is capable of detecting from 20 to 10<sup>6</sup> HIV-1 RNA copies/ml of plasma. Negative, low positive and high positive controls were used in each RNA extraction and RT-PCR assay as per manufacturer's instructions.



### 4.3.3 Sequencing and phylogenetic analysis

*env* C2-V5 sequences were reported previously (307). *gag* and *nef* sequences were obtained using the procedures and primers as previously described (205, 220, 309). Briefly, viral sequences were derived from 12, 16, and 9 time points for *gag*-p17 and -p24, *env*-gp120, and *nef*, respectively. Sequences spanned 8 years of untreated HIV-1 infection and included at least one post-ART time point. Viral sequencing was not performed during late ART due to inability to detect viral RNA in plasma.

Sequences bearing open reading frames (~90% of all sequences determined) were first aligned with the Pileup program in the GCG suite (Genetics Computer Group, Madison, WI) and then manually edited (205, 206). Both viral divergence from the founder strain and viral diversity were estimated at each time point. To estimate viral diversity, we determined the mean and standard deviation for pairwise nucleic acid distances between all sequences obtained at each time point. To estimate viral divergence, we compared sequences from each visit to a founder sequence that was approximated as the consensus sequence found at the initial virus-positive time point. The mean and standard deviation for all pairwise comparisons were then calculated.

### 4.3.4 Synthetic peptides

Peptide sequences representing autologous Gag, Env, and Nef MHC class I - associated variants evolving in our study participant during infection were synthesized (SynBioSci, Livermore, CA) and used in T cell priming and memory T cell functional assays. Epstein-Barr virus (EBV) BMLF1<sub>280-288</sub> (GL9, GLCTLVAML) (provided by the NIH AIDS Research Program) was used as a control peptide sequence in the functional assays. The Los Alamos HIV Molecular

Immunology Database was referred to for defining MHC Class I epitopes based on being known as optimal epitopes or based on affinity, T cell receptor usage, computational epitope prediction or functional studies. For ease of interpretation, the naturally evolving peptide sequences of subject 8 are referred to in order of their detection post-SC. Consequently, we defined early post-SC (0-2.8 yr post-SC), late post-SC (3.25-7.8 yr), early cART (8.3-10.1yr) and late cART (12.4-13.1 or >12.4yr) time points.

#### **4.3.5 *In silico* and *in vitro* analysis of peptide binding affinity**

HLA peptide binding predictions of the sequences under investigation were scored using the netMHCpan 2.4 server ([www.cbs.dtu.dk/services/NetMHCpan](http://www.cbs.dtu.dk/services/NetMHCpan)) (151, 241). *In silico* (predicted) IC<sub>50</sub> values were computed with binding affinity of peptides for MHC class I. Strong binders were assigned as having an IC<sub>50</sub> threshold of 50 nM and weak binders as having a threshold of 500nM. A fluorescence polarization (FP)–based assay was used to experimentally screen and identify high affinity binding peptides to HLA molecules (Pure Protein LLC, Oklahoma City, OK). Briefly, the assay utilizes fluorescently labeled control peptides and recombinant soluble HLA-A\*0201 and B\*0702 molecules to test for the competitive binding between a labeled reference peptide and the peptide or the peptide mix being investigated. The binding affinity of the competitor peptide is expressed as the concentration inhibiting 50% (IC<sub>50</sub>) of the binding of the labeled peptide (48). The followings are the binding affinity categories based on the log IC<sub>50</sub>: high affinity < 3.7, medium < 4.7, low < 5.5, and no affinity < 6.0 (48).

#### 4.3.6 Generation of dendritic cells (DC)

Monocyte-derived DC were generated from subject 8 and two healthy HIV-1 negative adults as previously described (67) with minor modifications. Briefly, CD14<sup>+</sup> monocytes were positively selected using anti-CD14 monoclonal antibody (mAb) coated magnetic beads (StemCell Technologies, Vancouver, Canada) or Percoll density separation (Sigma-Aldrich, Saint Louis, MO). DC were generated by culture of the purified monocytes with 1,000U/ml recombinant GM-CSF (Bayer Healthcare, Montville, NJ) and 1,000 U/ml recombinant IL-4 (R & D Systems, Minneapolis, MN). On day 5, immature DC were treated for 48 h with recombinant CD40L (0.5 µg/ml; Enzo, Farmingdale, New York) for use in memory T cell assays or CD40L (0.5 µg/ml) and interferon  $\gamma$  (IFN- $\gamma$ ; 1000 U/ml; R&D) for use in priming assays.

#### 4.3.7 *In vitro* priming

*In vitro* priming of autologous PBMC was performed as previously described with minor modifications (67). Briefly, DC were derived from PBMC obtained from subject 8 during virus suppressive cART and the HIV-1 negative, adult volunteers. Autologous DC matured with CD40L and IFN- $\gamma$  were incubated with 10 µg/ml of HIV-1 peptides in IMDM medium (Gemini Bio-Products, West Sacramento, CA) containing 10% heat-inactivated fetal calf serum (FCS) (Gemini Bio-Products) for 2 hr at 37°C in a 5% CO<sub>2</sub> atmosphere. The DC were harvested and re-suspended with autologous PBMC at a responder-to-stimulator (T:DC) ratio of 10:1. Autologous PBMC from subject 8 were obtained from cryopreserved cells prior to SC. After 3 days, the co-cultures were fed with fresh IMDM/10% FCS supplemented with recombinant IL-15 (2.5ng/ml; PeproTech, Rocky Hill, NJ), IL-2 (50 U/ml; Chiron, Emeryville, CA) and IL-7 (10 ng/ml; Miltenyi, Auburn,

CA). This was repeated at 2-3 day intervals thereafter for 2 weeks. PBMC were then re-stimulated with autologous DC loaded with the same set of peptides as in the primary stimulation at a responder-to-stimulator (T:DC) ratio of 10:1. These cells were harvested after a total of 21 days of culture and used in IFN- $\gamma$  ELISPOT assays.

#### **4.3.8 IFN $\gamma$ ELISPOT assay**

ELISPOT assays were performed as previously described (67, 156). Briefly, 96 well plates were coated overnight with 1  $\mu$ g/ml anti-human IFN $\gamma$  mAb 1-D1K (Mabtech, Stockholm, Sweden) at 4°C. DC matured with CD40L were loaded with 10  $\mu$ g/ml HIV-1 peptides or control EBV peptides in IMDM/10% FCS for 2 hr at 37°C. Control wells contained T cells in the presence of mature DC. Autologous PBMC in IMDM/10% FCS were added to wells at a responder-to-stimulator ratio of 10:1 and were incubated for 18 hr at 37 °C in a 5% CO<sub>2</sub> atmosphere. Following incubation, wells were washed with PBS/0.05% Tween-20 (Fisher Scientific, Pittsburgh, PA) and were treated with biotinylated anti-IFN- $\gamma$  mAb (1  $\mu$ g/ml; Mabtech, Stockholm, Sweden). Plates were washed with PBS/0.05% Tween 20 and incubated with an avidin-peroxidase complex (Vectastain ABC Kit, Vector Laboratories, Burlingame, CA) for 45 min at room temperature. Plates were washed with 0.05% Tween 20/PBS and PBS alone to remove unbound complexes followed by peroxidase staining with diaminobenzidine solution (Sigma, St Louis, MO) for 5 min at RT. IFN- $\gamma$  spot-forming cells (SFC) were enumerated using an AID ELISPOT reader (Cell Technology, Columbia, MD). Results reported represent mean values of duplicates and are expressed as spot forming cells/10<sup>6</sup> PBMC. T cell responses were considered positive after subtraction of the mean number of spots stimulated by DC alone from the mean number of spots induced by peptide-loaded DC.

### 4.3.9 Statistical analysis

The following statistical analyses were carried out: Pearson correlation between 1) predicted ( $IC_{50}$ ) and experimental ( $\log IC_{50}$ ) MHC binding, 2) viral load and divergence and diversity, 3) MHC binding and magnitude of T cell responses, 4) MHC binding and percent positive T cell responses, 5) the frequency of occurrence of variants and the percent positive T cell responses. In addition, a two-tailed paired-T test was used to compare the proportion of positive primary responses in our study participant as well as to compare subject 8 primary responses targeting naturally evolving sequences to those observed against the same sequences when testing our priming model with cells from two healthy donors. Bonferroni posthoc comparisons were applied to compare memory responses targeting contemporaneous Gag, Env and Nef variant sequences at early, late, early ART or late ART time intervals. Statistical analyses were conducted using GraphPad Prism software (version 4) and SPSS software (version 17.0).

## 4.4 RESULTS

### 4.4.1 Clinical and virologic characteristics of the study participant

Subject 8 enrolled in the MACS in November 1984, 3.2 years prior to SC to HIV-1. He was negative for both hepatitis B and C viruses throughout the period of study. PBMC and plasma samples were collected biannually from the time of enrollment. Within the first 3 years after SC (early post-SC: 0-2.8 years), the number of CD4<sup>+</sup> T cells decreased and the number of CD8<sup>+</sup> T cells increased, with an inversion in the CD4:CD8 T cell ratio (**Figure 26**).

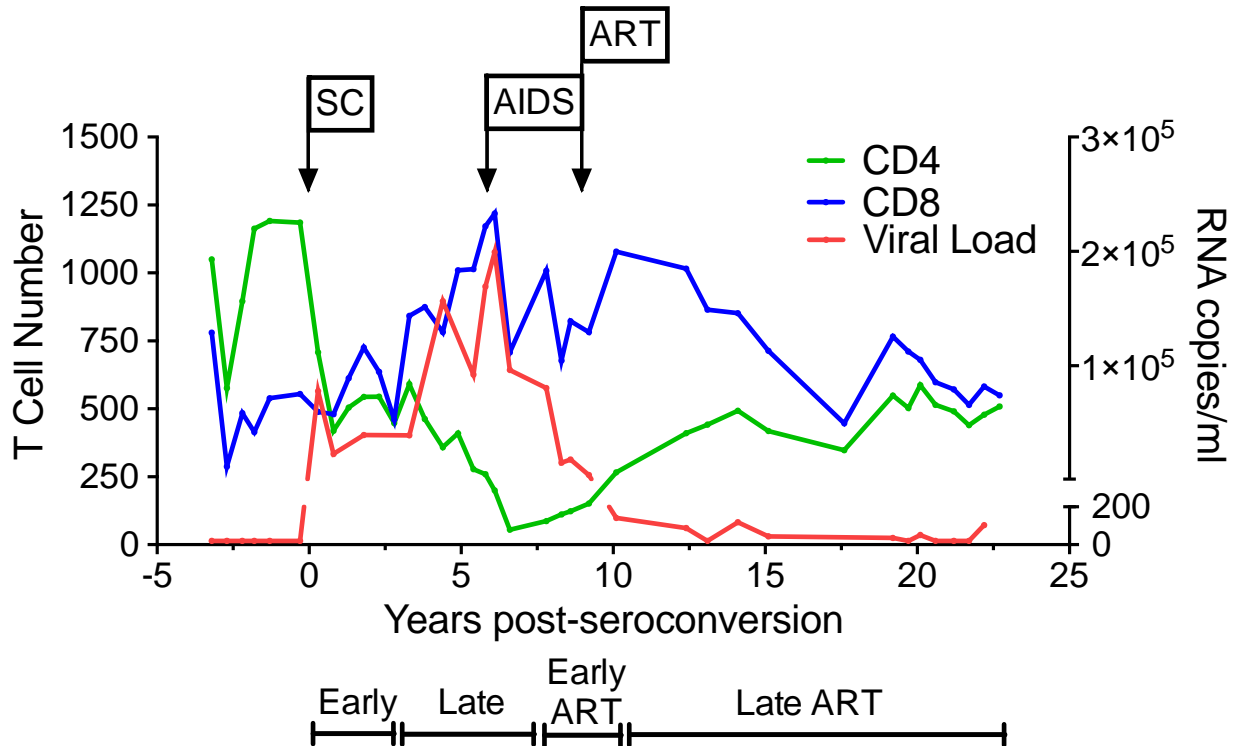


**Figure 26. Clinical course of HIV-1 infection in the study participant**

Plasma viral load (red line), CD4<sup>+</sup> (green line), and CD8<sup>+</sup> (blue line) T cell counts in subject 8 are shown. Subject 8 developed AIDS as per CDC guidelines 6.2 years post-SC. cART was administered 8.4 years post-SC. Time frames include early, late, early cART, and late cART and are defined as follow: 0-2.8 years post-SC, 3.3- 7.8 years post-SC, 8.3-10.1 years post-SC, and >12.4 years post-SC, respectively. SC, seroconversion.

Viral load increased sharply to  $7.8 \times 10^4$  RNA copies/ml at the first SC visit (0.3 years) and then reached a set point ranging from 23,092 to 39,608 RNA copies/ml up to 2.8 years. For the next 4.4 years (late post-SC: 3.3-7.8 years), the numbers of CD4<sup>+</sup> T cells decreased, reaching 200 cells/mm<sup>3</sup> 6.1 years post-SC (Stage 3 HIV-1 infection, AIDS) (300) while CD8<sup>+</sup> T cells continued to increase. This decline in CD4<sup>+</sup> T cells was associated with a rise in viral load that began approximately 3.8 years post-SC. A decline in viral load to a nadir of 80,470 copies/ml at 7.8 years post-SC was observed after development of AIDS and before initiation of cART at 8.3 years post SC. Overall, we observed a negative correlation between HIV-1 viral load and CD4<sup>+</sup> T cell counts ( $p=0.001$ ), as well as a positive correlation between viral load and CD8<sup>+</sup> T cell counts ( $p=0.0004$ ) before cART. Imposition of cART led to a decline in viral load to <200 RNA copies/ml during the first 1.8 years (early cART: 8.3-10.1 years). HIV-1 plasma viremia was maintained between <20 and 119 copies/ml through the next 10 years (late post-cART: >12.4 years). During this period of viral suppression, an increase in the CD4<sup>+</sup> T cell count was observed with levels ranging between 266 and 587 cells/mm<sup>3</sup>, with a concurrent decrease in CD8<sup>+</sup> T cell counts (**Figure 26**).

Taken together, these data demonstrate a typical course of HIV-1 infection from SC through development of AIDS, and recovery on cART. Consequently, we chose to use this participant in our longitudinal analysis of viral evolution and immunological responses to autologous HIV-1.

#### **4.4.2 Dynamics of viral evolution and epitope variants**

We examined the longitudinal changes in HIV-1 genes from subject 8 to define the effects of immune pressure during chronic, untreated infection and during cART. We sequenced 12, 16, and 9 time points that spanned >10 years of infection for *gag*-p17/-p24, *env*, and *nef* genes,

respectively. We next determined the pairwise diversity and divergence from the founder virus population at each time point. As expected (307), viral diversification and divergence in each HIV-1 gene gradually increased with time (**Figure 27**).

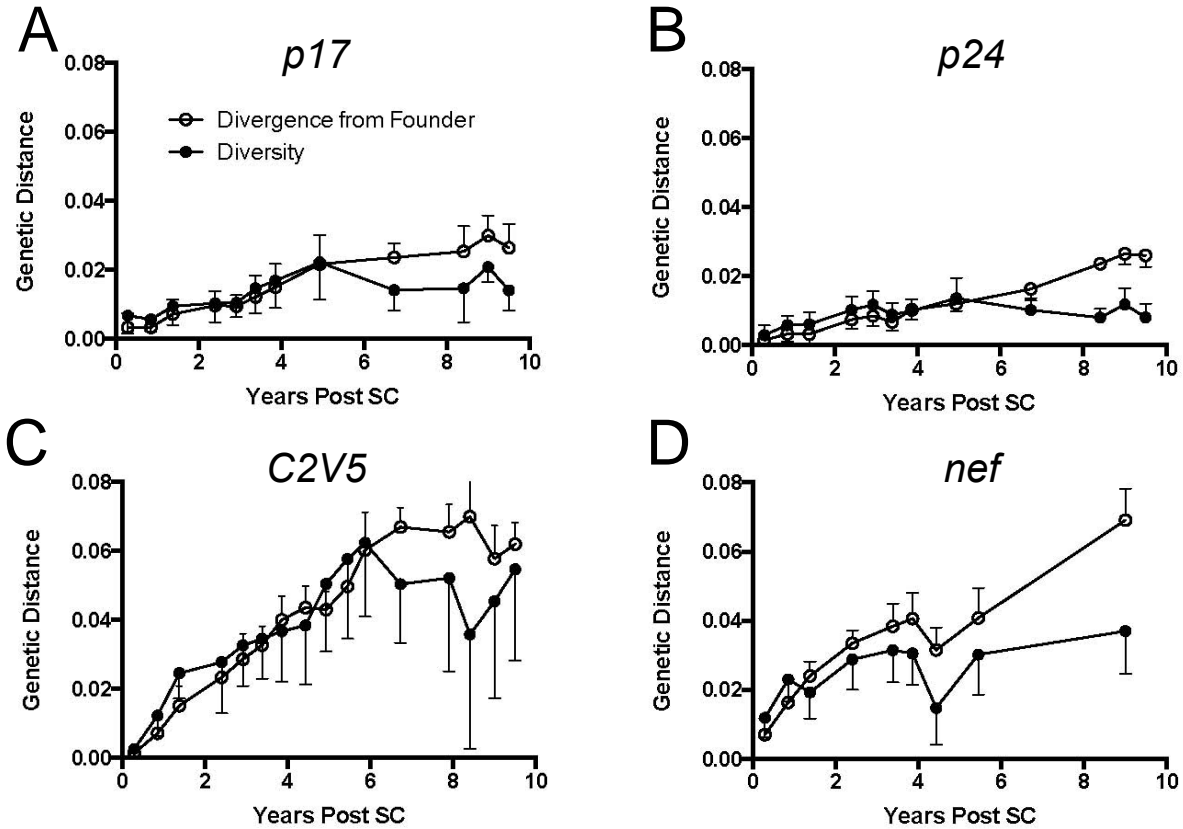


**Figure 27. Dynamics of genetic diversity and divergence of HIV-1**

(○) Divergence and (●) diversity of (A) *gag* p17, (B) *gag* p24, (C) *env*, and (D) *nef* are plotted (y-axis) for each gene during the course of HIV-1 infection. Subject 8 developed AIDS 6.2 years post-SC and cART was administered at 8.4 years post-SC. Trends in pairwise distance diversity and divergence from the founder virus are plotted through time from seroconversion to 10.1 years post-SC. SC, seroconversion.

Diversity accumulated linearly in *gag* p17 (**Figure 27A**) and *gag* p24 (**Figure 27B**) and then shrank, with the peak being about 4.9 years post-SC. Notably, diversification of *env* (**Figure 27C**) and *nef* (**Figure 27D**) proceeded faster than that of *gag*. A linear increase in diversity was observed until 6.1 years post-SC in *env*, when X4 viruses first appeared, and then diversity began to shrink (307). Diversification of the *nef* gene followed a different pattern, with diversification



appearing to slow appreciably before 4 years of infection, and, following a transient contraction, increased slowly thereafter. No clear plateau in divergence from the founder strain was noted in *nef* (**Figure 27D**).

In summary, the circulating viral populations within our study participant show increasing divergence from the founder virus. Interestingly, we observed a significant correlation between viral load and viral divergence ( $p < 0.01$ ) and diversity ( $p = 0.05$ ) up through 6.6 years post-SC, wherein viral load began a rapid decline prior to cART.

#### **4.4.3 Autologous HIV-1 peptide binding affinity for MHC class I**

The strength of peptide binding to MHC class I is a key determinant in CTL epitope immunogenicity (285). We therefore identified known HLA A\*0201- and B\*0702-restricted HIV-1 CTL epitopes in autologous sequences from subject 8 based on previously established immunologic activity (362). We also predicted additional HLA A\*0201- and B\*0702-restricted epitopes using the BioInformatics and Molecular Analysis Section (BIMAS) computational model (256). Accordingly, we identified 11 peptide families consisting of the Gag, Env, or Nef founder epitopes and their corresponding autologous variants that evolved during infection (**Table 5**). Epitope variants are referred to in Table 1 in order of their evolution in our study participant.

**Table 6. Longitudinal HIV-1 peptide sequences and their predicted and experimental HLA A and B affinity**

HIV-1 protein (epitope position)	Sequence <sup>a</sup>	HLA <sup>b</sup> restriction	MHC Class I Binding		Correlation coefficient	p value
			netMHCpan <sup>c</sup>	logIC <sub>50</sub> <sup>d</sup>		
<b>Gag</b>						
p17 77-85	SLFNTVATL	A*0201	139.2	3.81	0.9777	0.0002
	SLFNTVA <u>A</u> L	potential	41.9	3.84		
	SLFNTVAT <u>P</u>	potential	13108	5.24		
	SLF <u>S</u> TVATL	potential	106.9	3.66		
	SLFNTIATL	potential	55.12	3.92		
	SLY <u>N</u> TVATL	A*0201	223.2	3.86		
p24 16-24	SPRTLNAWV	B*0702	36.4	4.18	0.0357	NS <sup>e</sup>
	SPRTL <u>D</u> AWV	undefined	102.5	4.38		
	SPR <u>A</u> LNAWV	undefined	24.4	4.07		
	PPRTLNAWV	undefined	1221	4.22		
	SPR <u>P</u> LNAWV	undefined	20	4.18		
	SPRTL <u>S</u> AWV	undefined	36.9	6.08		
p24 19-27	TLNAWVKVV	A*0201	113.7	4.16	0.8439	0.034
	TL <u>D</u> AWVKVV	potential	85.6	4.30		
	<u>A</u> LNAWVKVV	potential	42.7	3.93		
	<u>P</u> LNAWVKVV	potential	2854.1	4.81		
	TL <u>S</u> AWVKVV	potential	105.4	4.18		
p24 143-151	RMYSPT <u>S</u> IL	potential	173.1	4.34	0.9738	0.0132
	RMYS <u>P</u> ISIL	potential	87.7	3.83		
	RMYS <u>P</u> ASIL	potential	281	4.78		
	RMYS <u>P</u> VSIL	potential	123.8	3.92		
<b>Env</b>						
gp160/120 298-307	RPNNNTRK <u>S</u> I	B*0702	14.7	3.56	0.0901	NS
	RPNNNTR <u>R</u> SI	undefined	9.3	3.99		
	R <u>S</u> NNNTRKSI	undefined	3120.83	4.33		
	RPNNNTRK <u>S</u> T	RS9 B*07	130	4.04		
	RPNN <u>S</u> TRKSI	undefined	12.6	3.87		
	RPNN <u>D</u> TRKSI	undefined	23.9	3.85		
	RPNNNTRK <u>R</u> I	undefined	49.7	4.32		
	RPNNNT <u>G</u> KRI	undefined	77.4	4.36		
	R <u>P</u> SNNTRKRI	undefined	34.4	4.17		
	R <u>P</u> TNNTRKSI	undefined	16.6	3.75		
	RPNNNTRK <u>C</u> I	undefined	67.8	4.63		

	RPNNNTRK <u>S</u> <u>L</u>	RS9 B*07	5.4	3.69		
341-349	TLEQVVKKL	potential	10358.5	5.34	0.7055	0.0006
	<u>A</u> LEQVVKKL	potential	4739.2	4.93		
	<u>M</u> LEQVVKKL	potential	2643.9	4.99		
	TL <u>A</u> QVVKKL	potential	1205.9	4.55		
	TLEQVVE <u>K</u> L	potential	3291.8	5.11		
	<u>I</u> LEQVVKKL	potential	4295.9	5.35		
	TLEQVV <u>N</u> KL	potential	3678.9	5.14		
	TL <u>D</u> <u>K</u> VVKKL	potential	3003.6	4.96		
	TL <u>G</u> <u>R</u> <u>V</u> <u>A</u> KKL	potential	8819.8	6.03		
	TL <u>G</u> <u>Q</u> <u>V</u> <u>V</u> <u>E</u> KL	potential	677.1	4.45		
	TL <u>D</u> <u>K</u> <u>V</u> <u>V</u> <u>E</u> KL	potential	431.5	4.36		
<b>Nef</b>						
68-76	FPVRPQVPL	B*0702	8.6	3.83	0.9766	0.0015
	F <u>S</u> VRPQVPL	potential	2500.2	4.85		
	FP <u>A</u> RPQVPL	potential	5.2	3.66		
	<u>S</u> PVRPQVPL	potential	8.4	3.67		
	FP <u>I</u> RPQVPL	potential	7.9	3.62		
77-85	RPMTWKGAL	potential	2.9	3.85	0.0733	NS
	RPMTW <u>K</u> <u>A</u> AL	potential	2.7	3.86		
	RPMT <u>Y</u> KGAL	potential	2.6	3.89		
	RPM <u>T</u> <u>R</u> <u>K</u> <u>A</u> AL	potential	2.1	3.82		
	RPMT <u>C</u> KGAL	potential	2.9	3.74		
	RPMT <u>Y</u> <u>K</u> <u>A</u> AL	B*0702	2.4	4.04		
	RP <u>I</u> <u>T</u> <u>Y</u> <u>K</u> <u>A</u> AL	potential	3.2	3.87		
128-137	TPGPGTRYPL	undefined	20.3	3.57	0.9076	<0.0001
	TPGPG <u>I</u> <u>R</u> <u>F</u> PL	undefined	43.7	3.4		
	TPGPG <u>I</u> <u>R</u> YPL	B7	34.8	3.78		
	TPGPG <u>I</u> <u>R</u> <u>Y</u> <u>P</u> <u>V</u>	undefined	142.3	3.74		
	TPGPG <u>I</u> <u>R</u> <u>F</u> <u>I</u>	undefined	150.3	3.77		
	T <u>S</u> GPGT <u>R</u> <u>F</u> PL	undefined	5462.9	4.85		
	<u>I</u> PGP <u>G</u> <u>R</u> <u>H</u> PL	undefined	16.8	3.51		
		B7				
	TPGPG <u>V</u> RYPL	supertype	30.3	3.64		
	TPGPG <u>P</u> RYPL	undefined	30.3	3.77		
	TPGPGT <u>R</u> PL	undefined	23.7	3.46		
	TPGPG <u>P</u> <u>R</u> <u>F</u> PL	undefined	35.9	3.66		
	TPGPG <u>I</u> <u>R</u> <u>Y</u> <u>P</u> <u>M</u>	undefined	36.1	3.5		
	TPGPG <u>P</u> <u>R</u> <u>Y</u> <u>P</u> <u>V</u>	undefined	117.7	3.82		
	TPGPG <u>P</u> <u>R</u> <u>Y</u> <u>P</u> <u>M</u>	undefined	33.2	3.57		
	T <u>K</u> GPG <u>I</u> <u>R</u> <u>F</u> PL	undefined	12856.5	5.41		

136-145	PLTFGWCFKL <sup>g</sup>	undefined	4173.8	6.48	0.00	NS
	PLTLGWCFKL	undefined	5994.1	6.10		
	PITFGWCFKL	undefined	16105.3	6.35		
	PVTFGWCFKL	undefined	19876.4	6.48		
	PLCFGWCFKL	undefined	3451.6	4.86		
	PVCFGWCFKL	undefined	18878.7	5.4		
	PMCFGWCFKL	undefined	2898.1	5.3		
	PLCFGWCFKP	undefined	36444.9	5.34		
180-189	VLVWRFDSSL	undefined	212.2	4.4	0.8315	0.0042
	VLVWKFDSSL	undefined	179.6	4.37		
	VLVWKSDSSL	undefined	401.3	4.76		
	VLVWKFDSSL	undefined	197.4	4.31		
	VLVWKFDSSL	undefined	330.1	4.82		
	VLVWKFDSSL	undefined	290.0	4.44		
	VLVWKFDSSL	undefined	154.6	4.22		

<sup>a</sup> These sequence variants of HIV-1 epitopes are listed in order of time of appearance during the course of infection.

<sup>b</sup> These are known or potential MHC class I epitopes defined by the HIV sequence database as HLA A\*0201 or B\*0702. A potential epitope is a single peptide having C-terminal anchor residues and internal anchors matching one or more motifs associated with the submitted HLA, but are *not* found in the HIV sequence database.

<sup>c</sup> This is the IC<sub>50</sub> (nM) prediction binding score of peptides under investigation. Strong binders have an IC<sub>50</sub> threshold of 50 and weak binders have a threshold of 500.

<sup>d</sup> logIC<sub>50</sub> is used to refer to the experimental (*in vitro*) binding of peptides to HLA A\*0201 or B\*0702. The followings are the binding affinity based on the log IC<sub>50</sub>: high affinity < 3.7, medium < 4.7, low < 5.5, and no affinity < 6.0.

<sup>e</sup> NS: Pearson correlation, between predicted and experimental MHC binding, is not significant, p value > 0.05.

<sup>f</sup> LTFGWCFKL can bind all five HLA-A2 supertypes alleles: A\*0201, A\*0202, A\*0203, A\*0206 and A\*6802.

An *in vitro* fluorescence polarization binding assay was performed for each variant (48). We also evaluated the predicted MHC-restricted binding affinity of variant epitope sequences within Gag, Env, and Nef by netMHCpan (151, 241). Lower experimental logIC<sub>50</sub> values and netMHCpan scores (IC<sub>50</sub>) correspond to actual and predicted higher peptide:MHC binding affinity, respectively. Significant positive correlations were found between observed and predicted MHC class I binding in the following families: SLFNTVATL (Gag p177-85), TLNAWVKVV (Gag

p24<sub>19-27</sub>), RMYSPTSIL (Gag p24<sub>143-151</sub>), TLEQVVKKL (Env gp160/120<sub>341-349</sub>), FPVRPQVPL (Nef<sub>68-76</sub>), TPGPGTRYPL (Nef<sub>128-137</sub>), and VLVWRFDSSL (Nef<sub>180-189</sub>) (Table 1).

Peptide variants were categorized based on their MHC class I affinity as determined by experimental log IC<sub>50</sub> values: high affinity binders < 3.7, medium affinity binders < 4.7, low affinity binders < 5.5 and no affinity binders < 6.0. Figure 28 shows: 1) medium binders constituted >97% of the Gag epitope pool at all three time points, 2) within Env contemporaneous epitopes, medium binders made up only 4% of the epitope pool early post-SC, but increased to 19.7% and 45.1% during late post-SC and early cART, respectively; frequency of high and low binders gradually decreased with this increase in medium binders, and 3) the frequency of Nef variants with medium binding affinity ranged from 50% to 70% through time with no trend in the fluctuation of low and high binder frequencies. Peptide variants with medium binding affinity were more frequent than variants with low or high binding affinity throughout chronic infection.

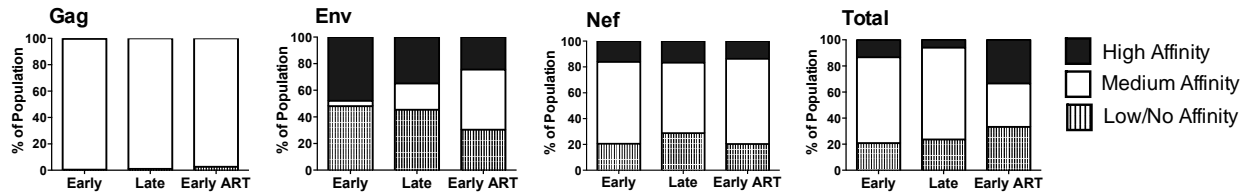


**Figure 28. Proportion of HIV-1 epitope variants exhibiting differential MHC class I affinities**

Epitope variants derived from autologous sequences from subject 8 were synthesized and evaluated for binding to soluble HLA A\*0201 or B\*0702 molecules by fluorescence polarization to determine a logIC<sub>50</sub> for each variant. Variants were separated into three distinct groups based on experimental logIC<sub>50</sub> values: high affinity (< 3.7), medium affinity (3.7-4.7), and low/no affinity (>4.7). The longitudinal changes in the proportion of these variants within the Gag, Env, and Nef epitopes of interest, as well as in all epitopes evaluated, are shown for early post-SC, late-post-SC, and early cART time points.

#### **4.4.4 Impact of peptide:MHC binding affinity on the breadth of memory T cell responses to autologous contemporaneous HIV-1 peptide sequences**

To better understand the impact of CTL epitope variation and the frequency of different binders on corresponding T cell responses, we longitudinally evaluated HIV-1 specific T cell responses targeting autologous known and predicted CTL epitope variants. Autologous PBMC were used as responder cells in IFN $\gamma$  ELISPOT to measure memory (recall) T cell responses stimulated by DC-loaded with peptide sequences. We first calculated the percent of naturally occurring Gag, Env, and Nef peptide variants that yielded positive *in vitro* T cell responses at early post-SC, late post-SC, or during cART time points (**Figure 29**) (207).

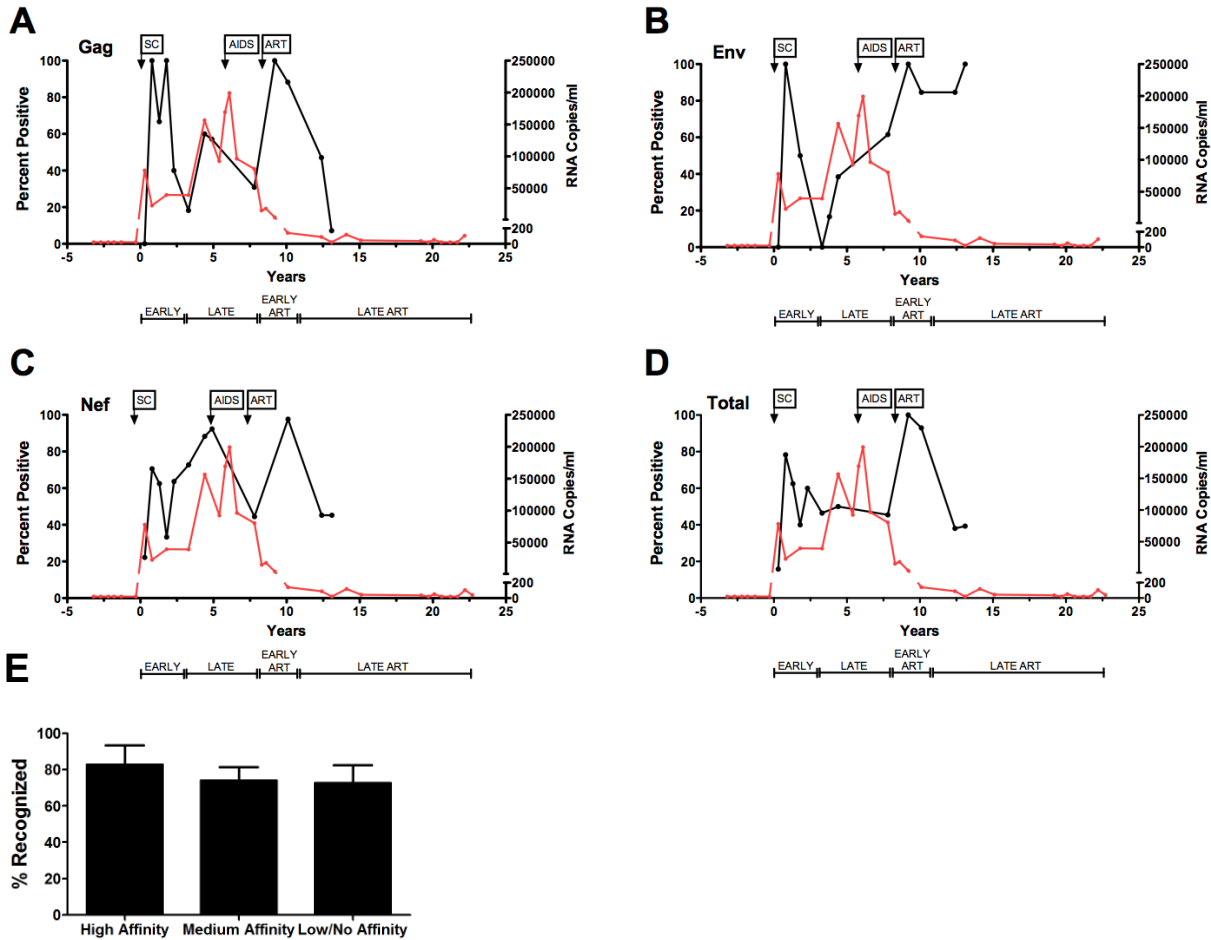


**Figure 29. The percent of autologous HIV-1 epitope variants that induced T cell responses**

Synthetic peptide sequences representing autologous variants of subject 8 were loaded onto mature autologous DC and used to stimulate cryopreserved autologous PMBC. PMBC were added to wells at a responder-to-stimulator ratio of 10:1. Epitope-specific T cell responses were measured by IFN $\gamma$  ELISPOT assay. The “percent positive” is defined as the percent of epitope variants to which we detected *in vitro* T cell responses at each time point. Viral load (red line) and percent positive (black line) to Gag variants (A), Env variants (B), Nef variants (C) and all variants tested (D) are shown across time. (E) The percent of variants with high, medium, or low/no affinity that were recognized at all time points by IFN $\gamma$  ELISPOT assay. Affinity binding categories are based on the values of log IC<sub>50</sub>: high affinity < 3.7, medium < 4.7, low/no affinity > 5.5. SC, seroconversion.

Viewing the data in this fashion allowed us to evaluate the overall breadth and efficiency of memory responses during progressive HIV-1 infection. The total percent of epitope variants inducing HIV-1-specific memory T cell responses peaked early post-SC, then declined and remained minimal shortly after establishment of the viral set point. This early T cell response was reflected in specific targeting of Gag, Env, and Nef variant sequences (**Figure 29A-C**). Overall,

we observed a tri-modal pattern in the breadth of T cell memory (**Figure 29D**). Following this early peak in T cell reactivity, there was a decline in responses to all three HIV-1 proteins. This pattern of immune reactivity was associated with an early decrease in plasma viral load to 23,092 copies of HIV-1 RNA, followed by relatively steady levels of HIV-1 RNA for ~3.0 years. The greatest breadth, i.e. the greatest “percent positive”, to Gag, Env, and Nef variants was observed during early cART (**Figure 29A-C**). This was associated with a decline in viral load to less than 200 copies/ml of plasma. During late cART, the total breadth of memory T cell responses declined for both Gag (**Figure 29A**) and Nef (**Figure 29C**) epitope variants. Memory responses to Env variants, however, remained relatively constant (**Figure 29B**). Interestingly, there was no significant difference in the percent of variants with high, medium, or low MHC class I affinity that induced detectable responses at any time point tested (**Figure 29E**). Overall, we observed significant correlations between the frequency of variants with high, medium, and low/no affinity and the percentage each of these contributed to the overall breadth of the autologous memory response early post-SC ( $p=0.003$ ,  $r^2=0.601$ ), late post-SC ( $p<0.0001$ ,  $r^2=0.827$ ), early cART ( $p<0.0001$ ,  $r^2=0.815$ ), and at late cART ( $p<0.0001$ ,  $r^2=0.816$ ). Taken together, we show that the breadth of memory T cell responses was associated with the frequency of occurrence of contemporaneous variants.

Our results indicate a typical course of progressive HIV-1 infection whereby an early increase in anti-HIV-1 CTL activity is associated with a decrease in HIV-1 viremia. As the untreated virus infection resulted in inexorable immune dysfunction, T cell reactivity no longer controlled viral replication. Initiation of cART was associated with control of viral replication and a temporal enhancement of anti-HIV-1 CTL responses that eventually declined to a low level, steady state (51, 167, 281).



#### 4.4.5 The changing magnitude of T cell memory responses targeting autologous HIV-1 variant sequences

We next assessed the longitudinal change in T cell responses to autologous Gag, Env, and Nef epitope variants (**Table 5**). Mature, autologous DC were loaded with synthetic peptides representing contemporaneous Gag, Env, and Nef CTL epitope variants and these peptides were used to stimulate PBMC in IFN $\gamma$  ELISPOT. Because sequencing data were not available for late cART time points, we used epitope variants reflecting circulating sequences during early cART in the late cART T cell memory assays. T cell memory responses to Gag families (SLFNTVATL, SPRTLNAW, TLNAWVKVV and RMYSPTSIL) ranged from 0 to 800 SFC/10<sup>6</sup> PBMC (**Figure 30**). Early post-SC we observed modest IFN $\gamma$  recall responses to 3 out of the 4 Gag families (SLFNTVATL, SPRTLNAW and TLNAWVKVV) (**Figure 30A-C**). These T cell responses decreased to low or undetectable levels late post-SC. More robust memory T cell responses were observed during early cART. In contrast, there were little or no memory responses to the RMYSPTSIL variants early post-SC, although these responses moderately increased late post-SC (**Figure 30D**). SLFNTVATL, TLNAWVKVV (known HLA A\*0201 epitopes), and SPRTLNAWV (known HLA-B\*0702 epitope) were in circulation at all time points. The magnitude of T cell responses to these variants consistently increased early following cART. These responses were either reduced or completely lost during late therapy. T cell responses targeting Gag variants circulating at early cART were statistically significant and higher than responses targeting variants circulating at early and late post-SC, and during late cART (**Figure 30E**).

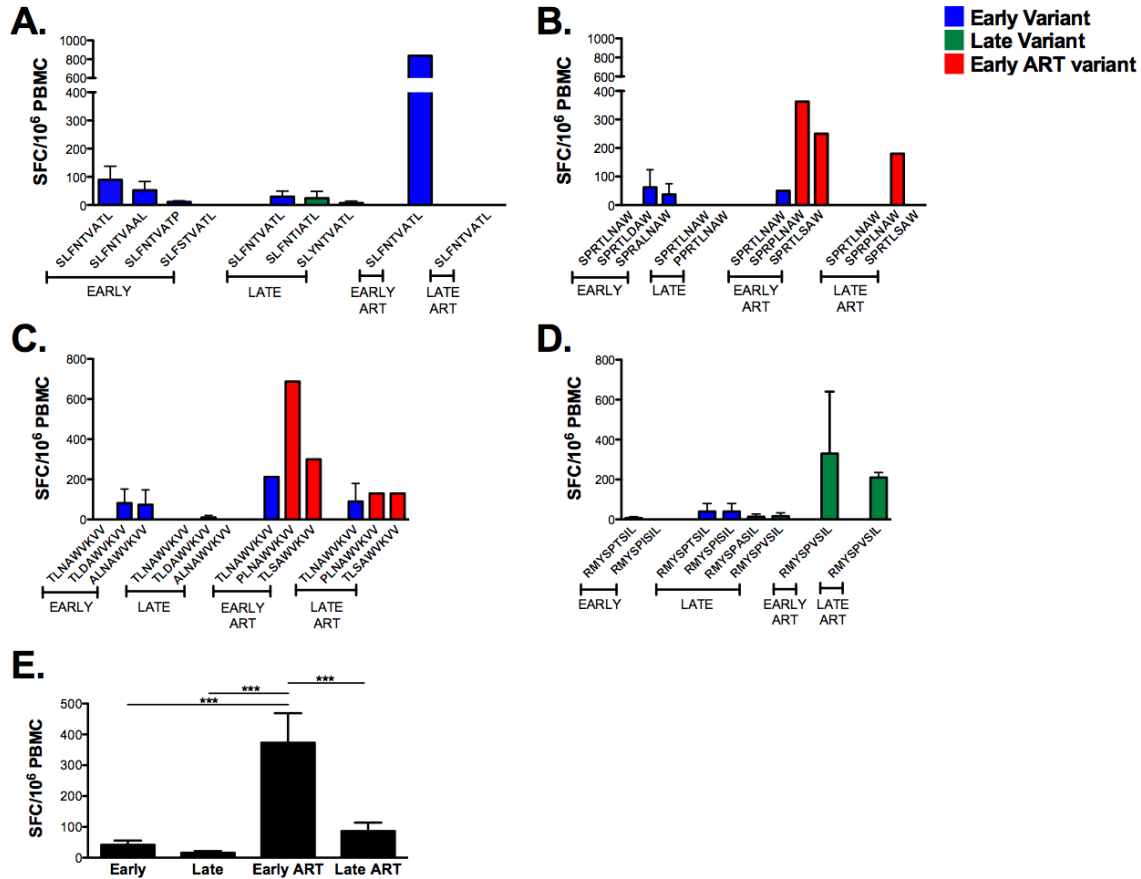


**Figure 30. Longitudinal changes in T cell responses against contemporaneous Gag epitope variants.** As previously described, synthetic 9 mer or 10 mer HIV-1 peptide sequences representing autologous contemporaneous variants of the study participant were loaded into mature autologous DC and were used to stimulate cryopreserved autologous PMBC at a responder-to-stimulator ratio of 10:1 in an IFN $\gamma$  ELISPOT assay. IFN $\gamma$  production (y-axis) to contemporaneous variants of (A) SLFNTVATL (p17 77-85), (B) SPRTLNAWV (p24 16-24), (C) TLNAVWVKVV (p24 19-27), and (D) RMYSPVSIL (p24 143-151) are shown across time. Blue histograms, early variants that emerged 0-2.8 years post-SC and tested with autologous PBMC; green histograms, late variants that emerged 3.3-7.8 years post-SC and tested with autologous PBMC; red histograms, early cART variants that emerged 8.3-10.1 years post-SC and tested with autologous PBMC. Epitope specific T cell responses labeled as late cART represent sequences evolving at early cART and assumed to linger through late cART(>10.1 years post-SC). (E) Mean Gag-specific memory responses detected early post-SC (0-3 years post-SC), late post-SC (3.25-7.75 years post-SC), early cART (8-10.25 years post-SC), and late cART (>10.5 years post-SC). SC, seroconversion, SFC, spot-forming cells. Standard deviation bars are shown when applicable. \*\*\*p<0.001

We next evaluated recall T cell responses to HIV-1 Env epitope variants. We observed strong T cell responses targeting the variants of RPNNNTRKSI late post-SC (**Figure 31A**). RPNNNTRKSI, a known HLA-B\*0702 epitope that lingered throughout infection, did not induce memory responses early post-SC; however, increasing responses were detected late post-SC and



responses (**Figure 32**). FPVRPQVPL, a founder sequence and a known B\*0702 epitope (**Table 5**), was frequently in circulation and stimulated low memory responses at all studied time points with a moderate increase following the administration of cART (**Figure 32A**). The founder sequences of the RPMTWKGAL family induced specific-memory responses *in vitro*. The switch observed in the dominant form of the estimated founder sequence RPMTWKGAL to become RPMTWKAAL was associated with maintenance of the ability of the latter to induce memory responses until early cART (**Figure 32B**). These responses were lost during late therapy. RPMTWKAAL is also identified as a known B\*0702 epitope whereas the remaining variants are identified as potential epitopes (**Table 6**).

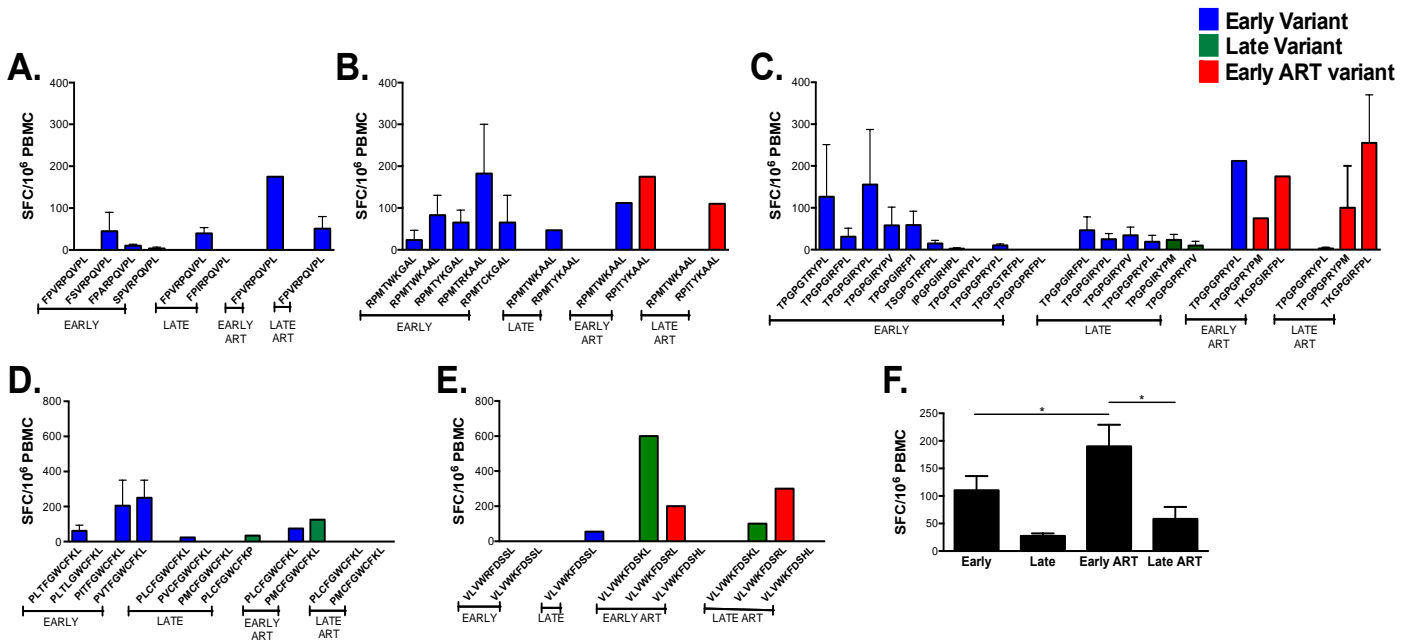


**Figure 32. Longitudinal changes in T cell responses against contemporaneous Nef epitope variants.** As previously described for Gag and Env, synthetic contemporaneous variants of Nef peptide sequences were

loaded into mature autologous DC and were used to stimulate PBMC in an IFN $\gamma$  ELISPOT assay. Nef-specific IFN $\gamma$  responses (y-axis) to contemporaneous variants of the (A) FPVRPQVPL (68-76), (B) RPMTWKGAL (77-85), (C) TPGPGTRYPL (128-137), (D) PLTFGWCFKL (136-145), and (E) VLVWRFDSSL (180-189) epitopes are shown across time. Blue histograms, early variants that evolved 0-2.8 years post-SC and tested with autologous PBMC; green histograms, late variants that evolved 3.3-7.8 years post-SC and tested with autologous PBMC; red histograms, early cART variants that evolved 8.3-10.1 years post-SC and tested with autologous PBMC. T cell responses labeled as late cART represent sequences that evolved during early cART and were assumed to linger through (>10.1 years post-SC). (F) Mean Nef-specific memory responses detected early post-SC (0-3 years post-SC), late post-SC (3.25-7.75 years post-SC), early cART (8-10.25 years post-SC), and late cART (>10.5 years post-SC) time points. SC, seroconversion, SFC, spot-forming cells. Standard deviation bars are shown when applicable. \*p<0.05

The majority of TPGPGTRYPL variants that evolved early post-SC induced low to moderate memory responses (**Figure 32C**); responses to the variants lingering to late time points were reduced. Early and late cART time points were associated with maintenance of moderate responses to contemporaneous sequences and loss of response to one of the studied founder sequences (TPGPGTRYPL). Responses to TPGPGIRYPL, a HLA B\*07 epitope (**Table 5**), were reduced with time whereas the TPGPGVRYPL variant, a B\*07 supertype, was not able to stimulate memory responses early post-SC. LTFGWCFKL (**Table 5**) is reported by the Los Alamos database to bind all five HLA-A2 supertype alleles: A\*0201, A\*0202, A\*0203, A\*0206 and A\*6802. Memory responses to two 10mers containing variants of LTFGWCFKL (PLCFGWCFKL and PMCFGWCFKL) induced no-to-low memory responses; the latter recovered during therapy with eventual loss at late cART time points (**Figure 32D**). VLVWKFDSKL and VLVWKFDSRL evolved late post-SC and during early cART time points, respectively, and were the only variants in this family to induce moderate to high memory responses (**Figure 32E**). Pairwise comparisons showed statistical differences in mean memory responses between early and early cART time points as well as between late and early cART time points (**Figure 32F**).

We evaluated the impact of MHC class I affinity on the magnitude of memory T cell responses throughout infection (**Figure 33**). Our data show that Gag, Env and Nef peptide variants

with high or medium affinity induce similar responses early post-SC while low binders as classified by the FP-assay induce statistically significant higher responses as compared to high binders (**Figure 33A**). Later during infection (i.e. late, early cART, and late cART), variants with high, medium and low binding affinity stimulated similar IFN $\gamma$  responses (**Figure 33B-D**).

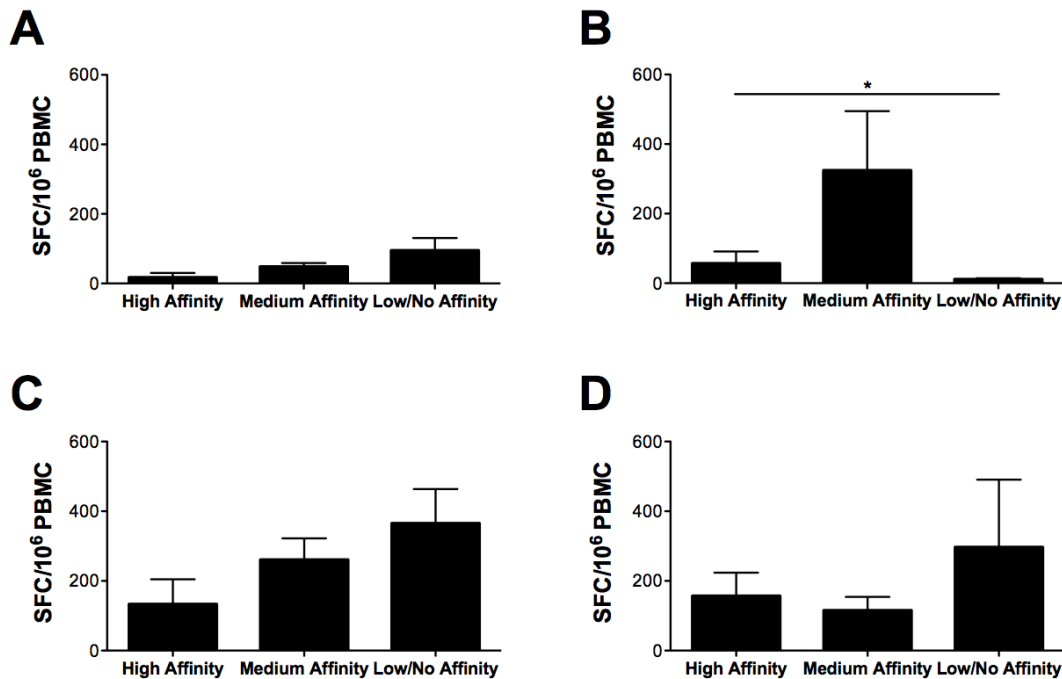


**Figure 33. T cell responses specific for HIV-1 epitope variants with differential MHC class I affinity.** Mean T cell responses to variants with high affinity < 3.7, medium affinity < 4.7, and low/no affinity >4.7 that were detected (A), late (B), early cART (C), and late cART (D) time points. SC, seroconversion. \*p<0.05

Being a known or potential HLA-A\*0201 or HLA-B80702, the magnitude of T cell responses elicited by the tested peptide variants with high and medium binding affinity was generally similar at different time point post-SC. Low affinity binders of Gag, Env, and Nef variants tested *in vitro* variably induced T cell responses with a clear increasing magnitudes following cART.

#### **4.4.6 Broad and high magnitude primary T cell responses to naturally-evolving variants in HIV-1-positive and healthy donors**

We have previously demonstrated the ability of mature monocyte-derived DC from HIV-1-naïve donors to induce broadly reactive primary CD8<sup>+</sup> T cell responses (67). Little is known about the ability to prime anti-HIV T cell immunity specific for variants that evolved during natural infection. Thus, we next determined the capacity of DC isolated from subject 8 during cART to prime autologous pre-SC T cells. Autologous DC matured with CD40-L and IFN- $\gamma$  (104, 156) were loaded with contemporaneous Gag (**Figure 34A**), Env (**Figure 34B**), and Nef (**Figure 34C**) peptide sequences that emerged at early, late, or cART time points post-SC. These DC were then used in a 21-day *in vitro* priming assay. The magnitude of primary T cell responses was tested in an IFN $\gamma$  ELISPOT assay.

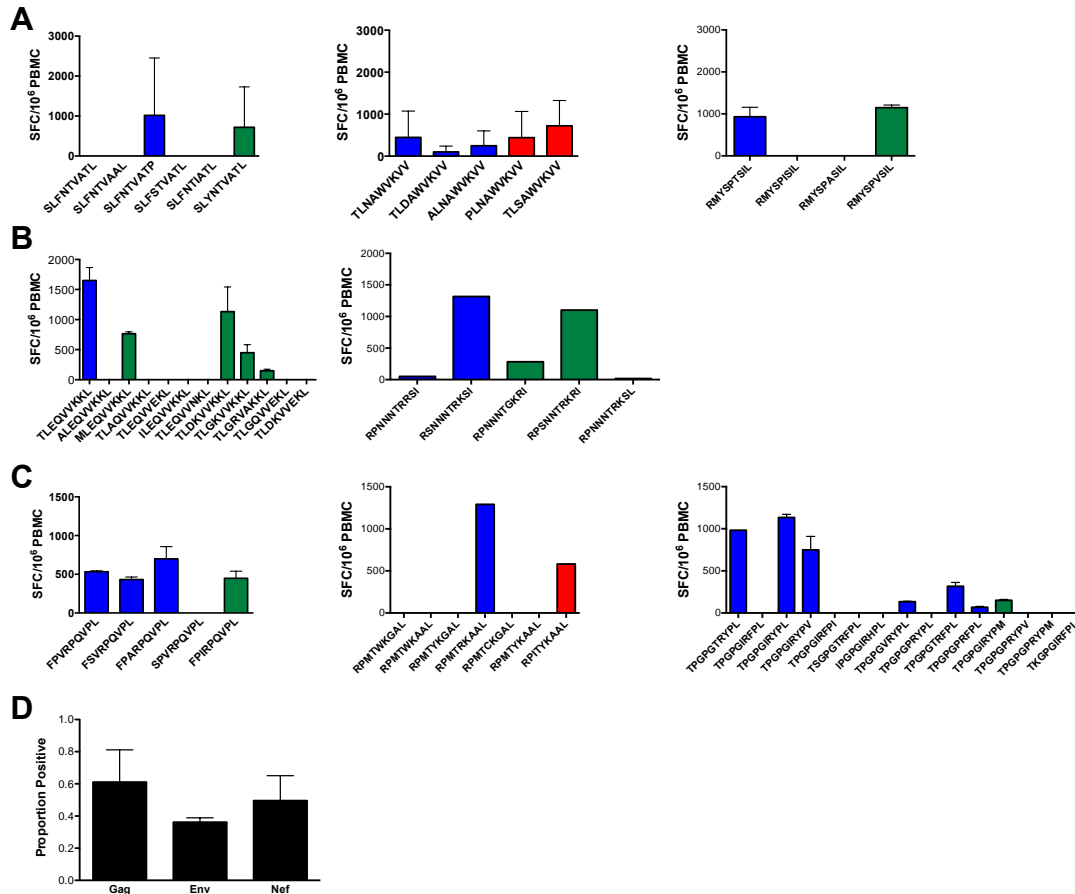


**Figure 34. *In vitro*-induced primary T cell responses specific for autologous HIV-1 epitope variants.** Mature DC loaded with autologous peptide epitope variants were used to prime autologous T cells isolated from the study participant prior to seroconversion. The magnitude of primary T cell responses were tested by IFN $\gamma$  ELISpot. Primary T cell responses were induced against epitope variants derived from (A) Gag (SLFNTVATL, TLNAWVKV, RMYSPSIL), (B) Env (TLEQVVKKL, RPNNTRRSI), and (C) Nef (FPVRPQVPL, RPMTWKGAL, TPGPGTRYPL) and evolving early post-SC (blue), late post-SC (green), and/or during early cART (red). The proportion of Gag, Env, and Nef variants to which positive primary responses were detected is shown in (D). SC, seroconversion; SFC, spot-forming cells.

Of the 59 peptides tested, HIV-naïve, pre-SC T cells were primed to 9/15 (60%) Gag, 10/17 (58.8%) Env, and 13/27 (48.4%) Nef variants. Among these 32 sequences eliciting primary responses, moderate ( $\geq 100$  SFC) to strong ( $\geq 500$  SFC) primary IFN- $\gamma$  responses were noted to known HLA-A\*0201 or HLA-B\*0702 epitopes SLYNTVATL (p17), naturally evolving at late time points; TLNAWVKV (p24) identified as a founder sequence; FPVRPQVPL (Nef), a founder sequence; TPGPGVRYPL emerging early post-SC and TPGPGIRYPL (Env), a founder sequence (**Table 6**).



The peptide families containing SLYNTVATL, TLNAWVKVV and FPVRPQVPL, harbor variant sequences with potential CTL epitopes (**Table 6**). Variants of three out of the five remaining families of peptides tested in our priming model: i.e. RMYSPTSIL (Gag), TLEQVVKKL (Env), and RPMTWKGAL (Nef) are also defined as potential MHC class I - restricted epitopes (**Table 6**). In summary, a total of 16 out of 32 variants induced strong primary responses (>500 SFC) (**Figure 34**).

To determine the breadth of primary T cell responses, the proportion of variants inducing positive primary responses was defined as the number of variant sequences inducing a positive primary T cell response /total number of variants tested within a respective family. The proportion of variants that stimulated primary responses was not dependent on the HIV-1 protein from which these variants were derived, as we observed no significant differences between primary responses targeting Gag, Env, and Nef peptide variants (**Figure 34D**). When combined, variants of Gag, Env, and Nef with low, binding affinity induced primary T cell responses with comparable breadth and magnitude as variants with high or medium affinity (**Figure 35**).

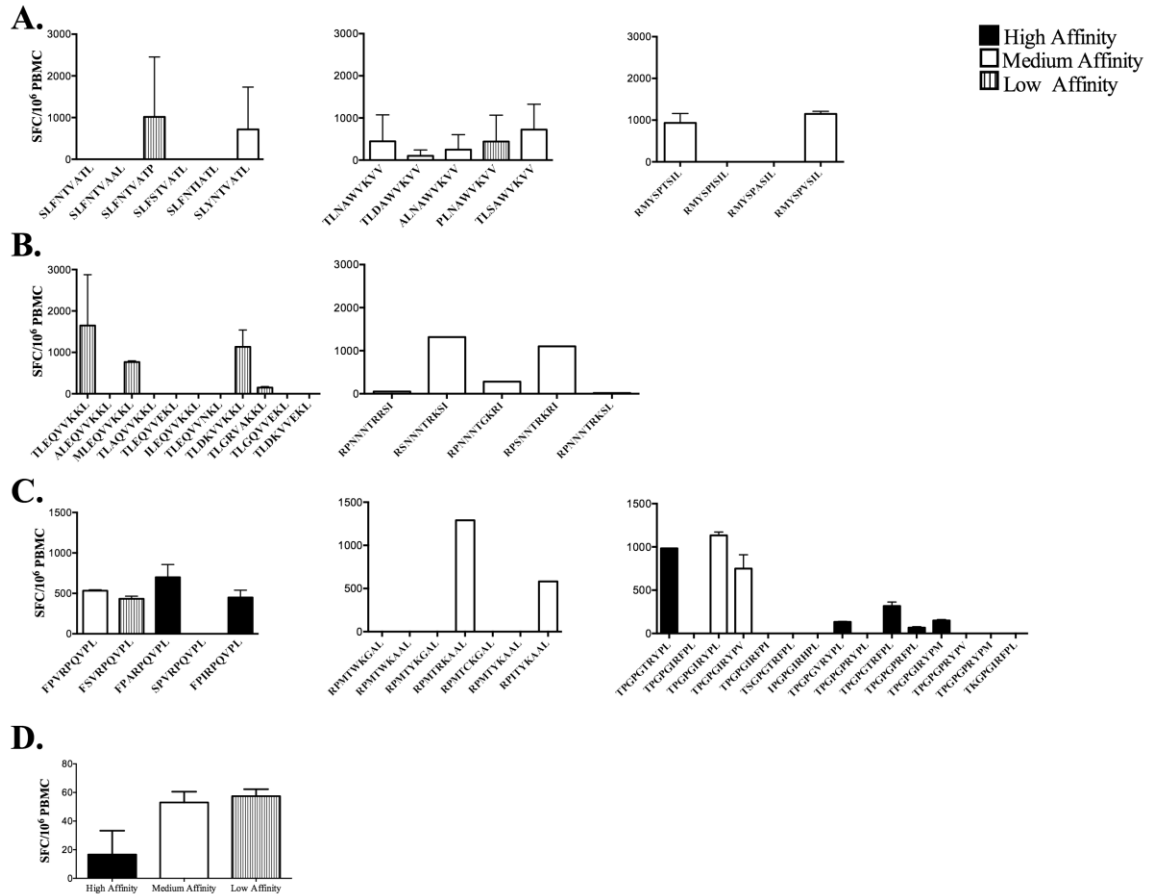


**Figure 35. Primary T cell responses induced in vitro against autologous epitope variants with differential MHC class I affinities.**

Mature DC loaded with autologous peptide epitope variants were used to prime autologous T cells isolated from the study participant prior to seroconversion. The magnitude of primary T cell responses were tested by IFN $\gamma$  ELISpot. Primary T cell responses were induced against epitope variants derived from (A) Gag (SLFNTVATL, TLNAWVKVY, RMYSPSIL), (B) Env (TLEQVVKKL, RPNNTRRSI), and (C) Nef (FPVRPQVPL, RPMTWK GAL, TPGPGTRYPL) and possessing high (black), medium (white), or low (striped) affinity for MHC class I. The proportion of variants with high, medium, or low MHC class I affinity to which positive primary responses were detected is shown in (D). SC, seroconversion; SFC, spot-forming cells.

Taken together, our results indicate that substantial primary T cell responses are induced by our model to a diverse number of HIV-1 peptide variants of the virus proteome. Being a known, potential, or undefined HLA-matched epitope, with high, medium, or low binding affinity did not influence the ability of our priming model to stimulate robust T cell responses in an entirely autologous system.

To evaluate the person-to-person variation in T cell priming capacity of the HIV-1 variant peptides from subject 8, we used PBMC from 2 healthy, HIV-1 naïve, HLA matched (HLA-A2/B7) donors. SLYNTVATL (Gag p17), TLNAWVKVV (Gag p24), FPVRPQVPL (Nef) and their naturally evolving variants were tested. T cells from donor 0038 responded to all SLYNTVATL (6/6) variants, 4 out of 5 TLNAWVKVV variants and all (5/5) FPVRPQVPL variants. Similarly, donor 2256 responded to all variants except one within the FL9 family (**Figure 36**). We found no significant difference between the magnitude of the IFN $\gamma$  primary responses stimulated by peptide variants of our HIV-positive study participant and those of HIV-naïve volunteers.

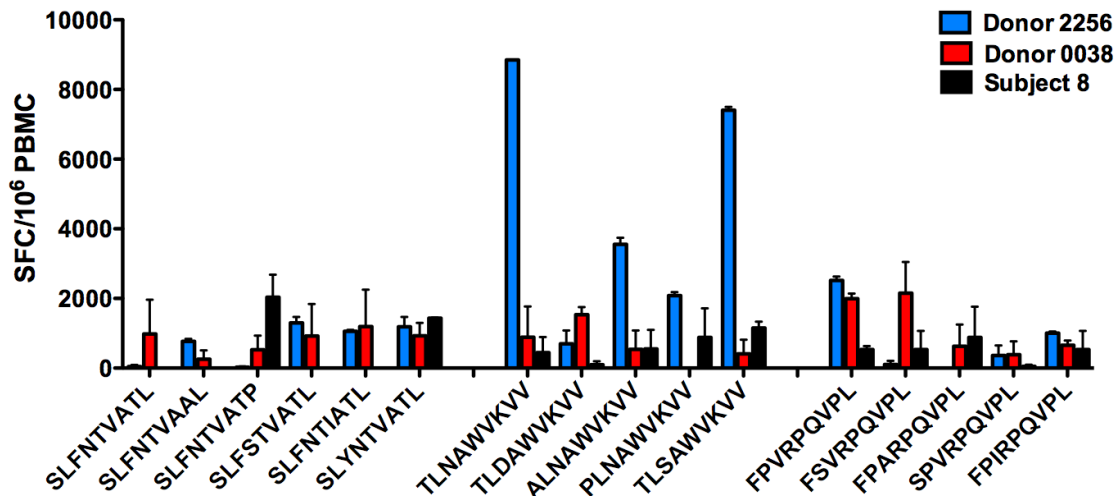


**Figure 36. Primary T cell responses specific for patient-derived HIV-1- epitope variants induced in HIV-1-negative donors.**

Mature DC isolated from HLA A2/B7-matched, HIV-1-negative donors (donors 2256 and 0038) were loaded with epitope variants detected in subject 8 and were used to stimulate autologous PBMC. The magnitude of primary T cell responses was tested by IFN- $\gamma$  ELISpot. Variants of the SLFNTVATL, TLNAWVKVV, and FPVRPQVPL epitopes (x-axis) were used in our priming model. SFC, spot-forming cells.

## 4.5 DISCUSSION

We report the evolution of HIV-1 in an infected subject across time and the impact of HIV-1 variants and respective MHC class I binding affinities on the breadth and the magnitude of T cell memory responses. Our data show that with higher sequence diversity, the proportion of T cell memory responses targeting contemporaneous variant peptide sequences of the proteome increases. It has been previously reported that the continuous presence of antigen is important for the maintenance of CTL responses (308, 347). Moreover, Liu et al. (207) recently reported in the cART-naïve setting that a balance is likely needed between the presence of antigen and prolonged antigen stimulation. Along similar lines, our results suggest the dynamic ability of evolving viral sequences to continuously exist and stimulate specific T cell responses.

T cell responses directed against individual known or optimal peptide sequences (Gag: SLFNTVATL, SLYNTVATL, TLNAWVKVV; Env: RPNNTRKSI; Nef: FPVRPQVPL, RPMTYKAAL, TPGPGVRYPL) evolving early during infection were temporally enhanced during early cART, followed by a decline or complete loss in late cART. We have previously observed such a temporal effect on CTL activity to consensus HIV-1 epitopes (281). This observation was not limited to optimal epitopes as similar trends were observed against potential epitopes and previously undefined epitopes (**Table 6**). Moreover, our results show a clear correlation between the frequency of autologous peptide variants during infection and the breadth, but not the magnitude, of these responses. These results are in agreement with the lack of correlation between the magnitude of CTL responses and HLA binding affinity (40, 320). Importantly, our data indicate that the breadth of T cell responses targeting contemporaneous epitopes representing different parts of the HIV-1 proteome is comparable early post-SC, late post-

SC, or during cART regardless of the experimental binding capacity to the cognate MHC class I molecules.

Even though a small repertoire of Gag, Env, and Nef peptide families were used in this study, all of the tested autologous HIV-1 epitope variants maintained a functionally detectable or predicted level of binding to MHC class I. Further assessment of peptide binding to MHC and its relation to T cell memory responses will need to categorize percent recognized (T cell reactive) and percent non-recognized (T cell non-reactive) variants in relation to viral peptides exhibiting a broader range of MHC binding. This is especially important since a number of mechanisms such as T cell escape, change in the antigen load and T cell exhaustions (325) could lead to decline of T cell responses during HIV-1 infection.

The minimum impact of MHC class I affinity observed in this study suggests that the breadth of recognition of peptide variants could be partially due to the promiscuity of TCR (49). Limited TCR diversity within cognate clonotypes has been suggested to facilitate immune escape through loss of CD8<sup>+</sup> T cell recognition (78, 272). Recently, dominant HIV-specific CD8<sup>+</sup> T cell clonotypes were found to persist *in vivo* for long periods of time while being able to cross-recognize naturally occurring epitope variants (332). A high clonotypic turnover of HIV-specific CD8<sup>+</sup> T cells was described following initiation of HAART or upon appearance of viral mutations; moreover, authors showed new cognate clonotypes during decreased or limited antigen load (161). These clonotypes became dominant and were characterized by high functional capabilities. While we don't have data on the evolution of HIV-specific CD8<sup>+</sup> T cell repertoire clonal composition in our participant or the functional profiles of the detected T cell responses, we believe that we might be dealing with a similar reconstitution post cART.

In our study, T cell responses were detected to 81% (63/78) of the total tested variants in the study participant, 8 of which are classified as optimal epitopes and 29 as potential epitopes as described by the Los Alamos HIV database. Post-STEP trial emphasis has been on the benefit of maximizing the T cell coverage, i.e. breadth, of the contemporaneous forms of the virus (225). Even though correlation between the breadth of the CTL responses and the containment of virus *in vivo* has been controversial (3, 111, 206), we and others (285) believe that the probability of inducing protective anti-HIV CTL responses is likely to be enhanced by broader range of immunogenic epitopes presented professionally by APC. We acknowledge the limitation of monitoring viral sequences longitudinally from one subject in addition to the limited repertoire of peptide epitopes tested in this study; hence, we might have missed important motifs implicated in better MHC binding and consequently effective T cell responses.

The genetic diversity of HIV-1 and the propensity of the virus to undergo escape mutations are major hurdles for long-term immune control of HIV-1. With the current lack of a preventive HIV-1 vaccine, alternatives are needed to improve the quality of the immune responses targeting the virus and thus reducing its transmission. It has been proposed that the magnitude and the quality of the memory T cell pool is affected by the activation of naïve CD8<sup>+</sup> T cells by licensed DC and that excessive antigenic stimulation leads to terminal differentiation and impairment of these memory CD8<sup>+</sup> T cells (363). We have previously demonstrated the potent capability of mature monocyte-derived DC from uninfected donors to induce a broad spectrum of primary CD8<sup>+</sup> T cell responses targeting epitopes in Gag, Env, and Nef (67). Our *in vitro* model was successful at priming HIV-naïve CD8<sup>+</sup> T cells to consensus HIV-1 epitopes as well as other viral peptides *in vitro*. A series of events have been described to be involved in triggering the stimulation of the

TCR on naïve CD8<sup>+</sup> T cells. The TCR and signaling by co-stimulatory and cytokine receptors drive the magnitude and the quality of the response (273).

Consequently, we have proposed the enhancement of the primary responses of naïve CD8<sup>+</sup> T cells to a broad array of HIV-1 epitopes while patients are on cART for better control of viral replication and disease (280). In this study, we confirm the ability of our *in vitro* model to stimulate autologous pre-SC naïve T cells from our study participant against 54% (32/59) of tested autologous peptide variants that emerged at different stages pre- and post-therapy. Moderate to strong primary responses were induced to variants from a variety of known and potential Gag, Env, and Nef epitopes in an entirely autologous system. Moreover, the time post-SC at which the epitope variant evolved did not affect the magnitude of the primary T cell responses. The elicited primary responses were not exclusive to already defined known and potential epitopes. A number of variant sequences of Env and Nef were not defined by the Los Alamos HIV database, yet had predicted and experimental HLA-binding affinity. Taken together, this *in vitro* priming model stimulates primary T cell responses regardless of the nature (i.e. known or undefined), origin (HIV-1 protein), and MHC binding affinity (high, medium or low binders) of the tested HIV-1 epitope variants. Even though cART has been successful at controlling HIV-1 viral load, immune recovery is still a challenge (72). Our model suggests by-passing this obstacle by using DC to generate primary CTL *in vivo* while subjects are under suppressive cART (280).

As a proof-of-concept, we demonstrated the ability of our priming model to prime autologous T cells derived from 2 HIV-1 naïve volunteers to a broad range of Gag and Nef peptide variants derived from the study subject. 25% and 75 % of these peptides were known and potential HLA A\*0201 and HLA B\*0702 epitopes, respectively, as defined by the Los Alamos HIV Immunology Database. Our model was able to generate primary responses targeting

immunodominant (SL9, FL9) and subdominant (TV9) epitopes and their variants. It is well established that immunodominant HIV-specific CTL responses can exert selection pressure on the virus during primary infection (9, 27). Even though subdominant epitopes stimulate T cells less frequently, the elicited responses are protective (40, 43, 93, 165). Our model does not differentiate between viral sequences based on immunodominance. A significant difference was observed between the magnitudes of these *in vitro* primary responses generated by cells of our normal donors. The reason for failure to detect similar *in vitro* primary responses between the 2 normal donors could be due to differences in T cell precursor frequencies. Importantly, we found no difference between the magnitudes of primary responses of our 2 healthy donors targeting HIV-1 evolving variant sequences derived from our study participant when compared to those targeting the same variants using pre-SC or HIV-naïve cells from our study participant. These findings show that, prior to HIV infection and immune dysfunction, the naïve T cell repertoire found within subject 8 was capable of recognizing and responding to primary stimulation against the variants that evolved after seroconversion. The mutations that evolved after infection, particularly those that appeared late post-SC, may have evolved to specifically evade T cell recognition. This obviously would have implications in immunotherapy approaches, which aim to induce primary responses against these “late evolving” viral variants. Fortunately, we show the induction of primary responses against these variants prior to SC, thus suggesting therapies implicated during cART, when immune restoration has occurred, may be successful at inducing CTL specific for autologous viral variants.

While we acknowledge the need for further exploration of the specific TCR clonotypic repertoire associated with emerging viral variants and its ability to control HIV-1 replication, we believe that the present work highlight the importance of primary responses against HIV-1 variants



in a continuous environment of competition between HIV-1 and the virus specific T cell responses. In fact, a recent study on mutations within the KK10 epitope at different positions suggest the capacity of KK10-specific CD8<sup>+</sup> T cell responses to attract an array of cross-reactive clonotypes from the existing repertoire to control HIV-1 infection (194). We believe the described primary responses might be similarly capable of assembling T cell clonotypes to control the ability of emerging viral variants to affect TCR recognition. This however requires further investigation.

With the clonal exhaustion of CD8<sup>+</sup> T cells as a result of chronic HIV-1 infection and the pressure exerted on memory T cells to recognize wild-type and mutant variants, we and others (15) believe that an effective T cell response would have to generate a long lasting protection environment. Engineering DC to prime naïve T cells to immune escape variants (280) could be a potential approach to overcome the challenges faced by circulating memory T cells.

#### **4.6 ACKNOWLEDGEMENTS**

We thank John Mellors for access to Taqman® assay, Kelly Gordon for technical assistance, and the volunteers of the Pittsburgh site of the Multicenter AIDS Cohort Study. This work was supported in part by NIH grants R01-AI-40388, R37-AI-41870, U01-AI-35041 and T32-AI065380.

## 5.0 THE ROLE OF DEFECTIVE AND CROSS-REACTIVE RECALL T CELL RESPONSES IN HIV-1 INFECTION

### 5.1 ABSTRACT

The ability of HIV-1 to rapidly accumulate mutations provides the virus with an effective means of escaping CD8<sup>+</sup> cytotoxic T lymphocyte (CTL) responses. Here we describe how subtle alterations in CTL epitopes expressed by naturally occurring HIV-1 variants can result in an incomplete escape from CTL recognition, providing the virus with a selective advantage. Rather than paralyzing the CTL response, these epitope modifications selectively induce the CTL to produce pro-inflammatory cytokines in the absence of target killing. Importantly, instead of dampening the immune response through CTL elimination of variant antigen-expressing immature dendritic cells (iDC), a positive CTL-to-DC immune feedback loop dominates whereby the iDC differentiate into mature pro-inflammatory DC. Moreover, these CTL-programmed DC exhibit a superior capacity to mediate HIV-1 *trans*-infection of T cells. This discordant induction of CTL helper activity in the absence of killing likely contributes to the chronic immune activation associated with HIV-1 infection, and can be utilized by HIV-1 to promote viral dissemination and persistence. Our findings highlight the need to address the detrimental potential of eliciting dysfunctional cross-reactive memory CTL responses when designing and implementing anti-HIV-1 immunotherapies.

I performed several of the memory and priming experiments discussed in this chapter, generated multiple figures, and performed statistical analyses. The work in this chapter was published as: Selective induction of CTL ‘helper’ rather than killer activity by natural epitope

variants promotes DC-mediated HIV-1 dissemination. Mailliard RB, Smith KN, Fecek RJ, Rappocciolo G, Nascimento EJM, Marques ET, Watkins SC, Mullins JI, Rinaldo CR. *Journal of Immunology*, 2013.

## 5.2 BACKGROUND

Effective CD8<sup>+</sup> cytotoxic T lymphocyte (CTL) responses are critical for the control of HIV-1 infection (238). Early in HIV-1 infection, the immune system responds vigorously and seemingly appropriately with the induction of strong CTL responses that coincide with the resolution of acute viremia (189). In primate models of SIV as well as HIV-1 in humans, those who limit progression and maintain relatively low virus loads mount and maintain potent and long-term anti-viral CTL activity. However, in most cases of HIV-1 infection, the virus escapes from immune control, causing a variety of complications that directly and indirectly negatively impact the cellular immune response, creating a state of persistent immune activation, eventually leading to T cell senescence and disease progression (81).

One way HIV-1 evades immune elimination is through its ability to rapidly mutate. CTL epitopes resulting from divergence of the infecting viral strains during viral replication have been shown to occur during acute and chronic stages of infection, emerging due to immune selective pressure provided by antigen specific CTL responses (132). While these genetic changes pose an inherent risk of adversely impacting viral fitness (206), their establishment likely provides the pathogen with a selective advantage. Minor viral protein modifications within CTL epitopes have been shown to contribute to immune escape by causing changes in antigen processing, reduced capacity to bind to the MHC class-I molecule, and alterations in the ability of T cell receptors to

interact with the presented peptides, all of which can reduce the effectiveness of memory CTL responses (184).

There is, however, evidence that contrasts with the concept that viral mutations driven by CTL immune pressure lead to the establishment of viral escape variants that paralyze antigen-specific CTL responders. Cale *et al.* (50) found CTL epitope variants of SIV arise during the acute stages of infection while in the presence of pre-existing variant reactive CTL. While these CTL efficiently recognize newly acquired variants, they fail to control the evolving and eventual fixation of mutant escape epitopes. Similarly, during chronic stages of HIV-1 infection, highly avid antigen specific CTL responses against autologous virus can be maintained without impact on viral evolution (94, 160). These CTL responses diminish as the subjects received antiviral therapy, suggesting that CTL were indeed actively responding to virus (94). Moreover, the presence of active antigen-cognizant CTL that fail to impact viral evolution or epitope divergence can be found in high frequency along with high viral load during progression to AIDS (94, 144).

It remains unclear why the pre-existing antigen-reactive CTL described in these studies lack the ability to provide sufficient immune pressure to either influence further viral evolution or impede the establishment of the recognized variants. It is conceivable that the CTL detected *ex vivo* are dysfunctional or suppressed *in vivo* as a result of the harsh environmental conditions associated with chronic viral assault. Furthermore, it is possible that any continued change to these epitopes might be more detrimental to the overall fitness and survival of the virus than the CTL response itself. However, data from previous reports suggest that HIV-1 can evolve directly into the path of pre-existing antigen responsive CTL rather than evolve away from CTL pressure, even when viral fitness would permit (50, 60). Another plausible explanation is that the presentation of some altered peptide variants can simply trigger detectable yet ineffective responses from

previously established cross-reactive CTL. Nevertheless, the potential benefit that may exist for the virus to evade such ineffective CTL activity is apparently outweighed by the advantage in maintaining it.

In the present study, we explore the notion that incomplete immune escape from sub-optimal CTL responses could provide an advantage for the pathogen. Using an *in vitro* DC-based CTL priming system, we show that minor viral changes in CTL epitopes can selectively induce the helper rather than killer function of cross-reactive CTL to promote their dysfunctional dialogue with HIV-1 antigen-expressing DC. As a result, an inflammatory state continues, promoting DC survival and acquisition of characteristics ideal for mediating HIV-1 dissemination through *trans* infection of CD4<sup>+</sup> T cells.

## 5.3 METHODS

### 5.3.1 Media, reagents, and cell lines

Cell cultures and lines were maintained in Iscove's Modified Dulbecco's Medium (IMDM; Invitrogen) containing 10% heat inactivated FBS (Gemini Bio Products) and 1% penicillin/streptomycin (Invitrogen). The following factors were used: rhGM-CSF (Leukine<sup>®</sup>, Bayer), rhIL-2 (Proleukin<sup>®</sup> Chiron), IFN- $\alpha$  (Intron<sup>®</sup> A, Schering-Plough), rhIL-4, rhIL-6, rhIL-7, rhIL-15, rhTNF- $\alpha$ , rhIL-1 $\beta$  and rhIFN- $\gamma$  (R&D Systems). The CD40L-transfected J558 cell line (J558-CD40L) was a gift from Dr. P. Lane, University of Birmingham, UK. The HLA A2 expressing T2 cell line was provided by Dr. Walter Storkus, University of Pittsburgh.

### **5.3.2 Human subjects**

This research was part of the Pittsburgh portion of the Multicenter Aids Cohort Study (MACS) (87), and was approved by the University of Pittsburgh Institutional Review Board. Plasma and PBMC were collected and cryopreserved at biannual MACS visits beginning at the time of enrollment, and plasma viral RNA copies/ml and T cell counts were determined. Whole blood products (buffy coats) from healthy, anonymous, HIV-1 negative donors were purchased from the Central Blood Bank of Pittsburgh. HIV-1 screening was performed as part of the product release criteria.

### **5.3.3 Selection of HIV-1 epitopes**

Families of CTL epitope peptides chosen for this study were identified through extensive sequence analysis of plasma derived viral RNA samples collected throughout the course of infection from 3 HIV-1 infected MACS subjects. These sequence analyses allowed for the identification of autologous viral epitopes and determination of the appearance and establishment of epitope variants. Synthetic MHC class 1-restricted epitope and variant peptides were then generated. PBMC from each collection time point were screened by routine IFN- $\gamma$  ELISPOT assays for CTL reactivity against each peptide target. Reactivity of the pre-existing CTL responders against later established variants within certain epitope families was noted in each of the 3 subjects tested (data from one representative donor shown in Fig. S1, Table S1). Founder virus sequences from 3 epitope families, i.e., Gag<sub>77-85</sub> (SLFNTVATL), Gag<sub>151-159</sub> (TLNAWVKVV) and Nef<sub>72-80</sub> (FPVRPQVPL), identified from one subject of a common HLA

type (A\*0201 / B\*0702 positive) were selected to initiate *in vitro* CTL priming in MHC class I single allele- matched HIV-1 naïve donors.

#### **5.3.4 HIV-1 genetic sequencing**

Plasma HIV-1 RNA was isolated and amplified as previously described (307). Viral sequences were derived from 5' and 3' half genomes from 12, 16, and 9 time points for *gag*-p17, -p24, *env*-gp160, and *nef* respectively. An average of 12 clonal sequences was obtained per time point. Sequences bearing open reading frames were aligned with the Pileup program in the GCG suite (Genetics Computer Group, Madison, WI) (206).

#### **5.3.5 Dengue virus epitope sequences**

The dengue virus serotype 3 (DENV3) epitope NS<sub>3399-407</sub> (KLNDWDFVV) was identified through use of the human HLA A\*0201 transgenic mouse model previously described (257). The DENV2 (RTNDWDFVV) and DENV4 (KLTDWDFVV) serotype variants were identified from the NCBI Entrez Protein Database.

#### **5.3.6 Synthetic peptides**

The Los Alamos HIV Molecular Immunology Database was used to identify optimal MHC class I epitopes, whereas predicted MHC class I epitopes were defined based on the presence of known HLA specific anchor residues. HIV-1 associated peptide sequences were synthesized by

Sigma-Aldrich and SynBioSci, whereas the DENV associated peptides were synthesized by GenScript (Piscataway, NJ).

### **5.3.7 Analysis of peptide:MHC class I affinity**

A previously described (48) fluorescence polarization competitive binding assay was used to experimentally determine MHC class I peptide affinity (Pure Protein LLC, Oklahoma City, OK). Epitope variant peptides were classified as previously reported (48) based on the log IC<sub>50</sub> as being binders with high affinity <3.7, medium affinity 4.7> and low/no affinity > 5.5.

### **5.3.8 HLA typing**

High-resolution HLA molecular typing was performed by the University of Pittsburgh Medical Center Tissue Typing Laboratory. The *in vitro* priming studies were limited to HIV-1 seronegative donors confirmed to be HLA-A\*0201 and/or HLA-B\*0702 positive.

### **5.3.9 Generation of DC**

Monocytes were isolated and cultured for 5-7 days in IMDM containing 10% FBS in the presence of GM-CSF and IL-4 (both 1000 IU/ml) (R&D systems) to generate immature DC (iDC) as previously described (218). To induce CD83<sup>+</sup> mature DC, immature DC were differentially exposed, on day 5, to activation factors for 48h. Mature type-1 polarized DC used for CTL priming experiments were generated using the  $\alpha$ DC1 maturation cocktail previously described (218); TNF- $\alpha$  (50 ng/ml) was used as a single maturation factor for 'TNF- $\alpha$ -matured' DC.



### **5.3.10 Induction and expansion of primary CTL**

Induction and expansion of primary CTL from HIV-1 naïve donors was done using a protocol similar to that previously described (218). Briefly, CD8<sup>+</sup> T cells were isolated from HIV-1 seronegative donors using the EasySep (StemCell Technologies) negative selection isolation system. These T cells were plated at  $7.5 \times 10^5$  cells/well in 48 well plates and sensitized with 9mer peptide-pulsed  $\alpha$ DC1 ( $7.5 \times 10^4$  cells/well).  $\gamma$ -irradiated (3000 Rad) J558-CD40L cells were added to the cultures ( $5 \times 10^4$  cells/well). At day 4, rhIL-2 (50 IU/ml), rhIL-7 (10 ng/ml), and rhIL15 (1 ng/ml) were added to the cultures. Long term CTL lines were maintained with increased concentration of rIL-2 (200 IU/ml) and rhIL-7 (10 ng/ml) and re-sensitized with the priming relevant peptide-pulsed  $\gamma$ -irradiated (3000 Rad) HLA-A2+ T2 cells at a stimulator to T cell responder ratio of 1:5 every 14 days.

### **5.3.11 Short term expansion of CTL**

Memory CTL from HIV-1 positive subjects were generated using a short term expansion method previously described method with slight modifications (175). Briefly, PBMC ( $1 \times 10^5$  /well) were cultured in the presence of 9mer peptide antigens (1  $\mu$ g/ml) for 3 days and then supplemented with rIL-2 (200 IU/ml) and rhIL-7 (10 ng/ml) for an additional 7 days, at which time they were analyzed or maintained.

### **5.3.12 CTL and DC co-cultures**

CTL ( $2 \times 10^5$  cells/well) were added directly to day 5 autologous iDC cultures in the absence or presence of antigenic 9mer peptides (1  $\mu\text{g/ml}$ ). An irrelevant DENV associated HLA-A\*0201 restricted peptide (KLNDWDFVV) was also included as control where stated. Exposure time depended on the individual experiment. Human soluble TNF receptor I (sTNF-RI; 0.1  $\mu\text{g/ml}$ ; R&D Systems) or IFN $\gamma$  receptor 1 (IFN $\gamma$ -R1; 1  $\mu\text{g/ml}$ ; R&D Systems) were added for blocking studies.

### **5.3.13 HIV-1 infection and transmission assay**

HIV-Ba-L (R5 tropic virus) was propagated in PHA and IL-2 activated, normal donor PBMC and purified as described (20). Virus titers were determined by p24 ELISA (SAIC-Frederick). DC were differentially activated by addition of autologous CTL in the presence of an irrelevant epitope peptide (KLNDWDFVV- iDC<sub>CTL</sub>) or the relevant epitope specific variant (PLN9- mDC<sub>CTL</sub>), or TNF- $\alpha$  (mDC<sub>TNF $\alpha$</sub> ). T cells were removed from the co-cultures prior to use of DC in HIV-1 transmission assay using the positive isolation system EasySep (StemCell Technologies). The DC were incubated with virus at 37°C for 2hr at an MOI of  $10^{-4}$ , an MOI not sufficient to directly infect activated CD4<sup>+</sup> T cells, as previously shown (276). HIV-1 loaded DC were then washed extensively and incubated with autologous, activated CD4<sup>+</sup> T cells at a 1:10 ratio respectively. After 4 days, cell free supernatants were collected and measured for viral p24 by ELISA.

### 5.3.14 Flow cytometry

Anti-human CD86 (FITC), CD83 (PE) (Immunotech), anti-CD3 mAb (APC-Cy7, BD Bioscience), anti-CD8 mAb (PerCP-Cy5.5, BD Biosciences), anti-CD107a (PC5, Pharmingen), anti-TNF $\alpha$  (eFluor 450, eBiosciences), anti-IFN $\gamma$  (FITC, eBioscience), anti-IL-2 (APC Pharmingen) mAb reagents were used. Anti-CD28/CD49d (FastImmune) (BD Biosciences), Golgistop™ (BD Biosciences), Golgiplug™ (BD Biosciences) reagents were used for intracellular staining. Viability was determined using the LIVE/DEAD® Aqua Kit (Invitrogen) per manufacturer's instructions. Data were acquired using a LSR-II 12-color flow cytometer (BD Biosciences) and analyzed using FlowJo 7.6 (TreeStar Inc.). Polyfunctional responses were determined using a previously described multi-parameter gating strategy (305) and displayed using the SPICE (5.2) program (Mario Roederer, NIAID, NIH).

### 5.3.15 ELISpot assays

PBMC ( $1 \times 10^5$ /well) and cultured CTL ( $3 \times 10^4$ /well) were tested for reactivity to 9mer peptide antigens by ELISpot assay as previously described with minor modifications (175). HLA-A2<sup>+</sup> T2 target cells ( $1 \times 10^4$  /well) were added to the assay as antigen presenting cells when testing HLA-A2<sup>+</sup> restricted CTL. Spots were counted with an automated ELISpot reader (AID GmbH). All data presented as spot forming units (SFUs) per  $10^5$  cells.

### 5.3.16 Cytotoxicity assays

CD4<sup>+</sup> T cell targets: PBMC were activated and cultured for 5 days in the presence of PHA (1µg/ml) and rIL-2 (100 IU/ml). The pre-activated CD4<sup>+</sup> T-cell targets were purified by negative selection (EasySep, StemCell Technologies) and pulsed with 1µg/mL target peptide for 1h and then washed. Peptide-pulsed targets were cultured at 37°C with CTL for 18h at ratios (CTL: target) of 3:1, 1:1, 0.3:1, and 0:1. Following incubation, cells were washed and stained with anti-CD4-V450 (BD Biosciences) and anti-CD8-APC-Cy7 (BD Biosciences). Cells were fixed and permeabilized with BD Cytofix/Cytoperm™ Fixation/Permeabilization Solution Kit (BD Bioscience). DNA of permeabilized cells was stained with 7-amino-actinomycin D (7-AAD) (BD Pharmingen) for 20 minutes at 37°C. To assess target cell death, DNA content was measured by gating on the singlet, CD4<sup>+</sup> target cells and analyzing 7-AAD intensity on a linear scale.

Immature DC targets: Peptide-pulsed autologous immature DC were used as targets in standard 4 h <sup>51</sup>Cr-release assays as previously described (218). Flow cytometry was used to measure the percent cell loss in CTL: DC co-cultures by determining the ratio of cell types recovered as determined by gating based on light scatter properties and expression of CD3 and CD86 on T cells and DC, respectively. Further analysis of cell viability on the DC gated events was achieved using LIVE/DEAD® Aqua amine-binding dye. CTL:DC exposure times varied.

### 5.3.17 DC production of immune mediators

Cytokine and chemokine production of DC was induced as previously described (218). DC were plated ( $2 \times 10^4$  cells/well) in a 96-well flat bottom plate and stimulated with J558-CD40L

cells ( $5 \times 10^4$  /well). Supernatants were collected at 24 h and tested by specific ELISA (Thermo Fisher) for the presence of IL-12p70, IL-6, CCL5, and CXCL10.

### **5.3.18 Scanning electron microscopy (SEM)**

Sterile 12 mm round glass coverslips were placed in the bottom of the well of day 5 iDC culture suspensions. CTL ( $2 \times 10^5$ /well) and specified peptides (1  $\mu$ g/ml) were added to the cultures. The glass coverslips were removed at 24h, fixed in 2.5% glutaraldehyde in PBS and post-fixed in aqueous 1% osmium tetroxide and washed with PBS. Samples were dehydrated through a graded ethanol series, critical point dried, and coated with 3.5 nm gold palladium. A JEOL JSM-6330F SEM was used at 3 kV for imaging.

### **5.3.19 Live cell imaging**

Imaging was performed using a Perkin Elmer Ultraview spinning disk confocal microscope equipped with a Nikon TE 2000E camera. A Metamorph (Molecular Devices) was used to collect all data and to drive the microscope. All images were collected using a 1.3 NA oil immersion 40 $\times$  objective with a 1 $\times$  coupler between the microscope and either the confocal or wide-field cameras. Cells were maintained at 37 $^\circ$ C in the microscope using a Harvard Apparatus heated stage insert. The XYZ stage used was made by ASI.

### 5.3.20 Statistical analysis

Data were analyzed using either paired Student's t-test (two-tailed) or one-way ANOVA followed by a Tukey post hoc test. Significance was determined at an  $\alpha$  of 0.05.

## 5.4 RESULTS

### 5.4.1 Use of DC to induce broadly cross-reactive HIV-1-specific CTL from HIV-1 naïve donors

Previous studies have shown that viral antigen specific CTL can actively persist and respond to certain target epitopes throughout the course of both SIV and HIV infection without providing sufficient immune pressure to induce selective change in their establishment (50, 60, 94, 144, 160). We hypothesize that such ineffective immune responses could represent the activity of previously established memory CTL sub-optimally cross-reacting to epitope variants. To ascertain whether early CTL responders generated against founder HIV-1 epitopes could indeed differentially cross-react to viral epitope variants arising at later time points of infection, we developed an *in vitro* strategy to study and characterize cross-reactive CTL responses to natural HIV-1 epitope variants. Our approach was to recapitulate the *in vivo* anti-HIV-1 CTL response using a previously described autologous dendritic cell-based *in vitro* model (15) to induce primary CTL responses in HIV-1 naïve donors using founder epitopes identified through the analysis of virus collected from MHC-class 1 matched HIV-1 positive donors. These CTL could be expanded and subsequently characterized for reactivity to naturally occurring epitope variants.

We first observed that T cells obtained early in HIV-1 infection recognized and produced IFN $\gamma$  in response to variants that did not evolve until after the time of T cell sampling, indicating the presence of cross-reactive T cells. We identified these cross-reactive responses in 10 HIV-1 Gag, Env, and Nef epitopes (**Table 7**).

**Table 7. Early memory anti-HIV CTL responses to early and late epitope variants**

CTL Epitope Origin (HXB2 position)	MHC Class I Restriction <sup>d</sup>	Early Memory CTL Reactivity Observed <sup>a</sup>			
		Early Variants <sup>b</sup>		Late Variants <sup>c</sup>	
		Affinity Category <sup>e</sup>	Amino Acid Sequence	Affinity Category	Amino Acid Sequence
Gag p17 (28-36)	A*2402	NA	QYKLRHIVW	NA	<b>KYRLKHIVW</b>
		NA		NA	<b>QYKLRHIVW</b>
Gag p17 (77-85)	A*0201	medium	SLFNTVATL	low	<b>SLFNTVATP</b>
		medium	SLFNTVAAL	medium	<b>SLFNTIATL</b>
				medium	<b>SLYNTVATL</b>
Gag p24 (16-24)	B*0702	medium	SPRTLNAWV	medium	<b>PPRTLNAWV</b>
		medium	SPRALNAWV		
Gag p24 (19-27)	A*02	medium	TLNAWVKVW	medium	<b>ALNAWVKVW</b>
		medium	TLDWVVKVW	medium	<b>PLNAWVKVW</b>
				medium	<b>TLSAWVKVW</b>
Env (298-307)	B*07	high	RPNNNTRKSI	medium medium	<b>RSNNNTRKSI</b> <b>RPNNNTRKCI</b>
Env (311-320)	A*0201	very low	IGPGRAFYAT	no affinity	<b>IGSGRAFYAT</b>
Env (341-349)	A*0201	low	TLEQVVKKL	low	<b>ALEQVVKKL</b>
				low	<b>MLEQVVKKL</b>
				low	<b>TLGQVVEKL</b>
				medium	<b>TLDKVVEKL</b>
Nef (68-76)	B*07	medium	FPVRPQVPL	high	<b>FPARPQVPL</b>
		low	FVSRPQVPL	high	<b>SPVRPQVPL</b>
Nef (128-137)	B*0702	high	TPGPGTRYPL	medium	<b>TPGPGIRFPI</b>
		medium	TPGPGIRYPL	medium	<b>TPGPGIRYPV</b>
		high	TPGPGIRFPL	low high	<b>TSGPGTRFPL</b> <b>TPGPGIRYPM</b>
Nef (180-189)	A*0201	medium	VLVWRFDSSL	low	<b>VLVWKFSSSL</b>

<sup>a</sup>PBMC obtained from an HIV-1+ MACS donor at early post-seroconversion time points were evaluated by IFN $\gamma$  ELISPOT for endogenous T cell responses to autologous epitope variants that evolved before and after PBMC sampling.

<sup>b</sup>Autologous MHC class I epitope variants that were present prior to PBMC sampling and induced positive T cell reactivity

<sup>c</sup>Autologous MHC class I epitope variants that evolved after PBMC sampling, yet induced positive T cell reactivity

<sup>d</sup>Autologous epitope variants were evaluated for MHC class I affinity and are defined according to their logIC<sub>50</sub> values: high affinity, log IC<sub>50</sub> < 3.7; medium affinity, 3.7 < log IC<sub>50</sub> < 4.7; low, 4.7 < log IC<sub>50</sub> < 6.0; no affinity, log IC<sub>50</sub> > 6.0

<sup>e</sup>Amino acid sequences represent the autologous Gag, Env, and Nef epitope variants derived from an HIV-1 infected patient

The order of epitope variant evolution *in vivo* is shown in **Figure 37**. Founder virus sequences from 3 epitope families identified from in this HIV-1 positive subject were selected to initiate *in vitro* CTL priming in HLA-matched (A\*0201 / B\*0702 positive) HIV-1 naïve donors.

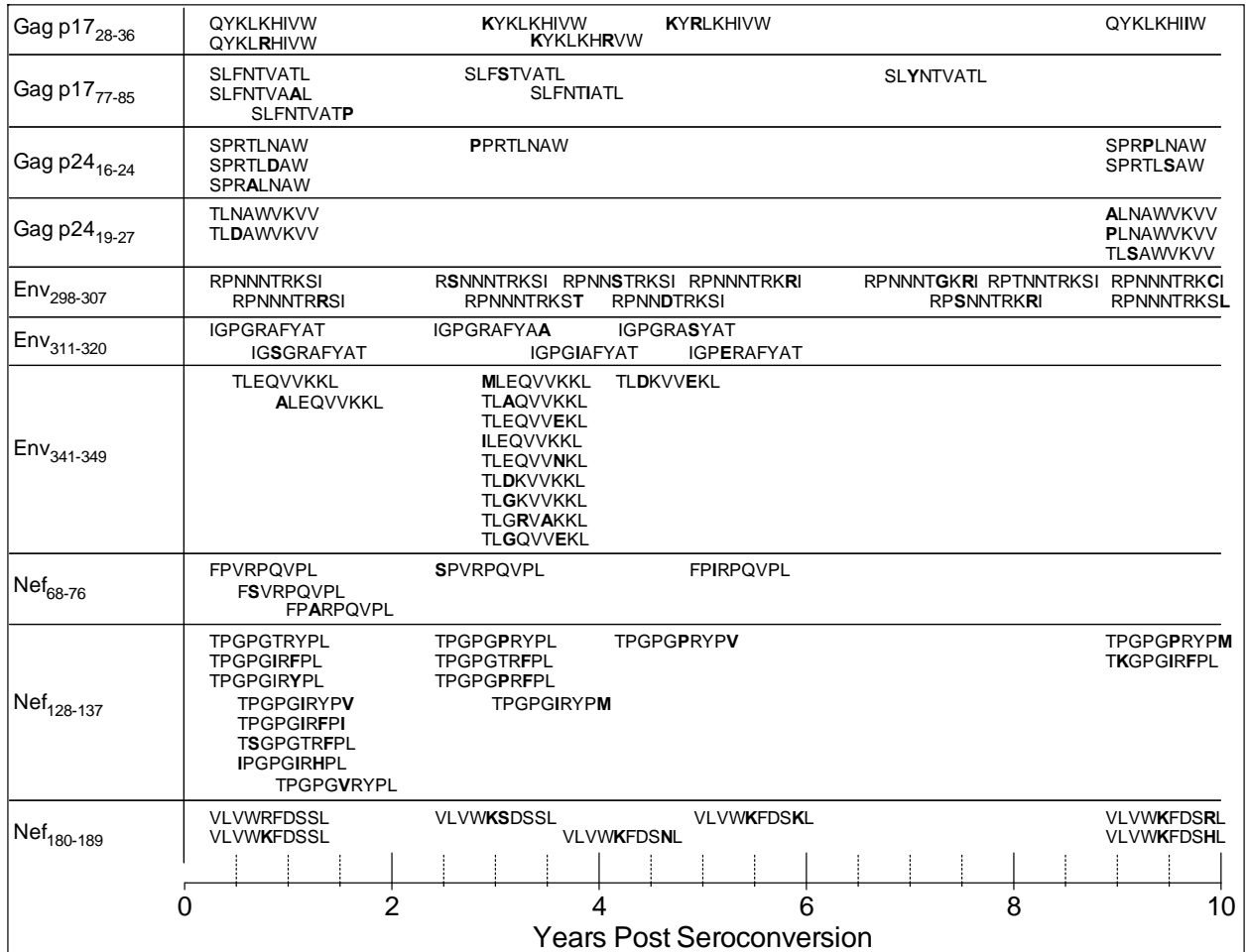


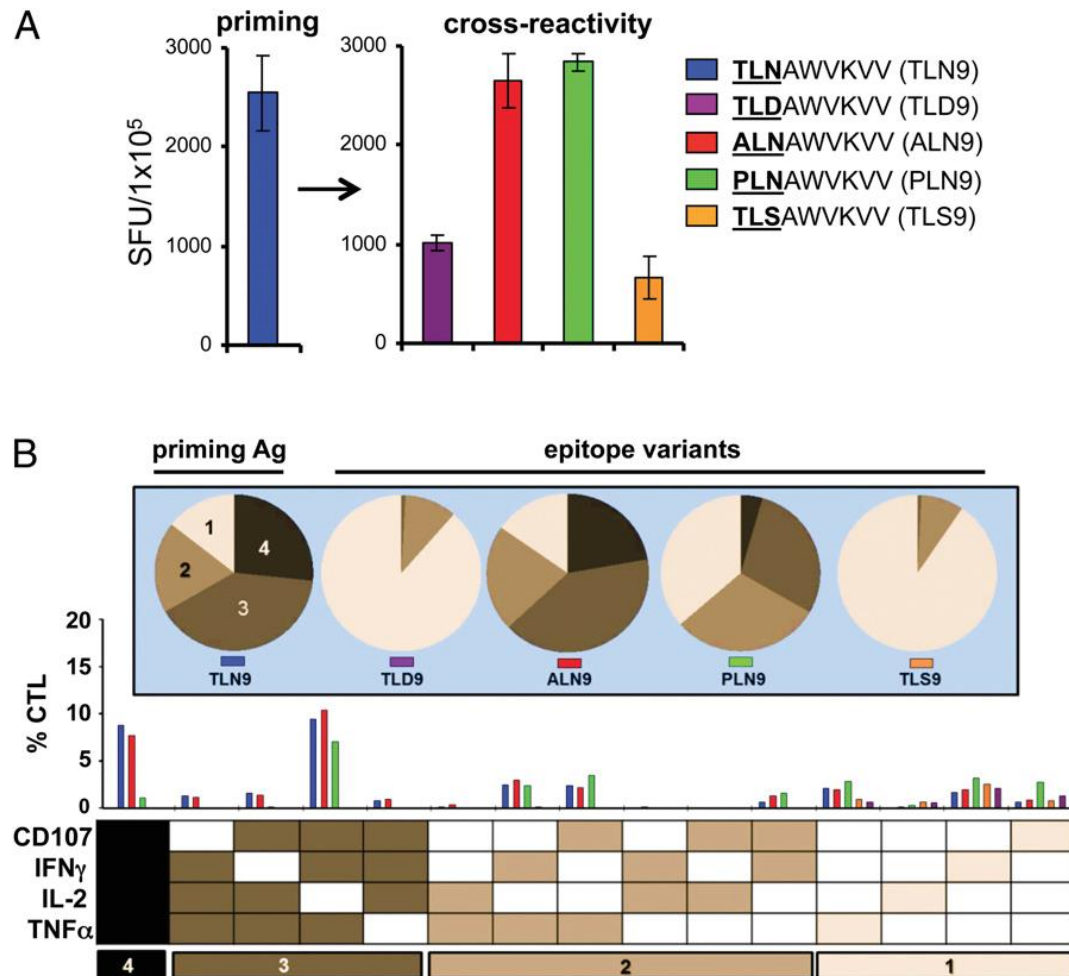
**Figure 37. Chronological evolution of autologous HIV-1 Gag, Env, and Nef epitope variants**

An outlined summary of the appearance of established CTL epitope variants. The amino acid mutations compared to the founder variants are in bold, and were determined by sequencing viral isolates at 13 time points ranging from 0.3 to 8.8 years post-seroconversion.

These were Gag<sub>77-85</sub> (SLFNTVATL), Gag<sub>151-159</sub> (TLNAWVKVW) and Nef<sub>72-80</sub> (FPVRPQVPL). The SLFNTVATL and TLNAWVKVW peptides are HLA-A\*0201 restricted, and the FPVRPQVPL peptide is HLA-B\*0702 restricted. Using this strategy, HIV-1 antigen-specific CTL responses against all 3 epitopes were successfully generated as determined by IFN-



$\gamma$  ELISPOT assay. Representative responses generated against variants of the TLN9 epitope are shown in **Figure 38**. In general, we found that CTL showed of cross-reactivity to all epitope variants, with some responses being comparable to that of the priming peptide (**Figure 38A**).



Primary CTL from an HIV naïve donor were generated against the HLA-A2 restricted, HIV-1 associated epitope p24 Gag<sub>151-159</sub> TLNAWVKVV (TLN9), maintained in culture, and tested for compared responsiveness to natural epitope variants. (A) IFN $\gamma$  ELISPOT results recorded as net spot forming units (SFU) /10<sup>5</sup> cells (non-specific background subtracted). Error bars represent  $\pm$  standard deviation of assay replicates. (B) Polyfunctional analysis of CTL cross-reactivity using intracellular cytokine staining and multi-parameter flow cytometry. The bar graph represents the percentage of CD3<sup>+</sup>CD8<sup>+</sup> T cells induced to express any combination of the 4 immune factors, IFN- $\gamma$ , TNF- $\alpha$ , IL-2 and CD107 (below), and were color coded based on the peptide used for stimulation. Pie charts (above) indicate the relative amount of polyfunctional responses to the individual peptide, with darker shades having higher degrees of polyfunctionality. The numbers at the bottom delineate groups with the indicated numbers of responses. Responses within each of these groups are summed to obtain the fractions shown in the pie charts. The data sets shown were generated using one representative CTL culture of 6 independently established each generated from different donors.

For example, TLNAWVKVV (TLN9) primed CTL induced responses of similar magnitude when re-challenged with either the cognate peptide or variant peptides ALNAWVKVV

(ALN9) and PLNAWVKVV (PLN9), with more apparent differences found only with decreasing antigen concentration (data not shown). Similar cross-reactivity was found with CTL lines generated against Gag<sub>77-85</sub> (SLFNTVATL) and Nef<sub>72-80</sub> (FPVRPQVPL) (data not shown). For sake of transparency, we chose to focus the rest of this report on CTL generated against the TLN9 epitope. However it is important to note that the findings we report translate across the peptide families tested.

#### **5.4.2 Phenotypic characterization of cross-reactive CTL lines**

We used intracellular cytokine staining (ICS) and flow cytometry analysis to compare the cytokine producing capacity and polyfunctional profiles of the CTL stimulated with either cognate or variant peptides. In doing so, we found that the peptides that induced the highest magnitude of responses also induced the most polyfunctional responses in the CTL (**Figure 38A and B**). Specifically, the TLN9-induced CTL reacted comparably in magnitude and polyfunctionality when exposed to the cross-reactive variants ALN9 and PLN9 as they did to the cognate TLN9 peptide, but reacted to the TLD9 and TLS9 epitope variants with less magnitude and polyfunctionality.

Even though the magnitude and quality of the CTL responses to some of the epitope variants seemed comparable to that of the cognate priming peptide, we noted subtle phenotypic differences. For example, when the priming peptide TLN9 or late viral variant PLN9 was used as the peptide stimulator, the cytokine profile and overall percentage of the responding CTL were similar (**Figure 38 and Figure 39A**).

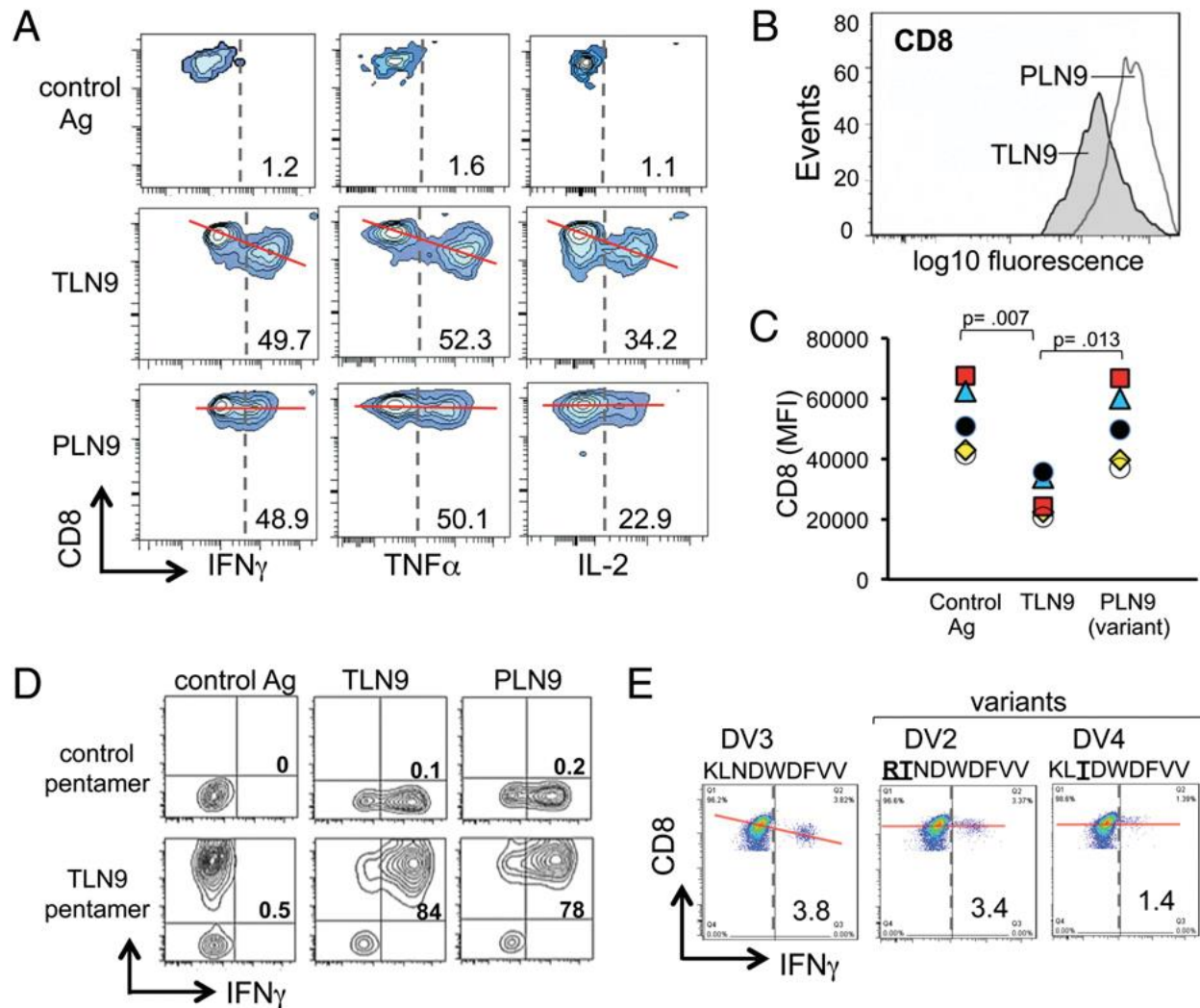


**Figure 39. Differential expression of the T cell co-receptor CD8 on cross-reactive CTL**  
 (A) HIV-1 p24 Gag<sub>151-159</sub> specific CTL were stimulated with either the relevant priming peptide TLNAWVKVV (TLN9), the epitope variant peptide PLNAWVKVV (PLN9), or an irrelevant DENV3 associated HLA-A\*0201 restricted control peptide (KLNDWDFVV) and assessed for dual expression of CD8 and each of the cytokines TNF- $\alpha$ , IFN- $\gamma$ , and IL-2. (B) Single parameter histogram display comparing CD8 expression of differential peptide-induced IFN- $\gamma$  producing CTL. (C) Comparison of CD8 expression on TLN9 specific CTL following their differential stimulation with either their cognate priming peptide TLN9, the epitope variant PLN9, and an irrelevant peptide control. Data plotted as mean fluorescence intensity (MFI) using CTL generated from 5 different HIV-1 naive donors (each represented by a unique symbol). Peptide responsive cells were analyzed by gating on the IFN- $\gamma$  producing T cells. Statistical significance was determined by one-way ANOVA followed by a Tukey post hoc test. (D) TLN9-specific CTL assessed for dual expression of the TCR specific MHC class 1 pentamer (A\*0201, TLNAWVKVV) stain and IFN- $\gamma$  following differential peptide stimulation. (E) HLA-A\*0201 restricted DENV3 NS3<sub>339-407</sub> epitope specific CTL were stimulated with either the priming peptide (KLNDWDFVV) or inter-serotype (DENV2 and DENV4) associated variant peptides and assessed for dual expression levels of CD8 and IFN- $\gamma$ . Red lines included a visual reference to compare relative differences in CD8 expression of antigen responsive CTL.

However, when stimulated with the priming peptide TLN9, the surface expression of CD8 on the peptide reactive CTL decreased, while its expression was maintained on the CTL exposed to the cross-reactive variant peptide PLN9 (**Figure 39A and B**). The differences observed in CD8 expression of CTL stimulated by the cognate TLN9 peptide compared to the variant PLN9 peptide was found to be consistent and statistically significant among CTL lines generated from 5 different donors (**Figure 39C**). Although not as striking, the expression level of CD3 followed the same pattern, with the variant peptide failing to down-regulate the expression of this surface marker (data not shown).

To verify that these differential responses were in fact occurring in cross-reactive CTL, and not the result of a simultaneous outgrowth of distinct T cell clones having different specificities, we further analyzed the CTL by flow cytometry using a fluorochrome labeled T cell receptor (TCR)-specific pentamer designed to recognize a TCR having specificity for the peptide TLN9 in the context of the MHC molecule HLA-A\*0201. The specific binding of this pentamer to those cells producing cytokines in response to either the TLN9 or the PLN9 peptide, and not the irrelevant peptide, clearly demonstrated that the same cell population was in fact cross-reactive to both of the related HIV-1 peptides (**Figure 39D**).

To determine if the observed relationship between CTL cross-reactivity and surface expression of CD8 was unique to HIV-1, we repeated CTL priming experiments using a dengue virus serotype 3 (DENV3)-associated HLA-A\*0201 restricted CTL epitope peptide (NS3<sub>399-407</sub>, KLNDWDFVV). The CTL generated against the DENV3 epitope were then tested for reactivity to the altered peptide sequences naturally associated with different DENV serotypes. Similar to the findings with the HIV-1 specific CTL, the DENV3 specific CTL displayed intense cytokine expression and down-regulation of CD8 in response to the relevant priming peptide

KLNDWDFVV, while the CD8 expression was maintained on the cells cross-reacting to the respective DENV2 and DENV4 serotype peptide variants **RT**NDWDFVV and KL**TD**WDFVV (**Figure 39E**). Therefore, the association between CTL expression of CD8 and cross-reactivity to natural viral variants appears to represent a basic immunological phenomenon.

These findings compelled us to revisit the HIV-1 positive donor samples we originally used for virus sequencing and epitope selection to see if a similar pattern in CD8 expression could be found in CTL obtained from natural infection (**Table 6, Figure 37**). We focused attention on the Gag<sub>77-85</sub> (SL**F**NTVATL) epitope family which demonstrated the most dominant and potentially cross-reactive early responses to the late variant SL**Y**NTVATL. Indeed, CTL expanded from early PBMC samples obtained from this donor 6 months post seroconversion which reacted to the late dominant variant SL**Y**NTVATL failed to down-regulate CD8 expression, while down-regulation occurred with exposure to the founder epitope peptide SL**F**NTVATL (**Figure 40**).

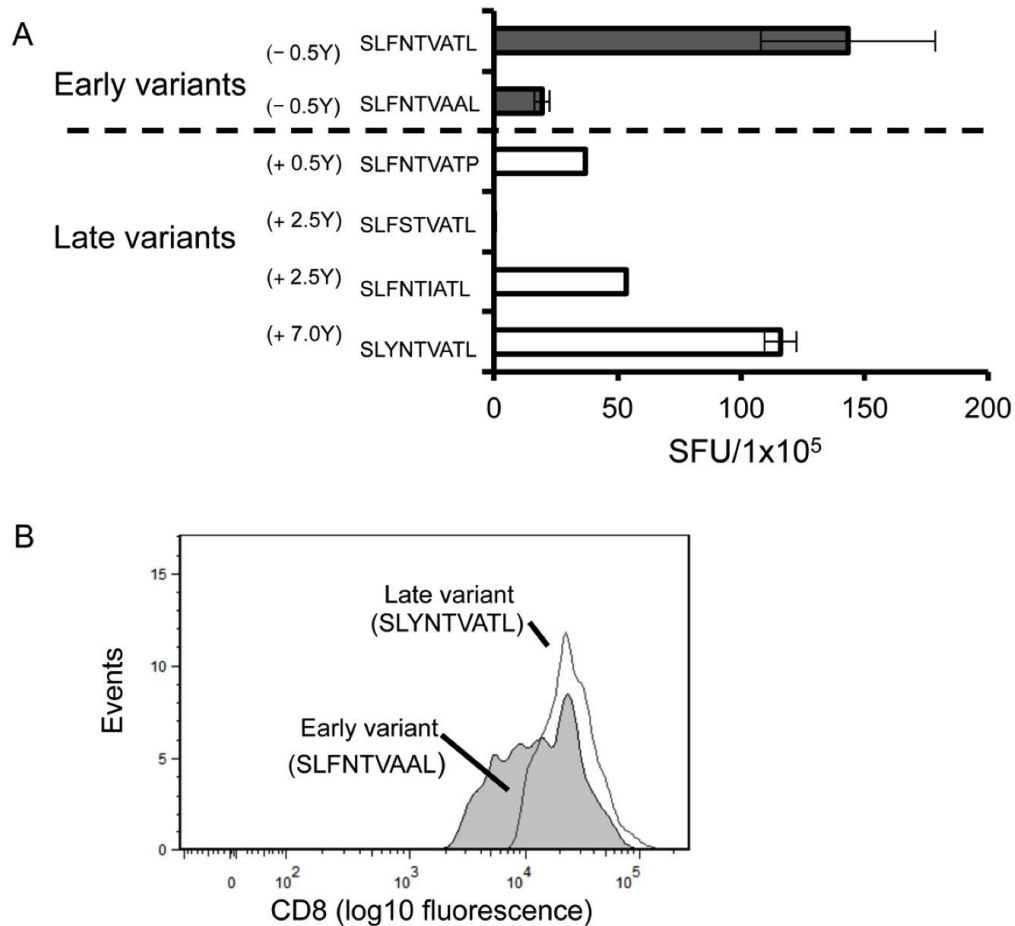


**Figure 40. CTL induced early post-seroconversion respond to late autologous HIV-1 epitope variants.**

Antigen-specific memory T cells were expanded in short-term cultures from PBMC isolated from an HIV-1 infected donor ~1 year post-seroconversion and were tested for reactivity to HIV-1 p17 Gag77-85 (SLFNTVATL; SL9) epitope peptide variants that arose throughout the course of infection. (A) IFN $\gamma$  ELISpot responses to HIV-1 peptide variants derived from virus detected at time points prior to (black bars, -0.5 years) and following (white bars, +0.5, 2.5, and 7.0 years) the collection date of PBMC. The dashed line indicates the relative collection time point (year 0) of the PBMC test sample. Error bars represent  $\pm$  SD. (B) Relative CD8 surface expression of antigen-activated, IFN $\gamma$ -producing CTL responding to early founder (SLFNTVATL) and late variant (SLYNTVATL) HIV-1-derived peptides. Data from one experiment representative of 3 independent tests performed with this epitope family. See Table 5 that lists additional cross-reactive CTL epitopes and their relative time points of detection.

### 5.4.3 Cytolytic function of cross-reactive HIV-1-specific CTL

A critical function of CTL is their ability to eliminate antigen-expressing targets. Therefore, we studied the cytotoxic effector responses of the CTL against antigen expressing autologous CD4<sup>+</sup> T cells as well as immature DC (iDC), both of which are known to be naturally

targeted by HIV-1 (121, 200). To examine CTL-induced cytotoxicity of pre-activated antigen expressing, CD4<sup>+</sup> T cells, we used DNA intercalating 7-aminoactinomycin D (7-AAD) to measure by flow cytometry the changes in DNA content associated with cell death. We detected a dramatic antigen specific decrease in the DNA histogram peak representing target cells in the diploid G1 phase of the cell cycle (**Figure 41 A and B**).

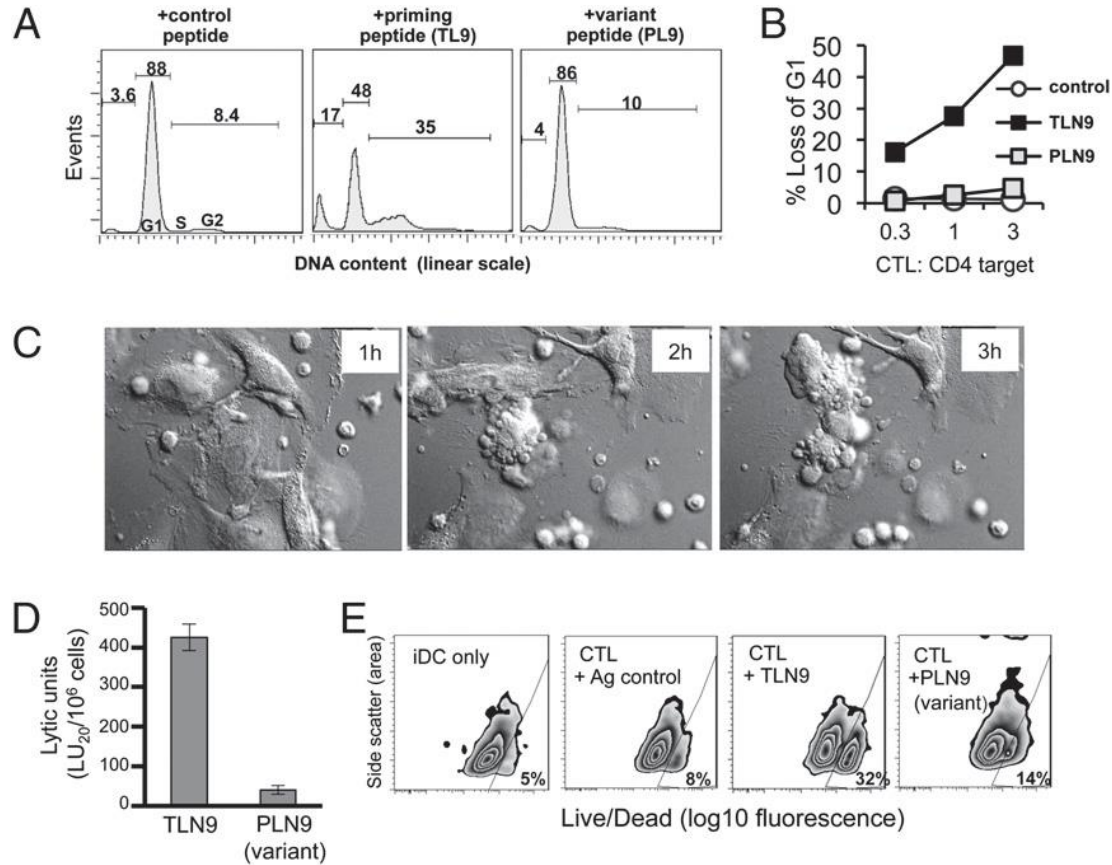


**Figure 41. Dysfunctional cytolytic capacity of cross-reactive HIV-1-specific CTL**

Purified autologous pre-activated CD4<sup>+</sup> T cells and immature DC that differentially expressed the cognate TLNAWVKVV (TLN9), variant PLNAWVKVV (PLN9), or irrelevant KLNDWDFVV peptide antigen were used as HIV-1 specific CTL targets in cytotoxicity assays. (A) Flow cytometry cell cycle analysis using 7-AAD staining to measure cellular DNA content of antigen-expressing CD4<sup>+</sup> T cell targets following an 18h co-culture with TLN9-specific CTL. Percent of target events within the G1 and S/G2 phase of the cell cycle and sub-G1 (apoptotic) regions are shown. Data shown from a representative experiment of 4 performed yielding similar results (B) Dose titration of CTL-induced cytotoxicity of antigen expressing CD4<sup>+</sup> T cell following an 18h co-culture. Results plotted as a percent loss of G1 compared to baseline target values in the absence of CTL. (C) Still frame pictures from a live cell time lapse (4h) video showing HIV p24 Gag<sub>151-159</sub> specific CTL lysis of autologous iDC target cells expressing the relevant peptide TLN9 (CTL:DC = 1:1). (D) A 4h <sup>51</sup>Cr-release assay showing differential ability of the CTL to kill autologous iDC expressing the relevant peptide TLN9 but not the cross-reactive variant PLN9. (E) Flow cytometry viability assessment using LIVE/DEAD® Aqua staining of autologous iDC co-cultured for 6h with the CTL at a 3:1 (CLT:DC) ratio in the absence or presence of either the irrelevant control peptide KLNDWDFVV, the relevant TLN9 peptide, or the epitope variant peptide PLN9.

This was accompanied by an early increase in the S/G2 region (within 5 hours, data not shown), and followed by an increase in the sub-diploid DNA apoptotic region after 16 h co-culture (**Figure 41A, middle panel**). These results were indicative of a CTL-induced toxic arrest of the targets at the S/G2 phase of the target cell cycle. This cytotoxic activity and loss of DNA in the G1 peak increased in a CTL dose dependent manner (**Figure 41B**). Interestingly, CD4<sup>+</sup> T cell targets labeled with an optimal concentration of the variant peptide PLN9 were not effectively killed (**Figure 41A, right panel, and 41B**).

A similar pattern of cytotoxicity was found when analyzing iDC targets. In addition to representing a normal CTL function of eliminating infected target cells, lysis of antigen-expressing iDC represents a negative feedback mechanism used by CTL to dampen successful type-1 immune responses (148). Using live cell microscopy, we were able to visualize the capacity of *in vitro* primed CTL to kill TLN-9 antigen-expressing autologous iDC targets (**Figure 41C**). Within 4 hours, at a 1:1 effector to target ratio, a substantial number of iDC targets were lysed. The ability of the CTL to kill antigen-expressing iDC was tested by standard 4 h <sup>51</sup>Cr-release cytotoxicity assays. As expected and in accord with previous reports (148, 342), the CTL showed lytic activity against iDC exposed to 1 μg/ml of the priming cognate antigen. However, this effector function was dramatically reduced when iDC were labeled with the same concentration of the variant peptide PLN9 (**Figure 41D**). This difference in killing activity was also apparent when analyzing antigen expressing iDC cultures by flow cytometry following their 6h exposure to CTL at a 3:1 (CTL:DC) ratio. In the representative experiment described, of the remaining iDC that could be recovered from priming peptide co-cultures, 32% were determined to be dead compared to only 14% and 8.3% recovered from the co-cultures containing the variant peptide and control peptide respectively (**Figure 41E**). This was in addition to an initial 49% reduction in the total number of



iDC recovered from the cultures that contained the priming peptide, compared to a reduction of only 8.5% from the cultures having the variant peptide as compared to control cultures (data not shown).

#### 5.4.4 Activation and programming of variant antigen-expressing DC by cross-reactive CTL

Although the CTL we evaluated showed a substantial reduction in killing capacity towards the iDC expressing PLN9 variant epitope, striking changes in DC morphology were seen after 24 h through light microscopic evaluation of the co-cultures, suggesting the occurrence of some level of CTL-induced DC activation. These DC partially adhere and developed a pronounced webbed network of long cellular extensions between neighboring cells (**Figure 42A, right panel**).

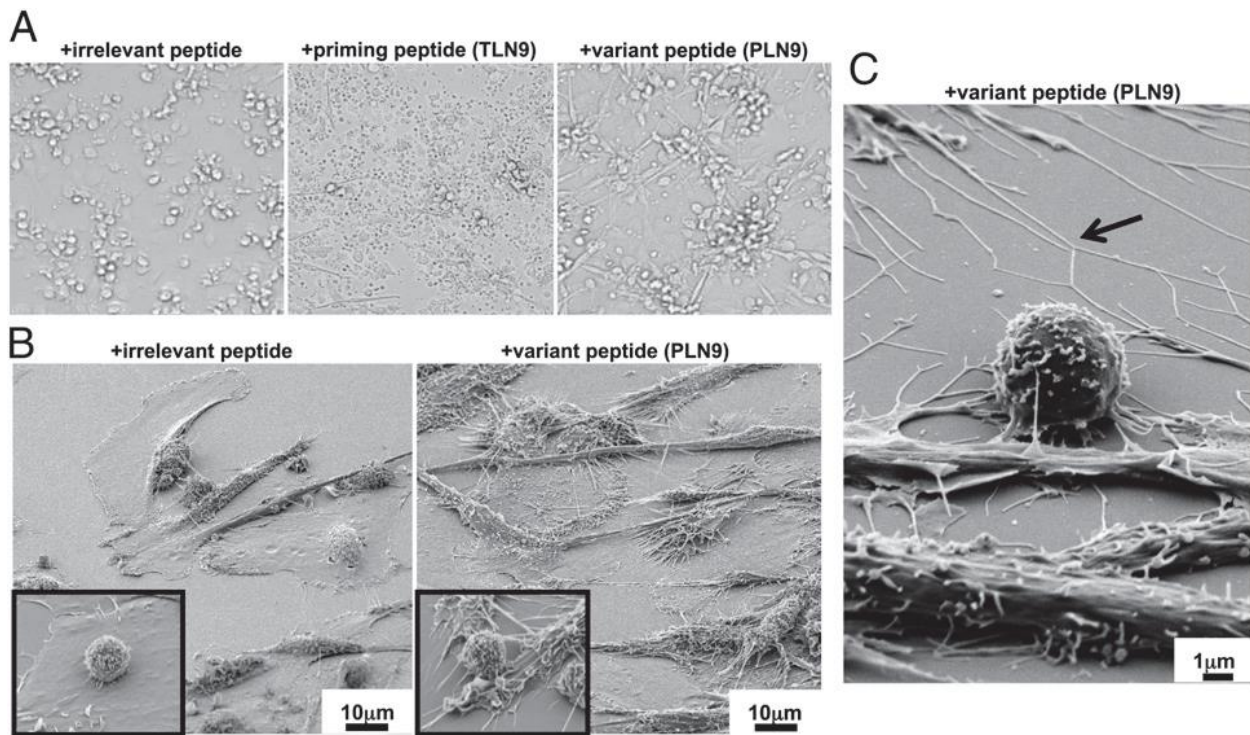


**Figure 42. Cross-reactive CTL induce micro/nanotube extensions on DC expressing variant peptide.** (A) Light microscopy of iDC:CTL co-cultures following a 24h incubation in the presence of the irrelevant DENV3 associated peptide KLNDWDFVV (left panel), the relevant HIV-1 associated priming peptide TLNAWVKVV

(TLN9) (middle panel), and the epitope variant peptide PLNAWVKVV (PLN9) (right panel). Cellular debris in the priming peptide culture indicates a massive degree CTL-induced DC death while the elongated adherent cells in the peptide variant culture suggest cross-reactive CTL dependent DC activation. (B) Scanning electron microscopy (SEM) images of HIV-1 peptide TLN9 specific CTL and autologous iDC co-cultures after 24h in the presence of an irrelevant DENV3 NS3<sub>339-407</sub> (left) or the of epitope variant peptide PLN9 (600X) (right). Insets images are from the respective cultures showing CTL (smaller round cell) and DC in contact at an enhanced magnification (6000X). (C) SEM image of the iDC: CTL co-cultures after 24 h incubation in the presence of the HIV-1 epitope variant peptide PLN9 highlighting what appears to be intercellular-connecting micro/nanotube formations (arrow) induced by the cross-reactive CTL (6000X).

This was in sharp contrast to the iDC expressing the control irrelevant peptide (**Figure 42A, left panel**) which went relatively unchanged, while the iDC expressing the TLN9 peptide failed to survive the extended exposure with the CTL (**Figure 42A, middle panel**). Scanning electron microscopy (SEM) used to examine the changes in DC morphology in detail provided evidence of what appeared to be the induction of interconnected micro/nanotube formations exclusively in the DC:CTL co-cultures containing the variant peptide (**Figure 42B and C**). These cellular formations appeared to be similar to the previously described tunneling membrane connections reported to facilitate intercellular communication and transfer of small molecules (343) as well as pathogens, including HIV-1 (101, 312).

Flow cytometric analysis of the surface expression levels of the DC maturation markers CD86 and CD83 revealed that the cross-reactive CTL were in fact inducing maturation of those DC expressing the variant antigen compared to iDC exposed to peptide alone, or to CTL in the presence of an irrelevant peptide (**Figure 43A and B**). While there were signs of low level non-specific CTL induced activation of DC, this was much less pronounced compared to the high degree of maturation that was dramatically induced by variant peptide (**Figure 43A and B**). Of the factors produced by these CTL as measured by ICS flow cytometry, TNF $\alpha$  and IFN $\gamma$  were the most likely candidates to contribute to this DC activation. Therefore we used the TNF $\alpha$  and IFN $\gamma$  inhibitors, sTNF-rec1 and sIFN $\gamma$ -rec1, respectively, to assess whether either factor was involved. While sIFN $\gamma$ -rec1 did not inhibit the CTL-induced DC maturation, CD86 enhancement was

partially reduced with the inclusion of sTNF-rec1 (**Figure 43B**), suggesting that CTL-derived TNF $\alpha$  played a role in the CTL-induced DC maturation. The fact that the CTL-induced DC enhancement of CD86 expression was not entirely blocked by the addition of sTNF-rec1 suggested that other factors along with TNF $\alpha$  likely contributed to this DC maturation.

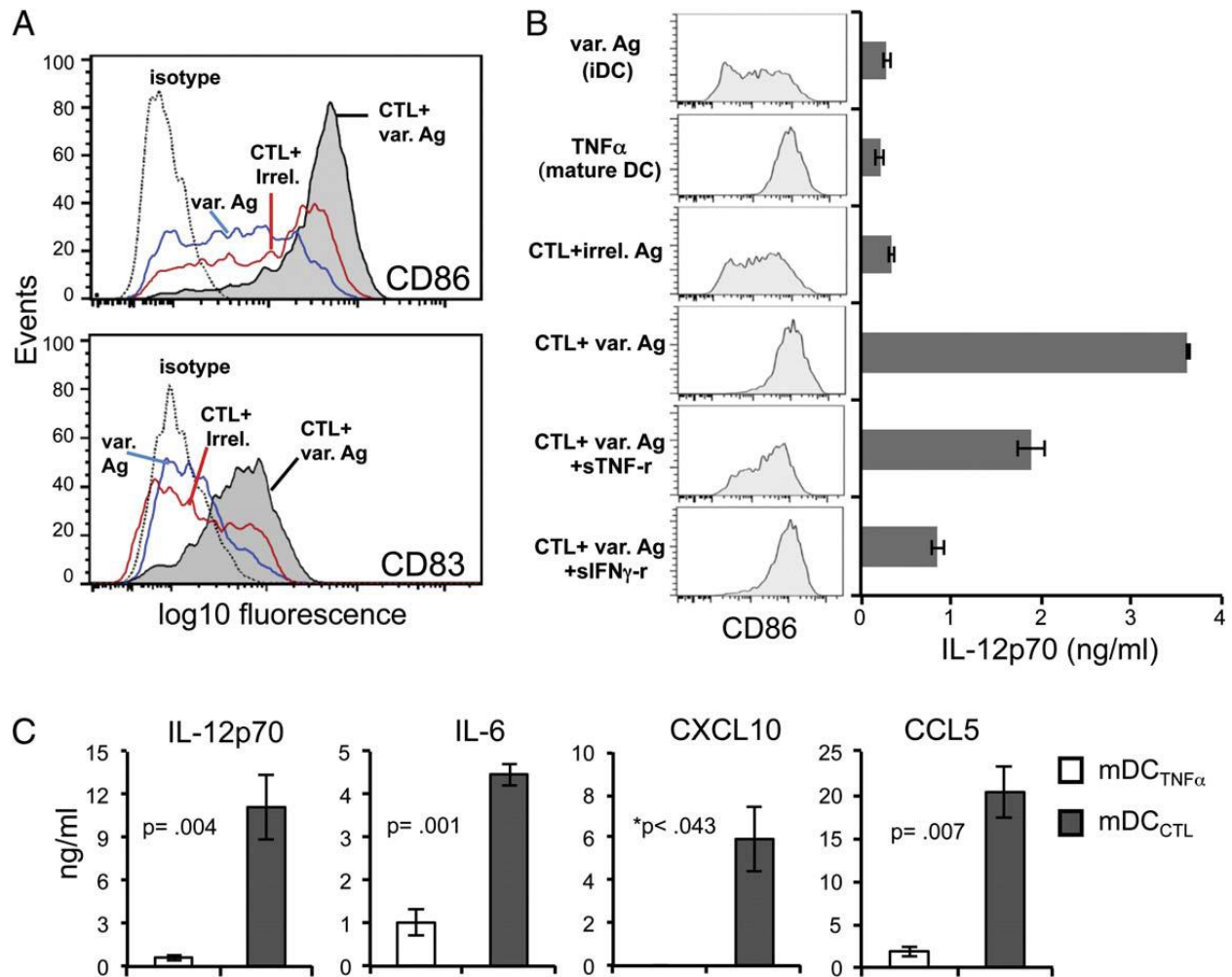


**Figure 43. Cross-reactive HIV-1-specific CTL induce mature proinflammatory programmed DC**

DC were characterized following 24h co-culture with HIV-1 antigen TLNAWVKVV (TLN9)-specific CTL in the presence of cognate or variant peptide. (A) Impact of cross-reactive CTL on the maturation status of variant peptide PLNAWVKVV (PLN9)-expressing iDC as determined by surface expression of CD86 and CD83. iDC were exposed to PLN9 peptide only (blue line), CTL and irrelevant control peptide KLNDWDFVV (CTL+irrel., red line), or to both CTL and PLN9 peptide (shaded histogram). The dashed line denotes the isotype control of the CTL: PLN9 condition. Isotype controls for the other conditions were recorded but not shown. (B) Impact of the presence of TNF $\alpha$  blocker (sTNF-R1; 0.1 $\mu$ g/ml) or an IFN $\gamma$  blocker (sIFN $\gamma$ -R1; 1 $\mu$ g/ml) on cross-reactive CTL-induced maturation of PLN9 (var. Ag) expressing DC. iDC and CTL were co-cultured for 48h, followed by assessment of DC surface expression of CD86 and capacity to produce IL-12p70. TNF $\alpha$  (50ng/ml) stimulated DC were a positive control for DC maturation and iDC exposed to PLN9 (var. Ag) peptide in the absence of CTL served as the iDC control. Error bars represent the standard deviation of assay triplicates. Data are from one experiment representative of 3 performed. (C)

Comparison of cytokine and chemokine producing capacity of mature DC following a 48h exposure of iDC to either TNF $\alpha$  (50ng/ml; mDC<sub>TNF $\alpha$</sub> ) to or variant peptide stimulated cross-reactive CTL (mDC<sub>CTL</sub>) in response to CD40L stimulation as determined by ELISA. Data presented as mean  $\pm$  standard error of 4 independent experiments using 4 different donors. \*Actual values for mDC<sub>TNF $\alpha$</sub>  were consistently below detection limits of the assay for CXCL10. Therefore, p values were recorded as < the calculated value substituting the assay detection limit as the DC<sub>TNF $\alpha$</sub>  value for CXCL10. Significance was determined using two-tailed paired t tests.

In addition to inducing DC maturation, the cross-reactive CTL triggered the type-1 polarization of the maturing DC, characterized by their enhanced IL-12p70 producing capacity upon subsequent stimulation with CD40 ligand (**Figure 43B**). This was in stark contrast to DC matured with exposure to exogenous TNF- $\alpha$  (50 ng/ml) which similarly expressed high levels of CD86, but instead had a more IL-12p70 “exhausted” phenotype (198), in which the ability to produce this cytokine is curtailed (**Figure 43B and C**). As was found with maturation, addition of sTNF-rec1 partially inhibited the CTL-dependent enhancement of DC IL-12p70 expression (**Figure 43B**). Moreover, while IFN- $\gamma$  did not appear to play a role in DC maturation with regard to surface expression of CD86 (**Figure 43B**) and CD83 (not shown), the addition of sIFN $\gamma$ -rec1 dramatically reduced their IL-12p70 producing capacity (**Figure 43B**). When both blocking reagents were used simultaneously, additive effects were not observed (data not shown). The finding that either of these inhibitors could interfere with DC polarization is in line with previous studies showing that the combined exposure of iDC to both a maturation inducing stimulus and IFN $\gamma$ , but neither alone, can promote this high IL-12 producing mature DC phenotype (168). In addition to IL-12p70, when compared to the TNF- $\alpha$ -matured non-polarized DC, these CTL-programmed mature DC consistently produced higher levels of IL-6 as well as the pro-inflammatory chemokines CXCL10 and CCL5 (**Figure 43C**), factors that can attract and promote their interaction with activated effector T cells, including CCR5 expressing CD4<sup>+</sup> T cells typically targeted by HIV-1 (223).

#### **5.4.5 Expression levels of cognate antigen can determine killer versus helper role of CTL**

Low concentrations of viral antigenic peptides have been previously shown to activate CTL without causing down-regulation of TCR (38). Therefore, we questioned if the cognate peptide expression level could reach a threshold that would allow for the selective induction of CTL ‘help’ in the absence of iDC killing as observed with optimal expression of altered viral peptide variants. When CTL and iDC were co-cultured in the presence of high concentration (1.0 to .01  $\mu\text{g/ml}$ ) of the TLN9 peptide, iDC were effectively recognized as cytolytic targets as mentioned previously (**Figure 44A and B**). However, killing capacity of the CTL was reduced with decreasing concentration of cognate peptide, with a substantial drop in killing occurring at .001  $\mu\text{g/ml}$  (**Figure 44A and B**). This decrease in killing capacity was inversely associated with an increase in CD8 expression (**Figure 44A**). When left in culture for 24 h, those DC that survived the exposure to CTL in the presence of .001  $\mu\text{g/ml}$  of TLN9 peptide differentiated into high CD86 expressing mature DC (**Figure 44C**), similar to when a high concentration of the PLN9 variant peptide was used (**Figure 43A and B**).

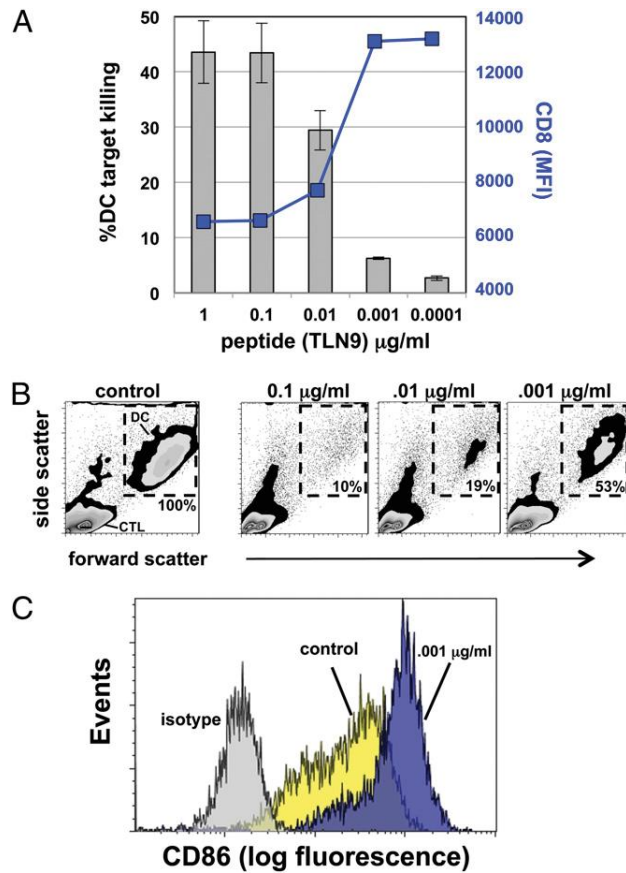


**Figure 44. Concentration of cognate Ag determines differential shift in CTL killer versus helper activity**

(A) Gray bars indicate percentage of iDC killed in a 6h co-culture with CTL at a 3:1 (CLT:DC) ratio by flow cytometry viability assessment using LIVE/DEAD® Aqua Kit discrimination. The blue line represents the relative CD8 expression (MFI) of TLN9 reactive CTL. Error bars represent  $\pm$  standard error of three experiments. (B) Flow cytometry data showing percent DC recovery after overnight co-culture with CTL in relation to antigen concentration as determined by light scatter gating of DC region (dashed gates) compared to CTL in the presence of antigen control (0.1  $\mu\text{g/ml}$  shown). (C) Relative expression of CD86 on surviving DC following 24h exposure to CTL and low concentration of either cognate (blue) or control (yellow) antigen.

#### 5.4.6 CTL programmed DC show enhanced ability to mediate HIV-1 transmission to T cells

DC are known to play a critical role in HIV dissemination through *trans* infection of CD4<sup>+</sup> T cells, with the efficiency of this *trans*-infection being greatly influenced by the status and mode of DC activation (355). Because the CTL programmed DC expressed the phenotypic, morphologic, and functional qualities ideal for activating and attracting activated CD4<sup>+</sup> T cells,

we speculated that they may be superior in mediating transmission of HIV-1 infection to CD4<sup>+</sup> T cell. To test this, HIV-1 *trans*-infection assays were performed comparing the CTL-matured DC to both immature (CTL exposed) and TNF- $\alpha$ -matured DC. The differentially activated DC were purified and pulsed for a short time with a concentration of R5-tropic HIV-1 previously determined to be suboptimal for direct infection of activated CD4<sup>+</sup> T cells (276), and subsequently co-incubated with autologous activated CD4<sup>+</sup> T cells for 4 days. We found that the efficiency of HIV-1 *trans* infection was consistently greatest when using the CTL-matured DC (**Figure 45**). Importantly, viral p24 concentrations remained below detectable levels in conditions where DC or CD4<sup>+</sup> T cells alone (data not shown) were exposed to the suboptimal concentration of virus.

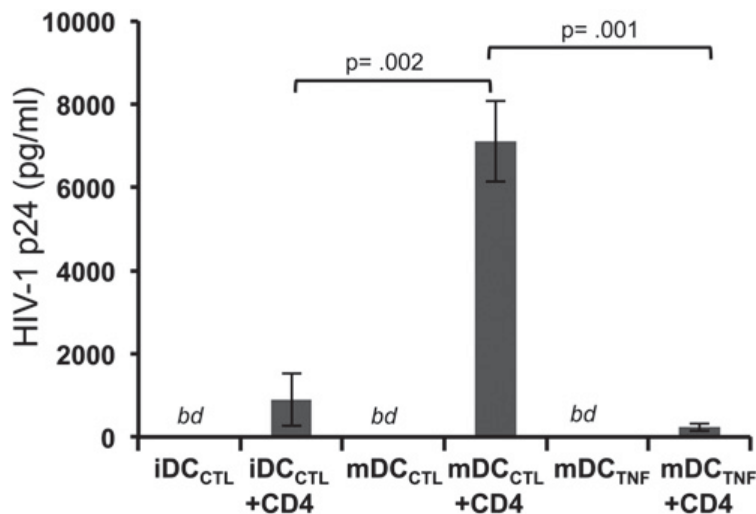


**Figure 45. DC matured by cross-reactive CTL are superior mediators of HIV-1 transmission to CD4<sup>+</sup> T cells.**

Immature DC were differentially stimulated for 48h with either CTL in the presence of the non CTL activating irrelevant peptide KLNDWDFVV (iDC<sub>CTL</sub>), CTL in the presence of the of the cognate priming peptide TLNAWVKVV (TLN9) (not shown), activating PLNAWVKVV (PLN9) epitope variant peptide (mDC<sub>CTL</sub>), or 50ng/ml of TNF- $\alpha$  (mDC<sub>TNF $\alpha$</sub> ). CTL were removed from the co-cultures and the differentially activated DC were incubated with HIV-1 R5 tropic virus at an MOI of 10<sup>-4</sup> at 37°C for 2h. Virus loaded DC were then co-incubated with autologous pre-activated CD4<sup>+</sup> T cells for 4 days at a DC:T cell ratio of 1:10. Cell free supernatants were tested by for levels of HIV-1 p24 by ELISA. DC initially present in co-cultures containing the CTL/TL9 peptide combination did not survive the 48h incubation (see Fig. 6A, middle panel) and therefore were not used in the *trans*-infection assay. Data presented as the combined mean concentration of p24 measured from supernatants collected from three separate *trans*-infection co-culture experiments  $\pm$  standard error using autologous cells generated from one representative donor. Data was analyzed using a one-way ANOVA followed by a Tukey post hoc test. *bd* = below detection limits of the assay.

## 5.5 DISCUSSION

CTL selective pressure is usually considered in the context of the antigen reactive CTL having the ability to kill infected target cells and inhibit viral production. CTL escape mutations that would allow infected cells to survive a cellular attack would thus provide an obvious selective advantage to the virus. However, the functions of antigen specific CTL are not limited to their killer effector role. They also play important immunoregulatory helper functions by producing cytokines and chemokines that influence the quality and character of the immune response (216). In addition, they can regulate the extent of the immune response by limiting the survival of antigen presenting cells (148). Therefore, it is likely that these functions are targeted by viruses and contribute to shaping the viral variant selection process.

We propose that the incomplete immune escape from CTL recognition through the establishment of partially activating epitope variants provides a selective advantage for the virus. Instead of totally bypassing the CTL response, these modifications can selectively promote the helper activity of the CTL while inhibiting their capacity to kill antigen expressing targets. Importantly, when the CTL effectors encounter such variant antigen presenting iDC, instead of dampening the immune response as a result of recognition of the iDC as cytolytic targets (148), a positive CTL to DC immune feedback loop dominates whereby the CTL provides helper signals to activate the HIV-1 antigen expressing DC, programming them to differentiate into a highly stimulatory, pro-inflammatory type of mature DC.

It is this viral ‘baiting’ of pre-existing CTL that allows the virus to utilize the CTL’s ability to program the phenotypic, morphologic, and functional character of the DC, the cell type that has been shown to be exploited by HIV-1 for dissemination and immune escape (121, 200). As shown in this study, iDC that survive the antigen-specific interaction with the cross-reactive effector CTL



undergo a dramatic physical transformation *in vitro*. These DC rapidly sprout widespread micro- and nanotube-like extensions, allowing them to develop extensive interconnected cellular networks. Pathogens such as HIV-1 have been known utilize such cellular connections for cell-to-cell spread (101, 312). Therefore, altered CTL responses against epitope variants *in vivo* may actually promote the development of these complex cellular networks that can be exploited as an escape route by HIV-1, thereby allowing for intercellular spread without exposure to neutralizing antibodies, and establishment of a potentially latent reservoir.

Instead of having a diminished capacity to produce inflammatory factors upon maturation, DC that are programmed to mature by variant cross-reactive CTL have qualities consistent with type-1 polarized DC (DC1) (218), producing enhanced levels of cytokines, such as IL12p70 and IL-6, as well as chemokines such as CXCL10 and CCL5. Such characteristics provide the mature CTL-induced DC1 with the ability to efficiently interact with antigen specific naïve CD4<sup>+</sup> T cells as well as attract activated CCR5<sup>+</sup>CD4<sup>+</sup> T cells, the cells preferentially targeted by HIV-1 (85, 95, 209). Together, these characteristics likely contribute to the superior ability of CTL-induced DC1 to facilitate *trans* infection of CD4<sup>+</sup> T cells as we report in this study. This notion supports a previous study that indicates DC1 to be effective mediators of HIV-1 *trans* infection (294). These results suggest that HIV-1 may utilize and benefit from the activity of cross-reactive CTL *in vivo* by promoting DC mediated viral spread.

The immunoregulatory helper roles of CD8<sup>+</sup> T cells and their ability to modulate DC function have been previously described (137, 216, 288, 321). It is known that they can participate in heterologous immune responses to promote antiviral and anticancer immunity (239, 345), and contribute to a DC-mediated positive immunoregulatory feedback mechanism supporting success driven, type-1 immune responses (169). In our experience, however, the effectiveness of such

direct DC-mediated CD8<sup>+</sup> T cell ‘help’ greatly depends on the activation status of the T cells, and is limited to the activity of either naïve or resting memory CD8<sup>+</sup> T cells (216, 239). The direct, antigen-specific interaction of fully activated CTL with DC typically results in a negative outcome with significant DC lysis (148, 239, 342), as we also have shown in this report. One novel finding from our study is that the presentation of altered peptide antigen can selectively promote the helper rather than killer function of the fully activated and otherwise potent effector CTL. The fact that these two CTL functions can occur either separately or simultaneously reinforces previous reports suggesting that data generated using common assays to measure and assess CTL function, such as ELISPOT and ICS flow cytometry, should be interpreted with caution (208, 330).

In this study, CTL killing activity was associated with the selective down-regulation and possible internalization of CD8 following antigenic stimulation as previously described (215). It has been suggested that the down-regulation of CD8 and CD3 serves to focus the CTL response on targets expressing high levels of antigen, limiting the response to protect against ‘self’ damage (215, 356). While exposure to low concentrations of viral antigenic peptides can activate CTL without causing down-regulation of TCR (38), we show that an altered viral peptide presented at high concentrations can likewise activate CTL without impacting TCR and CD8 expression. Importantly, we found the expression of the degranulation marker CD107a on the variant peptide activated CTL was not directly indicative of killing activity, a finding in line with that reported by others (350). Our data suggest that a decrease in CD8 expression is a reliable surrogate marker for measuring cytolytic function. Regardless of their lack of impact on CD8 expression, the variant peptides induced CTL production of cytokines at levels that had significant biological impact on DC function. Consistent with previous reports (77, 354, 357), this involvement of the T cell co-receptor CD8 appears to be a critical factor in determining the quality of the cross-reactive CTL

response. The possibility that a virus may target the role of CD8 engagement during antigen specific interaction to selectively drive the helper versus killer function is intriguing.

We propose that an escape strategy in which the virus only partially evades, or even evolves towards partial CTL recognition to allow an ineffective CTL response to persist, provides the virus with a novel mechanism for survival. In contrast to what might be expected, the successful establishment of a CTL escape variant does not necessarily ensure an outcome favorable to the virus. In fact, it has been shown that the efficient selective escape from successful CTL responses by Gag epitope variants correlates with a decrease, rather than an increase in viral load, which was suspected to be due to loss in viral fitness (47, 160). Alternatively, the selective induction of an inefficient or incomplete CTL response could provide the virus with an immune ‘smoke screen’ to impede a more direct and effective antiviral CTL attack while limiting the need for excessive epitope modifications that would otherwise pose a threat to viral fitness. The proposed benefit of HIV-1 to selectively induce such a host response would suggest the likelihood that there would be an enrichment, at a population level, of certain epitope variants that would characteristically promote CTL helper activity in the absence of killing rather than completely abrogate CTL recognition. The immunodominant HLA-A\*2010 restricted SL9 (SLYNTVATL) epitope, may represent such an example. While SL9 is widely targeted during chronic rather than acute infection (129), with often robust and potentially cross-reactive CTL responses, these attacks characteristically lack strong selective pressure (45, 46, 129, 160). This is true even when viral fitness pressure does not appear to be a major counteractive force to resist this immune pressure and epitope diversification (60). This suggests that these CTL responses are sub-optimal for target elimination, and that the potential benefit of the virus to evade this immune activity is outweighed by the advantage of maintaining it.

Our results fit with the “original antigenic sin” (185) model, whereby ineffective cross-reactive memory responses (in this case CTL memory) induced from an earlier exposure to virus hinders effective priming and expansion of naïve T cell responders specific against new viral variants. Such cross-reactive memory responses can interfere with the effectiveness of vaccines designed to elicit antigen specific cellular immunity, and may have partially contributed to the peculiar results of the STEP HIV-1 vaccine trial which showed a trend of increased HIV-1 infections observed in those receiving the vaccine (97). Genetic analysis of breakthrough virus in recipients of the STEP vaccine uncovered evidence for vaccine-associated divergence of Gag specific CTL epitopes (286). It is conceivable that narrow CTL responses elicited by this vaccine and the establishment of a limited pool of effector memory T cells allowed the virus to create an inflammatory response favorable for productive infection.

Our study adds a novel dimension to the idea of “original antigenic sin” by suggesting that in the setting of HIV-1 infection, the promiscuous nature of the CTL response is specifically exploited by an evolving virus to modulate the function of the DC to create an environment suitable for its spread and persistence within the host. Our results also point to the notion that this selective induction of CTL helper versus killer function is a general phenomenon, and not restricted to a specific virus, viral epitope, or HLA type, and therefore may be implicated in a broad range of diseases. This is supported by the fact that similar results were obtained when examining CTL responses to epitopes variants derived from DENV, a virus that upon secondary infection with heterotypic serotypes can lead to cross-reactive immune memory responses associated with severe disease including dengue hemorrhagic fever (287). Therefore, developing novel strategies to specifically disrupt or avoid this positive immune feedback loop may prove critical for the design

of more effective immunotherapeutic therapies for a wide range of diseases including HIV-1 infection.

## **5.6 ACKNOWLEDGEMENTS**

We thank Weimin Jiang, Blair Gleeson, Donna Stolz, Louise Borowski, Ravikumar Muthuswamy, Nancy McCarthy, Bill Buchanan, and the volunteers of the Pittsburgh site of the MACS for their contributions to this report. This work was supported by the NIAID grants U01 AI-35041, R37 AI-41870, and T32 AI-065380.

## **6.0 PRIMARY *IN VITRO* DC STIMULATION OF NAÏVE CD8<sup>+</sup> T CELLS FACILITATES ELIMINATION OF THE HIV-1 RESERVOIR**

A recent surge in HIV-1 research has focused on developing immunotherapies to eradicate the autologous viral reservoir via cytotoxic T lymphocyte (CTL)-mediated immune responses. To clear infection, new CTL must be primed from naïve precursors or memory CTL must be reactivated, as the endogenous effector memory populations fail to control viral replication during cART interruption. It has yet to be shown if naïve T cells derived from subjects on cART can be primed into effector CTL specific for the autologous reservoir, as they failed to prime effectively prior to cART. We hypothesize that naïve CD8<sup>+</sup> T cells derived from subjects on cART, in the absence of viral burden, can be primed into CTL specific for the autologous HIV-1 reservoir. To address this, we isolated highly pure populations of naïve and memory CD4<sup>+</sup> and CD8<sup>+</sup> T cells from HIV-1 infected subjects on cART or PBMC from these same subjects prior to seroconversion. T cells were used in an *in vitro* model of dendritic cell (DC) immunotherapy, in which autologous DC were loaded with inactivated HIV-1 derived from the autologous cART reservoir and were used to induce primary CD8<sup>+</sup> T cell responses from naïve precursors or to re-stimulate memory populations. IFN $\gamma$  ELISpot and viral suppression assays were used to evaluate primary CTL effector function against autologous viral antigen. DC from HIV-1 infected subjects on cART induced primary CTL that suppressed the survival of virally-infected CD4<sup>+</sup> T cells. Moreover, these primary CTL were specific for the autologous Gag proteome and enhanced the breadth of responses to those found in re-stimulated memory populations. Primary responses during cART did not differ from those induced pre-seroconversion. We show for the first time that naïve T cells from HIV-1 infected subjects on cART can respond to primary *in vitro* DC vaccination against the

autologous reservoir and are capable of suppressing viral replication. Additionally, we show that chronic, untreated infection did not permanently impair CTL priming to autologous virus. These data support the use of DC immunotherapies targeting the autologous reservoir in HIV-1 infected subjects on cART.

Viral isolation and purification from subjects on cART was assisted by Deena Ratner and the laboratory of Dr. Phalguni Gupta. I performed all other experiments, including ELISpots and viral suppression assays, generated all figures and performed all statistical analyses. Data analysis was assisted by Dr. Charles R. Rinaldo and Dr. Robbie B. Mailliard.

## **6.1 BACKGROUND**

Combination antiretroviral therapy (cART) has greatly reduced the morbidity and mortality associated with chronic HIV-1 infection. While on cART, subjects experience partial CD4<sup>+</sup> T cell recovery and decreases in AIDS-defining opportunistic infections, and many maintain plasma viremia at levels undetectable by standard assays (<50 copies/ml) (1, 28, 252). Despite this, viral reservoirs persist in the blood, gut-associated lymphoid tissues (GALT), and other lymphatics even after long-term suppressive therapy (62, 109, 110, 140, 263). Importantly, the frequency of anti-HIV-1 CD4<sup>+</sup> and CD8<sup>+</sup> T cells decreases, presumably due to low antigenic stimulation consequent to the lower viral load (233, 267, 281). Thus, partial immune reconstitution is achieved during cART, but the functionality of the reconstituted immune system is limited (115). When subjects are removed from cART due to drug toxicity or treatment noncompliance, there is an associated rebound in HIV-1 load and resumption of disease progression (61, 109, 110, 221, 340, 352).

It is presumed from studies in the SIV nonhuman primate model (299, 358) and observational studies in HIV-1-infected humans (22, 42, 189, 193, 254) that T cell immunity is the most important parameter in controlling virus infection in absence of cART and is paramount in controlling infection in concert with cART (42, 189, 254, 299). It has been proposed that induction of a broad and high magnitude CTL response that is specific for the patient's own, unique (autologous) virus will be effective at eliminating HIV-1-infected cells (255, 289). Unfortunately, a hallmark of HIV-1 pathogenesis is the ability of the virus to escape host CTL responses through chronic immune activation and dysregulation (41, 172, 230) and genetic mutations during the early and chronic phases of the infection (132) (8, 9, 93, 246). Therapeutic approaches have therefore aimed to enhance anti-HIV-1 CTL activity in subjects on cART, when the viral burden is minimized and partial immune reconstitution has occurred (17, 251, 351, 366). However, latently-infected cells do not express viral proteins during suppressive cART and are therefore undetectable by the immune system (310). Hence, to effectively control HIV-1 replication and ultimately cure HIV-1 infection, a "shock and kill" approach has been proposed. In this concept, cells harboring the latent virus reservoir are induced (the "kick") to produce viral protein antigens, together with a potent immunotherapy that induces cytotoxic T lymphocytes (CTL) specific for the patient's own, unique (autologous) virus (the "kill") (82).

These immunotherapies aim to induce primary immunity from naïve CD8<sup>+</sup> T cells or reactivate a dormant or dysfunctional recall CD8<sup>+</sup> T cell response in subjects on cART. We have previously shown that monocyte-derived dendritic cells (DC) engineered *ex vivo* are capable of revealing CD8<sup>+</sup> T cell responses to autologous and consensus HIV-1 peptide antigens in subjects on cART and during untreated infection (chapters 3 and 4 above) (155), thus supporting the use of DC in treatments that reactivate HIV-1-specific recall T cells. Additionally, Shan *et. al.*



demonstrated the ability of *ex vivo* antigen-stimulated CD8<sup>+</sup> T cells to eradicate reactivated CD4<sup>+</sup> T cells harboring latent HIV-1 (306), again underscoring the potential usefulness of reinvigorating a quiescent CTL response. It is currently unclear, however, if the repertoire and function of naïve and memory T cells in these subjects have been sufficiently restored to respond to a potent DC immunotherapy targeting the viral reservoir.

Abnormalities in T cell receptor (TCR) diversity and function, including responsiveness to neo-antigens, have been reported following chronic HIV-1 infection (178). It may be that naïve T cells present in long term, HIV-1 chronically infected subjects on cART do not have the TCR repertoire or functional capacity to respond to primary stimulation against autologous HIV-1, or that viral escape has specifically evaded potential recognition by this new repertoire of naïve T cells. Additionally, prolonged antigenic stimulation in chronic infection results in T cell exhaustion that persists during cART (41, 172, 230). DC, the most potent antigen-presenting cells, may further exhaust the HIV-1-specific memory subset in an immunotherapy. We believe naïve CD8<sup>+</sup> T cells from subjects on long-term suppressive cART can successfully respond to primary DC stimulation against the autologous HIV-1 reservoir, and that they will be superior CTL in comparison to memory T cells that have undergone the same stimulation.

To address these hypotheses, we established an *in vitro* model of dendritic cell (DC) immunotherapy to evaluate priming of naïve CD8<sup>+</sup> T cells and “re-conditioning” of memory CD8<sup>+</sup> T cells targeting the autologous HIV-1 cART reservoir. For the first time, we show that naïve CD8<sup>+</sup> T cells from subjects on cART can be primed to the HIV-1 reservoir and can eliminate infected CD4<sup>+</sup> T cells following an *in vitro* DC prime-boost regimen. We also show that memory T cells exposed to the same stimulation secrete proinflammatory cytokines but do not have CTL

effector function. Together, these data support use of DC immunotherapy targeting the naïve subset in subjects on cART.

## 6.2 METHODS

### 6.2.1 Study subjects

Four HIV-1 infected subjects were chosen from the MACS, a natural history study of men who have sex with men for which the methodologies have been described previously (87, 171). Human subject approval was obtained from the University of Pittsburgh Institutional Review Board. These subjects were chosen based on their prolonged enrollment in the study (>20 years), typical course of disease progression, and favorable response to combination antiretroviral therapy (cART). Subject S1 was determined to be HLA A\*0201/B\*0702 positive by high resolution PCR genotyping (Tissue Typing Laboratory, University of Pittsburgh Medical Center), whereas subjects S2, S3, and S8 were positive for the HLA A\*2402 allele. All four subjects were enrolled in the MACS prior to seroconversion to HIV-1. Seropositivity was confirmed by positive enzyme-linked immunosorbent assay (ELISA) for the presence of HIV-1 p24 and a Western blot with bands corresponding to at least two of the Gag, Pol, and Env proteins (171). Blood specimens and epidemiological and clinical data were collected at each visit, as described previously (307). All four subjects progressed to AIDS as defined by the CDC ( $<200$  CD4<sup>+</sup> T cells/mm<sup>3</sup>) within 8.3 years after seroconversion. These subjects received combination ART (cART) and maintained plasma HIV-1 RNA below 20 copies/ml at most post-cART visits.

### 6.2.2 Induction and isolation of HIV-1 from latently-infected CD4<sup>+</sup> T cells

We used a previously described virus culture assay to induce HIV-1 production by latently-infected CD4<sup>+</sup> T cells obtained during or immediately prior to cART (195, 311) in subjects S2, S3, and S8. Briefly,  $1 \times 10^6$  CD4<sup>+</sup> T cells were isolated from cryopreserved PBMC obtained <2 years post-cART using a negative CD4<sup>+</sup> T cell enrichment kit per the manufacturer's instructions (STEMCELL Technologies Inc, Vancouver, BC).  $1 \times 10^7$  fresh, irradiated PBMC from an HIV-1-negative donor were co-cultured with patient-derived CD4<sup>+</sup> T cells in IMDM supplemented with 10% heat-inactivated fetal bovine serum (FBS), 50 µg/ml gentamicin (Life Technologies, Carlsbad, CA), 100 U/ml IL-2 (Prometheus Labs, San Diego, CA), and 1 µg/ml PHA (Sigma-Aldrich, St. Louis, MO) at 37°C in a 5% CO<sub>2</sub> atmosphere. On day 2,  $4 \times 10^6$  CD4<sup>+</sup> lymphoblasts that had been activated for 2 days with 100 U/ml IL-2 and 0.5 µg/ml PHA were added to the virus cultures. On day 7 and every 7 days thereafter, CD4<sup>+</sup> lymphoblasts were again added to the virus cultures, splitting cells and replenishing media as needed. The presence of HIV-1 in culture supernatants was evaluated every 3 days by p24 ELISA (Zeptometrix, Buffalo, NY). Cultures were terminated and supernatants were collected when the concentration of p24 reached or exceeded 20,000 pg/ml. The virus was filtered 5 times through centrifugal filtration devices (Millipore, Billerica, MA) to remove any contaminating cytokines from the prolonged cell culture. The purified virus was then resuspended in RPMI/10% FBS, and frozen at -80°C until use. p24 ELISA was performed on each aliquot to determine the concentration of virus in each sample.

### 6.2.3 HIV-1 sequencing and peptide synthesis

For subject S1, sequencing of plasma HIV-1 was performed as described previously (307). For subjects S2, S3, and S8, only *gag* sequencing was performed. To do this, viral RNA was manually extracted from cell culture supernatants using a viral RNA mini kit (Qiagen, Valencia, CA). cDNA synthesis was performed using Nef3 (TAAGTCATTGGTCTTAAAGGTACC) and RT2 (GTATGTCATTGACAGTCCAGC) primers with SuperScript III Reverse Transcriptase (200 U/ml; Invitrogen, Carlsbad, CA). Endpoint dilution methodology was used prior to viral gene amplification to avoid template resampling. Multiplex first-round PCR was performed with the Gag1 (GAGGCTAGAAGGAGAGAGATGG) and RT2 primers. Singleplex second round PCR was performed with Gag2 (GTGCGAGAGCGTCGGTATTAAGCG) and RSP15R (CAATCCCCCTATCATTTTTGGTTTCC) primers. PCR products were run on a QIAxcel automated electrophoresis system (Qiagen, Valencia, CA) and Sanger sequencing was performed on samples with positive bands (High Throughput Genomics Center, Seattle, WA).

For subject S1, 11 peptides representing autologous variants of known HLA A\*0201 and B\*0702 CTL epitopes were synthesized. For subjects S2, S3, and S8, a library of 18mers representing the consensus autologous Gag sequence detected during cART was generated using PeptGen on The Los Alamos Database website (<http://www.hiv.lanl.gov/content/immunology>) and was synthesized for each subject (Sigma Aldrich, St. Louis, MO). Peptides were resuspended in 50µl sterile DMSO and were frozen in AIM V at 1mg/ml at -80°C.

#### **6.2.4 Isolation of monocytes and peripheral blood lymphocytes**

PBMC were purified from leukapheresis product by Ficoll density separation, and was further separated into monocytes and peripheral blood lymphocytes (PBL) by Percoll density separation. Monocytes and PBMC were frozen in FBS/10% DMSO in aliquots of 10M cells/vial. Fresh peripheral blood lymphocytes (PBL) were used immediately for purification of naïve and non-naïve CD4<sup>+</sup> and CD8<sup>+</sup> T cells.

#### **6.2.5 Purification of naïve and non-naïve CD4<sup>+</sup> and CD8<sup>+</sup> T cells**

Fresh PBL were resuspended in PBS and stained with CD3 PerCP (BD Pharmingen), CD4 Pacific Blue (BD Pharmingen), CD8 PerCp-Cy5.5 (BD Pharmingen), CD45RA APC-Cy7 (BD Pharmingen), CD62L APC (BD Pharmingen), CD31 PE (BD Pharmingen), and CCR7 FITC (R&D Systems). Cells were washed with PBS and resuspended at 10<sup>7</sup>/ml in IMDM/10% FBS. Naïve CD4<sup>+</sup> (CD3<sup>+</sup>/CD4<sup>+</sup>/CD45RA<sup>+</sup>/CD62L<sup>+</sup>/CCR7<sup>+</sup>/CD31<sup>+</sup>) and naïve CD8<sup>+</sup> (CD3<sup>+</sup>/CD4<sup>+</sup>/CD45RA<sup>+</sup>/CD62L<sup>+</sup>/CCR7<sup>+</sup>) T cells, as well as the non-naïve CD4<sup>+</sup> and CD8<sup>+</sup> T cells were purified to >97% using a BD FACS Aria IIu sorter. Purified naïve populations were tested for the presence of contaminating memory cells in an overnight IFN $\gamma$  ELISpot assay using a combination of CMV, EBV, and flu peptides as antigen.

### 6.2.6 Generation of monocyte-derived DC and CTL effector populations

Monocyte-derived DC were generated from each subject as previously described (67) with minor modifications. Briefly, monocytes were thawed and cultured in 10% FBS/IMDM with 1,000 U/ml recombinant GM-CSF (Bayer Healthcare, Montville, NJ) and 1,000 U/ml recombinant IL-4 (R & D Systems, Minneapolis, MN). On day 5, ~0.5 million immature DC (iDC) were incubated with 50,000 pg of purified autologous AT-2 inactivated HIV-1 or peptide epitope variant (5µg/ml) for 2h. iDC were then treated with recombinant CD40L (0.5 µg/ml; Enzo, Farmingdale, New York) and IFN-γ (1000 U/ml; R&D Systems) for 48h. Mature, antigen-loaded DC were harvested and γ-irradiated (3,000 Rads) to kill any contaminating memory T cells in the DC cultures.

Mature, antigen-loaded DC were co-cultured with PBMC obtained prior to seroconversion, naïve CD4<sup>+</sup> and CD8<sup>+</sup> T cells (used for priming) obtained post-cART, or non-naïve CD4<sup>+</sup> and CD8<sup>+</sup> T cells (used for *in vitro* sensitization) obtained post-cART at a DC:T cell ratio of 1:10 for 12 days, supplementing recombinant IL-2 (100 IU/ml; Chiron, Emeryville, CA), IL-7 (10 ng/ml; Miltenyi, Auburn, CA), and IL-15 (2.5ng/ml; PeproTech, Rocky Hill, NJ) every 3 days. T cell cultures were then restimulated with mature, autologous DC loaded with the peptide antigen used in the initial stimulation or autologous AT-2 inactivated HIV-1 and were cultured for an additional 7 days, again supplementing with IL-2, IL-7, and IL-15 every 3 days. Bulk T cells were isolated from primary and IVS cultures by negative selection using a T cell enrichment kit (EasySep, STEMCELL Technologies). *Ex vivo* T cells were generated by isolating bulk T cells from contemporaneous PBMC using a negative T cell enrichment kit (EasySep, STEMCELL Technologies) and culturing in IMDM/10% FBS supplemented with IL-2 (100 IU/ml) and IL-7 (10 ng/ml) for 2d. *Ex vivo*, primary, and IVS T cells were then used in functional assays.

### 6.2.7 IFN $\gamma$ ELISpot

ELISpot assays were performed as previously described (67, 156). Briefly, 96 well plates were coated overnight with 1  $\mu\text{g/ml}$  anti-human IFN $\gamma$  mAb 1-D1K (Mabtech, Stockholm, Sweden) at 4°C. For subject S1, CD8<sup>+</sup> T cells were isolated from pre-seroconversion *in vitro* priming cultures or from PBMC obtained late post-cART using a custom CD8<sup>+</sup> negative isolation kit without the CD56 marker (EasySep, STEMCELL Technologies, Vancouver, BC). For analysis of responses against peptide epitopes, CD8<sup>+</sup> T cells were incubated with 1  $\mu\text{g/ml}$  relevant peptide or EBV for 18h at 37°C in a 5% CO<sub>2</sub> atmosphere. For analysis of responses against overlapping Gag 18mers in subjects S2, S3, and S8, autologous iDC were loaded with 1  $\mu\text{g/ml}$  individual 18mers or a positive control pool consisting of CMV, EBV, and flu peptides for 2 hr at 37°C. *Ex vivo*, *in vitro* priming, and *in vitro*-sensitized (IVS) T cells were incubated with antigen-loaded iDC at a stimulator:responder ratio of 1:10 in IMDM/10% FBS for 18 hr at 37°C in a 5% CO<sub>2</sub> atmosphere. Following incubation, wells were washed with PBS/0.05% Tween-20 (Fisher Scientific, Pittsburgh, PA) and were treated with biotinylated anti-IFN $\gamma$  mAb (1  $\mu\text{g/ml}$ ; Mabtech, Stockholm, Sweden). Plates were washed with PBS/0.05% Tween 20 and incubated with an avidin-peroxidase complex (Vectastain ABC Kit, Vector Laboratories, Burlingame, CA) for 45 min at room temperature. Plates were washed with 0.05% Tween 20/PBS and PBS alone to remove unbound complexes followed by peroxidase staining with diaminobenzidine solution (Sigma, St Louis, MO) for 5 min at RT. IFN $\gamma$  spot-forming cells (SFC) were enumerated using an AID ELISpot reader (Cell Technology, Columbia, MD). Results reported represent the mean values of duplicates when available and are expressed as SFC/10<sup>6</sup>. T cell responses were considered positive and antigen-specific after subtraction of the mean number of spots stimulated by DC alone plus 2 standard deviations.

## 6.2.8 Generation of autologous HIV-1-infected CD4<sup>+</sup> T cells

Autologous CD4<sup>+</sup> T cells were infected with autologous HIV-1 as described previously with minor modifications (56, 290). Contemporaneous PBMC were depleted of CD8<sup>+</sup> T cells using a CD8 T cell positive isolation kit (EasySep, STEMCELL Technologies). The CD8<sup>neg</sup> population was cultured for 2d in IMDM/10% FBS in the presence of IL-2 (100 IU/ml) and PHA (1 µg/ml; Sigma-Aldrich) to induce T cell activation. Activated cells were washed and incubated for 1h in IMDM/10% FBS containing 5 µg of polybrene per ml. Cells were again washed and resuspended in the concentration of purified autologous HIV-1 that resulted in 10-30% of the cells being infected after an additional 3d incubation in IMDM/10% FBS and IL-2 (100 IU/ml). After 3 days of incubation, CD4<sup>+</sup> T cells were isolated by negative selection using a CD4<sup>+</sup> T cell enrichment kit (EasySep, STEMCELL Technologies) and were stained for surface expression of CD8-PerCP-Cy5.5 (BD Pharmingen) and intracellular expression of HIV-1 core antigens using the KC57-FITC antibody (Beckman Coulter, Brea, CA) per the manufacturer's instructions to confirm we had generated a pure population of CD8<sup>neg</sup> T cells, of which 10-30% were positive for HIV-1 (290).

## 6.2.9 HIV-1-specific cytotoxicity assay

CD8<sup>+</sup> T cells were isolated from *ex vivo*, primary, and secondary cultures by negative selection using a custom CD8<sup>+</sup> T cell enrichment kit without the CD56 marker (EasySep, STEMCELL Technologies) and were immediately evaluated for cytotoxic effector function by co-culture with fresh autologous infected CD4<sup>+</sup> T cells at various effector:target ratios for 18h at 37°C. The baseline percent of infection was determined by incubation of infected CD4<sup>+</sup> T cells without



CD8<sup>+</sup> T cells. Co-cultures were harvested and stained for surface expression of CD8-PerCP-Cy5.5 (BD Pharmingen) and intracellular expression of HIV-1 core antigens using the KC57-FITC antibody (Beckman Coulter, Brea, CA) per the manufacturer's instructions. Samples were run on a BD LSRFortessa™ flow cytometer (BD Biosciences) and were analyzed using FlowJo version 9.6.4. The percent of infected CD4<sup>+</sup> T cells was determined by gating on the CD8<sup>neg</sup> population and then on the KC-57 (HIV core antigen)-positive subset. The percent reduction in infected CD4<sup>+</sup> T cells was determined for each condition at each E:T ratio and is in relation to the baseline infection rate.

#### **6.2.10 Statistical analyses**

Comparisons in IFN $\gamma$  production to autologous peptide epitopes pre-seroconversion and post-cART, as well as in the responses to p17 and p24 peptide antigens, were performed using student's T test. Comparisons in *ex vivo* and primary T cell responses were performed using a paired T test, whereas evaluation of differences in IFN $\gamma$  production between all three T cell conditions was performed using a two-way ANOVA with Tukey's multiple comparisons post-test. Differences in CTL killing among the 3 T cell conditions were evaluated using a two-way ANOVA with Sidak's multiple comparisons post-test. All figures and statistics were generated using GraphPad Prism 6 (GraphPad Software, Inc., La Jolla, CA).

## 6.3 RESULTS

### 6.3.1 Primary CD8<sup>+</sup> T cell responses induced from pre-seroconversion and post-cART naïve precursors

It is currently unclear if naïve CD8<sup>+</sup> T cells from HIV-1-infected subjects who were infected for many years without cART are restored in their ability to respond to primary stimulation against autologous HIV-1 antigens after long-term cART. Studies have shown the function and repertoire of naïve CD8<sup>+</sup> T cells are diminished after years of chronic infection. To determine if our sorted naïve CD8<sup>+</sup> T cells were capable of responding to and recognizing autologous HIV-1 epitope variants at a level similar to what would have been observed prior to infection, we first performed Gag, Env, and Nef single-genome sequencing on plasma HIV-1 derived from subject S1 post-cART. We then synthesized 11 variants of known CTL epitopes that were detected by sequencing. Autologous monocyte-derived DC from the same time point as sequencing were matured with CD40L and IFN $\gamma$  and were loaded with each of the 11 epitope variants. Because of limited cell numbers prior to seroconversion and the lack of any existing memory CD8<sup>+</sup> T cells to HIV-1 at this time point, we used bulk PBMC as our responders in the pre-seroconversion condition. Antigen-loaded DC were then used to induce primary T cell responses in these pre-seroconversion PBMC or purified naïve CD8<sup>+</sup> T cells obtained from the same time point as sequencing (“contemporaneous”, post-cART T cells). Following a 19-day DC prime-boost regimen, CD8<sup>+</sup> T cells were isolated and the resulting responses were evaluated by IFN $\gamma$  ELISpot (**Figure 46**).

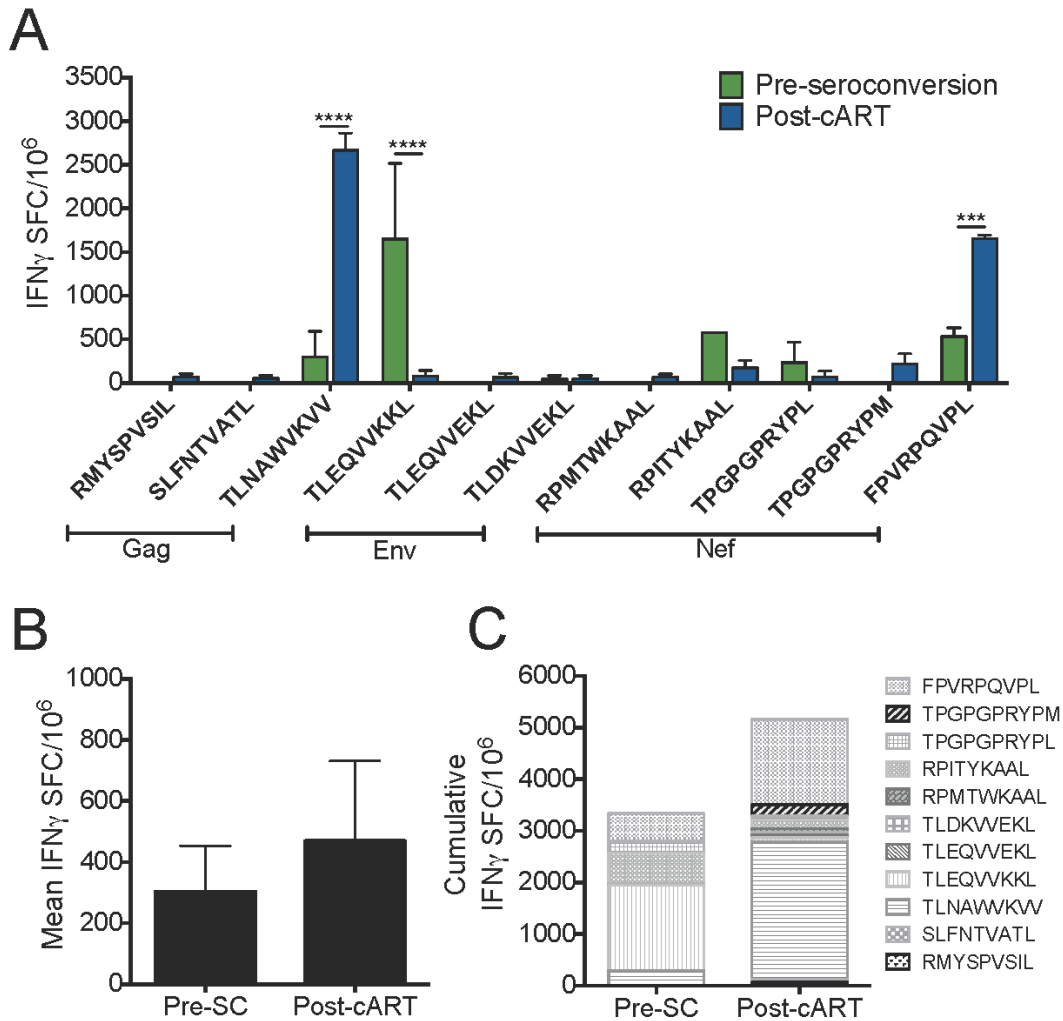


**Figure 46. Primary CD8<sup>+</sup> T cell responses specific for autologous epitope variants induced pre-seroconversion and post-cART in subject S1**

Monocyte-derived DC were matured with CD40L and IFN $\gamma$  and were loaded with individual peptides representing autologous HLA A\*0201 and B\*0702 epitope variants. Antigen-loaded DC were used to stimulate primary T cell responses in PBMC obtained prior to seroconversion or purified contemporaneous naïve CD8<sup>+</sup> T cells (post-cART). IFN $\gamma$  production was evaluated by an overnight ELISpot assay. (A) T cell responses to each individual epitope variant, (B) mean IFN $\gamma$  production, and (C) the cumulative response from all variants are shown as the number of spot-forming cells (SFC) per 10<sup>6</sup> for the pre-seroconversion and post-cART T cell conditions. Error bars represent the standard deviation of duplicate wells in (A) or the response to all variants in (B). Pre-SC, pre-seroconversion. \*\*\*p<0.001, \*\*\*\*p<0.0001

In cells obtained prior to seroconversion, we detected primary responses to 6 of the 11 variants tested, whereas we observed responses of varying magnitudes to all variants in the post-cART condition (**Figure 46A**). We observed significant differences in IFN $\gamma$  production between

the two conditions in only three of the variants tested. Responses to TLNAWVKVV and FPVRPQVPL were significantly higher post-cART compared to the pre-seroconversion condition ( $p < 0.0001$  and  $p = 0.0004$ , respectively). Interestingly, only the TLEQVVKKL variant induced a higher response in the pre-seroconversion condition ( $p < 0.0001$ ). There was no difference in mean IFN $\gamma$  production when the responses to each variant were averaged for the pre-seroconversion and post-cART conditions ( $p = 0.581$ ), with the post-cART T cells producing an average of 469 SFC/10<sup>6</sup> compared to 303 SFC/10<sup>6</sup> in pre-seroconversion T cells (**Figure 46B**). To evaluate the overall magnitude of the primary response, we summed the IFN $\gamma$  production that was detected in each set of T cells, with a sum of 3,333 SFC/10<sup>6</sup> in pre-seroconversion cells and 5,269 SFC/10<sup>6</sup> in post-cART CD8<sup>+</sup> T cells (**Figure 46C**). In cells derived from pre-seroconversion PBMC, however, the response is more evenly distributed across 5 different variants, whereas in the post-cART CD8<sup>+</sup> T cells the response is primarily toward the FPVRPQVPL and TLNAWVKVV variants.

Nonetheless, these data indicate a sufficient capacity of naïve CD8<sup>+</sup> T cells derived after many years of chronic infection and suppressive cART to develop primary responses against autologous epitope variants. Because these variants were in circulation during cART, it can be hypothesized that an effective CTL response was not generated to these variants *in vivo*. Additionally, an effective DC immunotherapy would need to generate a response that is more broad and of higher magnitude than the endogenous T cell response, as these CTL failed to control infection naturally. We therefore aimed to determine if the primary responses generated *in vitro* from naïve, contemporaneous (post-cART) precursors were comparable to those generated to the same variants *in vivo*. Contemporaneous bulk CD8<sup>+</sup> T cells were stimulated in an overnight IFN $\gamma$  ELISpot assay with the same autologous HIV-1 epitope variants.

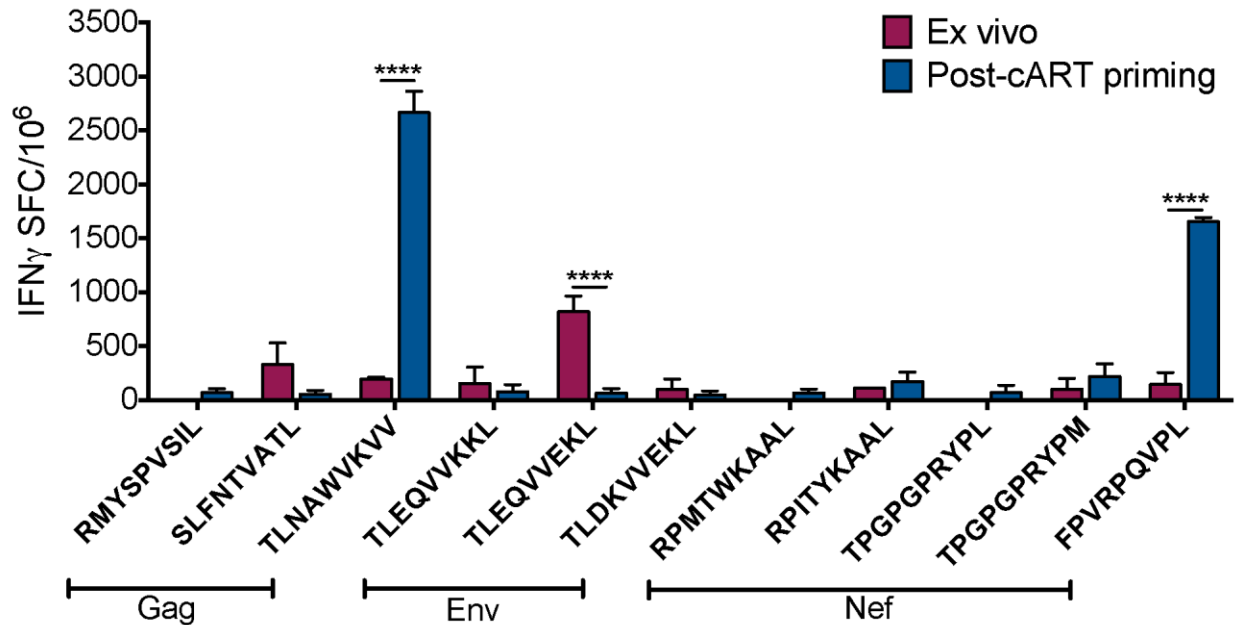


**Figure 47. Comparison of primary and recall CD8<sup>+</sup> T cell responses to autologous HIV-1 epitope variants in subject S1**

CD8<sup>+</sup> T cells were isolated from contemporaneous T cells pre-activated with IL-2 and IL-7 (*ex vivo*) or from the priming cultures that used contemporaneous naïve precursors (post-cART priming). *Ex vivo* and primary IFN $\gamma$  production to 11 autologous variants of HLA A\*0201- and B\*0702-restricted CTL epitopes was evaluated in an overnight ELISpot assay. Responses to each variant are shown as the number of spot-forming cells (SFC) per 10<sup>6</sup>. Error bars represent the standard deviation of duplicate wells. \*\*\*\*p<0.0001

We detected responses to 8 of the variants tested in the *ex vivo* condition (**Figure 47**), compared to all of the variants in the post-cART priming condition (**Figures 46A and 47**). Similar to the pattern observed in pre-seroconversion primary responses, the *ex vivo* T cell response was significantly lower than the post-cART primary response to the TLNAWVKVV (p<0.0001) and FPVRPQVPL (p<0.0001) variants. *Ex vivo* IFN $\gamma$  production in response to TLEQVVEKL was significantly higher than that detected in the post-cART priming condition (p<0.0001). Overall, there was no significant difference between the two conditions in 8 out of the 11 variants tested, and there was no difference in mean IFN $\gamma$  production by both conditions (data not shown), indicating a failure of our DC-based priming method to induce a response from naïve precursors

that is of greater magnitude than the endogenous recall T cell response when targeting autologous HIV-1 epitope variants.

### **6.3.2 Ex vivo T cells recognize autologous Gag p17 and p24 with variable breadth and magnitude**

We showed above that DC loaded with autologous HIV-1 peptide antigen induce primary responses from naïve precursors that are largely indistinguishable from the responses generated during infection. It could be hypothesized that using a limited number of individual peptide epitopes did not accurately reflect the breadth and magnitude of responses that were present endogenously or that can be generated using a DC stimulation. We therefore expanded our study to include three additional subjects who were under long-term suppressive cART (>13 years) following 8-10 years of untreated HIV-1 infection. We first wanted to assess the breadth and magnitude of the endogenous recall T cell response that was generated during infection and that currently makes up the memory repertoire against the autologous reservoir virus. These are the responses that would be stimulated during a therapeutic treatment interruption or a reactivation of the latent reservoir, and we therefore wanted a more broad understanding of the memory repertoire that was generated against the autologous virus.

Autologous HIV-1 was reactivated and isolated from CD4<sup>+</sup> T cells using a previously described method (195, 311). In subjects S2 and S3, this virus was obtained after >5 years post-cART, whereas in subject S8 this virus was isolated immediately prior to cART. The isolated viruses were deemed “contemporaneous”, as HIV-1 is unlikely to undergo significant evolution under suppressive cART (166, 303, 304). We performed single-genome *gag* p17-p24 sequencing on the reactivated virus and generated a library of 120, 114, and 115 overlapping 18mers

representing the autologous consensus Gag sequence of subjects S2, S3, and S8, respectively. Bulk T cells were isolated from each subject at the most recent study visit (>13 years post-cART) and were activated for 2 days in the presence of IL-2 and IL-7. This brief period of activation was performed to allow proper detection of an antigen-specific response in freeze-thawed T cells. These *ex vivo* cells were evaluated in an IFN $\gamma$  ELISpot assay for responses to each 18mer using immature dendritic cells (iDC) as our antigen-presenting cells.

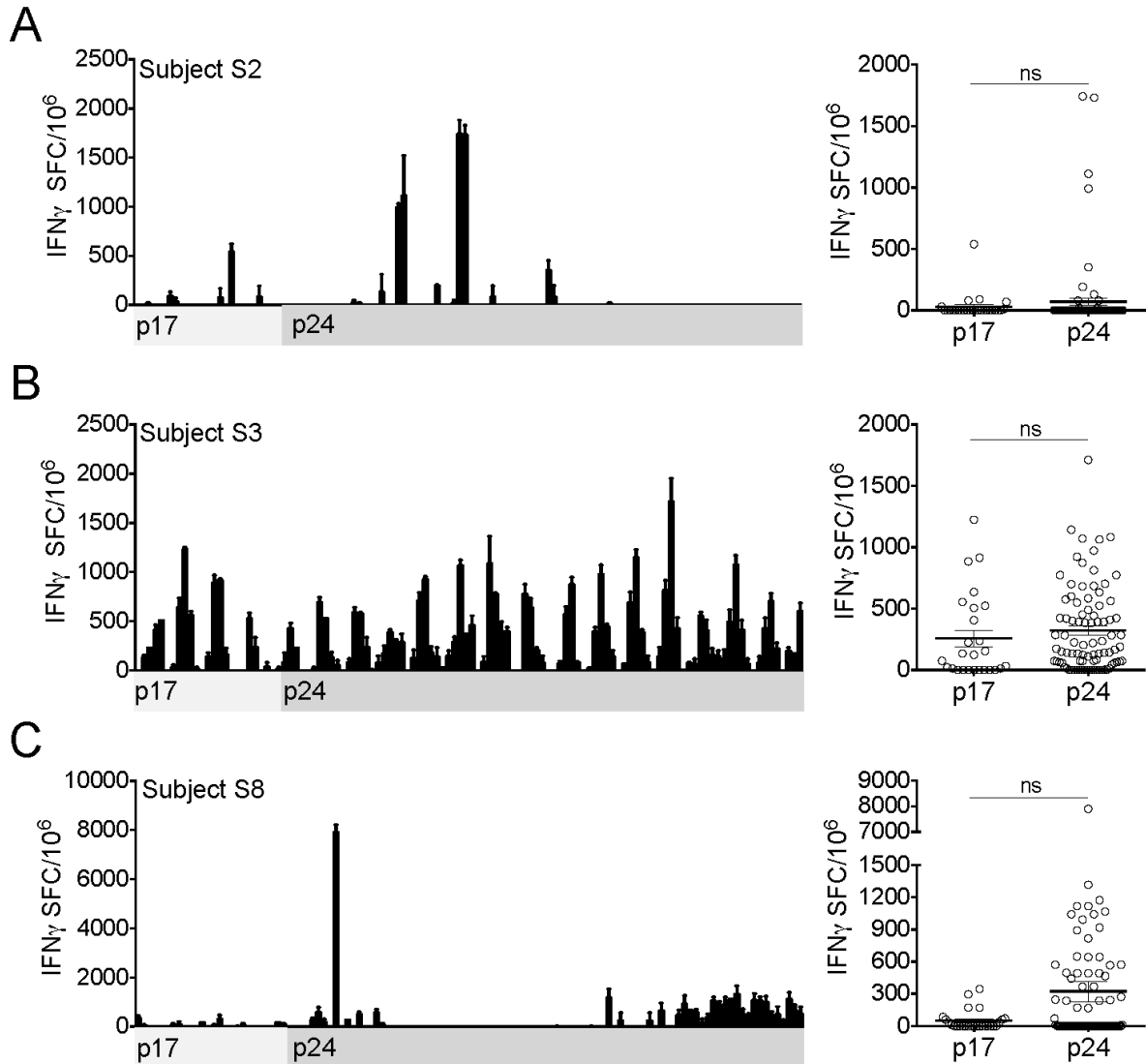


**Figure 48. *Ex vivo* T cell responses to autologous, contemporaneous Gag peptide antigen**

Autologous monocyte-derived immature DC were loaded with individual 18mers representing autologous contemporaneous Gag p17 and p24 sequences and were used to stimulate pre-activated, *ex vivo* T cells in an overnight IFN $\gamma$  ELISpot assay. Responses to each 18mer are shown as the number of spot-forming cells (SFC) per 10 $^6$  in duplicate wells (left panels) or the mean response to each p17 and p24 peptide (right panels) in subjects (A) S2, (B) S3, and (C) S8. All responses are shown with the mean background +2 standard deviations subtracted. Error bars represent the standard deviation of duplicate wells (left panels) or the standard error of the mean of all p17 or p24 peptide responses (right panels).

In subject S2, we detected recall T cell responses to 21/120 peptides (17.5%), with responses ranging from 10 to 1,740 SFC/10 $^6$  (**Figure 48A**). Within the Gag p17 protein, 6/27 (22.2%) peptides induced responses, whereas only 15/93 (16.1%) p24 peptides induced responses.



In subject S3, we detected responses to 91/114 (79.8%) peptides, with IFN $\gamma$  production ranging from 13 to 1,713 SFC/10<sup>6</sup>. In p17, 18/26 (69.2%) peptides were recognized whereas 72/88 (81.8%) peptides were recognized in p24 (**Figure 48B**). In subject S8, 47/115 (40.9%) peptides were recognized and responses to these ranged from 10 to 7,896 SFC/10<sup>6</sup> (**Figure 48C**). In this subject, we detected IFN $\gamma$  production in response to 11/27 (40.7%) p17 peptides and 36/88 (40.9%) p24 peptides. There were no significant differences in the mean IFN $\gamma$  response between p17 and p24 in any of the subjects, suggesting an equal distribution of the response between the two Gag regions (**Figure 48 A, B, and C**).

In summation, subjects S2 and S8 showed limited breadth in their endogenous responses to autologous Gag peptide antigen. In subject S3, we detected responses of high magnitude that broadly targeted the two proteins. Despite this, these T cells failed to control the virus in chronic HIV-1 infection. As we now evaluated IFN $\gamma$  production in response to many autologous peptide antigens, these responses serve as a baseline for which to compare our *in vitro* method of enhancing ant-HIV-1 CD8<sup>+</sup> T cell immunity.

### **6.3.3 T cells primed to autologous HIV-1 *in vitro* are of higher breadth and magnitude than responses detected *ex vivo***

We next aimed to determine if DC loaded with whole autologous virus could induce a broad primary response from contemporaneous naïve precursors. Immature DC were loaded with autologous AT-2 inactivated HIV-1, matured with CD40L and IFN $\gamma$ , and were cultured with purified contemporaneous naïve T cells in an *in vitro* 19 day prime-boost regimen. Primary CD3<sup>+</sup> T cells were isolated and evaluated for IFN $\gamma$  production against the overlapping 18mers previously

used in **Figure 48** to determine if a broad and robust response was generated against the autologous Gag sequence using our *in vitro* priming method.

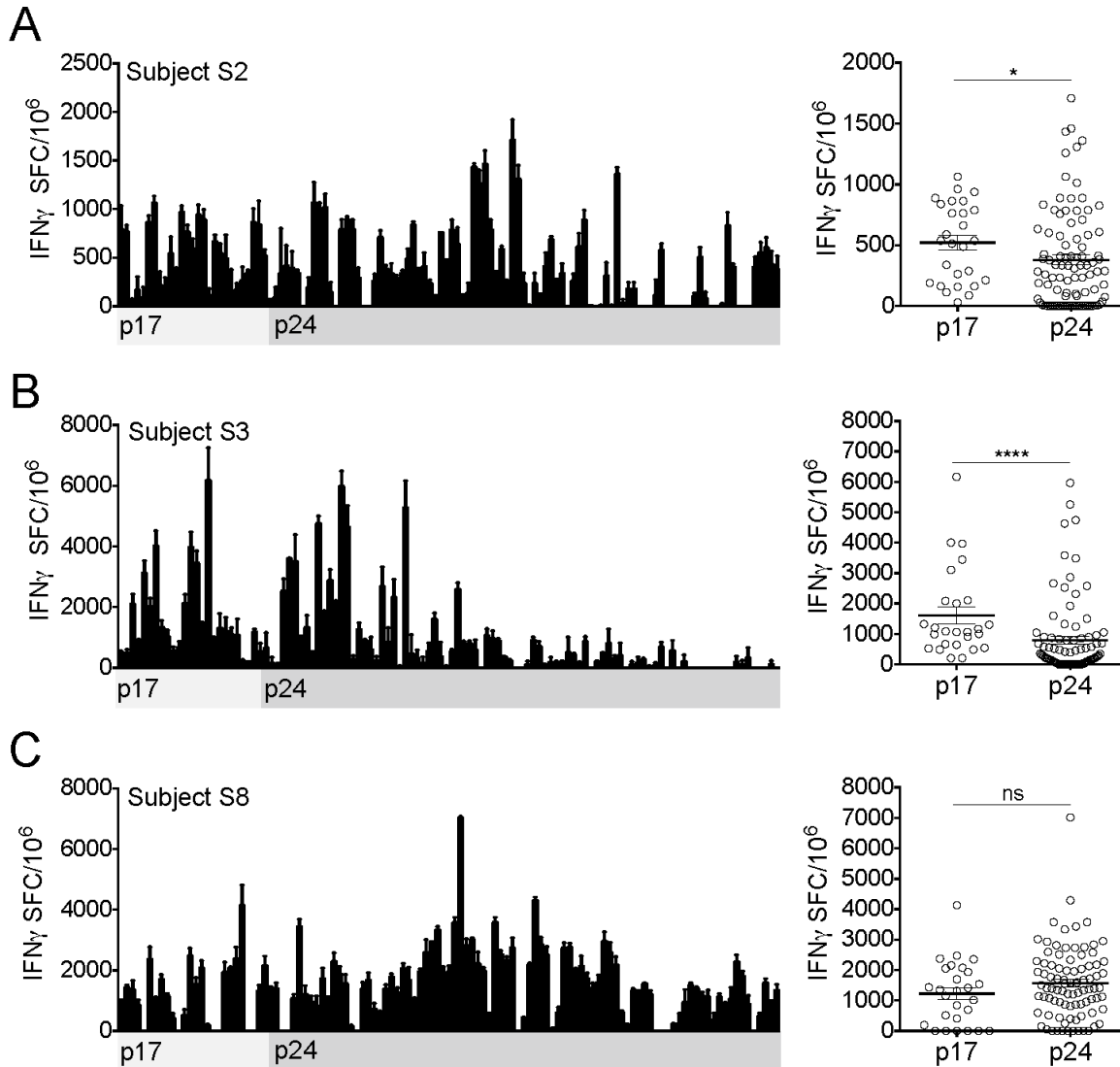


**Figure 49. Primary T cell responses specific for contemporaneous Gag p17 and p24 peptide antigens**  
 Contemporaneous immature DC (iDC) were loaded with autologous, AT-2 inactivated HIV-1 and were matured with CD40L and IFN $\gamma$  for 2 days. Mature antigen-loaded DC were  $\gamma$ -irradiated and used to stimulate primary HIV-1-specific T cells from purified contemporaneous naïve precursors. Autologous monocyte-derived iDC were loaded with individual 18mers representing autologous contemporaneous Gag p17 and p24 sequences and were used to stimulate pre-activated, *ex vivo* T cells in an overnight IFN $\gamma$  ELISpot assay. Responses to each 18mer are shown as the number of spot-forming cells (SFC) per  $10^6$  in duplicate wells (left panels) or the mean response to each p17 and p24 peptide (right panels) in subjects (A) S2, (B) S3, and (C) S8. All responses are shown with the mean background +2 standard deviations subtracted. Error bars represent the standard deviation of duplicate wells (left panels) or the standard error of the mean of all p17 or p24 peptide responses (right panels). ns, not significant. \*\*\*\* $p < 0.0001$ , \* $p < 0.05$ .

In subject S2, we generated primary responses against 99/120 (82.5%) of the 18mers tested, with 100% of p17 and 72/93 (77.4%) of p24 peptides being recognized and responses ranging from 10 to 1,708 SFC/10<sup>6</sup> (**Figure 49A, left panel**). The mean IFN $\gamma$  production against p17 peptides was significantly higher than the response against p24 peptides ( $p=0.014$ ), despite there being 8 p24 peptides that induced responses >1,000 SFC/10<sup>6</sup> compared to only one variant inducing this magnitude of response in p17 (**Figure 49A, right panel**). In subject S3, primary IFN $\gamma$  production ranged from 30 to 5,967 SFC/10<sup>6</sup>, with a total of 95/114 (83.3%) peptides being recognized. Within p17, 100% of peptides were recognized, whereas 69/88 (78.4%) of p24 peptides were recognized (**Figure 49B, left panel**). Mean IFN $\gamma$  production in response to the p17 peptides was significantly higher than the mean response to p24 peptides ( $p<0.0001$ , **Figure 49B, right panel**). Among the peptides inducing IFN $\gamma$  production, the range is similar between the two proteins, with a range of 207 to 6,167 SFC/10<sup>6</sup> in p17 and 63 to 5,966 SFC/10<sup>6</sup> in p24, despite more peptides inducing no response in p24 than p17. In subject S8, we detected primary responses against 101/115 (87.8%) peptides that ranged from 54 to 4,294 SFC/10<sup>6</sup>, with 21/27 (77.8%) p17 peptides and 80/88 (90.9%) p24 peptides giving a positive response (**Figure 49C, left panel**). There was no significant difference in the mean IFN $\gamma$  production against peptides from p17 and p24 (**Figure 49C, right panel**).

We then compared the primary responses induced from naïve precursors to those detected against the same peptide antigens in contemporaneous *ex vivo* T cells. This comparison would allow us to determine if using DC loaded with whole, autologous HIV-1 induced a primary response that was of higher magnitude and breadth than the endogenous recall response.

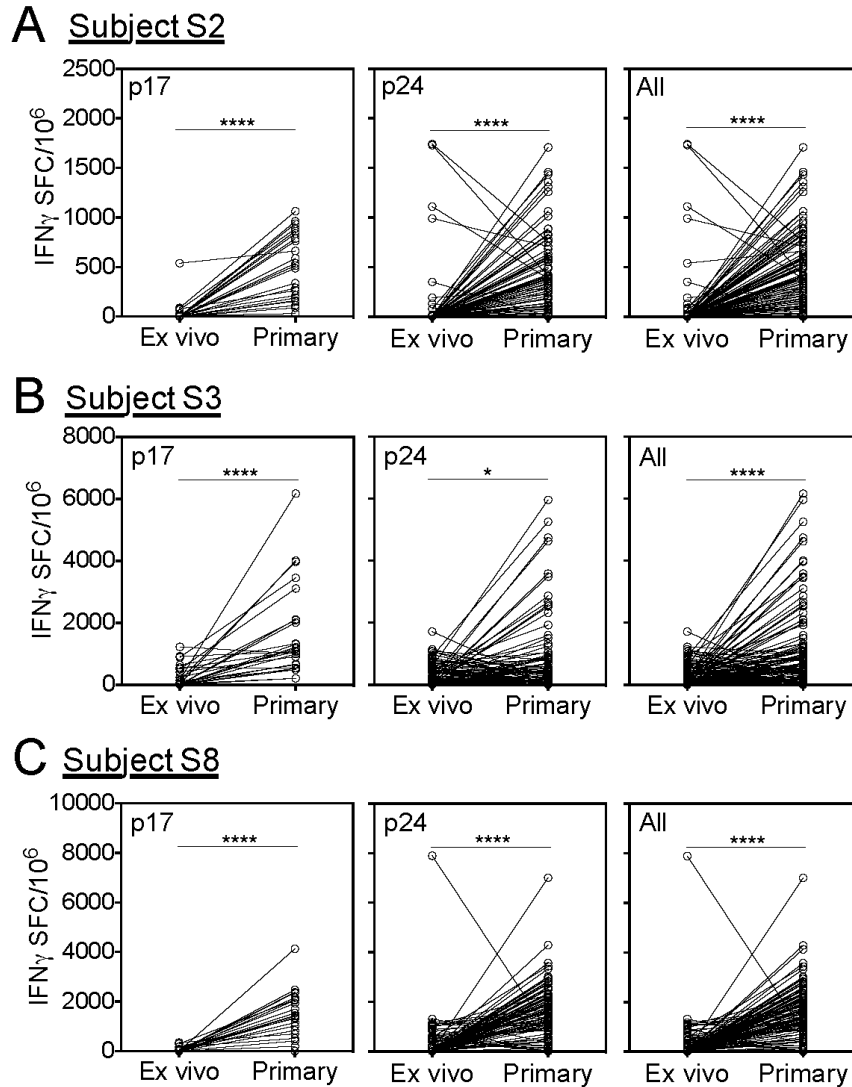


**Figure 50. Priming of naïve T cells to autologous HIV-1 induces antigen-specific responses that are of greater magnitude than the endogenous recall response**

The IFN $\gamma$  ELISpot data generated in figures 48 and 49 were evaluated in pairwise comparisons for differences in the magnitude between the endogenous *ex vivo* response and the primary response induced *in vitro* in subjects (A) S2, (B) S3, and (C) S8. The differences between responses against peptides from the p17 (left panels) and p24 (middle panels) proteins were evaluated, as well as the difference in response to all peptides combined (right panels). \* $p < 0.05$ , \*\*\*\* $p < 0.0001$

In subjects S2 (**Figure 50A**), S3 (**Figure 50B**), and S8 (**Figure 50C**) we were able to generate significantly higher primary responses from naïve precursors in comparison to the endogenous responses generated *in vivo*. In fact, when we evaluated responses to peptide antigens

based on the protein from which they were derived, primary responses were significantly higher than *ex vivo* responses against the p17 peptides (**Figure 50, left panels**,  $p < 0.0001$  for all) and p24 peptides (**Figure 50, middle panels**) for subjects S2 ( $p < 0.0001$ ), S3 ( $p = 0.039$ ), and S8 ( $p < 0.0001$ ).

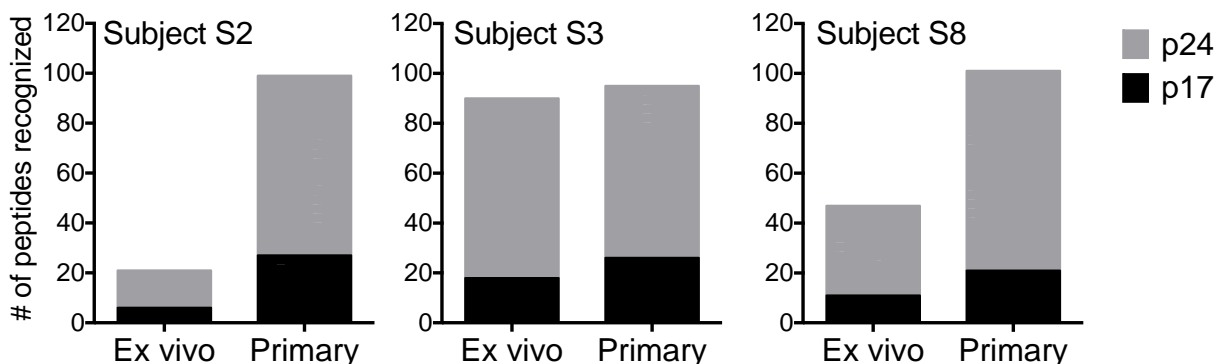


**Figure 51. Primary stimulation of naïve T cells increases the breadth of responses to autologous HIV-1 antigen**

The number of Gag p17 (black) and p24 (gray) 18mers that induced responses above background (the average SFC/10<sup>6</sup> of duplicate wells without peptide plus 2 standard deviations) and were greater than 10 SFC/10<sup>6</sup> in *ex vivo* and primary T cells were counted for subjects S2 (left panel), S3 (middle panel), and S8 (right panel).

We then wanted to determine if naïve T cell priming also enhanced the breadth of the response, i.e. the number of peptide variants that were recognized. In all three subjects, the number of variants that induced IFN $\gamma$  production was higher in the primary condition than in *ex vivo* T cells (**Figure 51**). These findings suggest that, not only did our *in vitro* priming method successfully prime naïve T cells to whole inactivated HIV-1, but the resulting T cells recognize autologous Gag antigens with a higher breadth and affinity than endogenous T cells.

Comparing primary and *ex vivo* IFN $\gamma$  production to autologous HIV-1 antigen derived from the reservoir virus allows us to conclude that naïve T cells from subjects on long-term cART are capable of mounting primary responses that are of significantly higher magnitude than the response generated *in vivo* if they are given the appropriate stimulation and are in the absence of chronic

immune dysfunction. However, these findings do not address the effects of a DC prime-boost regimen on the existing dysfunctional T cell population.

#### **6.3.4 DC sensitization of non-naïve T cells results in responses of variable breadth and magnitude against autologous Gag antigens**

While inducing a primary response using DC immunotherapy would allow us to pick the antigen to which we want the cells to respond, it has been proposed that reactivating the quiescent, dysfunctional memory response may be effective as well. In fact, DC can “re-condition” dysfunctional T cell responses to melanoma-associated antigens from those predominantly producing the type-2 cytokine IL-5 to those producing the type-1 cytokine IFN $\gamma$  (346). Additionally, it has yet to be explored how a long-term DC stimulation would impact an antigen-specific population with regulatory and exhaustion defects from years of chronic HIV-1 infection (162, 269, 296). We therefore used purified T cells that were not included in the “naïve” sorting gate (“non-naïve” cells) in our *in vitro* priming model. Since these cells were probably largely antigen-experienced, the T cells resulting from this protocol were deemed “secondary”. Following the 19-day DC stimulation with autologous AT-2 inactivated HIV-1, we evaluated the expanded, secondary T cells for IFN $\gamma$  production against the overlapping Gag 18mers used previously.

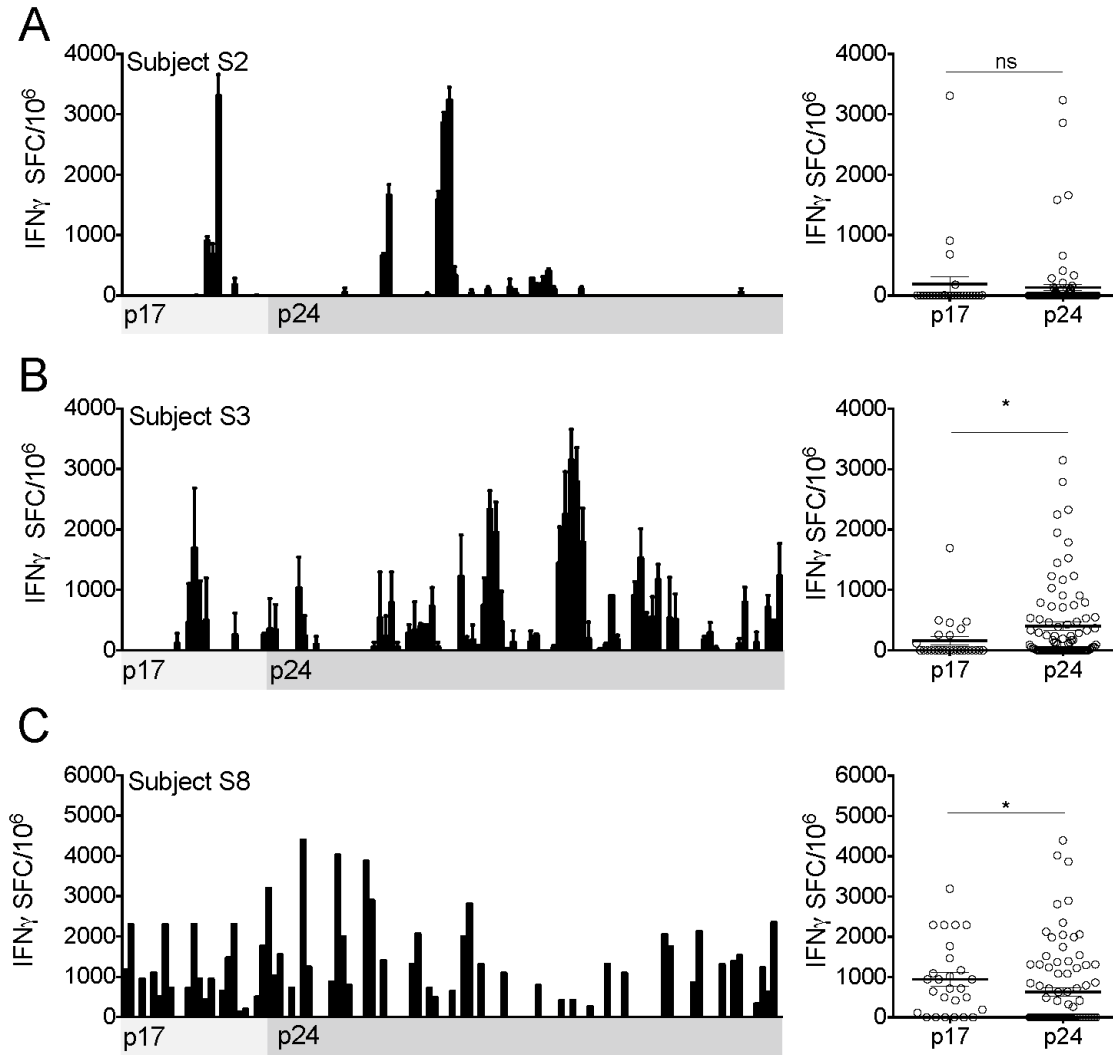


**Figure 52. Secondary, DC-stimulated T cell responses to autologous Gag peptides**

Contemporaneous immature DC (iDC) were loaded with autologous, AT-2 inactivated HIV-1 and were matured with CD40L and IFN $\gamma$  for 2 days. Mature antigen-loaded DC were  $\gamma$ -irradiated and used to stimulate autologous contemporaneous non-naïve T cells. Autologous monocyte-derived iDC were loaded with individual 18mers representing autologous contemporaneous Gag p17 and p24 sequences and were used to stimulate secondary T cells in an overnight IFN $\gamma$  ELISpot assay. Responses to each 18mer are shown as the number of spot-forming cells (SFC) per  $10^6$  in duplicate wells (left panels) or the mean response to each p17 and p24 peptide (right panels) in subjects (A) S2, (B) S3, and (C) S8. Responses in subjects S2 and S3 are shown with the mean background +2 standard deviations subtracted. Responses in subject S8 are shown as the number of SFC/ $10^6$  in single wells above background. Error bars represent the standard deviation of duplicate wells (left panels) or the standard error of the mean of all p17 or p24 peptide responses (right panels). ns, not significant. \* $p < 0.05$ .

In subject S2, secondary T cells responded to 23/120 (19.2%) peptides, with 4/27 (14.8%) p17 and 19/93 (20.4%) p24 peptides inducing IFN $\gamma$  production (**Figure 52A**). Pairwise comparisons showed no significant difference in the mean IFN $\gamma$  response induced by peptides

derived from either protein. Secondary T cell responses were more prevalent in subject S3, with 62/114 (54.4%) giving positive results (**Figure 52B**). We detected responses to 8/26 (30.8%) p17 peptides and 54/88 (61.4%) p24 peptides in this subject. The average response generated against p24 peptides was significantly higher than that generated against p17 peptides ( $p=0.014$ ). Finally, IFN $\gamma$  production by secondary T cells from subject S8 was observed in 58/115 (50.4%) peptides, with 21/27 (77.8%) p17 and 37/88 (42.0%) p24 peptides inducing responses (**Figure 52C**). The average response induced by p24 peptides was significantly lower than the response induced against p17 peptides ( $p=0.01$ ) in this subject.

As we already showed a significant enhancement of the response to autologous antigens when using primary T cells compared to *ex vivo* T cells, we next wanted to determine how the secondary response compares to the previous two T cell conditions. We therefore determined if secondary T cells enhanced the endogenous response and if they were of a different magnitude than the primary T cells induced from naïve precursors. By combining the data generated in figures 48, 49, and 52, we were able to observe stark differences between the three T cell conditions.

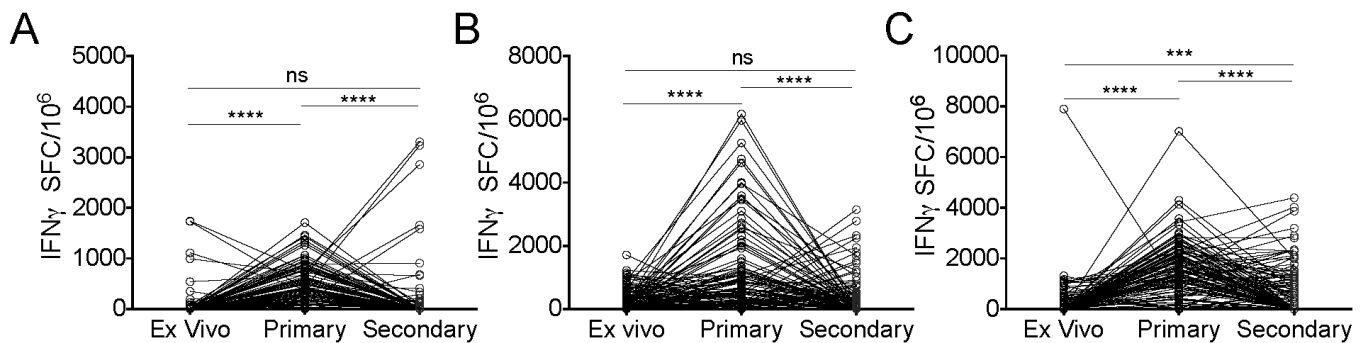


**Figure 53. Comparison of IFN $\gamma$  responses to all autologous Gag antigens evaluated in *ex vivo*, primary, and secondary T cells**

The IFN $\gamma$  ELISpot data generated in figures 48, 49, and 52 were evaluated in pairwise comparisons for differences in the magnitude between the endogenous *ex vivo* response and the primary and secondary responses induced *in vitro* in subjects (A) S2, (B) S3, and (C) S8. Responses are shown as the mean number of spot forming cells (SFC) above background in duplicate wells for each Gag 18mer in each T cell condition. ns, not significant. \*\* $p<0.01$ , \*\*\* $p<0.0001$



When comparing the responses of all three T cell conditions, primary IFN $\gamma$  production was significantly higher than the secondary response in subjects S2 (**Figure 53A**), S3 (**Figure 53B**), and S8 (**Figure 53C**) ( $p < 0.00001$  for all). The secondary T cell response was not different from the *ex vivo* response in subjects S2 and S3, however it was higher than the *ex vivo* response in subject S8 ( $p = 0.0001$ ). These findings indicate that DC-mediated stimulation of non-naïve T cells was unable to enhance the endogenous HIV-1-specific T cell response in 2 of the 3 subjects. Despite this, we still observed high magnitude IFN $\gamma$  responses to at least a few of the Gag 18mers in each subject, with more being recognized following secondary stimulation in subjects S3 and S8 than in subject S2.

It is plausible that the differences observed in mean IFN $\gamma$  production were skewed because of the high number of peptides that induced no response in the *ex vivo* condition. We therefore wanted to determine if the magnitude of the IFN $\gamma$  response was specifically increased in response to peptide antigens to which we detected responses in the *ex vivo* condition. Evaluating the data in this fashion would allow us to determine if *in vitro* priming or secondary stimulation specifically enhanced the responses that were already present in the *ex vivo* condition. We therefore compared IFN $\gamma$  ELISpot data for the Gag 18mers that induced positive responses in *ex vivo* T cells (**Figure 54**).

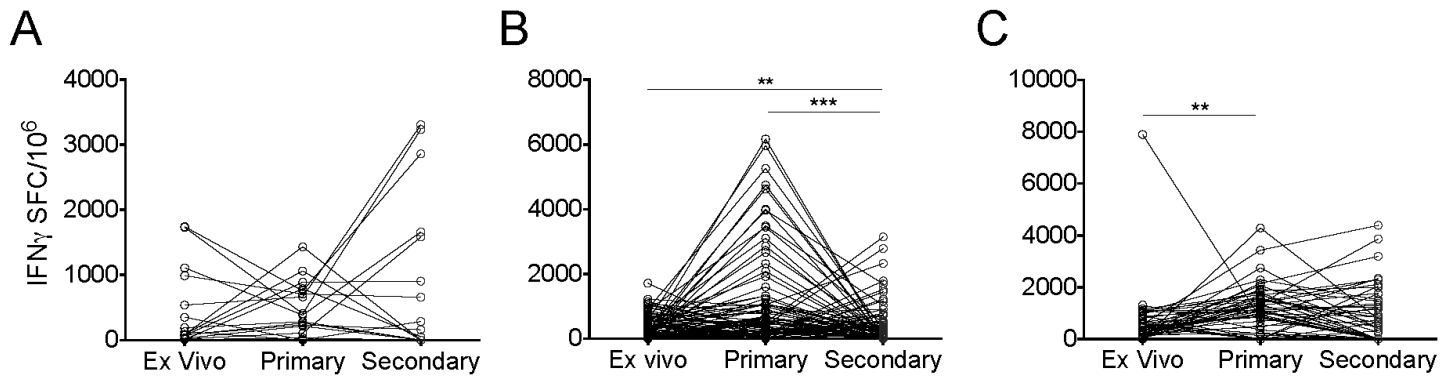


**Figure 54. Comparison of IFN $\gamma$  responses specific for autologous Gag antigens that induced responses in *ex vivo* T cells**

The IFN $\gamma$  ELISpot data shown in figure 53 were transformed to only include responses to variants to which we detected positive IFN $\gamma$  production in the *ex vivo* condition in subjects (A) S2, (B) S3, and (C) S8. Responses are shown as the mean number of spot forming cells (SFC) above background in duplicate wells for each Gag 18mer in each T cell condition. Error bars represent the mean of all values  $\pm$  SEM. \*\* $p < 0.01$ , \*\*\* $p < 0.001$

Surprisingly, the significant differences observed between the *ex vivo* and primary responses in subjects S2 and S3 (**Figure 53 A and C**, respectively) were completely abrogated when adjusting our analysis to only include variants giving positive responses in the *ex vivo* condition (**Figure 54A and B**). Only subject S8 retained the difference between the *ex vivo* and primary conditions (**Figure 54C**). Additionally, there was no longer a difference between the primary and secondary conditions in subjects S2 and S8 (**Figure 54 A and C**, respectively). Of note, secondary responses were significantly lower than *ex vivo* responses in subject S3 after removal of variants that induced no response in *ex vivo* T cells (**Figure 54B**). These data give a closer insight into the dynamics of the response within the breadth of the *ex vivo* condition, and show no universal enhancement of either *in vitro* priming or secondary stimulation compared to *ex vivo*.

### 6.3.5 Analysis of CTL effector function against autologous HIV-1-infected CD4<sup>+</sup> T cells

We showed above that *in vitro* sensitization of non-naïve T cells results in IFN $\gamma$  production that is significantly lower than the primary response generated from naïve precursors, but is still high in magnitude against some of the Gag antigens evaluated, particularly those that induced responses in the *ex vivo* condition. While IFN $\gamma$  production is a good way to validate the existence of an immune response, it is not necessarily correlative of a cytolytic effector function. We previously described a mechanism by which cytokine secretion is not necessarily correlative of CTL killing, and in fact activation of antigen-specific T cells with a similar, but different antigen resulted in high levels of cytokine production without the associated CTL response (217). We therefore needed to determine if the IFN $\gamma$  production detected in *in vitro*-sensitized and primary CD8<sup>+</sup> T cells was indicative of CTL effector function, and if the DC-based secondary stimulation or priming methods were able to generate CTL capable of eliminating autologous infected CD4<sup>+</sup> T cells with greater efficiency than the endogenous CD8<sup>+</sup> T cells that were generated *in vivo*. To address this, we evaluated primary and secondary CD8<sup>+</sup> T cells for their ability to kill autologous CD4<sup>+</sup> T cells infected with the autologous contemporaneous virus that was derived from latently-infected cells and compared this CTL elimination to that observed in *ex vivo* CD8<sup>+</sup> T cells.

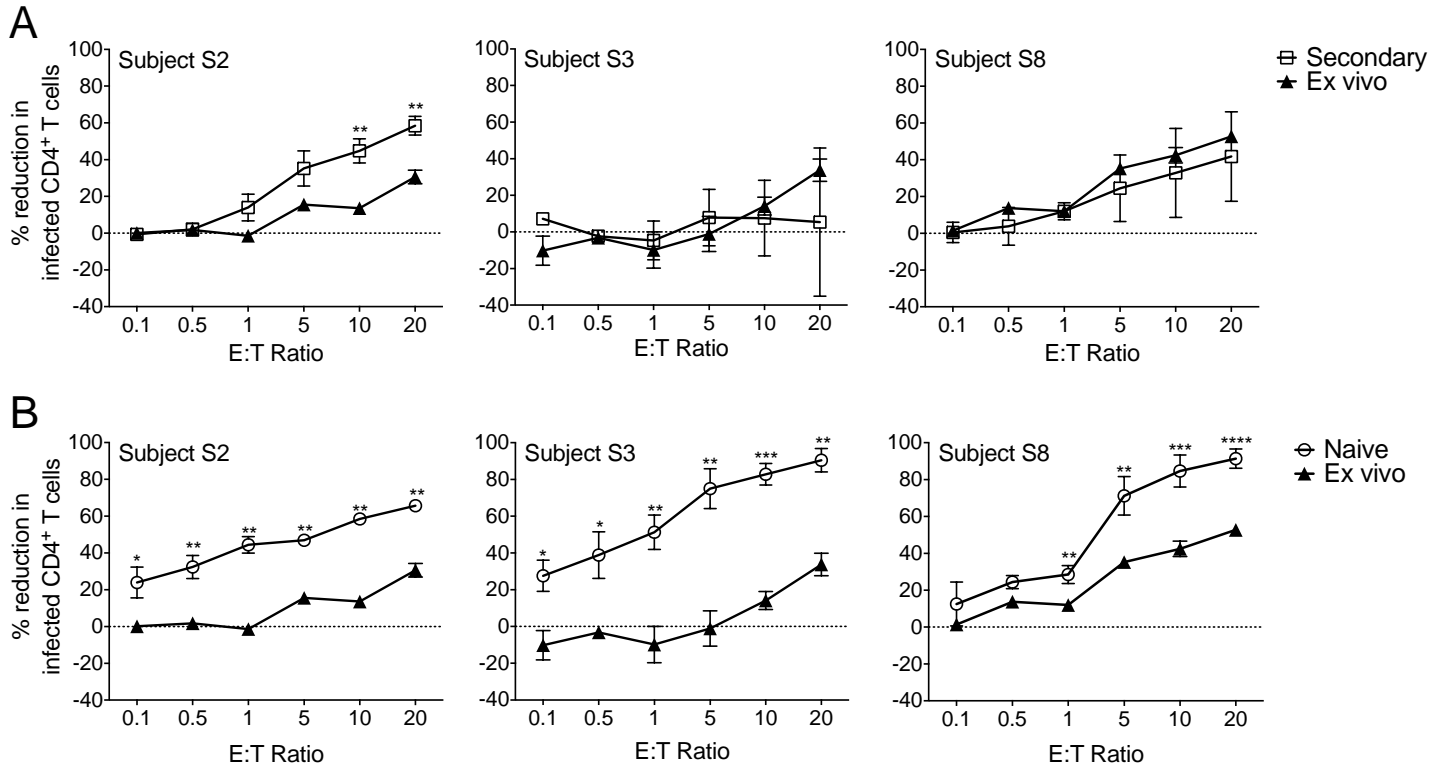


**Figure 55. *Ex vivo*, primary, and secondary CTL-mediated reductions in autologous CD4<sup>+</sup> T cells infected with the autologous HIV-1 reservoir virus**

Contemporaneous autologous CD4<sup>+</sup> T cells from subjects S2 (left panel), S3 (middle panel), and S8 (right panel) were infected for at least 2d with autologous HIV-1 derived from the cART reservoir to obtain a population in which 10-30% of the cells stained positive for intracellular HIV-1 by flow cytometry. *Ex vivo* (black triangle), primary (open circle), and secondary (open square) CD8<sup>+</sup> T cells were isolated and co-cultured with infected CD4<sup>+</sup> T cells for 18h at various effector:target ratios. Data are shown as the mean percent reduction in infected CD4<sup>+</sup> T cells compared to infected targets without effector CD8<sup>+</sup> T cells. Percent reduction was determined by flow cytometry and is shown as a comparison in the percent reduction induced by (A) secondary and (B) primary CD8<sup>+</sup> T cells to endogenous CD8<sup>+</sup> T cells stimulated *ex vivo* with IL-2 and IL-7 for 2d. \*p<0.05, \*\*p<0.01, \*\*\*p<0.001, \*\*\*\*p<0.0001

In subject S2, we did not observe secondary or *ex vivo* CTL elimination of virally-infected targets until the 1:1 E:T ratio (**Figure 55A**, left panel). CTL killing peaked at the 20:1 ratio at 30.6% and 58.4% in the *ex vivo* and secondary conditions, respectively. Secondary CD8<sup>+</sup> T cells significantly enhanced CTL killing above the *ex vivo* condition only at the 10:1 (p=0.004) and 20:1 (p=0.003) ratios. In subject S3, there was no identifiable pattern in target killing with increasing E:T ratios (**Figure 55A**, middle panel). Killing by *ex vivo* CD8<sup>+</sup> T cells was largely indistinguishable from the killing observed by secondary CD8<sup>+</sup> T cells, with no significant

differences seen at any of the E:T ratios. In subject S8, there was a general trend of increased reduction in infected targets with increased E:T ratios, however secondary CD8<sup>+</sup> T cell killing was not significantly greater than killing by *ex vivo* CD8<sup>+</sup> T cells at any of the ratios (**Figure 55A**, right panel). These data suggest that DC secondary stimulation of CD8<sup>+</sup> T cells does not increase their cytolytic effector capabilities, despite our detection of IFN $\gamma$  production in response to autologous Gag peptide antigen.

When evaluating CTL killing by primary T cells, we observed increases with each E:T ratio in all three subjects (**Figure 55B**). In subjects S2 (**Figure 55B**, left panel) and S3 (**Figure 55B**, middle panel), CTL killing by primary CD8<sup>+</sup> T cells was significantly greater than the killing observed by *ex vivo* CD8<sup>+</sup> T cells at every E:T ratio evaluated, with primary CTL killing peaking at 65.6% and 90.5%, respectively, at the 20:1 ratio. In subject S8, primary CTL killing was greater than *ex vivo* killing at the 1:1 (p=0.005), 5:1 (p=0.004), 10:1 (p=0.0007), and 20:1 (p<0.0001) ratios (**Figure 55B**, right panel), and peaked at 91.4%. Collectively, the data from these subjects show that inducing a primary CTL response from naïve precursors results in CTL that eliminate infected CD4<sup>+</sup> T cells more effectively than the endogenous *ex vivo*-stimulated CTL.

## 6.4 DISCUSSION

In this study we have shown for the first time that naïve CD8<sup>+</sup> T cells from subjects on long-term suppressive cART can respond to primary DC stimulation against the autologous HIV-1 reservoir and are capable of exerting effector CTL function on CD4<sup>+</sup> T cells infected with this same virus. We further show that primary CTL derived from naïve precursors have superior cytolytic activity when compared with the endogenous, *ex vivo* response, thus showing that our

method of *in vitro* priming significantly enhanced the CTL response against the autologous reservoir.

A major issue in HIV-1 immunotherapy approaches is which subset or subsets of T cells should be targeted for enhancement of antiviral activity by the HIV-1 antigen-loaded DC. We propose that DC immunotherapy should target naïve T cell precursors in order to prime CTL *de novo*, and avoid or even inhibit activation of the existing, dysfunctional memory T cell population in an effort to revitalize their CTL function. We have previously proposed that CTL should be primed from naïve precursors, as the endogenous memory T cell population has already failed to control virus prior to cART (280). This is problematic, however, as studies have revealed decreases in the prevalence and function of naïve T cells following HIV-1 infection compared to uninfected controls (17, 91, 145, 364). Failure of naïve T cells from subjects on cART to respond to neo-antigens has also been reported (178). Perturbations in naïve T cells have been acknowledged as a potential mechanism by which CTL fail to control virus (178), as narrowing of the T cell receptor (TCR) repertoire decreases the number of unique antigens to which T cells can respond and therefore reduces the likelihood of generating a primary response to HIV-1 variants *in vivo* (120, 127).

Prior to this study, it was unclear if naïve CD8<sup>+</sup> T cells in these individuals were sufficiently restored in function and repertoire to respond to primary stimulation against the highly mutated HIV-1 reservoir. We show here that naïve CD8<sup>+</sup> T cells from subjects on cART can be primed to HIV-1 derived from the autologous reservoir and recognize a broad array of autologous Gag antigens. Primary IFN $\gamma$  production by these cells was also associated with enhanced cytolytic effector function against CD4<sup>+</sup> T cells infected with the autologous virus. We recognize that our study does not compare naïve T cell function in HIV-1 negative donors and acknowledge that a

disparity may still exist in the function of naïve T cells in HIV-1-infected subjects. However, our data show that even if the function and repertoire of naïve CD8<sup>+</sup> T cells is perturbed in subjects on cART, it is still sufficient to respond to and eradicate autologous virus. Additionally, our *in vitro* findings should be interpreted with caution and are not necessarily indicative of immunotherapy success *in vivo*. Our results merely show that naïve CD8<sup>+</sup> T cells, in a controlled environment, have the repertoire and function that is required to respond to a primary HIV-1-specific stimulation.

We have recently shown that cross-reactive CD8<sup>+</sup> T cells that secrete proinflammatory cytokines in response to HIV-1 epitope variants do not have a cytolytic effector function and in fact induce maturation of bystander DC, which then promote HIV-1 dissemination (chapter 5 above) (217). It was from these findings that we decided to evaluate the effects of a potential DC immunotherapy on the memory CD8 population and compare how this response was altered from the one that was generated during HIV-1 infection. Because a DC immunotherapy implemented on memory CD8<sup>+</sup> T cells is not “priming”, we labeled this process a “secondary” stimulation. We initially hypothesized that secondary CD8<sup>+</sup> T cells would exhibit some level of CTL activity against infected CD4<sup>+</sup> T cells, albeit at a predicted lower efficacy than the killing observed in CTL derived from naïve precursors. Because the residual CD8<sup>+</sup> T cell responses were likely specific for the autologous contemporaneous reservoir or the virus that was in circulation immediately prior to cART, we believed a reinvigoration of this response would be efficacious at inducing CTL effector function. Since these CD8<sup>+</sup> T cells were likely specific for the virus with which we were using in our secondary stimulation, there was no reason to suspect we would observe the negative effects of cross-reactive T cell responses. Following DC secondary stimulation, these cells secreted high levels of IFN $\gamma$  in response to a portion of the autologous Gag 18mers. While not all

regions of Gag were recognized by secondary CD8<sup>+</sup> T cells, some induced relatively robust responses that were greater than 4,000 SFC/10<sup>6</sup>. To our surprise, secondary stimulation resulted in CTL activity that was largely indistinguishable from the killing observed *ex vivo*, suggesting a DC immunotherapy may not enhance the cytolytic capacity of memory T cells but may instead result in a population of CD8<sup>+</sup> T cells with limited breadth but high IFN $\gamma$  secreting potential and limited CTL function.

Cytokine secretion in the absence of CTL killing is not a new phenomenon. Loffredo *et al.* showed that IFN $\gamma$  and TNF $\alpha$  production by CD8<sup>+</sup> T cells in response to HIV-1 epitope variants was detectable at higher concentrations of peptide antigen, yet was not associated with elimination of target cells expressing the escape variant (208). Another study demonstrated that escape variant-specific T cell responses identified in ELISpot assays failed to predict CD8<sup>+</sup> T cell recognition of cells infected with the variant virus (330). Studies in the nonhuman primate model have shown that cytokine-producing cells vary greatly in their ability to suppress SIV replication (63), thus further highlighting the possibility that a single correlate of viral control may not exist, and that an anti-HIV-1 CTL response may be composed of a multitude of factors (339).

These findings are somewhat contrasting to those reported by Shan *et al.*, which showed peptide stimulation of recall CD8<sup>+</sup> T cells facilitates elimination of the viral reservoir (306). These findings would suggest that recall CD8<sup>+</sup> T cells are capable of being revitalized to recognize and kill infected cells. However, this protocol used a 6 day peptide stimulation, which is not comparable to our potent 21-day DC stimulation method and does not support the longevity of the CTL response. The results of *in vitro* peptide stimulation are not comparable to those that would be induced *in vivo*, as a peptide vaccine would be readily processed and presented by an antigen-presenting cell, such as a DC, before encountering a T cell. This could then lead to the inability



to eradicate the HIV-1 reservoir that we describe here. Additionally, this study evaluated HIV-1 elimination over the course of 8 days, whereas we report potent CTL activity after 18 hours, suggesting DC stimulation may be more effective at inducing a robust anti-HIV-1 response.

The present study, while novel, includes a small number of subjects and the findings of which should therefore be applied with caution. While we anticipate that our findings will hold true in most subjects on cART, further work must be completed to determine the generalizability of our conclusions. Future work should increase the number of subjects to determine if our findings represent a generalized phenomenon across HLA types and different patterns of disease progression. Additionally, subjects who received cART early after becoming infected with HIV-1 may respond to primary DC stimulation with more success than those who received cART after chronic infection. These are all factors that should be addressed in continuing work. Nonetheless, this study provides novel insight into the residual function of naïve CD8<sup>+</sup> T cells in HIV-1-infected subjects on cART and supports further research evaluating the efficacy of DC immunotherapies.

## **6.5 ACKNOWLEDGEMENTS**

We thank Dr. Robbie Mailliard for help with technical and experimental planning, Dr. Phalguni Gupta and his laboratory, particularly Deena Ratner, for help designing and executing autologous virus assays, Dr. Jim Mullins and his laboratory, particularly Kim Wong and Brendan Larsen for performing sequencing on patient-derived virus, Dr. John Mellors for access to his Taqman® assay, Kelly Gordon for technical assistance, and the volunteers of the Pittsburgh site of the Multicenter AIDS Cohort Study. This work was supported in part by NIH grants R01-AI-40388, R37-AI-41870, U01-AI-35041 and T32-AI065380.

## 7.0 DISCUSSION AND SUMMARY

CTL are a vital component in the immunological response to HIV-1 infection (42, 189, 254, 299). Mutational escape in CTL epitopes contributes to viral persistence and the eventual progression to AIDS (58, 165). Broad and high magnitude CTL responses have been detected in subjects who control infection without cART, and declining CTL responses have been reported in subjects who progress (19, 83) (24). An underlying issue is that no clear correlate of CTL efficacy exists. Longitudinal studies describing HIV-1-specific CTL responses typically used consensus peptide epitopes to stimulate PBMC, thereby ignoring autologous differences in epitope composition and the role of the APC in stimulating recall T cell responses. Accurately assessing these recall responses is paramount in the development of immunotherapies that aim to enhance the breadth and magnitude of the endogenous response.

CTL failure in chronic infection can be attributed to a combination of several factors, including mutational escape, increases in regulatory mechanisms, and T cell exhaustion. Although partial immune restoration occurs during cART, residual CTL primed before cART still exist. Due to low antigenic stimulation, it is likely that new CTL are not generated under this reconstituted immune system. Curative approaches for HIV-1-infected subjects on cART have therefore focused on generating new CTL from naïve precursors or reinvigorating dysfunctional CTL with a potent APC. DC, the most potent APC, are the most promising tool for generating robust anti-HIV-1 CTL. Despite this, perturbations in the naïve T cell repertoire following chronic HIV-1 infection have left many to hypothesize that naïve T cells in subjects on cART are not capable of recognizing or responding to the autologous virus. Additionally, recall T cells have been shown to be

detrimental if stimulated with HIV-1 epitope variants and could therefore do more harm than good in the context of a DC immunotherapy.

My work has provided valuable, novel insight into the immune responses generated to autologous HIV-1 in chronic infection and in the methods of detecting and stimulating antigen-specific T cell responses. In initial studies, I identified clinical correlates of HIV-1 evolution and identified signatures of positive selection in CTL epitopes in HIV-1-infected subjects. Sites under positive selection accumulated at an equal rate in *gag* and *env*, hence we can conclude that the driving force for adaptive selection was acting uniformly on both genes. Notably, the number of codons under positive and negative selection did not differ between *gag* and *env*, suggesting the high divergence and diversity observed in *env* was not due to increased selective pressures but was potentially due to higher rates of random polymerase errors. This furthermore shows that adaptive selection was equally targeted against the two proteins in spite of significant differences in genetic evolution. Our observation that positive selection was not specific to CTL epitopes shows an efficient epitope-specific response was not generated during natural HIV-1 infection. Of note, we did not observe amino acid changes within all of the known CTL epitopes. It is plausible that mutations within these epitopes were detrimental to viral fitness, but there was no evidence for compensatory mutations within or near any of the known CTL epitopes. Of course, these analyses are limited to the number of known epitopes for the HLA alleles found within our study subjects. Positive selection could have occurred in unidentified epitopes, and in fact it is likely that unidentified epitopes would have high rates of positive selection imposed on them.

I then used the findings from our *gag* and *env* sequence analysis to evaluate CD8<sup>+</sup> T cell responses to autologous variants of known and predicted HLA A\*2402-restricted epitopes. We identified several novel potential epitopes by using epitope prediction algorithms and generated a

peptide library consisting of known and predicted epitopes and their variants that evolved in each subject. We wanted to identify the effects of chronic HIV-1 infection on CD8<sup>+</sup> T cell responses to these variants. IFN $\gamma$  ELISpot assays showed that recall T cell responses to autologous epitope variants were detected at all stages of HIV-1 infection. Importantly, our findings show for the first time that primary CD8<sup>+</sup> T cell responses are generated *in vivo* to autologous virus and that they respond with the same breadth and magnitude to variants that evolved early or late post-seroconversion, suggesting these cells have the ability to respond to mutated “escape” variants.

We are not making the claim that our detection of cytokine secretion is indicative of CTL activity, but we are concluding that a primary response to these epitope variants was generated *in vivo*, although this response was likely of variable efficacy, as disease progression continued and many of the epitope variants persisted throughout infection. This CTL failure was likely due to insufficient antigen presentation or regulatory mechanisms that impeded their CTL effector function. We therefore evaluated the role of DC and T<sub>reg</sub> on antigen-specific responses. Mature, autologous DC revealed broad and robust CD8<sup>+</sup> T cell responses to autologous HIV-1 epitope variants regardless of disease progression, whereas the effects of T<sub>reg</sub> depletion were moderate at best. While we are not discounting the role of T<sub>reg</sub> in progressive HIV-1 infection, our data would suggest that antigen-loaded DC readily overcome any suppressive effect imposed by T<sub>reg</sub>. Nonetheless, these findings provide an in-depth understanding of the breadth of T cell responses that are generated to autologous HIV-1 antigens. Future studies should focus on the changes in cytolytic effector function against a select number of epitope variants throughout HIV-1 infection and should expand the study to include more subjects with a wide array of HLA alleles.

These longitudinal findings are primarily of academic interest and have minimal, if any, implications in DC-based immunotherapeutic approaches. We therefore evaluated the cytokine

secretion profiles of CD8<sup>+</sup> T cells stimulated with autologous epitope variants in the presence or absence of DC. We have previously shown that DC reveal polyfunctional responses specific for consensus MHC class I epitopes in subjects on cART (155), but studies have yet to evaluate how DC affect responses to autologous epitope variants. We observed a temporal increase in the ability of DC to reveal bifunctional and polyfunctional CD8<sup>+</sup> T cell responses with implementation of cART. These findings show that as subjects regain their health and immune function subsequent to decreases in viral load, DC are more capable of enhancing responses that are associated with CTL effector function. These findings support the function and potential therapeutic efficacy of a DC immunotherapy aimed at reviving the quiescent CTL response in subjects on cART. As our study evaluated a large number of peptide epitopes, it was impractical to assess CTL killing against each one. Future studies should determine if the enhanced cytokine profile observed with DC stimulation is associated with CTL elimination of target cells expressing the relevant antigen, and if differences in avidity exist between epitope variants.

Our next goal was to determine if HIV-1 infection permanently inhibited the generation of T cells that targeted late epitope variants. This is important for immunotherapeutic vaccines that aim to generate primary T cell responses against a late, reservoir virus. We have previously demonstrated the potent capability of mature monocyte-derived DC from uninfected donors to induce a broad spectrum of primary CD8<sup>+</sup> T cell responses targeting epitopes in Gag, Env, and Nef (67). In the present work, we showed that DC priming of PBMC obtained prior to seroconversion induced T cells that recognized autologous HIV-1 epitope variants that evolved after the subject became infected, specifically those variants evolving late post-seroconversion. That is, the naïve T cell repertoire found within subject 8 before infection and immune dysfunction was capable of recognizing and responding to primary stimulation against the variants that evolved

after seroconversion. It can therefore be assumed that the variants that evolved in this subject did not evolve to evade TCR or MHC recognition. This obviously would have implications in immunotherapy approaches, which aim to induce primary responses against these “late evolving” viral variants. Even though cART has been successful at controlling HIV-1 viral load, immune recovery is still a challenge (72). Our model suggests by-passing this obstacle by using DC to generate primary CTL *in vivo* while subjects are under suppressive cART (280). These observations suggest therapies implicated during cART, when immune restoration has occurred, may be successful at inducing CTL specific for autologous viral variants.

We then focused our work on the effects of DC stimulation on primary and recall CTL responses. We explored the notion that incomplete immune escape from sub-optimal CTL responses could provide an advantage for the pathogen. Using an *in vitro* DC-based CTL priming system, we show that evolutionary changes in CTL epitopes can induce a helper function in cross-reactive CTL to promote a dysfunctional interaction with HIV-1 antigen-expressing DC. These CTL do not exert their cytolytic function and instead promote DC maturation and HIV-1 dissemination. We propose that the virus partially evades CTL recognition to allow an ineffective CTL response to persist, thus allowing viral persistence in the absence of CTL elimination. The proposed benefit of HIV-1 to selectively induce such a host response suggests there could be an enrichment of certain epitope variants that promote CTL helper activity in the absence of effector function rather than completely evade CTL recognition. These findings could explain why robust T cell responses are detected to HIV-1 epitope variants that continue to persist in chronic infection. For example, T cell responses to the immunodominant HLA A\*0201-restricted SLYNTVATL (Gag p17<sub>77-85</sub>) epitope are readily detected on chronic infection, but fail to exert selective pressure

(45, 46, 129, 160). Perhaps the evolution of certain epitope variants is a form of “incomplete” immune escape and generates an immunological environment that is suitable for viral spread.

Based on the above findings, we hypothesized that a DC immunotherapy implemented during cART may be detrimental to the existing recall T cells, whereas it would be efficacious at inducing primary CTL responses from naïve precursors. We therefore developed an *in vitro* model of DC immunotherapy targeting the HIV-1 reservoir to evaluate the impact of this potent stimulation on naïve and memory T cells obtained from subjects on cART. For the first time, we show that naïve CD8<sup>+</sup> T cells from these subjects can be induced to recognize the autologous reservoir and are capable of exerting effector CTL function on CD4<sup>+</sup> T cells infected with this same virus. We further show that memory T cells exposed to this same stimulation exert an effector function that is indistinguishable from the response that was generated *in vivo*, indicating DC stimulation had no effect on this population of T cells. Importantly, we did observe IFN $\gamma$  production in response to several autologous Gag antigens, further supporting our previous findings that cytokine secretion is not necessarily indicative of CTL function.

Prior to this study, it was unclear if naïve CD8<sup>+</sup> T cells in these individuals were sufficiently restored in function and repertoire to respond to primary stimulation against the highly mutated HIV-1 reservoir. Primary CTL derived from naïve precursors had superior cytolytic activity when compared with the endogenous, *ex vivo* response and the secondary response, thus showing that our method of *in vitro* priming significantly enhanced the potential for viral eradication. These findings are somewhat contrasting to previous reports suggesting naïve T cells from subjects on cART were impaired in their ability to respond to neoantigens. Lange et. al. and Gelinck et. al. reported impaired primary responses to vaccinations in subjects on cART (122, 197), but also evaluated antibody responses mediated primarily by CD4<sup>+</sup> T cells. Dysfunctional naïve CD4<sup>+</sup> T

cells may exist in subjects on cART, but immunotherapies for these subjects that induce a CD8<sup>+</sup> T cell-mediated response would only require CD4<sup>+</sup> T cell functionality for bystander “help” (31, 44, 279, 301, 327, 328). Because of this, results from vaccines that aim to induce antibody-mediated immune responses in HIV-1-infected patients should be interpreted with caution when applying them to analyses of potential CTL-mediated immunotherapy efficacy. In addition, studies of primary immunity in HIV-1-infected subjects on cART typically compare responses to those observed in age-matched, uninfected controls. The *de novo* response generated in an HIV-1-infected person on cART may not be equivalent to that which is generated in an uninfected person, but it may be sufficient for viral clearance. Nonetheless, we show here that DC stimulation of naïve T cells may be more effective at inducing potent anti-HIV-1 CTL than DC stimulation of memory T cells. In addition, memory T cells stimulated with variants of their cognate antigen not only secreted proinflammatory cytokines in the absence of CTL effector function, but also promoted viral dissemination by DC, suggesting a DC immunotherapy may actually be detrimental to our efforts of HIV-1 eradication. Our proposed hypothesis is shown in **Figure 56**.



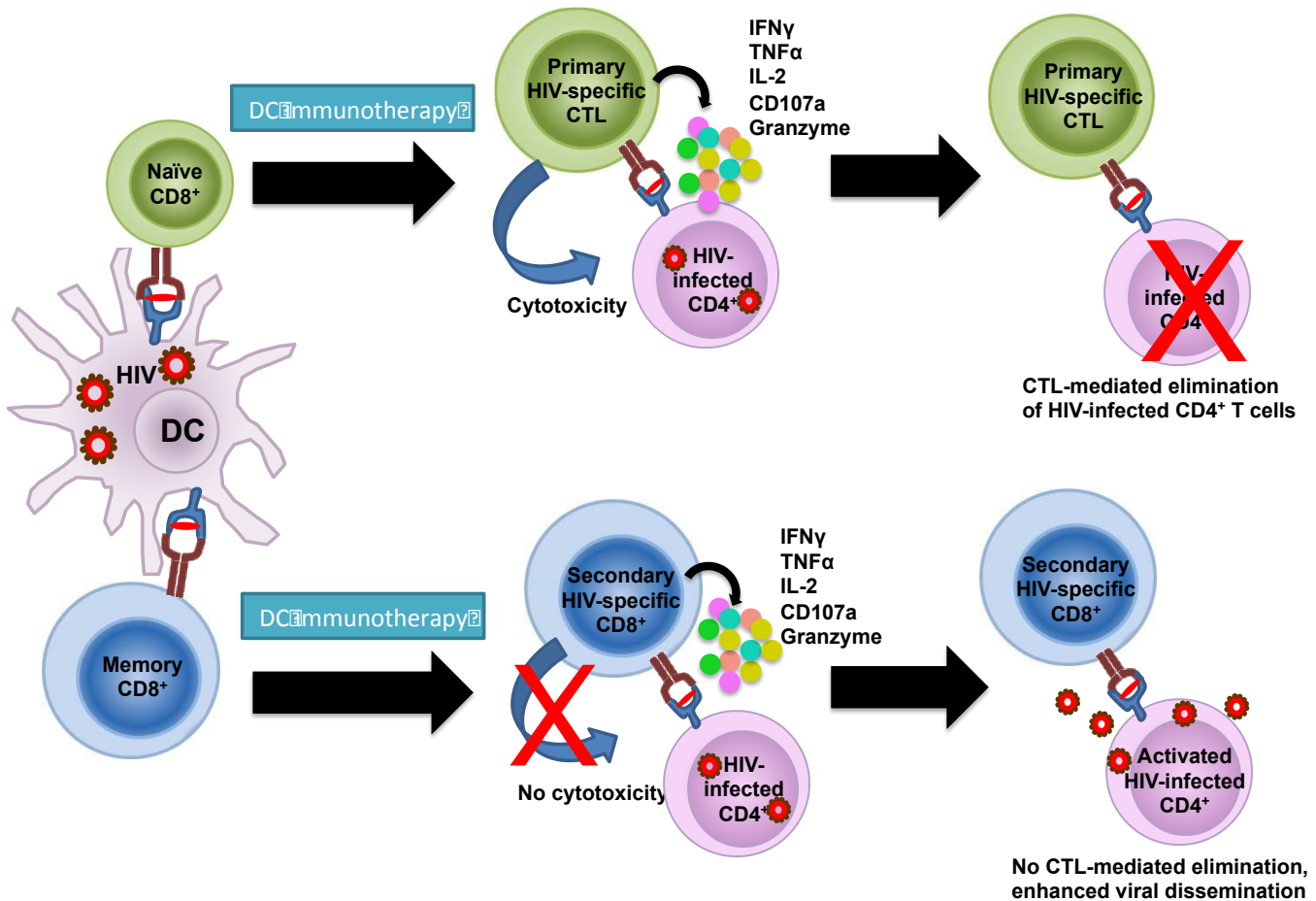


**Figure 56. Proposed effects of DC immunotherapy on naïve and memory CD8<sup>+</sup> T cells in HIV-1-infected subjects on cART**

DC stimulation of naïve CD8<sup>+</sup> T cells induces primary CTL that secrete proinflammatory cytokines and eliminate infected CD4<sup>+</sup> T cells. Secondary DC stimulation of memory CD8<sup>+</sup> T cells results in cytokine secretion without CTL effector function and promotes viral dissemination.

While our findings are significant and unprecedented, they represent an in-depth analysis of a limited number of patients. To further prove that the naïve repertoire in subjects on cART is capable of responding to DC-based priming against the HIV-1 reservoir, this study must be expanded to include more subjects with varying HLA phenotypes and atypical patterns of disease progression. Additionally, the time after infection at which the subjects received cART could impact the success of their response to neoantigens, as delayed initiation of cART negatively

affects immune restoration (341). Future studies should also evaluate the longitudinal changes in the TCR repertoire to determine how chronic HIV-1 infection affects the number and type of antigens that can be recognized by naïve T cells. Even if the repertoire is severely narrowed following infection and even during cART, we believe it will be sufficient to respond to primary stimulation against the HIV-1 reservoir if a potent DC is used.

In conclusion, the work presented within this dissertation utilized a completely autologous system to dissect the immune responses that are generated during natural HIV-1 infection and those that could be induced using an immunotherapy. We have provided novel insight into the ability of CD8<sup>+</sup> T cells to recognize, respond to, and eliminate autologous virus even after many years of untreated and treated infection. If successful, DC immunotherapies for HIV-1-infected persons on cART could eradicate the virus or allow these individuals to live disease-free in the absence of drug therapy. Such a treatment would have vast implications in the global health arena and would vastly improve the quality of life for those living with HIV-1.

## APPENDIX A

### LIST OF ABBREVIATIONS

AIDS	Acquired Immunodeficiency Syndrome
ANOVA	Analysis of Variance
APC	Antigen Presenting Cell
cART	Combination Antiretroviral Therapy
CD40L	CD40 ligand
CTL	Cytotoxic T Lymphocyte
DC	Dendritic Cell
ELISA	Enzyme-linked Immunosorbent Assay
ELISpot	Enzyme Linked Immunospot
E:T	Effector to Target ratio
FEL	Fixed Effects Likelihood
GM-CSF	Granulocyte Macrophage Colony Stimulating Factor
GTR	General Time-Reversible
HIV-1	Human Immunodeficiency Virus Type-1
HLA	Human Leukocyte Antigen
IC <sub>50</sub>	Inhibitory Concentration 50%
ICS	Intracellular Cytokine Staining
iDC	Immature Dendritic Cell

IFN $\gamma$	Interferon gamma
MACS	Multicenter AIDS Cohort Study
MHC	Major Histocompatibility Complex
MIP-1 $\beta$	Macrophage inflammatory protein-1beta
mRNA	Messenger Ribonucleic Acid
PBL	Peripheral Blood Lymphocytes
PBMC	Peripheral Blood Mononuclear Cells
PCR	Polymerase Chain Reaction
PolyI:C	Poly inosinic acid + cytidylic acid
PD-1	Programmed Death-1
RNA	Ribonucleic Acid
TCR	T Cell Receptor
TNF $\alpha$	Tumor Necrosis Factor alpha

APPENDIX B

SUPPLEMENTAL FIGURES

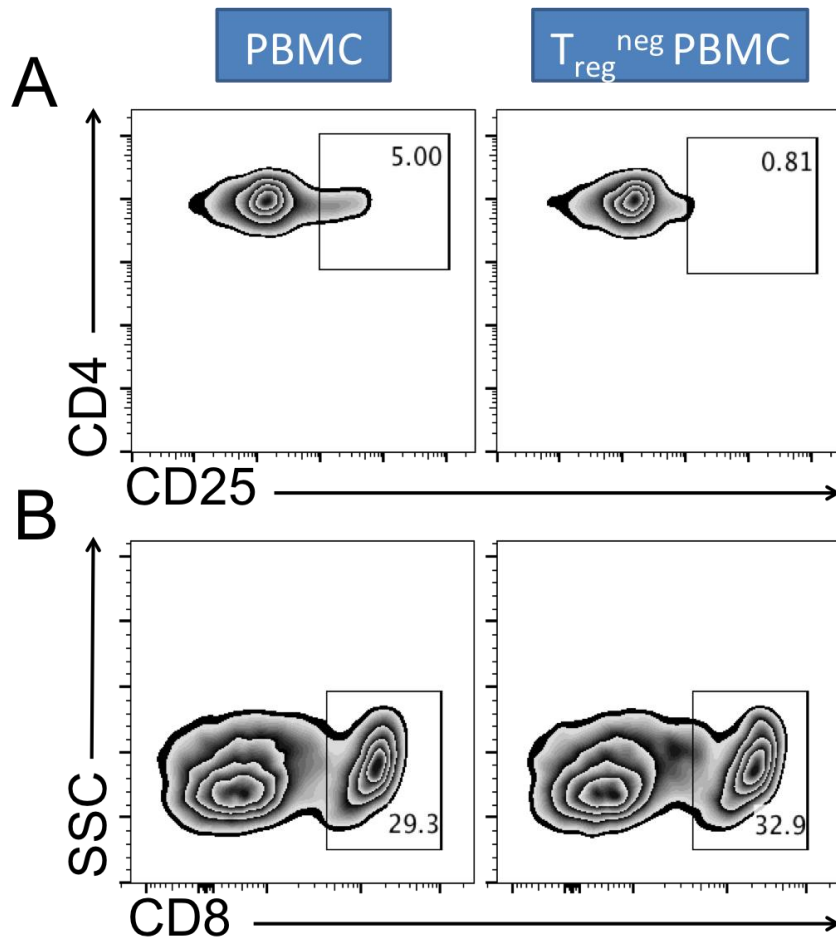


**Figure 57. Effects of T<sub>reg</sub> depletion on remaining T cell populations**  
PBMC were stained for T cell and T<sub>reg</sub> markers before or after depletion of CD4<sup>+</sup>CD25<sup>+</sup> cells by dual process magnetic bead separation. (A) The efficiency of the T<sub>reg</sub> depletion kit on removing CD4<sup>+</sup>CD25<sup>+</sup> T cells from PBMC populations. (B) The effect of T<sub>reg</sub> depletion on the frequency of CD8<sup>+</sup> T cells.

## BIBLIOGRAPHY

1. 2006. Epidemiology of HIV/AIDS--United States, 1981-2005. *MMWR Morb Mortal Wkly Rep* **55**:589-592.
2. **Abrahams, M. R., J. A. Anderson, E. E. Giorgi, C. Seoighe, K. Mlisana, L. H. Ping, G. S. Athreya, F. K. Treurnicht, B. F. Keele, N. Wood, J. F. Salazar-Gonzalez, T. Bhattacharya, H. Chu, I. Hoffman, S. Galvin, C. Mapanje, P. Kazembe, R. Thebus, S. Fiscus, W. Hide, M. S. Cohen, S. A. Karim, B. F. Haynes, G. M. Shaw, B. H. Hahn, B. T. Korber, R. Swanstrom, and C. Williamson.** 2009. Quantitating the multiplicity of infection with human immunodeficiency virus type 1 subtype C reveals a non-poisson distribution of transmitted variants. *Journal of virology* **83**:3556-3567.
3. **Addo, M. M., X. G. Yu, A. Rathod, D. Cohen, R. L. Eldridge, D. Strick, M. N. Johnston, C. Corcoran, A. G. Wurcel, C. A. Fitzpatrick, M. E. Feeney, W. R. Rodriguez, N. Basgoz, R. Draenert, D. R. Stone, C. Brander, P. J. Goulder, E. S. Rosenberg, M. Altfeld, and B. D. Walker.** 2003. Comprehensive epitope analysis of human immunodeficiency virus type 1 (HIV-1)-specific T-cell responses directed against the entire expressed HIV-1 genome demonstrate broadly directed responses, but no correlation to viral load. *Journal of virology* **77**:2081-2092.
4. **Ahlers, J. D., T. Takeshita, C. D. Pendleton, and J. A. Berzofsky.** 1997. Enhanced immunogenicity of HIV-1 vaccine construct by modification of the native peptide sequence. *Proceedings of the National Academy of Sciences of the United States of America* **94**:10856-10861.
5. **Allard, S. D., B. De Keersmaecker, A. L. de Goede, E. J. Verschuren, J. Koetsveld, M. L. Reedijk, C. Wylock, A. V. De Bel, J. Vandelloo, F. Pistor, C. Heirman, W. E. Beyer, P. H. Eilers, J. Corthals, I. Padmos, K. Thielemans, A. D. Osterhaus, P. Lacor, M. E. van der Ende, J. L. Aerts, C. A. van Baalen, and R. A. Gruters.** 2012. A phase I/IIa immunotherapy trial of HIV-1-infected patients with Tat, Rev and Nef expressing dendritic cells followed by treatment interruption. *Clin Immunol* **142**:252-268.
6. **Allen, T. M., M. Altfeld, S. C. Geer, E. T. Kalife, C. Moore, M. O'Sullivan K, I. Desouza, M. E. Feeney, R. L. Eldridge, E. L. Maier, D. E. Kaufmann, M. P. Lahaie, L. Reyor, G. Tanzi, M. N. Johnston, C. Brander, R. Draenert, J. K. Rockstroh, H. Jessen, E. S. Rosenberg, S. A. Mallal, and B. D. Walker.** 2005. Selective escape from CD8+ T-cell responses represents a major driving force of human immunodeficiency virus type 1 (HIV-1) sequence diversity and reveals constraints on HIV-1 evolution. *Journal of virology* **79**:13239-13249.
7. **Allen, T. M., M. Altfeld, X. G. Yu, K. M. O'Sullivan, M. Lichterfeld, S. Le Gall, M. John, B. R. Mothe, P. K. Lee, E. T. Kalife, D. E. Cohen, K. A. Freedberg, D. A. Strick, M. N. Johnston, A. Sette, E. S. Rosenberg, S. A. Mallal, P. J. Goulder, C. Brander, and B. D. Walker.** 2004. Selection, transmission, and reversion of an antigen-processing cytotoxic T-lymphocyte escape mutation in human immunodeficiency virus type 1 infection. *Journal of virology* **78**:7069-7078.
8. **Allen, T. M., P. Jing, B. Calore, H. Horton, D. H. O'Connor, T. Hanke, M. Piekarczyk, R. Ruddersdorf, B. R. Mothe, C. Emerson, N. Wilson, J. D. Lifson, I. M. Belyakov, J.**

- A. Berzofsky, C. Wang, D. B. Allison, D. C. Montefiori, R. C. Desrosiers, S. Wolinsky, K. J. Kunstman, J. D. Altman, A. Sette, A. J. McMichael, and D. I. Watkins.** 2002. Effects of cytotoxic T lymphocytes (CTL) directed against a single simian immunodeficiency virus (SIV) Gag CTL epitope on the course of SIVmac239 infection. *Journal of virology* **76**:10507-10511.
9. **Allen, T. M., D. H. O'Connor, P. Jing, J. L. Dzuris, B. R. Mothe, T. U. Vogel, E. Dunphy, M. E. Liebl, C. Emerson, N. Wilson, K. J. Kunstman, X. Wang, D. B. Allison, A. L. Hughes, R. C. Desrosiers, J. D. Altman, S. M. Wolinsky, A. Sette, and D. I. Watkins.** 2000. Tat-specific cytotoxic T lymphocytes select for SIV escape variants during resolution of primary viraemia. *Nature* **407**:386-390.
  10. **Allen, T. M., X. G. Yu, E. T. Kalife, L. L. Reyor, M. Lichterfeld, M. John, M. Cheng, R. L. Allgaier, S. Mui, N. Frahm, G. Alter, N. V. Brown, M. N. Johnston, E. S. Rosenberg, S. A. Mallal, C. Brander, B. D. Walker, and M. Altfeld.** 2005. De novo generation of escape variant-specific CD8+ T-cell responses following cytotoxic T-lymphocyte escape in chronic human immunodeficiency virus type 1 infection. *Journal of virology* **79**:12952-12960.
  11. **Almeida, J. R., D. A. Price, L. Papagno, Z. A. Arkoub, D. Sauce, E. Bornstein, T. E. Asher, A. Samri, A. Schnuriger, I. Theodorou, D. Costagliola, C. Rouzioux, H. Agut, A. G. Marcelin, D. Douek, B. Autran, and V. Appay.** 2007. Superior control of HIV-1 replication by CD8+ T cells is reflected by their avidity, polyfunctionality, and clonal turnover. *The Journal of experimental medicine* **204**:2473-2485.
  12. **Almeida, J. R., D. Sauce, D. A. Price, L. Papagno, S. Y. Shin, A. Moris, M. Larsen, G. Pancino, D. C. Douek, B. Autran, A. Saez-Cirion, and V. Appay.** 2009. Antigen sensitivity is a major determinant of CD8+ T-cell polyfunctionality and HIV-suppressive activity. *Blood* **113**:6351-6360.
  13. **Anderson, J. A., N. M. Archin, W. Ince, D. Parker, A. Wiegand, J. M. Coffin, J. Kuruc, J. Eron, R. Swanstrom, and D. M. Margolis.** 2011. Clonal sequences recovered from plasma from patients with residual HIV-1 viremia and on intensified antiretroviral therapy are identical to replicating viral RNAs recovered from circulating resting CD4+ T cells. *Journal of virology* **85**:5220-5223.
  14. **Angin, M., D. S. Kwon, H. Streeck, F. Wen, M. King, A. Rezai, K. Law, T. C. Hongo, A. Pyo, A. Piechocka-Trocha, I. Toth, F. Pereyra, M. Ghebremichael, S. J. Rodig, D. A. Milner, Jr., J. M. Richter, M. Altfeld, D. E. Kaufmann, B. D. Walker, and M. M. Addo.** 2012. Preserved function of regulatory T cells in chronic HIV-1 infection despite decreased numbers in blood and tissue. *The Journal of infectious diseases* **205**:1495-1500.
  15. **Appay, V., D. C. Douek, and D. A. Price.** 2008. CD8+ T cell efficacy in vaccination and disease. *Nature medicine* **14**:623-628.
  16. **Artimo, P., M. Jonnalagedda, K. Arnold, D. Baratin, G. Csardi, E. de Castro, S. Duvaud, V. Flegel, A. Fortier, E. Gasteiger, A. Grosdidier, C. Hernandez, V. Ioannidis, D. Kuznetsov, R. Liechti, S. Moretti, K. Mostaguir, N. Redaschi, G. Rossier, I. Xenarios, and H. Stockinger.** 2012. ExPASy: SIB bioinformatics resource portal. *Nucleic Acids Res* **40**:W597-603.
  17. **Autran, B., G. Carcelain, T. S. Li, C. Blanc, D. Mathez, R. Tubiana, C. Katlama, P. Debre, and J. Leibowitch.** 1997. Positive effects of combined antiretroviral therapy on CD4+ T cell homeostasis and function in advanced HIV disease. *Science* **277**:112-116.

18. **Autran, B., G. Carcelain, T. S. Li, G. Gorochov, C. Blanc, M. Renaud, M. Durali, D. Mathez, V. Calvez, J. Leibowitch, C. Katlama, and P. Debre.** 1999. Restoration of the immune system with anti-retroviral therapy. *Immunology letters* **66**:207-211.
19. **Baker, B. M., B. L. Block, A. C. Rothchild, and B. D. Walker.** 2009. Elite control of HIV infection: implications for vaccine design. *Expert Opin Biol Ther* **9**:55-69.
20. **Balachandran, R., P. Thampatty, A. Enrico, C. Rinaldo, and P. Gupta.** 1991. Human immunodeficiency virus isolates from asymptomatic homosexual men and from AIDS patients have distinct biologic and genetic properties. *Virology* **180**:229-238.
21. **Bandera, A., G. Ferrario, M. Saresella, I. Marventano, A. Soria, F. Zanini, F. Sabbatini, M. Airoidi, G. Marchetti, F. Franzetti, D. Trabattoni, M. Clerici, and A. Gori.** 2010. CD4+ T cell depletion, immune activation and increased production of regulatory T cells in the thymus of HIV-infected individuals. *PloS one* **5**:e10788.
22. **Bangham, C. R.** 2009. CTL quality and the control of human retroviral infections. *European journal of immunology* **39**:1700-1712.
23. **Bar, K. J., H. Li, A. Chamberland, C. Tremblay, J. P. Routy, T. Grayson, C. Sun, S. Wang, G. H. Learn, C. J. Morgan, J. E. Schumacher, B. F. Haynes, B. F. Keele, B. H. Hahn, and G. M. Shaw.** 2010. Wide variation in the multiplicity of HIV-1 infection among injection drug users. *Journal of virology* **84**:6241-6247.
24. **Barker, E., C. E. Mackewicz, G. Reyes-Teran, A. Sato, S. A. Stranford, S. H. Fujimura, C. Christopherson, S. Y. Chang, and J. A. Levy.** 1998. Virological and immunological features of long-term human immunodeficiency virus-infected individuals who have remained asymptomatic compared with those who have progressed to acquired immunodeficiency syndrome. *Blood* **92**:3105-3114.
25. **Barouch, D. H., and B. Korber.** 2010. HIV-1 vaccine development after STEP. *Annu Rev Med* **61**:153-167.
26. **Barouch, D. H., J. Kunstman, M. J. Kuroda, J. E. Schmitz, S. Santra, F. W. Peyerl, G. R. Krivulka, K. Beaudry, M. A. Lifton, D. A. Gorgone, D. C. Montefiori, M. G. Lewis, S. M. Wolinsky, and N. L. Letvin.** 2002. Eventual AIDS vaccine failure in a rhesus monkey by viral escape from cytotoxic T lymphocytes. *Nature* **415**:335-339.
27. **Barouch, D. H., P. F. McKay, S. M. Sumida, S. Santra, S. S. Jackson, D. A. Gorgone, M. A. Lifton, B. K. Chakrabarti, L. Xu, G. J. Nabel, and N. L. Letvin.** 2003. Plasmid chemokines and colony-stimulating factors enhance the immunogenicity of DNA priming-viral vector boosting human immunodeficiency virus type 1 vaccines. *Journal of virology* **77**:8729-8735.
28. **Battegay, M., R. Nuesch, B. Hirschel, and G. R. Kaufmann.** 2006. Immunological recovery and antiretroviral therapy in HIV-1 infection. *Lancet Infect Dis* **6**:280-287.
29. **Baum, P. D., J. J. Young, D. Schmidt, Q. Zhang, R. Hoh, M. Busch, J. Martin, S. Deeks, and J. M. McCune.** 2012. Blood T-cell receptor diversity decreases during the course of HIV infection, but the potential for a diverse repertoire persists. *Blood* **119**:3469-3477.
30. **Bazykin, G. A., J. Dushoff, S. A. Levin, and A. S. Kondrashov.** 2006. Bursts of nonsynonymous substitutions in HIV-1 evolution reveal instances of positive selection at conservative protein sites. *Proceedings of the National Academy of Sciences of the United States of America* **103**:19396-19401.



31. **Bennett, S. R., F. R. Carbone, F. Karamalis, R. A. Flavell, J. F. Miller, and W. R. Heath.** 1998. Help for cytotoxic-T-cell responses is mediated by CD40 signalling. *Nature* **393**:478-480.
32. **Berger, C. T., N. Frahm, D. A. Price, B. Mothe, M. Ghebremichael, K. L. Hartman, L. M. Henry, J. M. Brenchley, L. E. Ruff, V. Venturi, F. Pereyra, J. Sidney, A. Sette, D. C. Douek, B. D. Walker, D. E. Kaufmann, and C. Brander.** High-functional-avidity cytotoxic T lymphocyte responses to HLA-B-restricted Gag-derived epitopes associated with relative HIV control. *Journal of virology* **85**:9334-9345.
33. **Berger, C. T., N. Frahm, D. A. Price, B. Mothe, M. Ghebremichael, K. L. Hartman, L. M. Henry, J. M. Brenchley, L. E. Ruff, V. Venturi, F. Pereyra, J. Sidney, A. Sette, D. C. Douek, B. D. Walker, D. E. Kaufmann, and C. Brander.** 2011. High-Functional-Avidity Cytotoxic T Lymphocyte Responses to HLA-B-Restricted Gag-Derived Epitopes Associated with Relative HIV Control. *Journal of virology* **85**:9334-9345.
34. **Bergmann, C. C., L. Tong, R. V. Cua, J. L. Sensintaffar, and S. A. Stohlman.** 1994. Cytotoxic T cell repertoire selection. A single amino acid determines alternative class I restriction. *J Immunol* **152**:5603-5612.
35. **Bernardin, F., D. Kong, L. Peddada, L. A. Baxter-Lowe, and E. Delwart.** 2005. Human immunodeficiency virus mutations during the first month of infection are preferentially found in known cytotoxic T-lymphocyte epitopes. *Journal of virology* **79**:11523-11528.
36. **Betts, M. R., and A. Harari.** 2008. Phenotype and function of protective T cell immune responses in HIV. *Current opinion in HIV and AIDS* **3**:349-355.
37. **Betts, M. R., M. C. Nason, S. M. West, S. C. De Rosa, S. A. Migueles, J. Abraham, M. M. Lederman, J. M. Benito, P. A. Goepfert, M. Connors, M. Roederer, and R. A. Koup.** 2006. HIV nonprogressors preferentially maintain highly functional HIV-specific CD8+ T cells. *Blood* **107**:4781-4789.
38. **Betts, M. R., D. A. Price, J. M. Brenchley, K. Lore, F. J. Guenaga, A. Smed-Sorensen, D. R. Ambrozak, S. A. Migueles, M. Connors, M. Roederer, D. C. Douek, and R. A. Koup.** 2004. The functional profile of primary human antiviral CD8+ T cell effector activity is dictated by cognate peptide concentration. *J Immunol* **172**:6407-6417.
39. **Bi, X., Y. Suzuki, H. Gatanaga, and S. Oka.** 2009. High frequency and proliferation of CD4+ FOXP3+ Treg in HIV-1-infected patients with low CD4 counts. *European journal of immunology* **39**:301-309.
40. **Bihl, F., N. Frahm, L. Di Giammarino, J. Sidney, M. John, K. Yusim, T. Woodberry, K. Sango, H. S. Hewitt, L. Henry, C. H. Linde, J. V. Chisholm, 3rd, T. M. Zaman, E. Pae, S. Mallal, B. D. Walker, A. Sette, B. T. Korber, D. Heckerman, and C. Brander.** 2006. Impact of HLA-B alleles, epitope binding affinity, functional avidity, and viral coinfection on the immunodominance of virus-specific CTL responses. *J Immunol* **176**:4094-4101.
41. **Boasso, A., G. M. Shearer, and C. Chougnet.** 2009. Immune dysregulation in human immunodeficiency virus infection: know it, fix it, prevent it? *J Intern Med* **265**:78-96.
42. **Borrow, P., H. Lewicki, B. H. Hahn, G. M. Shaw, and M. B. Oldstone.** 1994. Virus-specific CD8+ cytotoxic T-lymphocyte activity associated with control of viremia in primary human immunodeficiency virus type 1 infection. *Journal of virology* **68**:6103-6110.
43. **Borrow, P., H. Lewicki, X. Wei, M. S. Horwitz, N. Peffer, H. Meyers, J. A. Nelson, J. E. Gairin, B. H. Hahn, M. B. Oldstone, and G. M. Shaw.** 1997. Antiviral pressure

- exerted by HIV-1-specific cytotoxic T lymphocytes (CTLs) during primary infection demonstrated by rapid selection of CTL escape virus. *Nature medicine* **3**:205-211.
44. **Bourgeois, C., B. Rocha, and C. Tanchot.** 2002. A role for CD40 expression on CD8+ T cells in the generation of CD8+ T cell memory. *Science* **297**:2060-2063.
  45. **Brander, C., P. J. Goulder, K. Luzuriaga, O. O. Yang, K. E. Hartman, N. G. Jones, B. D. Walker, and S. A. Kalams.** 1999. Persistent HIV-1-specific CTL clonal expansion despite high viral burden post in utero HIV-1 infection. *J Immunol* **162**:4796-4800.
  46. **Brander, C., K. E. Hartman, A. K. Trocha, N. G. Jones, R. P. Johnson, B. Korber, P. Wentworth, S. P. Buchbinder, S. Wolinsky, B. D. Walker, and S. A. Kalams.** 1998. Lack of strong immune selection pressure by the immunodominant, HLA-A\*0201-restricted cytotoxic T lymphocyte response in chronic human immunodeficiency virus-1 infection. *The Journal of clinical investigation* **101**:2559-2566.
  47. **Brockman, M. A., Z. L. Brumme, C. J. Brumme, T. Miura, J. Sela, P. C. Rosato, C. M. Kadie, J. M. Carlson, T. J. Markle, H. Streeck, A. D. Kelleher, M. Markowitz, H. Jessen, E. Rosenberg, M. Altfeld, P. R. Harrigan, D. Heckerman, B. D. Walker, and T. M. Allen.** 2010. Early selection in Gag by protective HLA alleles contributes to reduced HIV-1 replication capacity that may be largely compensated for in chronic infection. *J Virol* **84**:11937-11949.
  48. **Buchli, R., R. S. VanGundy, H. D. Hickman-Miller, C. F. Giberson, W. Bardet, and W. H. Hildebrand.** 2005. Development and validation of a fluorescence polarization-based competitive peptide-binding assay for HLA-A\*0201--a new tool for epitope discovery. *Biochemistry* **44**:12491-12507.
  49. **Buseyne, F., and Y. Riviere.** 2001. The flexibility of the TCR allows recognition of a large set of naturally occurring epitope variants by HIV-specific cytotoxic T lymphocytes. *International immunology* **13**:941-950.
  50. **Cale, E. M., P. Hraber, E. E. Giorgi, W. Fischer, T. Bhattacharya, T. Leitner, W. W. Yeh, C. Gleasner, L. D. Green, C. S. Han, B. Korber, and N. L. Letvin.** 2011. Epitope-specific CD8+ T lymphocytes cross-recognize mutant simian immunodeficiency virus (SIV) sequences but fail to contain very early evolution and eventual fixation of epitope escape mutations during SIV infection. *J Virol* **85**:3746-3757.
  51. **Casazza, J. P., M. R. Betts, B. J. Hill, J. M. Brenchley, D. A. Price, D. C. Douek, and R. A. Koup.** 2005. Immunologic pressure within class I-restricted cognate human immunodeficiency virus epitopes during highly active antiretroviral therapy. *Journal of virology* **79**:3653-3663.
  52. **CDC** 2013, posting date. HIV/AIDS Update. [Online.]
  53. **Champagne, P., G. S. Ogg, A. S. King, C. Knabenhans, K. Ellefsen, M. Nobile, V. Appay, G. P. Rizzardi, S. Fleury, M. Lipp, R. Forster, S. Rowland-Jones, R. P. Sekaly, A. J. McMichael, and G. Pantaleo.** 2001. Skewed maturation of memory HIV-specific CD8 T lymphocytes. *Nature* **410**:106-111.
  54. **Chan, D. C., and P. S. Kim.** 1998. HIV entry and its inhibition. *Cell* **93**:681-684.
  55. **Chen, Y., S. L. Carpenter, and S. J. Lamont.** 2000. A functional role for the Y box in regulating an MHC class II B gene promoter in chicken lymphocytes. *Immunogenetics* **51**:882-886.
  56. **Chen, Y., C. Rinaldo, and P. Gupta.** 1997. A semiquantitative assay for CD8+ T-cell-mediated suppression of human immunodeficiency virus type 1 infection. *Clin Diagn Lab Immunol* **4**:4-10.

57. **Chen, Z. K., and T. Frick.** 2000. Blockade of CD4 is more tolerogenic than blockade of Ag presentation via self MHC class II antigens. *Transplantation proceedings* **32**:2000.
58. **Chen, Z. W., A. Craiu, L. Shen, M. J. Kuroda, U. C. Iroku, D. I. Watkins, G. Voss, and N. L. Letvin.** 2000. Simian immunodeficiency virus evades a dominant epitope-specific cytotoxic T lymphocyte response through a mutation resulting in the accelerated dissociation of viral peptide and MHC class I. *J Immunol* **164**:6474-6479.
59. **Chevalier, M. F., and L. Weiss.** 2013. The split personality of regulatory T cells in HIV infection. *Blood* **121**:29-37.
60. **Christie, N. M., D. O. Willer, M. A. Lobritz, J. K. Chan, E. J. Arts, M. A. Ostrowski, A. Cochrane, M. A. Luscher, and K. S. MacDonald.** 2009. Viral fitness implications of variation within an immunodominant CD8+ T-cell epitope of HIV-1. *Virology* **388**:137-146.
61. **Chun, T. W., D. Engel, S. B. Mizell, L. A. Ehler, and A. S. Fauci.** 1998. Induction of HIV-1 replication in latently infected CD4+ T cells using a combination of cytokines. *The Journal of experimental medicine* **188**:83-91.
62. **Chun, T. W., D. C. Nickle, J. S. Justement, J. H. Meyers, G. Roby, C. W. Hallahan, S. Kottlilil, S. Moir, J. M. Mican, J. I. Mullins, D. J. Ward, J. A. Kovacs, P. J. Mannon, and A. S. Fauci.** 2008. Persistence of HIV in gut-associated lymphoid tissue despite long-term antiretroviral therapy. *The Journal of infectious diseases* **197**:714-720.
63. **Chung, C., W. Lee, J. T. Loffredo, B. Burwitz, T. C. Friedrich, J. P. Giraldo Vela, G. Napoe, E. G. Rakasz, N. A. Wilson, D. B. Allison, and D. I. Watkins.** 2007. Not all cytokine-producing CD8+ T cells suppress simian immunodeficiency virus replication. *Journal of virology* **81**:1517-1523.
64. **Clark, S. J., M. S. Saag, W. D. Decker, S. Campbell-Hill, J. L. Roberson, P. J. Veldkamp, J. C. Kappes, B. H. Hahn, and G. M. Shaw.** 1991. High titers of cytopathic virus in plasma of patients with symptomatic primary HIV-1 infection. *N Engl J Med* **324**:954-960.
65. **Coakley, E., C. J. Petropoulos, and J. M. Whitcomb.** 2005. Assessing chemokine co-receptor usage in HIV. *Curr Opin Infect Dis* **18**:9-15.
66. **Coffin, J. M.** 1996. *Retroviridae: The viruses and their replication*. Lippincott-Raven, Philadelphia, PA.
67. **Colleton, B. A., X. L. Huang, N. M. Melhem, Z. Fan, L. Borowski, G. Rappocciolo, and C. R. Rinaldo.** 2009. Primary human immunodeficiency virus type 1-specific CD8+ T-cell responses induced by myeloid dendritic cells. *Journal of virology* **83**:6288-6299.
68. **Connolly, N., S. Riddler, J. Stanson, W. Gooding, C. R. Rinaldo, S. Ferrone, and T. L. Whiteside.** 2007. Levels of antigen processing machinery components in dendritic cells generated for vaccination of HIV-1+ subjects. *AIDS* **21**:1683-1692.
69. **Connolly, N. C., B. A. Colleton, and C. R. Rinaldo.** 2007. Treating HIV-1 infection with dendritic cells. *Curr Opin Mol Ther* **9**:353-363.
70. **Connolly, N. C., T. L. Whiteside, C. Wilson, V. Kondragunta, C. R. Rinaldo, and S. A. Riddler.** 2008. Therapeutic immunization with human immunodeficiency virus type 1 (HIV-1) peptide-loaded dendritic cells is safe and induces immunogenicity in HIV-1-infected individuals. *Clin Vaccine Immunol* **15**:284-292.
71. **Connors, M., J. A. Kovacs, S. Krevat, J. C. Gea-Banacloche, M. C. Sneller, M. Flanagan, J. A. Metcalf, R. E. Walker, J. Falloon, M. Baseler, I. Feuerstein, H. Masur, and H. C. Lane.** 1997. HIV infection induces changes in CD4+ T-cell phenotype and

- depletions within the CD4+ T-cell repertoire that are not immediately restored by antiviral or immune-based therapies. *Nature medicine* **3**:533-540.
72. **Corbeau, P., and J. Reynes.** 2011. Immune reconstitution under antiretroviral therapy: the new challenge in HIV-1 infection. *Blood* **117**:5582-5590.
  73. **Corey, L., M. J. McElrath, and J. G. Kublin.** 2009. Post-step modifications for research on HIV vaccines. *AIDS* **23**:3-8.
  74. **Cossarizza, A., F. Poccia, C. Agrati, G. D'Offizi, R. Bugarini, M. Pinti, V. Borghi, C. Mussini, R. Esposito, G. Ippolito, and P. Narciso.** 2004. Highly active antiretroviral therapy restores CD4+ Vbeta T-cell repertoire in patients with primary acute HIV infection but not in treatment-naive HIV+ patients with severe chronic infection. *J Acquir Immune Defic Syndr* **35**:213-222.
  75. **Couillin, I., B. Culmann-Penciolelli, E. Gomard, J. Choppin, J. P. Levy, J. G. Guillet, and S. Saragosti.** 1994. Impaired cytotoxic T lymphocyte recognition due to genetic variations in the main immunogenic region of the human immunodeficiency virus 1 NEF protein. *The Journal of experimental medicine* **180**:1129-1134.
  76. **Daar, E. S., T. Moudgil, R. D. Meyer, and D. D. Ho.** 1991. Transient high levels of viremia in patients with primary human immunodeficiency virus type 1 infection. *N Engl J Med* **324**:961-964.
  77. **Daniels, M. A., and S. C. Jameson.** 2000. Critical role for CD8 in T cell receptor binding and activation by peptide/major histocompatibility complex multimers. *The Journal of experimental medicine* **191**:335-346.
  78. **Davenport, M. P., D. A. Price, and A. J. McMichael.** 2007. The T cell repertoire in infection and vaccination: implications for control of persistent viruses. *Current opinion in immunology* **19**:294-300.
  79. **Day, C. L., D. E. Kaufmann, P. Kiepiela, J. A. Brown, E. S. Moodley, S. Reddy, E. W. Mackey, J. D. Miller, A. J. Leslie, C. DePierres, Z. Mncube, J. Duraiswamy, B. Zhu, Q. Eichbaum, M. Altfeld, E. J. Wherry, H. M. Coovadia, P. J. Goulder, P. Klenerman, R. Ahmed, G. J. Freeman, and B. D. Walker.** 2006. PD-1 expression on HIV-specific T cells is associated with T-cell exhaustion and disease progression. *Nature* **443**:350-354.
  80. **De Stefano, A., J. H. Burridge, V. T. Yule, and R. Allen.** 2004. Effect of gait cycle selection on EMG analysis during walking in adults and children with gait pathology. *Gait & posture* **20**:92-101.
  81. **Deeks, S. G.** 2011. HIV infection, inflammation, immunosenescence, and aging. *Annual review of medicine* **62**:141-155.
  82. **Deeks, S. G.** 2012. HIV: Shock and kill. *Nature* **487**:439-440.
  83. **Deeks, S. G., and B. D. Walker.** 2007. Human immunodeficiency virus controllers: mechanisms of durable virus control in the absence of antiretroviral therapy. *Immunity* **27**:406-416.
  84. **Delwart, E. L., H. W. Sheppard, B. D. Walker, J. Goudsmit, and J. I. Mullins.** 1994. Human immunodeficiency virus type 1 evolution in vivo tracked by DNA heteroduplex mobility assays. *Journal of virology* **68**:6672-6683.
  85. **Deng, H., R. Liu, W. Ellmeier, S. Choe, D. Unutmaz, M. Burkhart, P. Di Marzio, S. Marmon, R. E. Sutton, C. M. Hill, C. B. Davis, S. C. Peiper, T. J. Schall, D. R. Littman, and N. R. Landau.** 1996. Identification of a major co-receptor for primary isolates of HIV-1. *Nature* **381**:661-666.

86. **Deng, W., B. S. Maust, D. C. Nickle, G. H. Learn, Y. Liu, L. Heath, S. L. Kosakovsky Pond, and J. I. Mullins.** 2010. DIVEIN: a web server to analyze phylogenies, sequence divergence, diversity, and informative sites. *Biotechniques* **48**:405-408.
87. **Detels, R., L. Jacobson, J. Margolick, O. Martinez-Maza, A. Munoz, J. Phair, C. Rinaldo, and S. Wolinsky.** 2012. The multicenter AIDS Cohort Study, 1983 to. *Public Health* **126**:196-198.
88. **Dillon, S. M., K. B. Robertson, S. C. Pan, S. Mawhinney, A. L. Meditz, J. M. Folkvord, E. Connick, M. D. McCarter, and C. C. Wilson.** 2008. Plasmacytoid and myeloid dendritic cells with a partial activation phenotype accumulate in lymphoid tissue during asymptomatic chronic HIV-1 infection. *J Acquir Immune Defic Syndr* **48**:1-12.
89. **Dong, T., Y. Zhang, K. Y. Xu, H. Yan, I. James, Y. Peng, M. E. Blais, S. Gaudieri, X. Chen, W. Lun, H. Wu, W. Y. Qu, T. Rostron, N. Li, Y. Mao, S. Mallal, X. Xu, A. McMichael, M. John, and S. L. Rowland-Jones.** 2011. Extensive HLA-driven viral diversity following a narrow-source HIV-1 outbreak in rural China. *Blood* **118**:98-106.
90. **Doria-Rose, N. A., and M. Connors.** 2009. Antibody-secreting B cells in HIV infection. *Current opinion in HIV and AIDS* **4**:426-430.
91. **Douek, D. C., R. D. McFarland, P. H. Keiser, E. A. Gage, J. M. Massey, B. F. Haynes, M. A. Polis, A. T. Haase, M. B. Feinberg, J. L. Sullivan, B. D. Jamieson, J. A. Zack, L. J. Picker, and R. A. Koup.** 1998. Changes in thymic function with age and during the treatment of HIV infection. *Nature* **396**:690-695.
92. **Douek, D. C., L. J. Picker, and R. A. Koup.** 2003. T cell dynamics in HIV-1 infection. *Annu Rev Immunol* **21**:265-304.
93. **Draenert, R., S. Le Gall, K. J. Pfafferott, A. J. Leslie, P. Chetty, C. Brander, E. C. Holmes, S. C. Chang, M. E. Feeney, M. M. Addo, L. Ruiz, D. Ramduth, P. Jeena, M. Altfeld, S. Thomas, Y. Tang, C. L. Verrill, C. Dixon, J. G. Prado, P. Kiepiela, J. Martinez-Picado, B. D. Walker, and P. J. Goulder.** 2004. Immune selection for altered antigen processing leads to cytotoxic T lymphocyte escape in chronic HIV-1 infection. *The Journal of experimental medicine* **199**:905-915.
94. **Draenert, R., C. L. Verrill, Y. Tang, T. M. Allen, A. G. Wurcel, M. Boczanowski, A. Lechner, A. Y. Kim, T. Suscovich, N. V. Brown, M. M. Addo, and B. D. Walker.** 2004. Persistent recognition of autologous virus by high-avidity CD8 T cells in chronic, progressive human immunodeficiency virus type 1 infection. *Journal of virology* **78**:630-641.
95. **Dragic, T., V. Litwin, G. P. Allaway, S. R. Martin, Y. Huang, K. A. Nagashima, C. Cayanan, P. J. Maddon, R. A. Koup, J. P. Moore, and W. A. Paxton.** 1996. HIV-1 entry into CD4+ cells is mediated by the chemokine receptor CC-CKR-5. *Nature* **381**:667-673.
96. **Drummond, A. J., M. A. Suchard, D. Xie, and A. Rambaut.** 2012. Bayesian phylogenetics with BEAUti and the BEAST 1.7. *Mol Biol Evol* **29**:1969-1973.
97. **Duerr, A., Y. Huang, S. Buchbinder, R. W. Coombs, J. Sanchez, C. Del Rio, M. Casapia, S. Santiago, P. Gilbert, L. Corey, and M. N. Robertson.** 2012. Extended Follow-up Confirms Early Vaccine-Enhanced Risk of HIV Acquisition and Demonstrates Waning Effect Over Time Among Participants in a Randomized Trial of Recombinant Adenovirus HIV Vaccine (Step Study). *The Journal of infectious diseases*.

98. **Dybul, M., A. S. Fauci, J. G. Bartlett, J. E. Kaplan, and A. K. Pau.** 2002. Guidelines for using antiretroviral agents among HIV-infected adults and adolescents. *Ann Intern Med* **137**:381-433.
99. **Egger, M., M. May, G. Chene, A. N. Phillips, B. Ledergerber, F. Dabis, D. Costagliola, A. D'Arminio Monforte, F. de Wolf, P. Reiss, J. D. Lundgren, A. C. Justice, S. Staszewski, C. Leport, R. S. Hogg, C. A. Sabin, M. J. Gill, B. Salzberger, and J. A. Sterne.** 2002. Prognosis of HIV-1-infected patients starting highly active antiretroviral therapy: a collaborative analysis of prospective studies. *Lancet* **360**:119-129.
100. **El Ansary, M., S. Mogawer, S. A. Elhamid, S. Alwakil, F. Aboelkasem, H. E. Sabaawy, and O. Abdelhalim.** 2013. Immunotherapy by autologous dendritic cell vaccine in patients with advanced HCC. *J Cancer Res Clin Oncol* **139**:39-48.
101. **Eugenin, E. A., P. J. Gaskill, and J. W. Berman.** 2009. Tunneling nanotubes (TNT) are induced by HIV-infection of macrophages: a potential mechanism for intercellular HIV trafficking. *Cellular immunology* **254**:142-148.
102. **Evans, D. T., D. H. O'Connor, P. Jing, J. L. Dzuris, J. Sidney, J. da Silva, T. M. Allen, H. Horton, J. E. Venham, R. A. Rudersdorf, T. Vogel, C. D. Pauza, R. E. Bontrop, R. DeMars, A. Sette, A. L. Hughes, and D. I. Watkins.** 1999. Virus-specific cytotoxic T-lymphocyte responses select for amino-acid variation in simian immunodeficiency virus Env and Nef. *Nature medicine* **5**:1270-1276.
103. **Falster, K., K. Petoumenos, J. Chuah, A. Mijch, B. Mulhall, M. Kelly, and D. A. Cooper.** 2009. Poor baseline immune function predicts an incomplete immune response to combination antiretroviral treatment despite sustained viral suppression. *J Acquir Immune Defic Syndr* **50**:307-313.
104. **Fan, Z., X. L. Huang, P. Kalinski, S. Young, and C. R. Rinaldo, Jr.** 2007. Dendritic cell function during chronic hepatitis C virus and human immunodeficiency virus type 1 infection. *Clin Vaccine Immunol* **14**:1127-1137.
105. **Fan, Z., X. L. Huang, L. Zheng, C. Wilson, L. Borowski, J. Liebmann, P. Gupta, J. Margolick, and C. Rinaldo.** 1997. Cultured blood dendritic cells retain HIV-1 antigen-presenting capacity for memory CTL during progressive HIV-1 infection. *J Immunol* **159**:4973-4982.
106. **Fauci, A. S., G. Pantaleo, S. Stanley, and D. Weissman.** 1996. Immunopathogenic mechanisms of HIV infection. *Ann Intern Med* **124**:654-663.
107. **Fazekas de St Groth, B., and A. L. Landay.** 2008. Regulatory T cells in HIV infection: pathogenic or protective participants in the immune response? *AIDS* **22**:671-683.
108. **Finkel, T. H., G. Tudor-Williams, N. K. Banda, M. F. Cotton, T. Curiel, C. Monks, T. W. Baba, R. M. Ruprecht, and A. Kupfer.** 1995. Apoptosis occurs predominantly in bystander cells and not in productively infected cells of HIV- and SIV-infected lymph nodes. *Nature medicine* **1**:129-134.
109. **Finzi, D., J. Blankson, J. D. Siliciano, J. B. Margolick, K. Chadwick, T. Pierson, K. Smith, J. Lisziewicz, F. Lori, C. Flexner, T. C. Quinn, R. E. Chaisson, E. Rosenberg, B. Walker, S. Gange, J. Gallant, and R. F. Siliciano.** 1999. Latent infection of CD4+ T cells provides a mechanism for lifelong persistence of HIV-1, even in patients on effective combination therapy. *Nature medicine* **5**:512-517.
110. **Finzi, D., M. Hermankova, T. Pierson, L. M. Carruth, C. Buck, R. E. Chaisson, T. C. Quinn, K. Chadwick, J. Margolick, R. Brookmeyer, J. Gallant, M. Markowitz, D. D.**

- Ho, D. D. Richman, and R. F. Siliciano.** 1997. Identification of a reservoir for HIV-1 in patients on highly active antiretroviral therapy. *Science* **278**:1295-1300.
111. **Frahm, N., B. T. Korber, C. M. Adams, J. J. Szinger, R. Draenert, M. M. Addo, M. E. Feeney, K. Yusim, K. Sango, N. V. Brown, D. SenGupta, A. Piechocka-Trocha, T. Simonis, F. M. Marincola, A. G. Wurcel, D. R. Stone, C. J. Russell, P. Adolf, D. Cohen, T. Roach, A. StJohn, A. Khatri, K. Davis, J. Mullins, P. J. Goulder, B. D. Walker, and C. Brander.** 2004. Consistent cytotoxic-T-lymphocyte targeting of immunodominant regions in human immunodeficiency virus across multiple ethnicities. *Journal of virology* **78**:2187-2200.
112. **Fritzsche, B., N. Oberle, N. Eberhardt, S. Quick, J. Haas, B. Wildemann, P. H. Krammer, and E. Suri-Payer.** 2005. In contrast to effector T cells, CD4+CD25+FoxP3+ regulatory T cells are highly susceptible to CD95 ligand- but not to TCR-mediated cell death. *J Immunol* **175**:32-36.
113. **Fu, Y. X., and W. H. Li.** 1993. Statistical tests of neutrality of mutations. *Genetics* **133**:693-709.
114. **Furuta, Y., T. Bergstrom, G. Norkrans, and P. Horal.** 1994. HIV type 1 V3 sequence diversity in contact-traced Swedish couples at the time of sexual transmission. *AIDS research and human retroviruses* **10**:1187-1189.
115. **Gaardbo, J. C., H. J. Hartling, J. Gerstoft, and S. D. Nielsen.** 2012. Incomplete immune recovery in HIV infection: mechanisms, relevance for clinical care, and possible solutions. *Clin Dev Immunol* **2012**:670957.
116. **Garcia, F., N. Climent, L. Assoumou, C. Gil, N. Gonzalez, J. Alami, A. Leon, J. Romeu, J. Dalmau, J. Martinez-Picado, J. Lifson, B. Autran, D. Costagliola, B. Clotet, J. M. Gatell, M. Plana, and T. Gallart.** 2011. A therapeutic dendritic cell-based vaccine for HIV-1 infection. *J Infect Dis* **203**:473-478.
117. **Garcia, F., N. Climent, A. C. Guardo, C. Gil, A. Leon, B. Autran, J. D. Lifson, J. Martinez-Picado, J. Dalmau, B. Clotet, J. M. Gatell, M. Plana, and T. Gallart.** 2013. A dendritic cell-based vaccine elicits T cell responses associated with control of HIV-1 replication. *Sci Transl Med* **5**:166ra162.
118. **Garcia, F., E. de Lazzari, M. Plana, P. Castro, G. Mestre, M. Nomdedeu, E. Fumero, E. Martinez, J. Mallolas, J. L. Blanco, J. M. Miro, T. Pumarola, T. Gallart, and J. M. Gatell.** 2004. Long-term CD4+ T-cell response to highly active antiretroviral therapy according to baseline CD4+ T-cell count. *J Acquir Immune Defic Syndr* **36**:702-713.
119. **Garcia, F., A. Leon, J. M. Gatell, M. Plana, and T. Gallart.** 2012. Therapeutic vaccines against HIV infection. *Hum Vaccin Immunother* **8**:569-581.
120. **Gea-Banacloche, J. C., E. E. Weiskopf, C. Hallahan, J. C. Lopez Bernaldo de Quiros, M. Flanigan, J. M. Mican, J. Falloon, M. Baseler, R. Stevens, H. C. Lane, and M. Connors.** 1998. Progression of human immunodeficiency virus disease is associated with increasing disruptions within the CD4+ T cell receptor repertoire. *The Journal of infectious diseases* **177**:579-585.
121. **Geijtenbeek, T. B., D. S. Kwon, R. Torensma, S. J. van Vliet, G. C. van Duijnhoven, J. Middel, I. L. Cornelissen, H. S. Nottet, V. N. KewalRamani, D. R. Littman, C. G. Figdor, and Y. van Kooyk.** 2000. DC-SIGN, a dendritic cell-specific HIV-1-binding protein that enhances trans-infection of T cells. *Cell* **100**:587-597.
122. **Gelinck, L. B., C. M. Jol-van der Zijde, A. M. Jansen-Hoogendijk, D. M. Brinkman, J. T. van Dissel, M. J. van Tol, and F. P. Kroon.** 2009. Restoration of the antibody

- response upon rabies vaccination in HIV-infected patients treated with HAART. *AIDS* **23**:2451-2458.
123. **Giorgi, J. V., H. L. Cheng, J. B. Margolick, K. D. Bauer, J. Ferbas, M. Waxdal, I. Schmid, L. E. Hultin, A. L. Jackson, L. Park, and et al.** 1990. Quality control in the flow cytometric measurement of T-lymphocyte subsets: the multicenter AIDS cohort study experience. The Multicenter AIDS Cohort Study Group. *Clin Immunol Immunopathol* **55**:173-186.
  124. **Gojobori, T., E. N. Moriyama, and M. Kimura.** 1990. Molecular clock of viral evolution, and the neutral theory. *Proceedings of the National Academy of Sciences of the United States of America* **87**:10015-10018.
  125. **Gojobori, T., Y. Yamaguchi, K. Ieko, and M. Mizokami.** 1994. Evolution of pathogenic viruses with special reference to the rates of synonymous and nonsynonymous substitutions. *Idengaku zasshi* **69**:481-488.
  126. **Goldstein, J. S., T. Chen, E. Gubina, R. W. Pastor, and S. Kozlowski.** 2000. ICAM-1 enhances MHC-peptide activation of CD8(+) T cells without an organized immunological synapse. *European journal of immunology* **30**:3266-3270.
  127. **Gorochov, G., A. U. Neumann, A. Kereveur, C. Parizot, T. Li, C. Katlama, M. Karmochkine, G. Raguin, B. Autran, and P. Debre.** 1998. Perturbation of CD4+ and CD8+ T-cell repertoires during progression to AIDS and regulation of the CD4+ repertoire during antiviral therapy. *Nature medicine* **4**:215-221.
  128. **Gottlieb, G. S., L. Heath, D. C. Nickle, K. G. Wong, S. E. Leach, B. Jacobs, S. Gezahegne, A. B. van 't Wout, L. P. Jacobson, J. B. Margolick, and J. I. Mullins.** 2008. HIV-1 variation before seroconversion in men who have sex with men: analysis of acute/early HIV infection in the multicenter AIDS cohort study. *The Journal of infectious diseases* **197**:1011-1015.
  129. **Goulder, P. J., M. A. Altfeld, E. S. Rosenberg, T. Nguyen, Y. Tang, R. L. Eldridge, M. M. Addo, S. He, J. S. Mukherjee, M. N. Phillips, M. Bunce, S. A. Kalams, R. P. Sekaly, B. D. Walker, and C. Brander.** 2001. Substantial differences in specificity of HIV-specific cytotoxic T cells in acute and chronic HIV infection. *The Journal of experimental medicine* **193**:181-194.
  130. **Goulder, P. J., C. Brander, Y. Tang, C. Tremblay, R. A. Colbert, M. M. Addo, E. S. Rosenberg, T. Nguyen, R. Allen, A. Trocha, M. Altfeld, S. He, M. Bunce, R. Funkhouser, S. I. Pelton, S. K. Burchett, K. McIntosh, B. T. Korber, and B. D. Walker.** 2001. Evolution and transmission of stable CTL escape mutations in HIV infection. *Nature* **412**:334-338.
  131. **Goulder, P. J., R. E. Phillips, R. A. Colbert, S. McAdam, G. Ogg, M. A. Nowak, P. Giangrande, G. Luzzi, B. Morgan, A. Edwards, A. J. McMichael, and S. Rowland-Jones.** 1997. Late escape from an immunodominant cytotoxic T-lymphocyte response associated with progression to AIDS. *Nature medicine* **3**:212-217.
  132. **Goulder, P. J., and D. I. Watkins.** 2004. HIV and SIV CTL escape: implications for vaccine design. *Nat Rev Immunol* **4**:630-640.
  133. **Gouy, M., S. Guindon, and O. Gascuel.** 2010. SeaView version 4: A multiplatform graphical user interface for sequence alignment and phylogenetic tree building. *Mol Biol Evol* **27**:221-224.
  134. **Gras, L., A. M. Kesselring, J. T. Griffin, A. I. van Sighem, C. Fraser, A. C. Ghani, F. Miedema, P. Reiss, J. M. Lange, and F. de Wolf.** 2007. CD4 cell counts of 800 cells/mm<sup>3</sup>



- or greater after 7 years of highly active antiretroviral therapy are feasible in most patients starting with 350 cells/mm<sup>3</sup> or greater. *J Acquir Immune Defic Syndr* **45**:183-192.
135. **Grossman, Z., M. Meier-Schellersheim, W. E. Paul, and L. J. Picker.** 2006. Pathogenesis of HIV infection: what the virus spares is as important as what it destroys. *Nature medicine* **12**:289-295.
  136. **Grossman, Z., M. Meier-Schellersheim, A. E. Sousa, R. M. Victorino, and W. E. Paul.** 2002. CD4+ T-cell depletion in HIV infection: are we closer to understanding the cause? *Nature medicine* **8**:319-323.
  137. **Gurunathan, S., L. Stobie, C. Prussin, D. L. Sacks, N. Glaichenhaus, A. Iwasaki, D. J. Fowell, R. M. Locksley, J. T. Chang, C. Y. Wu, and R. A. Seder.** 2000. Requirements for the maintenance of Th1 immunity in vivo following DNA vaccination: a potential immunoregulatory role for CD8+ T cells. *J Immunol* **165**:915-924.
  138. **Haaland, R. E., P. A. Hawkins, J. Salazar-Gonzalez, A. Johnson, A. Tichacek, E. Karita, O. Manigart, J. Mulenga, B. F. Keele, G. M. Shaw, B. H. Hahn, S. A. Allen, C. A. Derdeyn, and E. Hunter.** 2009. Inflammatory genital infections mitigate a severe genetic bottleneck in heterosexual transmission of subtype A and C HIV-1. *PLoS pathogens* **5**:e1000274.
  139. **Haas, A., K. Zimmermann, and A. Oxenius.** 2011. Antigen-dependent and -independent mechanisms of T and B cell hyperactivation during chronic HIV-1 infection. *Journal of virology* **85**:12102-12113.
  140. **Haggerty, C. M., E. Pitt, and R. F. Siliciano.** 2006. The latent reservoir for HIV-1 in resting CD4+ T cells and other viral reservoirs during chronic infection: insights from treatment and treatment-interruption trials. *Curr Opin HIV AIDS* **1**:62-68.
  141. **Harari, A., C. Cellera, F. B. Enders, J. Kostler, L. Codarri, G. Tapia, O. Boyman, E. Castro, S. Gaudieri, I. James, M. John, R. Wagner, S. Mallal, and G. Pantaleo.** 2007. Skewed association of polyfunctional antigen-specific CD8 T cell populations with HLA-B genotype. *Proceedings of the National Academy of Sciences of the United States of America* **104**:16233-16238.
  142. **Harari, A., F. Vallelian, P. R. Meylan, and G. Pantaleo.** 2005. Functional heterogeneity of memory CD4 T cell responses in different conditions of antigen exposure and persistence. *J Immunol* **174**:1037-1045.
  143. **Harari, A., F. Vallelian, and G. Pantaleo.** 2004. Phenotypic heterogeneity of antigen-specific CD4 T cells under different conditions of antigen persistence and antigen load. *European journal of immunology* **34**:3525-3533.
  144. **Hay, C. M., D. J. Ruhl, N. O. Basgoz, C. C. Wilson, J. M. Billingsley, M. P. DePasquale, R. T. D'Aquila, S. M. Wolinsky, J. M. Crawford, D. C. Montefiori, and B. D. Walker.** 1999. Lack of viral escape and defective in vivo activation of human immunodeficiency virus type 1-specific cytotoxic T lymphocytes in rapidly progressive infection. *Journal of virology* **73**:5509-5519.
  145. **Hazenbergh, M. D., S. A. Otto, J. W. Cohen Stuart, M. C. Verschuren, J. C. Borleffs, C. A. Boucher, R. A. Coutinho, J. M. Lange, T. F. Rinke de Wit, A. Tsegaye, J. J. van Dongen, D. Hamann, R. J. de Boer, and F. Miedema.** 2000. Increased cell division but not thymic dysfunction rapidly affects the T-cell receptor excision circle content of the naive T cell population in HIV-1 infection. *Nature medicine* **6**:1036-1042.

146. **Hazenberg, M. D., S. A. Otto, B. H. van Benthem, M. T. Roos, R. A. Coutinho, J. M. Lange, D. Hamann, M. Prins, and F. Miedema.** 2003. Persistent immune activation in HIV-1 infection is associated with progression to AIDS. *AIDS* **17**:1881-1888.
147. **Herbeck, J. T., M. Rolland, Y. Liu, S. McLaughlin, J. McNevin, H. Zhao, K. Wong, J. N. Stoddard, D. Raugi, S. Sorensen, I. Genowati, B. Birditt, A. McKay, K. Diem, B. S. Maust, W. Deng, A. C. Collier, J. D. Stekler, M. J. McElrath, and J. I. Mullins.** 2011. Demographic processes affect HIV-1 evolution in primary infection before the onset of selective processes. *Journal of virology* **85**:7523-7534.
148. **Hermans, I. F., D. S. Ritchie, J. Yang, J. M. Roberts, and F. Ronchese.** 2000. CD8+ T cell-dependent elimination of dendritic cells in vivo limits the induction of antitumor immunity. *J Immunol* **164**:3095-3101.
149. **Hightower, G. K., J. K. Wong, S. L. Letendre, A. A. Umlauf, R. J. Ellis, C. C. Ignacio, R. K. Heaton, A. C. Collier, C. M. Marra, D. B. Clifford, B. B. Gelman, J. C. McArthur, S. Morgello, D. M. Simpson, J. A. McCutchan, I. Grant, S. J. Little, D. D. Richman, S. L. Kosakovsky Pond, and D. M. Smith.** 2012. Higher HIV-1 genetic diversity is associated with AIDS and neuropsychological impairment. *Virology* **433**:498-505.
150. **Hiscott, J., H. Kwon, and P. Genin.** 2001. Hostile takeovers: viral appropriation of the NF-kappaB pathway. *The Journal of clinical investigation* **107**:143-151.
151. **Hoof, I., B. Peters, J. Sidney, L. E. Pedersen, A. Sette, O. Lund, S. Buus, and M. Nielsen.** 2009. NetMHCpan, a method for MHC class I binding prediction beyond humans. *Immunogenetics* **61**:1-13.
152. **Hsu, F. J., C. Benike, F. Fagnoni, T. M. Liles, D. Czerwinski, B. Taidi, E. G. Engleman, and R. Levy.** 1996. Vaccination of patients with B-cell lymphoma using autologous antigen-pulsed dendritic cells. *Nat Med* **2**:52-58.
153. **Hu, W. S., and H. M. Temin.** 1990. Retroviral recombination and reverse transcription. *Science* **250**:1227-1233.
154. **Huang, X., Z. Fan, L. Zheng, and C. R. Rinaldo, Jr.** 2001. Stimulation of Anti-HIV-1 Cytotoxic T Lymphocytes by Dendritic Cells. *Methods Mol Med* **64**:441-453.
155. **Huang, X. L., Z. Fan, L. Borowski, R. B. Mailliard, M. Rolland, J. I. Mullins, R. D. Day, and C. R. Rinaldo.** 2010. Dendritic cells reveal a broad range of MHC class I epitopes for HIV-1 in persons with suppressed viral load on antiretroviral therapy. *PLoS one* **5**:e12936.
156. **Huang, X. L., Z. Fan, L. Borowski, and C. R. Rinaldo.** 2008. Maturation of dendritic cells for enhanced activation of anti-HIV-1 CD8(+) T cell immunity. *J Leukoc Biol* **83**:1530-1540.
157. **Huang, X. L., Z. Fan, L. Borowski, and C. R. Rinaldo.** 2009. Multiple T-cell responses to human immunodeficiency virus type 1 are enhanced by dendritic cells. *Clin Vaccine Immunol* **16**:1504-1516.
158. **Huang, X. L., Z. Fan, B. A. Colleton, R. Buchli, H. Li, W. H. Hildebrand, and C. R. Rinaldo, Jr.** 2005. Processing and presentation of exogenous HLA class I peptides by dendritic cells from human immunodeficiency virus type 1-infected persons. *J Virol* **79**:3052-3062.
159. **Hussain, S. K., W. Zhu, S. C. Chang, E. C. Breen, E. Vendrame, L. Magpantay, D. Widney, D. Conn, M. Sehl, L. P. Jacobson, J. H. Bream, S. Wolinsky, C. R. Rinaldo, R. F. Ambinder, R. Detels, Z. F. Zhang, and O. Martinez-Maza.** 2013. Serum levels of

- the chemokine CXCL13, genetic variation in CXCL13 and its receptor CXCR5, and HIV-associated non-hodgkin B-cell lymphoma risk. *Cancer Epidemiol Biomarkers Prev* **22**:295-307.
160. **Iversen, A. K., G. Stewart-Jones, G. H. Learn, N. Christie, C. Sylvester-Hviid, A. E. Armitage, R. Kaul, T. Beattie, J. K. Lee, Y. Li, P. Chotiarnwong, T. Dong, X. Xu, M. A. Luscher, K. MacDonald, H. Ullum, B. Klarlund-Pedersen, P. Skinhoj, L. Fugger, S. Buus, J. I. Mullins, E. Y. Jones, P. A. van der Merwe, and A. J. McMichael.** 2006. Conflicting selective forces affect T cell receptor contacts in an immunodominant human immunodeficiency virus epitope. *Nature immunology* **7**:179-189.
  161. **Janbazian, L., D. A. Price, G. Canderan, A. Filali-Mouhim, T. E. Asher, D. R. Ambrozak, P. Scheinberg, M. R. Boulassel, J. P. Routy, R. A. Koup, D. C. Douek, R. P. Sekaly, and L. Trautmann.** 2012. Clonotype and repertoire changes drive the functional improvement of HIV-specific CD8 T cell populations under conditions of limited antigenic stimulation. *J Immunol* **188**:1156-1167.
  162. **Jenabian, M. A., P. Ancuta, N. Gilmore, and J. P. Routy.** 2012. Regulatory T cells in HIV infection: can immunotherapy regulate the regulator? *Clin Dev Immunol* **2012**:908314.
  163. **Jensen, M. A., F. S. Li, A. B. van 't Wout, D. C. Nickle, D. Shriner, H. X. He, S. McLaughlin, R. Shankarappa, J. B. Margolick, and J. I. Mullins.** 2003. Improved coreceptor usage prediction and genotypic monitoring of R5-to-X4 transition by motif analysis of human immunodeficiency virus type 1 env V3 loop sequences. *Journal of virology* **77**:13376-13388.
  164. **Ji, J., and M. W. Cloyd.** 2009. HIV-1 binding to CD4 on CD4+CD25+ regulatory T cells enhances their suppressive function and induces them to home to, and accumulate in, peripheral and mucosal lymphoid tissues: an additional mechanism of immunosuppression. *International immunology* **21**:283-294.
  165. **Jones, N. A., X. Wei, D. R. Flower, M. Wong, F. Michor, M. S. Saag, B. H. Hahn, M. A. Nowak, G. M. Shaw, and P. Borrow.** 2004. Determinants of human immunodeficiency virus type 1 escape from the primary CD8+ cytotoxic T lymphocyte response. *The Journal of experimental medicine* **200**:1243-1256.
  166. **Joos, B., M. Fischer, H. Kuster, S. K. Pillai, J. K. Wong, J. Boni, B. Hirschel, R. Weber, A. Trkola, and H. F. Gunthard.** 2008. HIV rebounds from latently infected cells, rather than from continuing low-level replication. *Proceedings of the National Academy of Sciences of the United States of America* **105**:16725-16730.
  167. **Kalams, S. A., P. J. Goulder, A. K. Shea, N. G. Jones, A. K. Trocha, G. S. Ogg, and B. D. Walker.** 1999. Levels of human immunodeficiency virus type 1-specific cytotoxic T-lymphocyte effector and memory responses decline after suppression of viremia with highly active antiretroviral therapy. *Journal of virology* **73**:6721-6728.
  168. **Kalinski, P., C. M. Hilkens, E. A. Wierenga, and M. L. Kapsenberg.** 1999. T-cell priming by type-1 and type-2 polarized dendritic cells: the concept of a third signal. *Immunol Today* **20**:561-567.
  169. **Kalinski, P., and M. Moser.** 2005. Consensual immunity: success-driven development of T-helper-1 and T-helper-2 responses. *Nat Rev Immunol* **5**:251-260.
  170. **Karosiene, E., M. Rasmussen, T. Blicher, O. Lund, S. Buus, and M. Nielsen.** 2013. NetMHCIIpan-3.0, a common pan-specific MHC class II prediction method including all

- three human MHC class II isotypes, HLA-DR, HLA-DP and HLA-DQ. *Immunogenetics* **65**:711-724.
171. **Kaslow, R. A., D. G. Ostrow, R. Detels, J. P. Phair, B. F. Polk, and C. R. Rinaldo, Jr.** 1987. The Multicenter AIDS Cohort Study: rationale, organization, and selected characteristics of the participants. *American journal of epidemiology* **126**:310-318.
  172. **Katlama, C., S. G. Deeks, B. Autran, J. Martinez-Picado, J. van Lunzen, C. Rouzioux, M. Miller, S. Vella, J. E. Schmitz, J. Ahlers, D. D. Richman, and R. P. Sekaly.** 2013. Barriers to a cure for HIV: new ways to target and eradicate HIV-1 reservoirs. *Lancet* **381**:2109-2117.
  173. **Kaufmann, D. E., D. G. Kavanagh, F. Pereyra, J. J. Zaunders, E. W. Mackey, T. Miura, S. Palmer, M. Brockman, A. Rathod, A. Piechocka-Trocha, B. Baker, B. Zhu, S. Le Gall, M. T. Waring, R. Ahern, K. Moss, A. D. Kelleher, J. M. Coffin, G. J. Freeman, E. S. Rosenberg, and B. D. Walker.** 2007. Upregulation of CTLA-4 by HIV-specific CD4+ T cells correlates with disease progression and defines a reversible immune dysfunction. *Nature immunology* **8**:1246-1254.
  174. **Kearney, M., F. Maldarelli, W. Shao, J. B. Margolick, E. S. Daar, J. W. Mellors, V. Rao, J. M. Coffin, and S. Palmer.** 2009. Human immunodeficiency virus type 1 population genetics and adaptation in newly infected individuals. *Journal of virology* **83**:2715-2727.
  175. **Keating, S. M., P. Bejon, T. Berthoud, J. M. Vuola, S. Todryk, D. P. Webster, S. J. Dunachie, V. S. Moorthy, S. J. McConkey, S. C. Gilbert, and A. V. Hill.** 2005. Durable human memory T cells quantifiable by cultured enzyme-linked immunospot assays are induced by heterologous prime boost immunization and correlate with protection against malaria. *J Immunol* **175**:5675-5680.
  176. **Keele, B. F., E. E. Giorgi, J. F. Salazar-Gonzalez, J. M. Decker, K. T. Pham, M. G. Salazar, C. Sun, T. Grayson, S. Wang, H. Li, X. Wei, C. Jiang, J. L. Kirchherr, F. Gao, J. A. Anderson, L. H. Ping, R. Swanstrom, G. D. Tomaras, W. A. Blattner, P. A. Goepfert, J. M. Kilby, M. S. Saag, E. L. Delwart, M. P. Busch, M. S. Cohen, D. C. Montefiori, B. F. Haynes, B. Gaschen, G. S. Athreya, H. Y. Lee, N. Wood, C. Seoighe, A. S. Perelson, T. Bhattacharya, B. T. Korber, B. H. Hahn, and G. M. Shaw.** 2008. Identification and characterization of transmitted and early founder virus envelopes in primary HIV-1 infection. *Proceedings of the National Academy of Sciences of the United States of America* **105**:7552-7557.
  177. **Kelleher, C. C.** 2001. Evolution of cardio-vascular risk factors--light at the end of the tunnel? *Wiener klinische Wochenschrift* **113**:552-557.
  178. **Khoury, G., R. Rajasuriar, P. U. Cameron, and S. R. Lewin.** 2011. The role of naive T-cells in HIV-1 pathogenesis: an emerging key player. *Clin Immunol* **141**:253-267.
  179. **Kiepiela, P., K. Ngumbela, C. Thobakgale, D. Ramduth, I. Honeyborne, E. Moodley, S. Reddy, C. de Pierres, Z. Mncube, N. Mkhwanazi, K. Bishop, M. van der Stok, K. Nair, N. Khan, H. Crawford, R. Payne, A. Leslie, J. Prado, A. Prendergast, J. Frater, N. McCarthy, C. Brander, G. H. Learn, D. Nickle, C. Rousseau, H. Coovadia, J. I. Mullins, D. Heckerman, B. D. Walker, and P. Goulder.** 2007. CD8+ T-cell responses to different HIV proteins have discordant associations with viral load. *Nature medicine* **13**:46-53.
  180. **Kim, J. M., and S. H. Han.** 2011. Immunotherapeutic restoration in HIV-infected individuals. *Immunotherapy* **3**:247-267.

181. **Kimura, M.** 1979. The neutral theory of molecular evolution. *Scientific American* **241**:98-100, 102, 108 passim.
182. **Kimura, M.** 1991. The neutral theory of molecular evolution: a review of recent evidence. *Idengaku zasshi* **66**:367-386.
183. **Kimura, M.** 1977. Preponderance of synonymous changes as evidence for the neutral theory of molecular evolution. *Nature* **267**:275-276.
184. **Klenerman, P., Y. Wu, and R. Phillips.** 2002. HIV: current opinion in escapology. *Current opinion in microbiology* **5**:408-413.
185. **Klenerman, P., and R. M. Zinkernagel.** 1998. Original antigenic sin impairs cytotoxic T lymphocyte responses to viruses bearing variant epitopes. *Nature* **394**:482-485.
186. **Koibuchi, T., T. M. Allen, M. Lichterfeld, S. K. Mui, K. M. O'Sullivan, A. Trocha, S. A. Kalams, R. P. Johnson, and B. D. Walker.** 2005. Limited sequence evolution within persistently targeted CD8 epitopes in chronic human immunodeficiency virus type 1 infection. *Journal of virology* **79**:8171-8181.
187. **Kosakovsky Pond, S. L., A. F. Poon, A. J. Leigh Brown, and S. D. Frost.** 2008. A maximum likelihood method for detecting directional evolution in protein sequences and its application to influenza A virus. *Mol Biol Evol* **25**:1809-1824.
188. **Koup, R. A.** 1994. Virus escape from CTL recognition. *The Journal of experimental medicine* **180**:779-782.
189. **Koup, R. A., J. T. Safrit, Y. Cao, C. A. Andrews, G. McLeod, W. Borkowsky, C. Farthing, and D. D. Ho.** 1994. Temporal association of cellular immune responses with the initial control of viremia in primary human immunodeficiency virus type 1 syndrome. *Journal of virology* **68**:4650-4655.
190. **Krathwohl, M. D., T. W. Schacker, and J. L. Anderson.** 2006. Abnormal presence of semimature dendritic cells that induce regulatory T cells in HIV-infected subjects. *The Journal of infectious diseases* **193**:494-504.
191. **Kuniyasu, Y., T. Takahashi, M. Itoh, J. Shimizu, G. Toda, and S. Sakaguchi.** 2000. Naturally anergic and suppressive CD25(+)CD4(+) T cells as a functionally and phenotypically distinct immunoregulatory T cell subpopulation. *International immunology* **12**:1145-1155.
192. **Kuritzkes, D. R.** 2000. Neutropenia, neutrophil dysfunction, and bacterial infection in patients with human immunodeficiency virus disease: the role of granulocyte colony-stimulating factor. *Clin Infect Dis* **30**:256-260.
193. **Kuroda, M. J., J. E. Schmitz, W. A. Charini, C. E. Nickerson, M. A. Lifton, C. I. Lord, M. A. Forman, and N. L. Letvin.** 1999. Emergence of CTL coincides with clearance of virus during primary simian immunodeficiency virus infection in rhesus monkeys. *J Immunol* **162**:5127-5133.
194. **Ladell, K., M. Hashimoto, M. C. Iglesias, P. G. Wilmann, J. E. McLaren, S. Gras, T. Chikata, N. Kuse, S. Fastenackels, E. Gostick, J. S. Bridgeman, V. Venturi, Z. A. Arkoub, H. Agut, D. J. van Bockel, J. R. Almeida, D. C. Douek, L. Meyer, A. Venet, M. Takiguchi, J. Rossjohn, D. A. Price, and V. Appay.** 2013. A molecular basis for the control of preimmune escape variants by HIV-specific CD8+ T cells. *Immunity* **38**:425-436.
195. **Laird, G. M., E. E. Eisele, S. A. Rabi, J. Lai, S. Chioma, J. N. Blankson, J. D. Siliciano, and R. F. Siliciano.** 2013. Rapid quantification of the latent reservoir for HIV-1 using a viral outgrowth assay. *PLoS Pathog* **9**:e1003398.

196. **Lanave, C., G. Preparata, C. Saccone, and G. Serio.** 1984. A new method for calculating evolutionary substitution rates. *J Mol Evol* **20**:86-93.
197. **Lange, C. G., M. M. Lederman, K. Medvik, R. Asaad, M. Wild, R. Kalayjian, and H. Valdez.** 2003. Nadir CD4+ T-cell count and numbers of CD28+ CD4+ T-cells predict functional responses to immunizations in chronic HIV-1 infection. *AIDS* **17**:2015-2023.
198. **Langenkamp, A., M. Messi, A. Lanzavecchia, and F. Sallusto.** 2000. Kinetics of dendritic cell activation: impact on priming of TH1, TH2 and nonpolarized T cells. *Nature immunology* **1**:311-316.
199. **Learn, G. H., D. Muthui, S. J. Brodie, T. Zhu, K. Diem, J. I. Mullins, and L. Corey.** 2002. Virus population homogenization following acute human immunodeficiency virus type 1 infection. *Journal of virology* **76**:11953-11959.
200. **Lekkerkerker, A. N., Y. van Kooyk, and T. B. Geijtenbeek.** 2006. Viral piracy: HIV-1 targets dendritic cells for transmission. *Current HIV research* **4**:169-176.
201. **Lemey, P., S. L. Kosakovsky Pond, A. J. Drummond, O. G. Pybus, B. Shapiro, H. Barroso, N. Taveira, and A. Rambaut.** 2007. Synonymous substitution rates predict HIV disease progression as a result of underlying replication dynamics. *PLoS computational biology* **3**:e29.
202. **Leslie, A. J., K. J. Pfafferott, P. Chetty, R. Draenert, M. M. Addo, M. Feeney, Y. Tang, E. C. Holmes, T. Allen, J. G. Prado, M. Altfeld, C. Brander, C. Dixon, D. Ramduth, P. Jeena, S. A. Thomas, A. St John, T. A. Roach, B. Kupfer, G. Luzzi, A. Edwards, G. Taylor, H. Lyall, G. Tudor-Williams, V. Novelli, J. Martinez-Picado, P. Kiepiela, B. D. Walker, and P. J. Goulder.** 2004. HIV evolution: CTL escape mutation and reversion after transmission. *Nature medicine* **10**:282-289.
203. **Librado, P., and J. Rozas.** 2009. DnaSP v5: a software for comprehensive analysis of DNA polymorphism data. *Bioinformatics* **25**:1451-1452.
204. **Liu, J., K. L. O'Brien, D. M. Lynch, N. L. Simmons, A. La Porte, A. M. Riggs, P. Abbink, R. T. Coffey, L. E. Grandpre, M. S. Seaman, G. Landucci, D. N. Forthal, D. C. Montefiori, A. Carville, K. G. Mansfield, M. J. Havenga, M. G. Pau, J. Goudsmit, and D. H. Barouch.** 2009. Immune control of an SIV challenge by a T-cell-based vaccine in rhesus monkeys. *Nature* **457**:87-91.
205. **Liu, Y., J. McNevin, J. Cao, H. Zhao, I. Genowati, K. Wong, S. McLaughlin, M. D. McSweyn, K. Diem, C. E. Stevens, J. Maenza, H. He, D. C. Nickle, D. Shriner, S. E. Holte, A. C. Collier, L. Corey, M. J. McElrath, and J. I. Mullins.** 2006. Selection on the human immunodeficiency virus type 1 proteome following primary infection. *Journal of virology* **80**:9519-9529.
206. **Liu, Y., J. McNevin, H. Zhao, D. M. Tebit, R. M. Troyer, M. McSweyn, A. K. Ghosh, D. Shriner, E. J. Arts, M. J. McElrath, and J. I. Mullins.** 2007. Evolution of human immunodeficiency virus type 1 cytotoxic T-lymphocyte epitopes: fitness-balanced escape. *J Virol* **81**:12179-12188.
207. **Liu, Y., J. P. McNevin, S. Holte, M. J. McElrath, and J. I. Mullins.** 2011. Dynamics of viral evolution and CTL responses in HIV-1 infection. *PloS one* **6**:e15639.
208. **Loffredo, J. T., B. J. Burwitz, E. G. Rakasz, S. P. Spencer, J. J. Stephany, J. P. Vela, S. R. Martin, J. Reed, S. M. Piaskowski, J. Furlott, K. L. Weisgrau, D. S. Rodrigues, T. Soma, G. Napoe, T. C. Friedrich, N. A. Wilson, E. G. Kallas, and D. I. Watkins.** 2007. The antiviral efficacy of simian immunodeficiency virus-specific CD8+ T cells is

- unrelated to epitope specificity and is abrogated by viral escape. *Journal of virology* **81**:2624-2634.
209. **Lore, K., A. Smed-Sorensen, J. Vasudevan, J. R. Mascola, and R. A. Koup.** 2005. Myeloid and plasmacytoid dendritic cells transfer HIV-1 preferentially to antigen-specific CD4+ T cells. *The Journal of experimental medicine* **201**:2023-2033.
  210. **Lu, W., L. C. Arraes, W. T. Ferreira, and J. M. Andrieu.** 2004. Therapeutic dendritic-cell vaccine for chronic HIV-1 infection. *Nat Med* **10**:1359-1365.
  211. **Lubong Sabado, R., D. G. Kavanagh, D. E. Kaufmann, K. Fru, E. Babcock, E. Rosenberg, B. Walker, J. Lifson, N. Bhardwaj, and M. Larsson.** 2009. In vitro priming recapitulates in vivo HIV-1 specific T cell responses, revealing rapid loss of virus reactive CD4 T cells in acute HIV-1 infection. *PLoS One* **4**:e4256.
  212. **Macatangay, B. J., and C. R. Rinaldo.** 2010. Regulatory T cells in HIV immunotherapy. *HIV therapy* **4**:639-647.
  213. **Macatangay, B. J., M. E. Szajnik, T. L. Whiteside, S. A. Riddler, and C. R. Rinaldo.** 2010. Regulatory T cell suppression of Gag-specific CD8 T cell polyfunctional response after therapeutic vaccination of HIV-1-infected patients on ART. *PloS one* **5**:e9852.
  214. **Maddon, P. J., A. G. Dalgleish, J. S. McDougal, P. R. Clapham, R. A. Weiss, and R. Axel.** 1986. The T4 gene encodes the AIDS virus receptor and is expressed in the immune system and the brain. *Cell* **47**:333-348.
  215. **Maile, R., C. A. Siler, S. E. Kerry, K. E. Midkiff, E. J. Collins, and J. A. Frelinger.** 2005. Peripheral "CD8 tuning" dynamically modulates the size and responsiveness of an antigen-specific T cell pool in vivo. *J Immunol* **174**:619-627.
  216. **Mailliard, R. B., S. Egawa, Q. Cai, A. Kalinska, S. N. Bykovskaya, M. T. Lotze, M. L. Kapsenberg, W. J. Storkus, and P. Kalinski.** 2002. Complementary dendritic cell-activating function of CD8+ and CD4+ T cells: helper role of CD8+ T cells in the development of T helper type 1 responses. *The Journal of experimental medicine* **195**:473-483.
  217. **Mailliard, R. B., K. N. Smith, R. J. Fecek, G. Rappocciolo, E. J. Nascimento, E. T. Marques, S. C. Watkins, J. I. Mullins, and C. R. Rinaldo.** 2013. Selective induction of CTL helper rather than killer activity by natural epitope variants promotes dendritic cell-mediated HIV-1 dissemination. *J Immunol* **191**:2570-2580.
  218. **Mailliard, R. B., A. Wankowicz-Kalinska, Q. Cai, A. Wesa, C. M. Hilkens, M. L. Kapsenberg, J. M. Kirkwood, W. J. Storkus, and P. Kalinski.** 2004. alpha-type-1 polarized dendritic cells: a novel immunization tool with optimized CTL-inducing activity. *Cancer Res* **64**:5934-5937.
  219. **Malaspina, A., C. R. Rinaldo, R. P. Sekaly, J. Flores, and P. M. D'Souza.** 2011. "In vitro systems to characterize the immune response to HIV-1 and HIV-1 vaccine candidates", NIAID Workshop Report, Bethesda, August 4, 2010. *Vaccine* **29**:4647-4653.
  220. **Malhotra, U., F. Li, J. Nolin, M. Allison, H. Zhao, J. I. Mullins, S. Self, and M. J. McElrath.** 2007. Enhanced detection of human immunodeficiency virus type 1 (HIV-1) Nef-specific T cells recognizing multiple variants in early HIV-1 infection. *Journal of virology* **81**:5225-5237.
  221. **Markowitz, M., X. Jin, A. Hurley, V. Simon, B. Ramratnam, M. Louie, G. R. Deschenes, M. Ramanathan, Jr., S. Barsoum, J. Vanderhoeven, T. He, C. Chung, J. Murray, A. S. Perelson, L. Zhang, and D. D. Ho.** 2002. Discontinuation of antiretroviral therapy commenced early during the course of human immunodeficiency virus type 1

- infection, with or without adjunctive vaccination. *The Journal of infectious diseases* **186**:634-643.
222. **Masquelier, B., A. Taieb, S. Reigadas, B. Marchou, C. Cheneau, B. Spire, C. Charpentier, C. Leport, F. Raffi, G. Chene, and D. Descamps.** 2011. Cellular HIV-1 DNA quantification and short-term and long-term response to antiretroviral therapy. *The Journal of antimicrobial chemotherapy* **66**:1582-1589.
  223. **McDonald, D., L. Wu, S. M. Bohks, V. N. KewalRamani, D. Unutmaz, and T. J. Hope.** 2003. Recruitment of HIV and its receptors to dendritic cell-T cell junctions. *Science* **300**:1295-1297.
  224. **McDougal, J. S., P. J. Maddon, A. G. Dalgleish, P. R. Clapham, D. R. Littman, M. Godfrey, D. E. Maddon, L. Chess, R. A. Weiss, and R. Axel.** 1986. The T4 glycoprotein is a cell-surface receptor for the AIDS virus. *Cold Spring Harb Symp Quant Biol* **51 Pt 2**:703-711.
  225. **McElrath, M. J., S. C. De Rosa, Z. Moodie, S. Dubey, L. Kierstead, H. Janes, O. D. Defawe, D. K. Carter, J. Hural, R. Akondy, S. P. Buchbinder, M. N. Robertson, D. V. Mehrotra, S. G. Self, L. Corey, J. W. Shiver, and D. R. Casimiro.** 2008. HIV-1 vaccine-induced immunity in the test-of-concept Step Study: a case-cohort analysis. *Lancet* **372**:1894-1905.
  226. **McNeil, A. C., W. L. Shupert, C. A. Iyasere, C. W. Hallahan, J. A. Mican, R. T. Davey, Jr., and M. Connors.** 2001. High-level HIV-1 viremia suppresses viral antigen-specific CD4(+) T cell proliferation. *Proceedings of the National Academy of Sciences of the United States of America* **98**:13878-13883.
  227. **Meier, U. C., P. Klenerman, P. Griffin, W. James, B. Koppe, B. Larder, A. McMichael, and R. Phillips.** 1995. Cytotoxic T lymphocyte lysis inhibited by viable HIV mutants. *Science* **270**:1360-1362.
  228. **Mellors, J. W., C. R. Rinaldo, Jr., P. Gupta, R. M. White, J. A. Todd, and L. A. Kingsley.** 1996. Prognosis in HIV-1 infection predicted by the quantity of virus in plasma. *Science* **272**:1167-1170.
  229. **Meyaard, L., S. A. Otto, R. R. Jonker, M. J. Mijster, R. P. Keet, and F. Miedema.** 1992. Programmed death of T cells in HIV-1 infection. *Science* **257**:217-219.
  230. **Miedema, F., M. D. Hazenberg, K. Tesselaar, D. van Baarle, R. J. de Boer, and J. A. Borghans.** 2013. Immune Activation and Collateral Damage in AIDS Pathogenesis. *Front Immunol* **4**:298.
  231. **Migueles, S. A., A. C. Laborico, W. L. Shupert, M. S. Sabbaghian, R. Rabin, C. W. Hallahan, D. Van Baarle, S. Kostense, F. Miedema, M. McLaughlin, L. Ehler, J. Metcalf, S. Liu, and M. Connors.** 2002. HIV-specific CD8+ T cell proliferation is coupled to perforin expression and is maintained in nonprogressors. *Nature immunology* **3**:1061-1068.
  232. **Mocroft, A., A. N. Phillips, J. Gatell, B. Ledergerber, M. Fisher, N. Clumeck, M. Losso, A. Lazzarin, G. Fatkenheuer, and J. D. Lundgren.** 2007. Normalisation of CD4 counts in patients with HIV-1 infection and maximum virological suppression who are taking combination antiretroviral therapy: an observational cohort study. *Lancet* **370**:407-413.
  233. **Mollet, L., T. S. Li, A. Samri, C. Tournay, R. Tubiana, V. Calvez, P. Debre, C. Katlama, and B. Autran.** 2000. Dynamics of HIV-specific CD8+ T lymphocytes with



- changes in viral load. The RESTIM and COMET Study Groups. *J Immunol* **165**:1692-1704.
234. **Montaner, J. S., P. Reiss, D. Cooper, S. Vella, M. Harris, B. Conway, M. A. Wainberg, D. Smith, P. Robinson, D. Hall, M. Myers, and J. M. Lange.** 1998. A randomized, double-blind trial comparing combinations of nevirapine, didanosine, and zidovudine for HIV-infected patients: the INCAS Trial. Italy, The Netherlands, Canada and Australia Study. *JAMA* **279**:930-937.
  235. **Montes, M., C. Sanchez, D. E. Lewis, E. A. Graviss, C. Seas, E. Gotuzzo, and A. C. White, Jr.** 2011. Normalization of FoxP3(+) regulatory T cells in response to effective antiretroviral therapy. *The Journal of infectious diseases* **203**:496-499.
  236. **Moreno-Fernandez, M. E., P. Presicce, and C. A. Chougnet.** 2012. Homeostasis and function of regulatory T cells in HIV/SIV infection. *Journal of virology* **86**:10262-10269.
  237. **Murphy, K.** 2012. *Janeway's Immunobiology*, 8 ed. Garland Science, Taylor & Francis Group, LLC, New York, NY.
  238. **Musey, L., J. Hughes, T. Schacker, T. Shea, L. Corey, and M. J. McElrath.** 1997. Cytotoxic-T-cell responses, viral load, and disease progression in early human immunodeficiency virus type 1 infection. *The New England journal of medicine* **337**:1267-1274.
  239. **Nakamura, Y., P. Watchmaker, J. Urban, B. Sheridan, A. Giermasz, F. Nishimura, K. Sasaki, R. Cumberland, R. Muthuswamy, R. B. Mailliard, A. T. Larregina, L. D. Faló, W. Gooding, W. J. Storkus, H. Okada, R. L. Hendricks, and P. Kalinski.** 2007. Helper function of memory CD8+ T cells: heterologous CD8+ T cells support the induction of therapeutic cancer immunity. *Cancer Res* **67**:10012-10018.
  240. **Newton, P. J., I. V. Weller, I. G. Williams, R. F. Miller, A. Copas, R. S. Tedder, D. R. Katz, and B. M. Chain.** 2006. Monocyte derived dendritic cells from HIV-1 infected individuals partially reconstitute CD4 T-cell responses. *AIDS* **20**:171-180.
  241. **Nielsen, M., C. Lundegaard, T. Blicher, K. Lamberth, M. Harndahl, S. Justesen, G. Roder, B. Peters, A. Sette, O. Lund, and S. Buus.** 2007. NetMHCpan, a method for quantitative predictions of peptide binding to any HLA-A and -B locus protein of known sequence. *PloS one* **2**:e796.
  242. **Nielsen, M., C. Lundegaard, O. Lund, and C. Kesmir.** 2005. The role of the proteasome in generating cytotoxic T-cell epitopes: insights obtained from improved predictions of proteasomal cleavage. *Immunogenetics* **57**:33-41.
  243. **Nilsson, J., A. Boasso, P. A. Velilla, R. Zhang, M. Vaccari, G. Franchini, G. M. Shearer, J. Andersson, and C. Chougnet.** 2006. HIV-1-driven regulatory T-cell accumulation in lymphoid tissues is associated with disease progression in HIV/AIDS. *Blood* **108**:3808-3817.
  244. **Nixon, D. F., A. R. Townsend, J. G. Elvin, C. R. Rizza, J. Gallwey, and A. J. McMichael.** 1988. HIV-1 gag-specific cytotoxic T lymphocytes defined with recombinant vaccinia virus and synthetic peptides. *Nature* **336**:484-487.
  245. **O'Connor, D., T. Friedrich, A. Hughes, T. M. Allen, and D. Watkins.** 2001. Understanding cytotoxic T-lymphocyte escape during simian immunodeficiency virus infection. *Immunological reviews* **183**:115-126.
  246. **O'Connor, D. H., T. M. Allen, T. U. Vogel, P. Jing, I. P. DeSouza, E. Dodds, E. J. Dunphy, C. Melsaether, B. Mothe, H. Yamamoto, H. Horton, N. Wilson, A. L.**

- Hughes, and D. I. Watkins.** 2002. Acute phase cytotoxic T lymphocyte escape is a hallmark of simian immunodeficiency virus infection. *Nature medicine* **8**:493-499.
247. **O'Connor, D. H., A. B. McDermott, K. C. Krebs, E. J. Dodds, J. E. Miller, E. J. Gonzalez, T. J. Jacoby, L. Yant, H. Piontkivska, R. Pantophlet, D. R. Burton, W. M. Rehrauer, N. Wilson, A. L. Hughes, and D. I. Watkins.** 2004. A dominant role for CD8<sup>+</sup>-T-lymphocyte selection in simian immunodeficiency virus sequence variation. *Journal of virology* **78**:14012-14022.
248. **Oshiro, T. M., A. de Almeida, and A. J. da Silva Duarte.** 2009. Dendritic cell immunotherapy for HIV infection: from theory to reality. *Immunotherapy* **1**:1039-1051.
249. **Oshita, C., M. Takikawa, A. Kume, H. Miyata, T. Ashizawa, A. Iizuka, Y. Kiyohara, S. Yoshikawa, R. Tanosaki, N. Yamazaki, A. Yamamoto, K. Takesako, K. Yamaguchi, and Y. Akiyama.** 2012. Dendritic cell-based vaccination in metastatic melanoma patients: phase II clinical trial. *Oncol Rep* **28**:1131-1138.
250. **Otero, M., G. Nunnari, D. Leto, J. Sullivan, F. X. Wang, I. Frank, Y. Xu, C. Patel, G. Dornadula, J. Kulkosky, and R. J. Pomerantz.** 2003. Peripheral blood Dendritic cells are not a major reservoir for HIV type 1 in infected individuals on virally suppressive HAART. *AIDS research and human retroviruses* **19**:1097-1103.
251. **Pakker, N. G., D. W. Notermans, R. J. de Boer, M. T. Roos, F. de Wolf, A. Hill, J. M. Leonard, S. A. Danner, F. Miedema, and P. T. Schellekens.** 1998. Biphasic kinetics of peripheral blood T cells after triple combination therapy in HIV-1 infection: a composite of redistribution and proliferation. *Nature medicine* **4**:208-214.
252. **Palella, F. J., Jr., K. M. Delaney, A. C. Moorman, M. O. Loveless, J. Fuhrer, G. A. Satten, D. J. Aschman, and S. D. Holmberg.** 1998. Declining morbidity and mortality among patients with advanced human immunodeficiency virus infection. HIV Outpatient Study Investigators. *N Engl J Med* **338**:853-860.
253. **Pandrea, I., T. Gaufin, R. Gautam, J. Kristoff, D. Mandell, D. Montefiori, B. F. Keele, R. M. Ribeiro, R. S. Veazey, and C. Apetrei.** 2011. Functional cure of SIVagm infection in rhesus macaques results in complete recovery of CD4<sup>+</sup> T cells and is reverted by CD8<sup>+</sup> cell depletion. *PLoS pathogens* **7**:e1002170.
254. **Pantaleo, G., J. F. Demarest, H. Soudeyins, C. Graziosi, F. Denis, J. W. Adelsberger, P. Borrow, M. S. Saag, G. M. Shaw, R. P. Sekaly, and et al.** 1994. Major expansion of CD8<sup>+</sup> T cells with a predominant V beta usage during the primary immune response to HIV. *Nature* **370**:463-467.
255. **Pantaleo, G., C. Graziosi, and A. S. Fauci.** 1993. New concepts in the immunopathogenesis of human immunodeficiency virus infection. *N Engl J Med* **328**:327-335.
256. **Parker, K. C., M. A. Bednarek, and J. E. Coligan.** 1994. Scheme for ranking potential HLA-A2 binding peptides based on independent binding of individual peptide side-chains. *J Immunol* **152**:163-175.
257. **Pascolo, S., N. Bervas, J. M. Ure, A. G. Smith, F. A. Lemonnier, and B. Perarnau.** 1997. HLA-A2.1-restricted education and cytolytic activity of CD8(+) T lymphocytes from beta2 microglobulin (beta2m) HLA-A2.1 monochain transgenic H-2Db beta2m double knockout mice. *The Journal of experimental medicine* **185**:2043-2051.
258. **Perelson, A. S., P. Essunger, Y. Cao, M. Vesanen, A. Hurley, K. Saksela, M. Markowitz, and D. D. Ho.** 1997. Decay characteristics of HIV-1-infected compartments during combination therapy. *Nature* **387**:188-191.

259. **Pereyra, F., M. M. Addo, D. E. Kaufmann, Y. Liu, T. Miura, A. Rathod, B. Baker, A. Trocha, R. Rosenberg, E. Mackey, P. Ueda, Z. Lu, D. Cohen, T. Wrin, C. J. Petropoulos, E. S. Rosenberg, and B. D. Walker.** 2008. Genetic and immunologic heterogeneity among persons who control HIV infection in the absence of therapy. *The Journal of infectious diseases* **197**:563-571.
260. **Peters, B., S. Bulik, R. Tampe, P. M. Van Endert, and H. G. Holzhutter.** 2003. Identifying MHC class I epitopes by predicting the TAP transport efficiency of epitope precursors. *J Immunol* **171**:1741-1749.
261. **Phillips, R. E., S. Rowland-Jones, D. F. Nixon, F. M. Gotch, J. P. Edwards, A. O. Ogunlesi, J. G. Elvin, J. A. Rothbard, C. R. Bangham, C. R. Rizza, and et al.** 1991. Human immunodeficiency virus genetic variation that can escape cytotoxic T cell recognition. *Nature* **354**:453-459.
262. **Piantadosi, A., B. Chohan, D. Panteleeff, J. M. Baeten, K. Mandaliya, J. O. Ndinya-Achola, and J. Overbaugh.** 2009. HIV-1 evolution in gag and env is highly correlated but exhibits different relationships with viral load and the immune response. *Aids* **23**:579-587.
263. **Pierson, T., J. McArthur, and R. F. Siliciano.** 2000. Reservoirs for HIV-1: mechanisms for viral persistence in the presence of antiviral immune responses and antiretroviral therapy. *Annu Rev Immunol* **18**:665-708.
264. **Piguet, V., and R. M. Steinman.** 2007. The interaction of HIV with dendritic cells: outcomes and pathways. *Trends Immunol* **28**:503-510.
265. **Piketty, C., P. Castiel, L. Belec, D. Batisse, A. Si Mohamed, J. Gilquin, G. Gonzalez-Canali, D. Jayle, M. Karmochkine, L. Weiss, J. P. Aboulker, and M. D. Kazatchkine.** 1998. Discrepant responses to triple combination antiretroviral therapy in advanced HIV disease. *AIDS* **12**:745-750.
266. **Piqueras, B., J. Connolly, H. Freitas, A. K. Palucka, and J. Banchereau.** 2006. Upon viral exposure, myeloid and plasmacytoid dendritic cells produce 3 waves of distinct chemokines to recruit immune effectors. *Blood* **107**:2613-2618.
267. **Pitcher, C. J., C. Quittner, D. M. Peterson, M. Connors, R. A. Koup, V. C. Maino, and L. J. Picker.** 1999. HIV-1-specific CD4+ T cells are detectable in most individuals with active HIV-1 infection, but decline with prolonged viral suppression. *Nature medicine* **5**:518-525.
268. **Poli, G., G. Pantaleo, and A. S. Fauci.** 1993. Immunopathogenesis of human immunodeficiency virus infection. *Clin Infect Dis* **17 Suppl 1**:S224-229.
269. **Porichis, F., and D. E. Kaufmann.** 2012. Role of PD-1 in HIV pathogenesis and as target for therapy. *Curr HIV/AIDS Rep* **9**:81-90.
270. **Poss, M., A. G. Rodrigo, J. J. Gosink, G. H. Learn, D. de Vange Panteleeff, H. L. Martin, Jr., J. Bwayo, J. K. Kreiss, and J. Overbaugh.** 1998. Evolution of envelope sequences from the genital tract and peripheral blood of women infected with clade A human immunodeficiency virus type 1. *Journal of virology* **72**:8240-8251.
271. **Price, D. A., P. J. Goulder, P. Klenerman, A. K. Sewell, P. J. Easterbrook, M. Troop, C. R. Bangham, and R. E. Phillips.** 1997. Positive selection of HIV-1 cytotoxic T lymphocyte escape variants during primary infection. *Proceedings of the National Academy of Sciences of the United States of America* **94**:1890-1895.
272. **Price, D. A., S. M. West, M. R. Betts, L. E. Ruff, J. M. Brenchley, D. R. Ambrozak, Y. Edghill-Smith, M. J. Kuroda, D. Bogdan, K. Kunstman, N. L. Letvin, G. Franchini,**

- S. M. Wolinsky, R. A. Koup, and D. C. Douek.** 2004. T cell receptor recognition motifs govern immune escape patterns in acute SIV infection. *Immunity* **21**:793-803.
273. **Prlic, M., M. A. Williams, and M. J. Bevan.** 2007. Requirements for CD8 T-cell priming, memory generation and maintenance. *Current opinion in immunology* **19**:315-319.
274. **Rambaut, A., D. Posada, K. A. Crandall, and E. C. Holmes.** 2004. The causes and consequences of HIV evolution. *Nat Rev Genet* **5**:52-61.
275. **Rammensee, H., J. Bachmann, N. P. Emmerich, O. A. Bachor, and S. Stevanovic.** 1999. SYFPEITHI: database for MHC ligands and peptide motifs. *Immunogenetics* **50**:213-219.
276. **Rappocciolo, G., P. Piazza, C. L. Fuller, T. A. Reinhart, S. C. Watkins, D. T. Rowe, M. Jais, P. Gupta, and C. R. Rinaldo.** 2006. DC-SIGN on B lymphocytes is required for transmission of HIV-1 to T lymphocytes. *PLoS pathogens* **2**:e70.
277. **Reynolds, M. R., A. M. Weiler, K. L. Weisgrau, S. M. Piaskowski, J. R. Furlott, J. T. Weinfurter, M. Kaizu, T. Soma, E. J. Leon, C. MacNair, D. P. Leaman, M. B. Zwick, E. Gostick, S. K. Musani, D. A. Price, T. C. Friedrich, E. G. Rakasz, N. A. Wilson, A. B. McDermott, R. Boyle, D. B. Allison, D. R. Burton, W. C. Koff, and D. I. Watkins.** 2008. Macaques vaccinated with live-attenuated SIV control replication of heterologous virus. *The Journal of experimental medicine* **205**:2537-2550.
278. **Richman, D. D., T. Wrin, S. J. Little, and C. J. Petropoulos.** 2003. Rapid evolution of the neutralizing antibody response to HIV type 1 infection. *Proceedings of the National Academy of Sciences of the United States of America* **100**:4144-4149.
279. **Ridge, J. P., F. Di Rosa, and P. Matzinger.** 1998. A conditioned dendritic cell can be a temporal bridge between a CD4+ T-helper and a T-killer cell. *Nature* **393**:474-478.
280. **Rinaldo, C. R.** 2009. Dendritic cell-based human immunodeficiency virus vaccine. *Journal of internal medicine* **265**:138-158.
281. **Rinaldo, C. R., Jr., X. L. Huang, Z. Fan, J. B. Margolick, L. Borowski, A. Hoji, C. Kalinyak, D. K. McMahon, S. A. Riddler, W. H. Hildebrand, R. B. Day, and J. W. Mellors.** 2000. Anti-human immunodeficiency virus type 1 (HIV-1) CD8(+) T-lymphocyte reactivity during combination antiretroviral therapy in HIV-1-infected patients with advanced immunodeficiency. *Journal of virology* **74**:4127-4138.
282. **Ritola, K., C. D. Pilcher, S. A. Fiscus, N. G. Hoffman, J. A. Nelson, K. M. Kitrinos, C. B. Hicks, J. J. Eron, Jr., and R. Swanstrom.** 2004. Multiple V1/V2 env variants are frequently present during primary infection with human immunodeficiency virus type 1. *Journal of virology* **78**:11208-11218.
283. **Rodrigo, A. G., and J. I. Mullins.** 1996. Human immunodeficiency virus type 1 molecular evolution and the measure of selection. *AIDS research and human retroviruses* **12**:1681-1685.
284. **Roederer, M., J. G. Dubs, M. T. Anderson, P. A. Raju, L. A. Herzenberg, and L. A. Herzenberg.** 1995. CD8 naive T cell counts decrease progressively in HIV-infected adults. *The Journal of clinical investigation* **95**:2061-2066.
285. **Rolland, M., D. Heckerman, W. Deng, C. M. Rousseau, H. Coovadia, K. Bishop, P. J. Goulder, B. D. Walker, C. Brander, and J. I. Mullins.** 2008. Broad and Gag-biased HIV-1 epitope repertoires are associated with lower viral loads. *PloS one* **3**:e1424.
286. **Rolland, M., S. Tovanabutra, A. C. deCamp, N. Frahm, P. B. Gilbert, E. Sanders-Buell, L. Heath, C. A. Magaret, M. Bose, A. Bradfield, A. O'Sullivan, J. Crossler, T. Jones, M. Nau, K. Wong, H. Zhao, D. N. Raugi, S. Sorensen, J. N. Stoddard, B. S.**

- Maust, W. Deng, J. Hural, S. Dubey, N. L. Michael, J. Shiver, L. Corey, F. Li, S. G. Self, J. Kim, S. Buchbinder, D. R. Casimiro, M. N. Robertson, A. Duerr, M. J. McElrath, F. E. McCutchan, and J. I. Mullins.** 2011. Genetic impact of vaccination on breakthrough HIV-1 sequences from the STEP trial. *Nature medicine* **17**:366-371.
287. **Rothman, A. L.** 2011. Immunity to dengue virus: a tale of original antigenic sin and tropical cytokine storms. *Nat Rev Immunol* **11**:532-543.
288. **Ruedl, C., M. Kopf, and M. F. Bachmann.** 1999. CD8(+) T cells mediate CD40-independent maturation of dendritic cells in vivo. *The Journal of experimental medicine* **189**:1875-1884.
289. **Saez-Cirion, A., C. Lacabaratz, O. Lambotte, P. Versmisse, A. Urrutia, F. Boufassa, F. Barre-Sinoussi, J. F. Delfraissy, M. Sinet, G. Pancino, and A. Venet.** 2007. HIV controllers exhibit potent CD8 T cell capacity to suppress HIV infection ex vivo and peculiar cytotoxic T lymphocyte activation phenotype. *Proceedings of the National Academy of Sciences of the United States of America* **104**:6776-6781.
290. **Saez-Cirion, A., S. Y. Shin, P. Versmisse, F. Barre-Sinoussi, and G. Pancino.** 2010. Ex vivo T cell-based HIV suppression assay to evaluate HIV-specific CD8+ T-cell responses. *Nat Protoc* **5**:1033-1041.
291. **Sakaguchi, S., N. Sakaguchi, M. Asano, M. Itoh, and M. Toda.** 1995. Immunologic self-tolerance maintained by activated T cells expressing IL-2 receptor alpha-chains (CD25). Breakdown of a single mechanism of self-tolerance causes various autoimmune diseases. *J Immunol* **155**:1151-1164.
292. **Sakthivel, P., M. Gereke, and D. Bruder.** 2012. Therapeutic intervention in cancer and chronic viral infections: antibody mediated manipulation of PD-1/PD-L1 interaction. *Rev Recent Clin Trials* **7**:10-23.
293. **Salazar-Gonzalez, J. F., E. Bailes, K. T. Pham, M. G. Salazar, M. B. Guffey, B. F. Keele, C. A. Derdeyn, P. Farmer, E. Hunter, S. Allen, O. Manigart, J. Mulenga, J. A. Anderson, R. Swanstrom, B. F. Haynes, G. S. Athreya, B. T. Korber, P. M. Sharp, G. M. Shaw, and B. H. Hahn.** 2008. Deciphering human immunodeficiency virus type 1 transmission and early envelope diversification by single-genome amplification and sequencing. *Journal of virology* **82**:3952-3970.
294. **Sanders, R. W., E. C. de Jong, C. E. Baldwin, J. H. Schuitemaker, M. L. Kapsenberg, and B. Berkhout.** 2002. Differential transmission of human immunodeficiency virus type 1 by distinct subsets of effector dendritic cells. *J Virol* **76**:7812-7821.
295. **Sapp, M., J. Engelmayer, M. Larsson, A. Granelli-Piperno, R. Steinman, and N. Bhardwaj.** 1999. Dendritic cells generated from blood monocytes of HIV-1 patients are not infected and act as competent antigen presenting cells eliciting potent T-cell responses. *Immunology letters* **66**:121-128.
296. **Sauce, D., C. Elbim, and V. Appay.** 2013. Monitoring cellular immune markers in HIV infection: from activation to exhaustion. *Current opinion in HIV and AIDS* **8**:125-131.
297. **Scarlatti, G., E. Tresoldi, A. Bjorndal, R. Fredriksson, C. Colognesi, H. K. Deng, M. S. Malnati, A. Plebani, A. G. Siccardi, D. R. Littman, E. M. Fenyo, and P. Lusso.** 1997. In vivo evolution of HIV-1 co-receptor usage and sensitivity to chemokine-mediated suppression. *Nature medicine* **3**:1259-1265.
298. **Schenker, E. L., L. E. Hultin, K. D. Bauer, J. Ferbas, J. B. Margolick, and J. V. Giorgi.** 1993. Evaluation of a dual-color flow cytometry immunophenotyping panel in a multicenter quality assurance program. *Cytometry* **14**:307-317.

299. **Schmitz, J. E., M. J. Kuroda, S. Santra, V. G. Sasseville, M. A. Simon, M. A. Lifton, P. Racz, K. Tenner-Racz, M. Dalesandro, B. J. Scallon, J. Ghayeb, M. A. Forman, D. C. Montefiori, E. P. Rieber, N. L. Letvin, and K. A. Reimann.** 1999. Control of viremia in simian immunodeficiency virus infection by CD8+ lymphocytes. *Science* **283**:857-860.
300. **Schneider, E., S. Whitmore, K. M. Glynn, K. Dominguez, A. Mitsch, and M. T. McKenna.** 2008. Revised surveillance case definitions for HIV infection among adults, adolescents, and children aged <18 months and for HIV infection and AIDS among children aged 18 months to <13 years--United States, 2008. *MMWR Recomm Rep* **57**:1-12.
301. **Schoenberger, S. P., R. E. Toes, E. I. van der Voort, R. Offringa, and C. J. Melief.** 1998. T-cell help for cytotoxic T lymphocytes is mediated by CD40-CD40L interactions. *Nature* **393**:480-483.
302. **Schulze Zur Wiesch, J., A. Thomssen, P. Hartjen, I. Toth, C. Lehmann, D. Meyer-Olson, K. Colberg, S. Frerk, D. Babikir, S. Schmiedel, O. Degen, S. Mauss, J. Rockstroh, S. Staszewski, P. Khaykin, A. Strasak, A. W. Lohse, G. Fatkenheuer, J. Hauber, and J. van Lunzen.** 2011. Comprehensive analysis of frequency and phenotype of T regulatory cells in HIV infection: CD39 expression of FoxP3+ T regulatory cells correlates with progressive disease. *Journal of virology* **85**:1287-1297.
303. **Sedaghat, A. R., J. D. Siliciano, T. P. Brennan, C. O. Wilke, and R. F. Siliciano.** 2007. Limits on replenishment of the resting CD4+ T cell reservoir for HIV in patients on HAART. *PLoS pathogens* **3**:e122.
304. **Sedaghat, A. R., R. F. Siliciano, and C. O. Wilke.** 2008. Low-level HIV-1 replication and the dynamics of the resting CD4+ T cell reservoir for HIV-1 in the setting of HAART. *BMC infectious diseases* **8**:2.
305. **Seder, R. A., P. A. Darrah, and M. Roederer.** 2008. T-cell quality in memory and protection: implications for vaccine design. *Nat Rev Immunol* **8**:247-258.
306. **Shan, L., K. Deng, N. S. Shroff, C. M. Durand, S. A. Rabi, H. C. Yang, H. Zhang, J. B. Margolick, J. N. Blankson, and R. F. Siliciano.** 2012. Stimulation of HIV-1-specific cytolytic T lymphocytes facilitates elimination of latent viral reservoir after virus reactivation. *Immunity* **36**:491-501.
307. **Shankarappa, R., J. B. Margolick, S. J. Gange, A. G. Rodrigo, D. Upchurch, H. Farzadegan, P. Gupta, C. R. Rinaldo, G. H. Learn, X. He, X. L. Huang, and J. I. Mullins.** 1999. Consistent viral evolutionary changes associated with the progression of human immunodeficiency virus type 1 infection. *Journal of virology* **73**:10489-10502.
308. **Shin, H., S. D. Blackburn, J. N. Blattman, and E. J. Wherry.** 2007. Viral antigen and extensive division maintain virus-specific CD8 T cells during chronic infection. *The Journal of experimental medicine* **204**:941-949.
309. **Shriner, D., A. G. Rodrigo, D. C. Nickle, and J. I. Mullins.** 2004. Pervasive genomic recombination of HIV-1 in vivo. *Genetics* **167**:1573-1583.
310. **Siliciano, J. D., J. Kajdas, D. Finzi, T. C. Quinn, K. Chadwick, J. B. Margolick, C. Kovacs, S. J. Gange, and R. F. Siliciano.** 2003. Long-term follow-up studies confirm the stability of the latent reservoir for HIV-1 in resting CD4+ T cells. *Nature medicine* **9**:727-728.

311. **Siliciano, J. D., and R. F. Siliciano.** 2005. Enhanced culture assay for detection and quantitation of latently infected, resting CD4+ T-cells carrying replication-competent virus in HIV-1-infected individuals. *Methods Mol Biol* **304**:3-15.
312. **Sowinski, S., C. Jolly, O. Berninghausen, M. A. Purbhoo, A. Chauveau, K. Kohler, S. Oddos, P. Eissmann, F. M. Brodsky, C. Hopkins, B. Onfelt, Q. Sattentau, and D. M. Davis.** 2008. Membrane nanotubes physically connect T cells over long distances presenting a novel route for HIV-1 transmission. *Nature cell biology* **10**:211-219.
313. **Streeck, H., J. S. Jolin, Y. Qi, B. Yassine-Diab, R. C. Johnson, D. S. Kwon, M. M. Addo, C. Brumme, J. P. Routy, S. Little, H. K. Jessen, A. D. Kelleher, F. M. Hecht, R. P. Sekaly, E. S. Rosenberg, B. D. Walker, M. Carrington, and M. Altfeld.** 2009. Human immunodeficiency virus type 1-specific CD8+ T-cell responses during primary infection are major determinants of the viral set point and loss of CD4+ T cells. *J Virol* **83**:7641-7648.
314. **Suchard, M. S., E. Mayne, V. A. Green, S. Shalekoff, S. L. Donninger, W. S. Stevens, C. M. Gray, and C. T. Tiemessen.** 2010. FOXP3 expression is upregulated in CD4T cells in progressive HIV-1 infection and is a marker of disease severity. *PloS one* **5**:e11762.
315. **Tada, F., M. Abe, M. Hirooka, Y. Ikeda, Y. Hiasa, Y. Lee, N. C. Jung, W. B. Lee, H. S. Lee, Y. S. Bae, and M. Onji.** 2012. Phase I/II study of immunotherapy using tumor antigen-pulsed dendritic cells in patients with hepatocellular carcinoma. *Int J Oncol* **41**:1601-1609.
316. **Tajima, F.** 1989. Statistical method for testing the neutral mutation hypothesis by DNA polymorphism. *Genetics* **123**:585-595.
317. **Tang, H. L., and J. G. Cyster.** 1999. Chemokine Up-regulation and activated T cell attraction by maturing dendritic cells. *Science* **284**:819-822.
318. **Tanner, K., and D. Allen.** 2004. Approaches to biology teaching and learning: learning styles and the problem of instructional selection--engaging all students in science courses. *Cell biology education* **3**:197-201.
319. **Tenzer, S., B. Peters, S. Bulik, O. Schoor, C. Lemmel, M. M. Schatz, P. M. Kloetzel, H. G. Rammensee, H. Schild, and H. G. Holzhutter.** 2005. Modeling the MHC class I pathway by combining predictions of proteasomal cleavage, TAP transport and MHC class I binding. *Cell Mol Life Sci* **62**:1025-1037.
320. **Tenzer, S., E. Wee, A. Burgevin, G. Stewart-Jones, L. Friis, K. Lamberth, C. H. Chang, M. Harndahl, M. Weimershaus, J. Gerstoft, N. Akkad, P. Klenerman, L. Fugger, E. Y. Jones, A. J. McMichael, S. Buus, H. Schild, P. van Endert, and A. K. Iversen.** 2009. Antigen processing influences HIV-specific cytotoxic T lymphocyte immunodominance. *Nature immunology* **10**:636-646.
321. **Thomas, M. J., A. Noble, E. Sawicka, P. W. Askenase, and D. M. Kemeny.** 2002. CD8 T cells inhibit IgE via dendritic cell IL-12 induction that promotes Th1 T cell counter-regulation. *J Immunol* **168**:216-223.
322. **Tindall, B., and D. A. Cooper.** 1991. Primary HIV infection: host responses and intervention strategies. *AIDS* **5**:1-14.
323. **Trautmann, L., L. Janbazian, N. Chomont, E. A. Said, S. Gimmig, B. Bessette, M. R. Boulassel, E. Delwart, H. Sepulveda, R. S. Balderas, J. P. Routy, E. K. Haddad, and R. P. Sekaly.** 2006. Upregulation of PD-1 expression on HIV-specific CD8+ T cells leads to reversible immune dysfunction. *Nature medicine* **12**:1198-1202.

324. **Turk, G., M. M. Gherardi, N. Laufer, M. Saracco, R. Luzzi, J. H. Cox, P. Cahn, and H. Salomon.** 2008. Magnitude, breadth, and functional profile of T-cell responses during human immunodeficiency virus primary infection with B and BF viral variants. *Journal of virology* **82**:2853-2866.
325. **Turnbull, E. L., M. Wong, S. Wang, X. Wei, N. A. Jones, K. E. Conrod, D. Aldam, J. Turner, P. Pellegrino, B. F. Keele, I. Williams, G. M. Shaw, and P. Borrow.** 2009. Kinetics of expansion of epitope-specific T cell responses during primary HIV-1 infection. *J Immunol* **182**:7131-7145.
326. **Ueno, H., E. Klechevsky, R. Morita, C. Aspod, T. Cao, T. Matsui, T. Di Pucchio, J. Connolly, J. W. Fay, V. Pascual, A. K. Palucka, and J. Banchereau.** 2007. Dendritic cell subsets in health and disease. *Immunol Rev* **219**:118-142.
327. **Umeshappa, C. S., H. Huang, Y. Xie, Y. Wei, S. J. Mulligan, Y. Deng, and J. Xiang.** 2009. CD4+ Th-APC with acquired peptide/MHC class I and II complexes stimulate type 1 helper CD4+ and central memory CD8+ T cell responses. *J Immunol* **182**:193-206.
328. **Umeshappa, C. S., R. H. Nanjundappa, Y. Xie, A. Freywald, Q. Xu, and J. Xiang.** 2013. Differential requirements of CD4(+) T-cell signals for effector cytotoxic T-lymphocyte (CTL) priming and functional memory CTL development at higher CD8(+) T-cell precursor frequency. *Immunology* **138**:298-306.
329. **UNAIDS/WHO** 2010, posting date. 2010 AIDS Epidemic Update. [Online.]
330. **Valentine, L. E., S. M. Piaskowski, E. G. Rakasz, N. L. Henry, N. A. Wilson, and D. I. Watkins.** 2008. Recognition of escape variants in ELISPOT does not always predict CD8+ T-cell recognition of simian immunodeficiency virus-infected cells expressing the same variant sequences. *Journal of virology* **82**:575-581.
331. **van Baarle, D., A. Tsegaye, F. Miedema, and A. Akbar.** 2005. Significance of senescence for virus-specific memory T cell responses: rapid ageing during chronic stimulation of the immune system. *Immunology letters* **97**:19-29.
332. **van Bockel, D. J., D. A. Price, M. L. Munier, V. Venturi, T. E. Asher, K. Ladell, H. Y. Greenaway, J. Zaunders, D. C. Douek, D. A. Cooper, M. P. Davenport, and A. D. Kelleher.** 2011. Persistent survival of prevalent clonotypes within an immunodominant HIV gag-specific CD8+ T cell response. *J Immunol* **186**:359-371.
333. **van der Burg, S. H., M. J. Visseren, R. M. Brandt, W. M. Kast, and C. J. Melief.** 1996. Immunogenicity of peptides bound to MHC class I molecules depends on the MHC-peptide complex stability. *J Immunol* **156**:3308-3314.
334. **Van Gulck, E., V. F. Van Tendeloo, Z. N. Berneman, and G. Vanham.** 2010. Role of dendritic cells in HIV-immunotherapy. *Curr HIV Res* **8**:310-322.
335. **Van Gulck, E., E. Vlieghe, M. Vekemans, V. F. Van Tendeloo, A. Van De Velde, E. Smits, S. Anguille, N. Cools, H. Goossens, L. Mertens, W. De Haes, J. Wong, E. Florence, G. Vanham, and Z. N. Berneman.** 2012. mRNA-based dendritic cell vaccination induces potent antiviral T-cell responses in HIV-1-infected patients. *AIDS* **26**:F1-12.
336. **Vanderford, T. H., C. Bleckwehl, J. C. Engram, R. M. Dunham, N. R. Klatt, M. B. Feinberg, D. A. Garber, M. R. Betts, and G. Silvestri.** 2011. Viral CTL escape mutants are generated in lymph nodes and subsequently become fixed in plasma and rectal mucosa during acute SIV infection of macaques. *PLoS Pathog* **7**:e1002048.
337. **Vanham, G., and E. Van Gulck.** 2012. Can immunotherapy be useful as a "functional cure" for infection with Human Immunodeficiency Virus-1? *Retrovirology* **9**:72.



338. **Vergara-Rodriguez, P., S. Vibhakar, and J. Watts.** 2009. Metabolic syndrome and associated cardiovascular risk factors in the treatment of persons with human immunodeficiency virus and severe mental illness. *Pharmacol Ther* **124**:269-278.
339. **Vojnov, L., J. S. Reed, K. L. Weisgrau, E. G. Rakasz, J. T. Loffredo, S. M. Piaskowski, J. B. Sacha, H. L. Kolar, N. A. Wilson, R. P. Johnson, and D. I. Watkins.** 2010. Effective simian immunodeficiency virus-specific CD8+ T cells lack an easily detectable, shared characteristic. *Journal of virology* **84**:753-764.
340. **Volberding, P. A., and S. G. Deeks.** 1998. Antiretroviral therapy for HIV infection: promises and problems. *JAMA* **279**:1343-1344.
341. **Vrisekoop, N., R. van Gent, A. B. de Boer, S. A. Otto, J. C. Borleffs, R. Steingrover, J. M. Prins, T. W. Kuijpers, T. F. Wolfs, S. P. Geelen, I. Vulto, P. Lansdorp, K. Tesselaar, J. A. Borghans, and F. Miedema.** 2008. Restoration of the CD4 T cell compartment after long-term highly active antiretroviral therapy without phenotypical signs of accelerated immunological aging. *J Immunol* **181**:1573-1581.
342. **Watchmaker, P. B., J. A. Urban, E. Berk, Y. Nakamura, R. B. Mailliard, S. C. Watkins, S. M. van Ham, and P. Kalinski.** 2008. Memory CD8+ T cells protect dendritic cells from CTL killing. *J Immunol* **180**:3857-3865.
343. **Watkins, S. C., and R. D. Salter.** 2005. Functional connectivity between immune cells mediated by tunneling nanotubes. *Immunity* **23**:309-318.
344. **Wei, X., J. M. Decker, S. Wang, H. Hui, J. C. Kappes, X. Wu, J. F. Salazar-Gonzalez, M. G. Salazar, J. M. Kilby, M. S. Saag, N. L. Komarova, M. A. Nowak, B. H. Hahn, P. D. Kwong, and G. M. Shaw.** 2003. Antibody neutralization and escape by HIV-1. *Nature* **422**:307-312.
345. **Welsh, R. M., J. W. Che, M. A. Brehm, and L. K. Selin.** 2010. Heterologous immunity between viruses. *Immunological reviews* **235**:244-266.
346. **Wesa, A., P. Kalinski, J. M. Kirkwood, T. Tatsumi, and W. J. Storkus.** 2007. Polarized type-1 dendritic cells (DC1) producing high levels of IL-12 family members rescue patient TH1-type antimelanoma CD4+ T cell responses in vitro. *J Immunother* **30**:75-82.
347. **Wherry, E. J., D. L. Barber, S. M. Kaech, J. N. Blattman, and R. Ahmed.** 2004. Antigen-independent memory CD8 T cells do not develop during chronic viral infection. *Proceedings of the National Academy of Sciences of the United States of America* **101**:16004-16009.
348. **Wolfs, T. F., G. Zwart, M. Bakker, and J. Goudsmit.** 1992. HIV-1 genomic RNA diversification following sexual and parenteral virus transmission. *Virology* **189**:103-110.
349. **Wolinsky, S. M., B. T. Korber, A. U. Neumann, M. Daniels, K. J. Kunstman, A. J. Whetsell, M. R. Furtado, Y. Cao, D. D. Ho, and J. T. Safrit.** 1996. Adaptive evolution of human immunodeficiency virus-type 1 during the natural course of infection. *Science* **272**:537-542.
350. **Wolint, P., M. R. Betts, R. A. Koup, and A. Oxenius.** 2004. Immediate cytotoxicity but not degranulation distinguishes effector and memory subsets of CD8+ T cells. *The Journal of experimental medicine* **199**:925-936.
351. **Wong, J. K., H. F. Gunthard, D. V. Havlir, Z. Q. Zhang, A. T. Haase, C. C. Ignacio, S. Kwok, E. Emini, and D. D. Richman.** 1997. Reduction of HIV-1 in blood and lymph nodes following potent antiretroviral therapy and the virologic correlates of treatment failure. *Proceedings of the National Academy of Sciences of the United States of America* **94**:12574-12579.

352. **Wong, J. K., M. Hezareh, H. F. Gunthard, D. V. Havlir, C. C. Ignacio, C. A. Spina, and D. D. Richman.** 1997. Recovery of replication-competent HIV despite prolonged suppression of plasma viremia. *Science* **278**:1291-1295.
353. **Wood, E., R. S. Hogg, B. Yip, R. Quercia, P. R. Harrigan, M. V. O'Shaughnessy, and J. S. Montaner.** 2003. Higher baseline levels of plasma human immunodeficiency virus type 1 RNA are associated with increased mortality after initiation of triple-drug antiretroviral therapy. *The Journal of infectious diseases* **188**:1421-1425.
354. **Wooldridge, L., B. Laugel, J. Ekeruche, M. Clement, H. A. van den Berg, D. A. Price, and A. K. Sewell.** 2010. CD8 controls T cell cross-reactivity. *J Immunol* **185**:4625-4632.
355. **Wu, L., and V. N. KewalRamani.** 2006. Dendritic-cell interactions with HIV: infection and viral dissemination. *Nat Rev Immunol* **6**:859-868.
356. **Xiao, Z., M. F. Mescher, and S. C. Jameson.** 2007. Detuning CD8 T cells: down-regulation of CD8 expression, tetramer binding, and response during CTL activation. *The Journal of experimental medicine* **204**:2667-2677.
357. **Yachi, P. P., J. Ampudia, T. Zal, and N. R. Gascoigne.** 2006. Altered peptide ligands induce delayed CD8-T cell receptor interaction--a role for CD8 in distinguishing antigen quality. *Immunity* **25**:203-211.
358. **Yasutomi, Y., K. A. Reimann, C. I. Lord, M. D. Miller, and N. L. Letvin.** 1993. Simian immunodeficiency virus-specific CD8+ lymphocyte response in acutely infected rhesus monkeys. *Journal of virology* **67**:1707-1711.
359. **Yin, L., Z. C. Kou, C. Rodriguez, W. Hou, M. M. Goodenow, and J. W. Sleasman.** 2009. Antiretroviral therapy restores diversity in the T-cell receptor Vbeta repertoire of CD4 T-cell subpopulations among human immunodeficiency virus type 1-infected children and adolescents. *Clinical and vaccine immunology : CVI* **16**:1293-1301.
360. **Yokomaku, Y., H. Miura, H. Tomiyama, A. Kawana-Tachikawa, M. Takiguchi, A. Kojima, Y. Nagai, A. Iwamoto, Z. Matsuda, and K. Ariyoshi.** 2004. Impaired processing and presentation of cytotoxic-T-lymphocyte (CTL) epitopes are major escape mechanisms from CTL immune pressure in human immunodeficiency virus type 1 infection. *Journal of virology* **78**:1324-1332.
361. **Younes, S. A., B. Yassine-Diab, A. R. Dumont, M. R. Boulassel, Z. Grossman, J. P. Routy, and R. P. Sekaly.** 2003. HIV-1 viremia prevents the establishment of interleukin 2-producing HIV-specific memory CD4+ T cells endowed with proliferative capacity. *The Journal of experimental medicine* **198**:1909-1922.
362. **Yusim K, S. J., Honeyborne I, Calef C, Goulder PJ, Korber BT** 2004. Enhanced Motif Scan: A Tool to Scan for HLA Anchor Residues in Proteins, p. 25-36. in *HIV Immunology and HIV/SIV Vaccine Databases 2003*, Edited by: Korber BT, Brander C, Haynes BF, Koup R, Moore JP, Walker BD, and Watkins DI. Published by: Los Alamos National Laboratory, Theoretical Biology and Biophysics, Los Alamos, New Mexico. LA-UR 04-8162.
363. **Zehn, D., S. Y. Lee, and M. J. Bevan.** 2009. Complete but curtailed T-cell response to very low-affinity antigen. *Nature* **458**:211-214.
364. **Zhang, L., S. R. Lewin, M. Markowitz, H. H. Lin, E. Skulsky, R. Karanickolas, Y. He, X. Jin, S. Tuttleton, M. Vesanen, H. Spiegel, R. Kost, J. van Lunzen, H. J. Stellbrink, S. Wolinsky, W. Borkowsky, P. Palumbo, L. G. Kostrikis, and D. D. Ho.** 1999.

- Measuring recent thymic emigrants in blood of normal and HIV-1-infected individuals before and after effective therapy. *J Exp Med* **190**:725-732.
365. **Zhang, M., B. Gaschen, W. Blay, B. Foley, N. Haigwood, C. Kuiken, and B. Korber.** 2004. Tracking global patterns of N-linked glycosylation site variation in highly variable viral glycoproteins: HIV, SIV, and HCV envelopes and influenza hemagglutinin. *Glycobiology* **14**:1229-1246.
366. **Zhang, Z. Q., D. W. Notermans, G. Sedgewick, W. Cavert, S. Wietgreffe, M. Zupancic, K. Gebhard, K. Henry, L. Boies, Z. Chen, M. Jenkins, R. Mills, H. McDade, C. Goodwin, C. M. Schuwirth, S. A. Danner, and A. T. Haase.** 1998. Kinetics of CD4+ T cell repopulation of lymphoid tissues after treatment of HIV-1 infection. *Proceedings of the National Academy of Sciences of the United States of America* **95**:1154-1159.
367. **Zheng, Y. H., N. Lovsin, and B. M. Peterlin.** 2005. Newly identified host factors modulate HIV replication. *Immunology letters* **97**:225-234.